Combinatorial aspects of Coxeter groups

Dissertation

zur Erlangung des akademischen Grades

doctor rerum naturalium
(Dr. rer. nat.)

von Anna Franziska Reimann, M. Sc.

geb. am 31.12.1998 in Halberstadt

genehmigt durch die Fakultät für Mathematik
der Otto-von-Guericke-Universität Magdeburg

Gutachter: Prof. Dr. rer. nat. Petra Schwer

Prof. Dr. rer. nat. Volker Kaibel

Prof. Dr. rer. nat. Christophe Hohlweg

eingereicht am: 25. September 2025
Verteidigung am: 26. Januar 2026

Abstract

This thesis investigates aspects of Coxeter groups along two main lines of research, both using similar combinatorial methods.
After presenting the basic notions of graph theory together with the geometric and combinatorial foundations of Coxeter groups in Part I (Chapter 2), Part II is devoted to the study of folded galleries and Coxeter shadows. While folded galleries have numerous applications across mathematics, their rich intrinsic combinatorial structure remains only partially understood. This work aims to develop methods for describing folded galleries and shadows in affine Coxeter complexes with Weyl chamber orientations, establishing the foundation for extending these ideas to more general orientations. Central to this study is the introduction of *folding patterns* in Chapter 3, which encode the combinatorial possibilities of folding minimal galleries. The main result of this chapter is that we characterize all applicable folding patterns of a given minimal gallery by establishing a bijection between folding patterns and directed paths in Bruhat moment graphs in Theorem 3.3.9, reducing the complexity of the problem to the study of finite graphs. Furthermore, we also prove how to determine the spherical direction of the end alcove of a positively folded gallery with respect to Weyl chamber orientations by drawing another link to Bruhat moment graphs in Theorem 3.3.18. Building on these connections, we introduce *folding pattern polytopes* in Chapter 4, which describe the sets of end vertices of folded galleries with a given folding pattern. For a special subset of group elements, these tools allow us to provide a combinatorial framework for computing the complete Coxeter shadow in Theorem 4.3.12, while for arbitrary group elements, we propose the notion of the *Coxeter umbra* for the subset of the shadow constructed this way (cf. Theorem 4.4.4).
Part III addresses involutions in Coxeter groups, i.e., elements of order two. We study the number cc_2 of conjugacy classes of involutions, a group-theoretic invariant previously determined by Deodhar and Richardson [Deo82; Ric82], in Chapter 5. Our combinatorial approach (cf. Theorem 5.3.7) is based on the introduction of *higher-rank odd graphs*, a natural generalization of the odd graphs that have been used in the study of conjugacy classes of reflections (see [Bra+02]). This framework allows us to provide closed formulae for cc_2 in all irreducible finite and affine Coxeter groups in Theorems 5.4.3 and 5.4.4. Moreover, we apply our method to compute the number of conjugacy classes of involutions for triangle groups and right-angled Coxeter groups.
Uniting both directions of research is the pervasive use of graphs as our combinatorial tool of choice, which provides a common language for the objects under consideration.

Zusammenfassung

Diese Dissertation untersucht Aspekte von Coxeter-Gruppen entlang von zwei Hauptforschungsrichtungen, die auf ähnlichen kombinatorischen Methoden beruhen. Nachdem in Part I (Chapter 2) grundlegende Begriffe der Graphentheorie sowie die geometrischen und kombinatorischen Grundlagen von Coxeter-Gruppen dargestellt werden, widmet sich Part II der Untersuchung gefalteter Galerien und Coxeter-Schatten. Obwohl gefaltete Galerien zahlreiche Anwendungen in verschiedenen Teildisziplinen der Mathematik haben, ist ihre innere kombinatorische Struktur bislang nur teilweise verstanden. Ziel dieser Arbeit ist es, Methoden zur Beschreibung gefalteter Galerien und Schatten in affinen Coxeter-Komplexen mit Weyl-Kammer-Orientierungen zu entwickeln und damit die Grundlage für eine Erweiterung dieser Ideen auch auf andere Orientierungen zu schaffen. Zentral für unsere Untersuchungen ist die Einführung von *folding patterns* (dt. Faltungsmuster) in Chapter 3, die die kombinatorischen Möglichkeiten des Faltens minimaler Galerien kodieren. Das Hauptresultat dieses Kapitels besteht darin, dass wir alle anwendbaren Faltungsmuster für eine gegebene minimale Galerie charakterisieren, indem wir in Theorem 3.3.9 eine Bijektion zwischen Faltungsmustern und gerichteten Pfaden in Bruhat-Moment-Graphen herstellen und so die Komplexität des Problems auf die Untersuchung endlicher Graphen reduzieren. Darüber hinaus beweisen wir in Theorem 3.3.18, wie man die sphärische Richtung der End-Alkoven einer positiv gefalteten Galerie in Bezug auf Weyl-Kammer-Orientierungen bestimmt, indem wir eine weitere Verbindung zu Bruhat-Moment-Graphen herstellen. Aufbauend auf diesen Ergebnissen führen wir in Chapter 4 *folding pattern polytopes* (dt. Faltungsmuster-Polytope) ein, die die Menge der End-Ecken gefalteter Galerien zu einem gegebenen Faltungsmuster beschreiben. Für eine spezielle Teilmenge von Gruppenelementen ermöglichen uns diese Werkzeuge den Entwurf einer kombinatorischen Vorgehensweise zur Bestimmung des vollständigen Coxeter-Schattens in Theorem 4.3.12, während wir für beliebige Gruppenelemente den Begriff der *Coxeter-Umbra* für die auf diese Weise konstruierte Schattenteilmenge vorschlagen (vgl. Theorem 4.4.4).
Part III behandelt Involutionen in Coxeter-Gruppen, d.h. Elemente der Ordnung zwei. In Chapter 5 untersuchen wir die Anzahl cc_2 der Konjugationsklassen von Involutionen, ein gruppentheoretisches Invariant, das zuvor von Deodhar und Richardson [Deo82; Ric82] bestimmt wurde. Unser kombinatorischer Ansatz (vgl. Theorem 5.3.7) basiert auf der Einführung von *higher-rank odd graphs* (dt. ungeraden Graphen von höherem Rang), einer natürlichen Verallgemeinerung der Odd-Graphen, die in der Untersuchung von Konjugationsklassen von Spiegelungen verwendet werden (vgl. [Bra+02]). Dies erlaubt es uns, geschlossene Formeln für cc_2 in allen irreduziblen endlichen (Theorem 5.4.3) und affinen (Theorem 5.4.4) Coxeter-Gruppen anzugeben. Darüber hinaus wenden wir unsere Methode an, um die Anzahl der Konjugationsklassen von Involutionen für Dreiecksgruppen und rechtwinklige Coxeter-Gruppen zu berechnen.
Beide Teile der Dissertation verbindet der Einsatz von Graphen als bevorzugtes kombinatorisches Werkzeug, welches eine gemeinsame Sprache für die betrachteten Objekte bereitstellt.

Contents

Part I

Prequel

CHAPTER 1

Introduction

Coxeter groups are finitely generated groups that admit a presentation of the form

$$\langle s_1, \cdots, s_n |\ s_i^2 = 1,\ (s_i s_j)^{m_{ij}} = 1\ \forall i, j \in [n] \rangle,\ m_{ij} \in \mathbb{N}_{\geq 2} \cup \{\infty\}.$$

Their invention was motivated by the study of symmetry groups of convex polytopes, which are generated by reflections. Harold Scott MacDonald Coxeter translated this property to the abstract presentation, giving a full classification of finite Coxeter groups in 1935 [Cox35] and also classifying all discrete reflection groups in Euclidean space, leading to these groups being named in his honor. Compare also Figures A.1 and A.2.

From this invention, it is obvious that Coxeter groups naturally appear in geometry. However, their influence reaches far beyond: They are closely related to Weyl groups and thus appear in Lie theory as well as in numerous areas of mathematics ranging from algebra to combinatorics and beyond. Much like a chameleon, the study of Coxeter groups often allows both geometric and combinatorial approaches, making them a versatile bridge between disciplines of mathematics.

One generally distinguishes between three main classes of Coxeter groups: The finite groups, generated by reflections across the sides of a polytope, that act cocompactly on some n-sphere; the Euclidean or *affine* Coxeter groups, which are infinite groups that act cocompactly on some n-dimensional Euclidean space, and the rest, of which some act as geometric reflection groups on some hyperbolic space. Finite and Euclidean reflection groups are well understood due to their geometric nature and classification, but every Coxeter group is associated with natural constructions of spaces on which it acts discretely via reflection-like generators. Since Coxeter groups are generated by *involutions*, i.e., group elements of order 2, an important theme is the relation between involutions and reflections: In this setting, a *reflection* is defined as any conjugate of a simple generator s_i. All reflections are involutions, but not all involutions are reflections, raising questions about the discrepancy between those sets.

The rich combinatorial structure and the interplay between combinatorics and geometry motivated the introduction of further geometric and combinatorial objects related to Coxeter groups. In the 1990s, Peter Littelmann introduced *folded galleries*, a combinatorial substructure of the Coxeter complex, to study Kac-Moody algebras [Lit94; Lit95]. Since then, folded galleries in Coxeter groups have found applications in various areas of mathematics, for example to study the affine Grassmannian [GL05] and affine flag varieties [Mil+24], while also revealing an intricate combinatorial structure of their own that is not yet fully understood.

The aim of this thesis is to develop new methods for understanding folded galleries and involutions in Coxeter groups, using graphs as our primary combinatorial tool.

This thesis is organized as follows: Part I collects basic notions on graph theory as well as geometric and combinatoric foundations of Coxeter groups. The Chapters 3 to 5 contain our results, topicwise separated into in two parts. We focus on folded galleries in Part II, studying the combinatorial possibilities of folding galleries in affine Coxeter complexes in Chapter 3, and giving a closed description for the set of alcoves contained in the Coxeter shadow of certain group elements in Chapter 4. We address involutions in Coxeter groups in Part III, where we give a combinatorial approach to the number of conjugacy classes of involutions in all Coxeter groups in Chapter 5. Open questions and further directions of research that appeared throughout the text are gathered in Part IV, and Appendix A contains a reference table of irreducible spherical and affine Coxeter groups.

Part II: Combinatorics of folded galleries for Coxeter shadows

We will call $\gamma = (\mathbf{c}_0, p_1, \mathbf{c}_1, \ldots, p_n, \mathbf{c}_n)$ with alcoves $\mathbf{c}_i$ and panels p_i a *gallery*, and say that γ is *folded at* p_i, if $\mathbf{c}_{i-1} = \mathbf{c}_i$. See Figure 1.1 for an example: The orange gallery γ_2 is folded at its third and ninth panel. As mentioned above, folded galleries were introduced first by Peter Littelmann: They appeared in his *path model* to answer representation theoretic questions on symmetrizable Kac-Moody algebras [Lit94; Lit95]. He used the dimension of galleries to compute weight multiplicities of irreducible highest weight representations and determined the irreducible components of the tensor product of two highest weight representations of semisimple complex Lie algebras. Later, together with Gaussent [GL05], they proved correspondencies between folded galleries and Mirković-Vilonen polytopes. They interpreted folded galleries in the Bruhat-Tits buildings associated with a semisimple algebraic group and connected them to the structure of the corresponding affine Grassmannian. Since then, folded galleries have shown to be a valuable combinatorial tool for studying problems of broadly diversified topics, compare [Ram06; KM04; Sch06b; Ehr10; MST15].

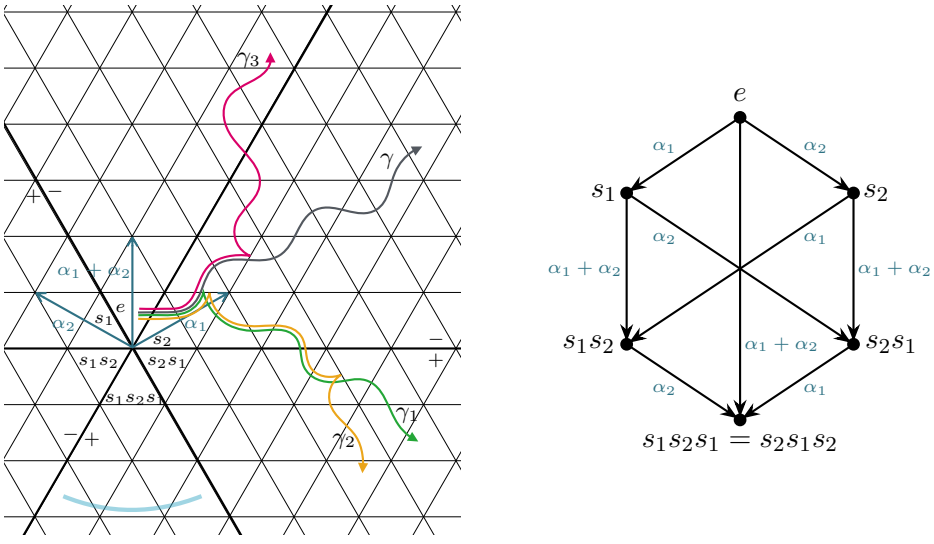

FIGURE 1.1. *On the left:* Coxeter complex of $\tilde{\mathtt{A}}_2$ with folded galleries. *On the right:* Bruhat moment graph of $\mathtt{A}_2$.

It then was a natural question to ask for the set of (end alcoves of) galleries that can be obtained from a given (minimal) gallery γ by folding it. This was approached by Graeber and Schwer in [GS20], starting to study folded galleries as combinatorial objects on their own, without pursuing a case of application, and introducing the notion of a *Coxeter shadow* for this set. Figure 1.2 illustrates an example of such a Coxeter shadow, demonstrating its remarkable regularity and partial symmetries, which motivate the search for a closed description.

The notion of shadows is closely related to the study of buildings. Milićević, Naqvi, Schwer, and Thomas showed in [Mil+24] that the shadow of an element $x \in W$ for an affine Coxeter system (W, S) with respect to a certain orientation is the image of a retraction based at infinity of the pre-image of another retraction in a thick affine building. In a different context, this observation already appeared in [Hit10]. As folded galleries, Coxeter shadows appear and have applications in various contexts, for example in the study of affine Grassmannians [GL05] and affine Deligne-Lusztig varieties [MST15; MST22]. An accessible and enyojable survey of these appearances is given by Schwer in [Sch22].

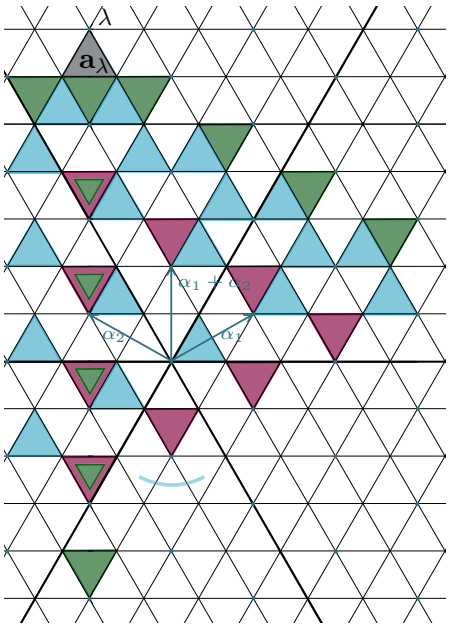

FIGURE 1.2. Shadow of a_λ with respect to ϕ_{w_0}. The orientation defining Weyl chamber is indicated by the light blue arc. The alcoves obtained by folding a minimal gallery for $\mathbf{a}_\lambda$ once are shown in green, by folding twice in blue, and folding three times in purple (cf. Figure 4.7).

So far, Coxeter shadows can be computed recursively [GS20; Mil+24], but they lack a closed description. This leads to the central research problem of this part of the thesis:

Give an explicit description of the alcoves contained in the Coxeter shadow $\mathrm{Sh}(x)$ *of a group element* x*.*

We address this question for a specific subset of group elements x with respect to a certain class of orientations of affine Coxeter complexes. For this, we will analyse the combinatoric possibilities to fold minimal galleries for x in Chapter 3, and then use these results to give a geometric construction of subsets of the Coxeter shadow which, in exceptional cases, cover it entirely in Chapter 4.

Chapter 3: Folding patterns for Coxeter shadows

To give an explicit description of Coxeter shadows, it is essential to understand the combinatorial options of folding minimal galleries without having to inspect every single panel that the gallery crosses. This arises the following question:

Given a minimal gallery γ for x, at which panels can γ be folded at positively only using the information given by the corresponding word and group element x?

We answer this question for a certain type of orientation of the Coxeter complex, called *Weyl chamber orientation*, using the Bruhat moment graph of the associated spherical Weyl group W_0. To the authors knowledge, moment graphs were first introduced by Goresky, Kottwitz and MacPherson [GKM97] to study the topology of a complex equivariantly formal variety, and later used by Peter Fiebig to interpret Lusztig's and Kazhdan-Lusztig's conjecture as problems on moment graphs [Fie07; Fie10]; compare also the survey [Fie16].
To obtain our main result, we use moment graphs associated with root systems of finite Coxeter groups, so called Bruhat graphs. As described in [BB06], Bruhat graphs also illustrate a poset structure on the elements of the Coxeter group, defined by the reflections of the group. For a gallery, we call the sequence of roots perpendicular to the hyperplanes containing the panels that the gallery is folded in the *folding pattern*. For example, the orange gallery γ_2 in Figure 1.1 has the folding pattern $(\alpha_1+\alpha_2, \alpha_1)$. Using this and the relation of spherical and affine Coxeter groups, we obtain the following result (compare Theorem 3.3.9):

Theorem. *Fix an affine Coxeter system (W, S) with associated spherical group W_0. Let the affine Coxeter complex be equipped with a Weyl chamber orientation ϕ_w, $w \in W_0$ and let γ be a minimal gallery starting in $\mathbf{c_f}$. Then the directed paths in the Bruhat moment graph of W_0 determine the possible ϕ_w-positive sequences of folding hyperplanes of γ.*

This result provides a complete description of the folding options of galleries with respect to Weyl chamber orientations. A crucial ingredient of the theorem is the periodicity of the orientation, which allows for a description of the folding options on the level of parallelism classes of hyperplanes instead of considering individual hyperplanes.

An example is shown in Figure 1.1: The green and orange galleries γ_1, γ_2 can be obtained from the unfolded minimal gallery γ by folding positively with respect to the Weyl chamber orientation defined by $s_1s_2s_1$, marked in blue. The galleries are folded in hyperplanes perpendicular to the roots $\alpha_1 + \alpha_2$, and $\alpha_1 + \alpha_2, \alpha_1$, respectively. This coincides with the labels of a directed path in the Bruhat moment graph, depicted on the right of Figure 1.1, starting in the node labeled s_2, which is the Weyl chamber γ ends in. One can see as well that γ_3 is not positively folded with respect to this orientation, since it is folded in a hyperplane perpendicular to the root α_2, and there is no directed edge leaving the node s_2 in the graph.

A further natural question concerns the inclusion of Coxeter shadows:

Given a group element x, is this element contained in the Coxeter shadow of another element y? That is, can a minimal gallery ending in $\mathbf{y}$ be positively folded with respect to a given orientation, such that the folded gallery ends in $\mathbf{x}$?

Regarding this question, we observe that folding obviously affects the spherical direction of the end alcove of a gallery. In Theorem 3.3.18, we draw a connection between the Bruhat moment graph of the associated spherical Coxeter group and the spherical direction of end alcoves of galleries, allowing us to deny such inclusions in certain cases.

It remains an open problem to generalize these results to other orientations.

This chapter is organized as follows: We introduce combinatorial galleries and provide some technical results in Section 3.1. Section 3.2 defines foldings of galleries, explains Coxeter shadows, and discusses some of their properties. Our main results of this chapter are presented and proven in Section 3.3.

Chapter 4: Umbrae of Coxeter shadows

We build upon the results of the previous chapter to construct alcoves of the Coxeter shadow, thereby answering our initial question to give an explicit description of the Coxeter shadow in the case of Weyl chamber orientations. From our earlier results, it follows that every alcove in the shadow can be obtained by applying a permissible folding pattern to a minimal gallery. To analyse this systematically, we begin by fixing a folding pattern and studying the set of alcoves obtained from it. More precisely, we ask:

Given a group element $x = t^\lambda w$ in an affine Coxeter group and a folding pattern $(\alpha_{j,i})_{i\in[n]}$ that can be fully applied to x. Which group elements y arise as end alcoves of folded galleries obtained from folding minimal galleries $\gamma : \mathbf{c_f} \rightsquigarrow \mathbf{x}$ with this pattern?

Taking the union over all folding patterns yields the Coxeter shadow.

We will not solve this problem in full generality for arbitrary x, but provide a construction of a subset of this set of alcoves. In the special case when $x = t^\lambda w$ with λ being regular and w a particular spherical direction, such that the alcove is the *gate* of λ, i.e, the alcove at λ that is closest to the origin of the Coxeter complex (cf. Definition 4.1.1), we obtain a complete description of the shadow. Gates are especially convenient because their galleries cross exactly the same hyperplanes as any minimal vertex-to-vertex gallery ending at λ. This property is essential since a part of our framework is formulated in terms of vertex-galleries.

Our construction relies on generalized root operators. Originally introduced by Gaussent and Littelmann [GL05] for positive simple roots to prove a dimension formula for positively folded galleries, they can be used to manipulate vertex-to-vertex galleries in a controlled way by adding or deleting folds and changing the position of folds. Building on the work of Milićević, Schwer, and Thomas [MST15], who used root operators to construct families of ϕ-positively folded galleries and thereby, in our language, identified certain alcoves in the Coxeter shadow, we adapt these tools to keep track of the folding pattern of the gallery and exhaust all options of applying a pattern to given minimal galleries.

Motivated further by the results of Schwer [Hit10], who proved that the vertices of alcoves in the Coxeter shadow lie in a polytope defined by the Weyl orbit of λ, we show that the end vertices of all folded galleries with fixed folding pattern obtained by this procedure are contained in a lattice polytope, which we introduce as the *folding pattern polytope*. The picture on the left of Figure 1.3 illustrates the folding pattern polytopes for the coroot λ for all applicable folding patterns.

By combining the vertices of the folding pattern polytope with the spherical directions of the corresponding end alcoves, obtained from the Bruhat graph in Chapter 3, we obtain a full description of the Coxeter shadow of gates (cf. Theorem 4.3.12):

Theorem (Coxeter shadow of gates)**.** *Let (W, S) be an affine Coxeter system with (W_0, S_0) the associated spherical system. Let the Coxeter complex $\Sigma = \Sigma(W, S)$ be equipped with a Weyl chamber orientation ϕ_w. Let further $x = t^\lambda u$ be the gate of λ and $\lambda \in T$ regular. Then $y = t^\mu v \in \mathrm{Sh}_{\phi_w}(x)$ if and only if μ is contained in the folding pattern polytope of x for an applicable folding pattern and v is the end node of the path labeled by the pattern starting in the node u in the undirected moment graph $\mathcal{G}^{un}_{W_0}$.*

Since the gate at λ is the alcove closest to the origin of the Coxeter complex, every minimal gallery to another alcove at λ also crosses the hyperplanes a gate gallery crosses, ensuring that the same foldings are permissible. The spherical direction of the end alcoves at the coroot lattice endpoints of the so folded galleries differ, but, as above, can be obtained by our results from Chapter 3. Since this construction of alcoves is the same procedure for all alcoves at a vertex λ, forming some kind of *core of the shadow*, we introduce the notion of the *Coxeter umbra* for this set of alcoves. Nevertheless, since the gallery may cross further hyperplanes, the umbra may not always yield the entire shadow. However, we will see examples of equality beyond gate shadows (cf. Figure 4.10), leading to Theorem 4.4.4 below.

Theorem (Umbrae and shadows)**.** *Let $\Sigma = (W, S)$ be an affine Coxeter complex with periodic orientation ϕ and let $x = t^\lambda w \in W$ with λ a regular coroot lattice point. Then*

$$\mathrm{Um}_\phi(x) \subseteq \mathrm{Sh}_\phi(x).$$

Furthermore, if $\mathbf{x} = \mathbf{a}_\lambda$, then $\mathrm{Um}_\phi(x) = \mathrm{Sh}_\phi(x)$.

The picture on the right of Figure 1.3 illustrates the alcoves contained in $\mathrm{Um}_\phi(x)$ highlighted in the set of grey alcoves of the shadow $\mathrm{Sh}_\phi(x)$.

In summary, for group elements in gate position, these results provide a closed description of the Coxeter shadow, fully answering our initial question in this case. The description of the difference between Coxeter shadows and umbrae, as well as generalizations to other orientations, remain open problems.

This chapter is organized as follows: We introduce gates of coroot lattice points, compute them for regular coroot lattice points, and examine some properties of their corresponding gate galleries in Section 4.1. Section 4.2 recalls root operators and their key properties. In Section 4.3, after introducing folding pattern polytopes, we present and prove our main result Theorem 4.3.12 of this chapter. In the last Section 4.4, we use this result

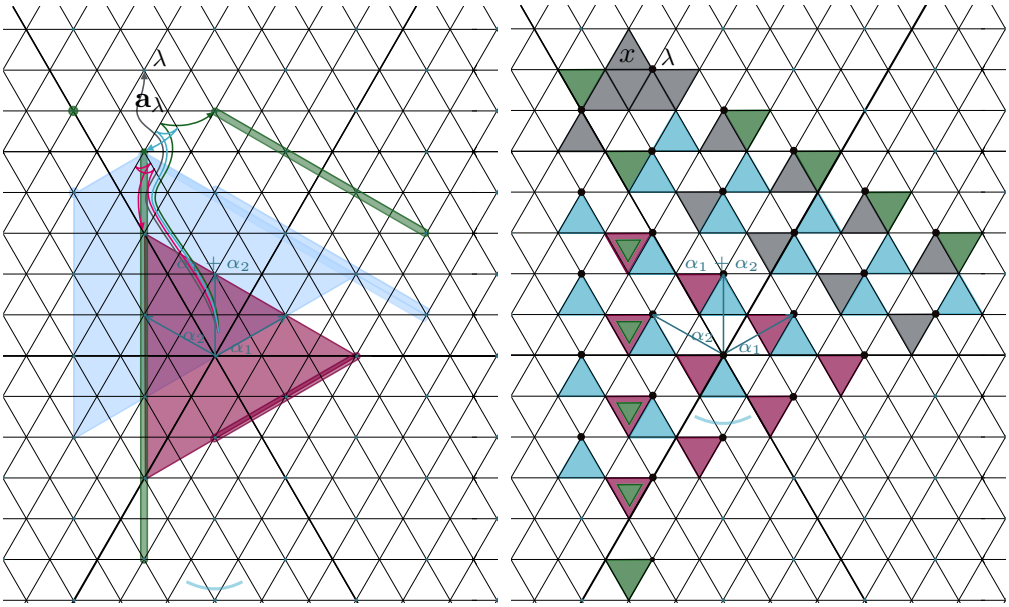

FIGURE 1.3. *On the left:* Folding pattern polytopes of $\mathbf{a}_\lambda$ for all applicable folding patterns of length 1 in green, length 2 in blue, and length 3 in purple (cf. Figures 4.4 to 4.6). Examples of folded galleries obtained from the minimal grey gallery are shown in the corresponding colours. *On the right:* Coxeter shadow of x with highlighted alcove sets $\mathcal{Y}_x$ of the Coxeter umbra. The green alcoves are obtained from folding pattern polytopes with folding patterns of length 1, the blue alcoves from patterns of length 2, and the brown alcoves from pattern with length 3, respectively. The non-highlighted alcoves are not contained in the Coxeter umbra.

to give an explicit description of the Coxeter umbra that, in some cases, *is* the Coxeter shadow, partly answering our intial question of this part of the thesis.

Part III: Involutions in Coxeter groups

Recall that an *involution* in a group W is a nontrivial element of order two. Recalling the presentation of Coxeter groups, we see that every Coxeter group is generated by a set S of involutions corresponding to (abstract) reflections under Tits' geometric representation. The set of all reflections is precisely the set of W-conjugates of the standard generators in S, which lead to the conjugacy classes of involutions being a natural and extensively studied object. Although every reflection is involutory, the converse does not hold in general: Not every involution is also a reflection. While the set of reflections depends on the choice of S, the set of involutions does not. This led to the following questions:

What can one say about the potential discrepancy between reflections and involutions in a given Coxeter group? When are these two sets equal? Is there a combinatorial characterization of conjugacy classes of involutions in terms of the Coxeter diagram of a given system?

Chapter 5: Conjugacy classes of of involutions in Coxeter groups

The study of the classification of conjugacy classes of involutions has a long history. Building on work of Frobenius [Fro00], Schur [Sch08], Young [You30a; You30b], and Specht [Spe37], conjugacy classes of involutions in (finite) Weyl groups were completely classified by Carter in terms of graphs in his 1972 paper [Car72]. Springer [Spr82], and also Deodhar [Deo82] and Richardson [Ric82] made substantial contributions in the early 1980s, showing in particular that conjugacy classes of involutions of W are determined by central involutions of certain spherical parabolic subgroups. By work of Moussong [Mou88], who proved that all Coxeter groups are CAT(0), Coxeter groups have solvable conjugacy problem as all CAT(0) groups do [BH99, Theorem III.Γ.1.12]. Later, Krammer [Kra09] provided a polynomial time algorithm for the solution of the conjugacy problem in all finite rank Coxeter groups. This led to the question whether there exist minimal length representatives of every conjugacy class.

Precise descriptions of conjugacy classes in all finite Coxeter groups and characterizations of their minimal length elements were given by Geck and Pfeiffer (see [GP93] and [GP00, Chapter 3]). The question on representatives already appeared in Cohen's book [Coh94] and was independently studied for twisted Coxeter groups by Geck, Kim, and Pfeiffer [GKP00], for all affine Coxeter groups by He and Nie [HN12], and for arbitrary Coxeter groups by Marquis [Mar21] (building up on the work of Geck and Pfeiffer in [GP93]). More recently, Milićević, Schwer and Thomas gave a closed, geometric description for all conjugacy classes in affine Coxeter groups [MST24] and, more generally, for arbitrary split subgroups of the full isometry group of Euclidean space [MST25].

For a Coxeter system (W_Γ, S) with Coxeter diagram Γ, denote by $\mathrm{cc}_2(W_\Gamma)$ the total number of conjugacy classes of involutions in W_Γ. In the works mentioned above, Deodhar and Richardson showed that $\mathrm{cc}_2(W_\Gamma) \leq 2^{|S|} - 1$ (by [Ric82, Theorem A]) and is thus finite, and that there is a procedure to determine this number by an algebraically determined subcollection of spherical parabolics in W_Γ (cf. [Deo82, Section 5]).

It turns out that one can combinatorially characterize the number of conjugacy classes of reflections as the number of connected components of the *odd graph* Γ_{odd}, obtained from the Coxeter diagram Γ by removing all edges with even or ∞ labels. See for example Lemma 3.6 in [Bra+02].

Recalling the last question mentioned above, this motivated the idea of generalizing the concept of odd graphs to determine the number of conjugacy classes of involutions (not just reflections) by counting connected components of higher rank odd graphs Γ^k, $1 \leq k \leq |V(\Gamma)|$. These graphs are derived directly from the Coxeter diagram Γ by identifying subgraphs corresponding to subgroups of *inc-type*, short for 'irreducible with nontrivial center', and studying their relations inside the diagram. The first graph Γ^1 coincides with the aforementioned odd graph. For the precise definitions see Section 5.2. In doing so, we give an alternative — in our view, more combinatorial — version of the Deodhar–Richardson method that could be easier to implement and that quickly outputs $\mathrm{cc}_2(W_\Gamma)$. We will prove our main result as Theorem 5.3.7 below:

Theorem (Counting conjugacy classes of involutions)**.** *Let Γ be a Coxeter diagram and, for each $k \geq 1$, write Γ^k for its corresponding k-odd graph (cf. Definition 5.2.9). Then,*

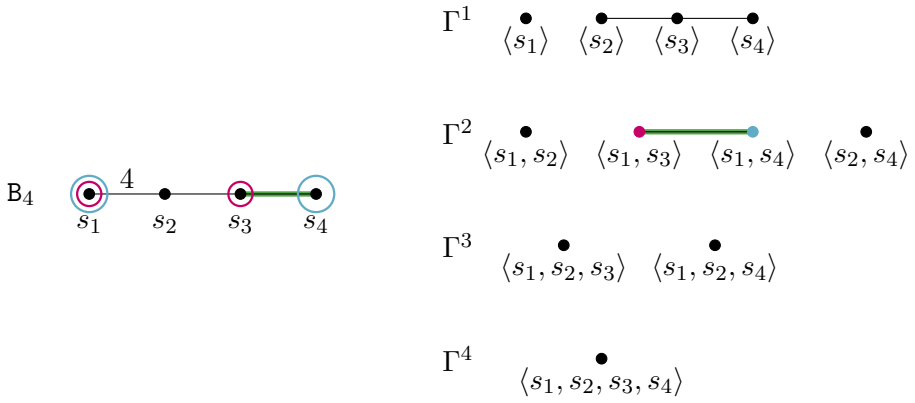

FIGURE 1.4. *On the left:* Coxeter diagram of $\mathtt{B}_4$. The pink and blue circles mark subdiagrams of type $\mathtt{A}_2$ which are odd-adjacent via the green edge. *On the right:* k-odd-graphs of $\mathtt{B}_4$. The two highlighted nodes of Γ^2 that correspond to the two subdiagrams spanned by the nodes of $\Gamma_{\mathtt{B}_4}$ labeled s_1 and s_3, and s_1 and s_4 are connected by the green edge. The other nodes of Γ^2 and Γ^3 are either of different types, or not odd-adjacent, and therefore isolated.

the cardinality of the set of connected components of Γ^k is equal to the cardinality of the set of conjugacy classes of involutions of rank k in the corresponding Coxeter group W_Γ. The total number $\mathrm{cc}_2(W_\Gamma)$ of conjugacy classes is obtained as

$$\mathrm{cc}_2(W_\Gamma) = \sum_{k=1}^{|V(\Gamma)|} |\pi_0(\Gamma^k)|.$$

An illustrative example of our method is given in Figure 1.4, where the four k-odd-graphs of the Coxeter group of type $\mathtt{B}_4$ are displayed.

The key ingredient to the proof of this result is the following theorem (Theorem 5.3.6), which provides an explicit criterion using odd-adjacency relations (cf. Section 5.2) for spherical standard parabolic subgroups with nontrivial centers to be conjugate.

Theorem (Conjugating parabolics with nontrivial centers)**.** *Let $\Gamma = (S, E)$ be a Coxeter diagram with $S = \{s_i | \ i \in I\}$ and write $W = W_\Gamma$ for the associated Coxeter group. For $J, K \subseteq I$, $J \neq K$ let W_J and W_K be the corresponding standard parabolic subgroups, and assume they are spherical with longest elements being central elements. Then the subgroup W_J is conjugate to W_K if and only if both following conditions hold:*

(1) There exist $\ell \in \mathbb{N}$ and $L, M, X \subseteq I$ such that $W_J = W_L \times W_X$ and $W_K = W_M \times W_X$ with $W_L \cong W_M \cong (\mathbb{Z}/2\mathbb{Z})^\ell$, and

(2) there exists a finite sequence of standard parabolic subgroups $W_1, \ldots, W_m$ such that $W_1 = W_J$, $W_m = W_K$, and W_i is odd-adjacent to W_{i+1} for $i = 1, \ldots, m-1$.

We view this theorem as a combinatorial form of Richardson's concept of W-equivalence, which is useful for dealing with concrete examples. A crucial ingredient of its proof is

Krammer's combinatorial version of results due to Deodhar, which we have restated as Theorem 5.3.1; see Krammer [Kra09, Section 3] and Deodhar [Deo82, Proposition 5.5] for the original statements. In the finite case this was shown earlier by Howlett [How80]. In our formulation, the Deodhar–Richardson procedure to fully determine conjugacy classes of involutions is obtained as follows (cf. Corollary 5.3.8).

Corollary (Representing conjugacy classes of involutions)**.** *With notation as above, the connected components of Γ^k are in bijection with the conjugacy classes of involutions of rank k. To obtain a representative for such a conjugacy class, one may choose any vertex in the corresponding connected component in Γ^k and take as representative the longest element in the parabolic subgroup corresponding to it.*

We use our methods to explicitly compute cc_2 in several cases in Section 5.4. Most prominently, we derive formulae for $\mathrm{cc}_2(W_\Gamma)$ for all irreducible spherical and affine Coxeter groups, besides explicitly computing $\mathrm{cc}_2(W_\Gamma)$ for all triangle groups. We also give an alternative, geometric way to compute cc_2 for right-angled Coxeter groups (RACGs).

Looking forward, it remains subject to further research whether the concept of k-odd graphs can be extended to study the number of conjugacy classes of torsion elements of order $m \neq 2$.

This chapter is organized as follows: We establish the notion of Coxeter groups of *inc-type* in Section 5.1 and collect helpful facts on them that allow us to transfer the problem of determining the number of conjugacy classes of involutions to the problem of counting the conjugacy classes of standard parabolic subgroups with irreducible components of inc-type. In Section 5.2, we introduce higher rank odd graphs and develop tools for their computation. After discussing some technical prerequisites, we present and prove our main results of this chapter in Section 5.3. We provide examples in Section 5.4, where we explicitly compute cc_2 for several subclasses of Coxeter groups, including the presentation of our closed formulae for cc_2 in irreducible spherical and affine Coxeter groups. The proofs of these formulae are found in Sections 5.5 and 5.6.

CHAPTER 2

Preliminaries

In this chapter, we will collect basic concepts and fix our notation for the rest of this thesis. As graphs will be our combinatorial tool of choice to study Coxeter groups, we will give a very compact collection of notions required for our formulations in Section 2.1. The more comprehensive Section 2.2 will give a brief introduction to Coxeter groups and their geometry.

2.1. Basic concepts of graph theory

Throughout this text, graphs will appear in various contexts to describe or visualize combinatorial properties of objects we are interested in. The goal of this section is to introduce the notation we will use for graphs below, following the textbook of Diestel [Die05].

Definition 2.1.1 (Graphs)**.** A *graph* (or *diagram*) is a tuple of sets $\mathcal{G} = (V, E)$ with $E \subseteq V^2$. The elements of V are called *nodes* or *vertices* of the graph, the elements of E are called *edges*. If the edges $e \in E$ are unordered tuples $e = \{v, w\}$ with $v, w \in V$, we call the graph *undirected*. If the edges are vectors $e = (v, w)$ with *initial node* v and *terminal node* w, we call the graph *directed*. The edges then are referred to as *directed edges* or *arcs*. A graph is *finite*, if V is finite; otherwise it is called infinite. If every edge of a graph $\mathcal{G}$ connects distinct vertices and no two edges share more than one vertex, we say that $\mathcal{G}$ is *simple*.
Further, we can assign a *vertex labeling* or *edge labeling* to a given graph $\mathcal{G}$, which is a map $L_V : V(\mathcal{G}) \to L$, resp. $L_E : V(\mathcal{G}) \to L$ that assigns an element of the *label set* L to every vertex or edge.

Unless explicitly stated otherwise, by a 'graph' we will mean an undirected simple graph. There is a natural way to associate an undirected graph with a directed one by converting all directed edges to undirected edges. Compare Example 2.1.6.
We will denote most of the graphs by a calligraphic letter $\mathcal{G}$, while using the Greek uppercase letters Γ, Λ for Coxeter diagrams and presentation diagrams. These two special graphs will be introduced in Definition 2.2.3 and Definition 2.2.10. To visualize graphs, we will represent the vertices as dots, connecting them with arrows when they form a directed edge, and using lines for undirected edges. For an example, refer to Figure 2.1.

Definition 2.1.2 (Degree of vertices)**.** Let $\mathcal{G} = (V, E)$ be a graph and $v, w \in V$. We call w a *neighbour* of v if $\{v, w\} \in E$ and denote the set of neighbours of v by $\mathrm{Lk}(v)$. We call $|\mathrm{Lk}(v)|$ the *degree of the vertex* v and denote it by $\deg(v)$.

Certain subsets of graphs can also be considered graphs themselves:

Definition 2.1.3 (Subgraph)**.** Let $\mathcal{G} = (V, E)$ be a graph. The *full* (or *induced*) *subgraph* spanned by a subset $X \subseteq V(\mathcal{G})$ is the subgraph $\mathcal{G}_X$ of $\mathcal{G}$ whose vertex set is X and which contains all those edges in $E(\mathcal{G})$ whose incident vertices are in X.

Some subgraphs have special properties that are of great interest to us. For easier reference, we assign names to them:

Definition 2.1.4 (Paths, circles and trees)**.** Let $\mathcal{G} = (V, E)$ be a graph and let $\mathcal{G}_X$ be the subgraph induced by $X \subseteq V$. Then $\mathcal{G}_X$ is a

- *path in* $\mathcal{G}$, if $X = \{v_1, \cdots, v_k\}$ and $E(\mathcal{G}_X) = \{\{v_1, v_2\}, \{v_2, v_3\}, \cdots, \{v_{k-1}, v_k\}\}$. If $\mathcal{G}$ is a directed graph and the terminal vertex of every contained edge coincides with the initial vertex of the following edge, we call the path *directed*. Furthermore, we say that two vertices can be connected by a path in $\mathcal{G}$, when they are contained in the vertex set of a path in $\mathcal{G}$.
- *circle in* $\mathcal{G}$, if $\mathcal{G}_X$ is a path in $\mathcal{G}$ with vertex set $X = \{v_1, \cdots, v_k\}$ and $E(\mathcal{G}_X) = \{\{v_1, v_2\}, \{v_2, v_3\}, \cdots, \{v_k, v_1\}\}$.
- *forest*, if it does not contain a circle, and *tree*, if furthermore every two vertices of $\mathcal{G}_X$ can be connected by a path.

Notice that all these defintions can be applied to $\mathcal{G}_X = \mathcal{G}$. In this case, we call $\mathcal{G}$ a *path graph*, *circle graph*, or simply a *forest* or *tree*.

With this in mind, we can introduce:

Definition 2.1.5 (Connectivity)**.** Let $\mathcal{G} = (V, E)$ be a graph. A vertex $v \in V$ is called *isolated* if it is not joined by an edge to any other vertices, i.e., if $\deg(v) = 0$. A graph all of whose vertices are isolated is called *discrete*. A *connected component* of $\mathcal{G}$ is a maximal nonempty full subgraph all of whose vertices can be connected by a path. We denote by $\pi_0(\mathcal{G})$ the *set of connected components* of the graph $\mathcal{G}$, and $\mathcal{G}$ is *connected* when $\mathcal{G} \neq \emptyset$ and $|\pi_0(\mathcal{G})| = 1$.

Example 2.1.6. Figure 2.1 shows an example of a directed graph $\mathcal{G}_d$ on 8 vertices, along with its corresponding undirected graph $\mathcal{G}$. Notably, the vertices v_2, v_4, v_5, v_6 in $\mathcal{G}$ all have a degree of 2, while the vertices labeled v_1, v_7, v_8 have a degree of 1, and $\deg(v_3) = 3$. The subgraph spanned by $X = \{v_1, v_2, v_3\}$ forms a directed path in $\mathcal{G}_d$. Observe further that both graphs contain no circles, and that $\mathcal{G}$ is a tree.

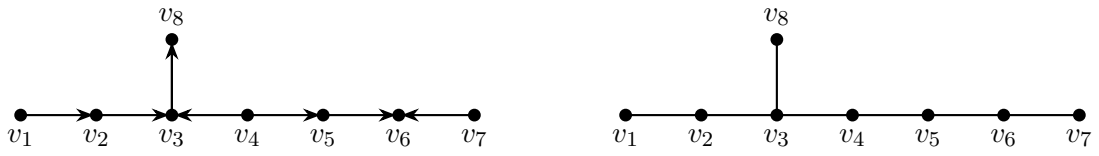

FIGURE 2.1. *On the left:* A directed graph $\mathcal{G}_d$ *On the right:* the corresponding undirected graph $\mathcal{G}$.

The following two constructions of subgraphs of undirected graphs will be important in Part III:

Definition 2.1.7 (Graph neighbourhoods)**.** Let $\mathcal{G} = (V, E)$ be an undirected graph. We define the *neighbourhood* $N_{\mathcal{G}}(X)$ of a subset of vertices $X \subseteq V$ in $\mathcal{G}$ as the subgraph of $\mathcal{G}$ induced by the vertex set

$$\{v_i \in V \setminus X \mid \text{ there exists } v_k \in X \text{ such that } \{v_i, v_k\} \in E\}.$$

In particular, for $X = \{v_i, v_j\}$, the neighbourhood $N_{\mathcal{G}}(X)$ is the full subgraph of $\mathcal{G}$ with vertex set $(\mathrm{Lk}(v_i) \cup \mathrm{Lk}(v_j)) \setminus \{v_i, v_j\}$ and $\mathcal{G} \setminus N_{\mathcal{G}}(X)$ is the full subgraph on the vertices $V \setminus \{\mathrm{Lk}(v_i) \cup \mathrm{Lk}(v_j)\} \cup \{v_i, v_j\}$.

Definition 2.1.8 (Cocliques)**.** Let $\mathcal{G} = (V, E)$ be an undirected graph. A vertex set $X \subseteq V$ is called a *coclique* of $\mathcal{G}$ if the full subgraph $\mathcal{G}_X$ spanned by X is discrete. The *size* of a coclique is the cardinality of its vertex set.

Cocliques are also known as *independent sets* and sometimes referred to as *(internally) stable sets*; cf. [Ber01; GR01].

Example 2.1.9. Consider the graph $\mathcal{G}$ from Example 2.1.6 once again. It holds that $N_{\mathcal{G}}(v_3, v_4) = \{v_2, v_5, v_8\}$. Figure 2.2 illustrates the graph $\mathcal{G} \setminus N_{\mathcal{G}}(v_3, v_4)$. Observe that this graph has 3 connected components and that the two subgraphs spanned by the vertex sets $\{v_3, v_4\}$ and $\{v_6, v_7\}$ are both path graphs. Furthermore, the vertex set $X = \{v_1, v_3, v_6\}$ is a coclique in $\mathcal{G} \setminus N_{\mathcal{G}}(v_3, v_4)$ as well as in $\mathcal{G}$.

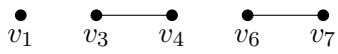

FIGURE 2.2. The graph $\mathcal{G} \setminus N_{\mathcal{G}}(v_3, v_4)$.

2.2. An introduction to Coxeter groups and their geometry

In this section, we will review the basic definitions and properties of Coxeter groups and establish the notation we will use throughout the text. Section 2.2.1 introduces Coxeter systems and complexes. Following that, we will discuss root systems in Section 2.2.2 and provide a bief introduction to Bruhat order on Coxeter groups in Section 2.2.3. The last two subsections focus on affine Coxeter groups. First, in Section 2.2.4, we collect essential concepts and observations regarding the geometry of affine Coxeter complexes. Then, we study orientations of Coxeter complexes in Section 2.2.5. For more background on Coxeter groups and their geometry, the reader may refer to one of the many good textbooks on the topic; the author especially recommends [Dav08], [AB08], [Hum90], and [BB06].

2.2.1. Coxeter systems and complexes. Coxeter groups are abstract reflection groups that generalize the symmetry groups of regular polyhedra. They are named after Harold S. M. Coxeter, who gave a classification of all finite groups that allow a certain presentation [Cox35]:

Definition 2.2.1 (Coxeter group, Coxeter system and reflections)**.** A group W is a *Coxeter group* if it is isomorphic to a finitely presented group of the form

$$\langle S \mid (s_i s_j)^{m_{i,j}} \ \forall i, j \in I \rangle,$$

where $S = \{s_i \mid i \in I\}$ for a finite index set I and $m_{i,i} = 1$ for all $i \in I$ and $m_{i,j} = m_{j,i} \in \mathbb{N}_{\geq 2} \cup \{\infty\}$ for all $i \neq j$. A sequence of generators $w = s_{i_1} s_{i_2} \cdots s_{i_m}$ with $i_j \in I$ is called a *word in* S with length $l(w) = m$ and represents, not necessarily uniquely, a group element that we usually denote by a letter x, y, or z. A pair (W, S) is called a *Coxeter system* of *rank* $n = |I| = |S|$. The elements of $R = \cup_{w \in W} wSw^{-1}$ are the *reflections* in W with respect to S.

Since all the information needed for the presentation is contained within the exponents $m_{i,j}$ of the products of generators, we can use the *Coxeter matrix* to store this information in a more compact form:

Definition 2.2.2 (Coxeter matrix)**.** Let (W, S) be a Coxeter system with $S = \{s_i \mid i \in I\}$ for a finite index set I. The matrix $M = M(W, S) \in (\mathbb{N} \cup \{\infty\})^{|S| \times |S|}$ with $M_{i,j} = m_{i,j}$ $\forall i, j \in I$ is called *Coxeter matrix* of (W, S).

By writing down symmetric matrices with diagonal entries equal to 1 and other entries in $\mathbb{N}_{\geq 2} \cup \{\infty\}$, we can construct numerous examples of Coxeter groups. As usual, we use *Coxeter diagrams*, also called *Coxeter-Dynkin diagrams*, to encode Coxeter systems:

Definition 2.2.3 (Coxeter diagram)**.** Let (W, S) be a Coxeter system. The undirected labeled graph $\Gamma = (V, E)$ with vertex set $V = S$ and edges $e = (s_i, s_j) \in E \Leftrightarrow m_{i,j} \geq 3$ with labels $m_{i,j}$ is called *Coxeter diagram*. The Coxeter matrix serves as the adjacency matrix for Γ, while edges labeled 2 are omitted. Usually, also edges labeled 3 are left unlabeled. We will sometimes use the terminology *odd-labeled* (or simply *odd*) when referring to edges of a Coxeter diagram which are unlabeled or labeled by an odd number. We call Γ (or W_Γ) *odd* or *even*, respectively, if all edges are odd-labeled, or even or ∞ labeled. Given a Coxeter diagram Γ, the associated Coxeter group is denoted by W_Γ.

Example 2.2.4. An example of a Coxeter group is the symmetric group S_3, which permutes the elements of a 3-element set. In the left picture of Figure 2.3, we observe that S_3 encodes the symmetries of a regular triangle as a reflection group: It permutes the vertices of the triangle through reflections along the dashed lines and by rotating the triangle. The group is generated by the two reflections s_1 and s_2, which correspond to the reflections along the diagonal dashed lines. When such a reflection is applied twice, we return to the original triangle. Combining both reflections results in a rotation of the triangle by $\frac{2\pi}{3}$; performing this rotation 3 times returns us to our original triangle. Thus, we can derive a presentation for S_3 that aligns with the structure of Coxeter groups:

$$S_3 = \langle s_1, s_2 |\ s_1^2 = s_2^2 = (s_1 s_2)^3 = 1 \rangle$$

with corresponding Coxeter matrix

$$M(S_3) = \begin{pmatrix} 1 & 3 \\ 3 & 1 \end{pmatrix}.$$

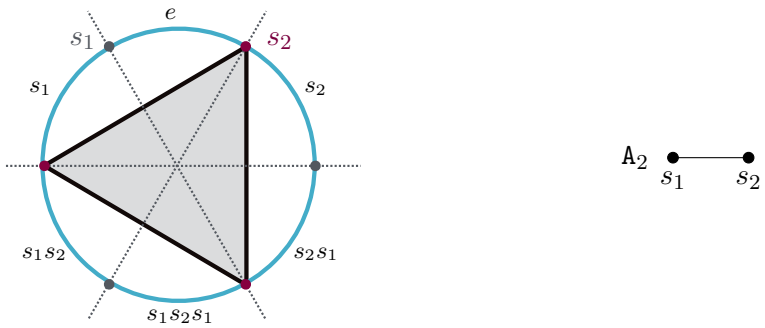

FIGURE 2.3. *On the left:* Coxeter complex of S_3. *On the right:* Coxeter diagram of type $\mathtt{A}_2$.

The Coxeter diagram of S_3 is shown in the right picture of Figure 2.3. Note that every symmetric group S_{n+1} is a Coxeter group. To see this, identify the transpositions $(1\ 2), \cdots, (n\ n{+}1)$ of the symmetric group with the generators $s_1, \cdots, s_n$. Then observe that all transpositions are involutions, two non-consecutive transpositions commute, and two consecutive transpositions form a cycle of length 3. This family of Coxeter groups is referred to as the *Coxeter groups of type* $\mathtt{A}_n$. Their diagrams are displayed in Figure A.1.

The union of Coxeter diagrams again gives a Coxeter diagram:

Definition 2.2.5 (Irreducible Coxeter groups)**.** We say that a Coxeter diagram Γ or the associated group W_Γ is *reducible* (or otherwise *irreducible*) if the graph Γ is a disjoint union of at least two nonempty full subgraphs Γ_1 and Γ_2. This is equivalent to stating that W_Γ decomposes as a direct product $W_{\Gamma_1} \times W_{\Gamma_2}$.

Some subgroups of Coxeter groups are Coxeter groups as well:

Definition 2.2.6 (Parabolic subgroups and closure)**.** Let (W, S) be a Coxeter system. A *standard parabolic subgroup* of W is a group of the form $W_J := \langle S_J \rangle$, where $J \subseteq I$ and $S_J := \{s_j \in S |\ j \in J\}$. The pair (W_J, S_J) then is again a Coxeter system whose Coxeter diagram is the full subgraph $\Gamma_J := \Gamma_{S_J}$ on S_J in Γ. A *parabolic subgroup* of W is any conjugate of a standard parabolic. The trivial group and W itself are considered parabolic subgroups, corresponding to the subsets $\emptyset$ and I of I, respectively. The *parabolic closure* $\mathrm{Pc}(X)$ of a subset $X \subset W$ is the smallest (with respect to set-theoretic containment) parabolic subgroup of W containing X.

Coxeter groups can be classified into three categories: The first category is the category of finite Coxeter groups. It includes products of the three infinite families $\mathtt{A}_n$ for $n \geq 1$, $\mathtt{B}_n$ for $n \geq 2$ and $\mathtt{D}_n$ for $n \geq 4$ of increasing dimension n, one infinite family $\mathtt{I}_2(m)$ for $m \geq 7$ in dimension 2, and eight exceptional types $\mathtt{E}_6, \mathtt{E}_7, \mathtt{E}_8, \mathtt{F}_4, \mathtt{G}_2, \mathtt{H}_2, \mathtt{H}_3$, and $\mathtt{H}_4$ of irreducible finite Coxeter groups. All of these groups act on some n-sphere. We call Γ (or W_Γ) *spherical*, if W_Γ is finite. Every spherical Coxeter group has a unique longest element (see [Hum90, p. I.1.8]) which we denote by w_0.
The second category is the category of affine Coxeter groups. These are infinite groups that are derived from finite Coxeter groups by adding a generator and one or two edges

in the Coxeter diagram, such that the finite Coxeter group is a quotient group of the affine Coxeter group when divided by a suitable normal abelian subgroup. There are four infinite families in this category: $\tilde{\mathtt{A}}_n$ for $n \geq 2$, $\widetilde{\mathtt{B}}_n$ for $n \geq 3$, $\widetilde{\mathtt{C}}_n$ for $n \geq 2$ and $\widetilde{\mathtt{D}}_n$ for $n \geq 4$ of increasing dimension n. In addition, there are six exceptional types $\widetilde{\mathtt{E}}_6, \widetilde{\mathtt{E}}_7, \widetilde{\mathtt{E}}_8, \widetilde{\mathtt{F}}_4, \widetilde{\mathtt{G}}_2$, and $\widetilde{\mathtt{I}}_1$. All affine Coxeter groups act cocompactly on some $\mathbb{R}^n$. A full list of the Coxeter diagrams for all types of finite and affine Coxeter groups is shown in Figures A.1 and A.2.
The third category includes all Coxeter groups that do not belong to the first two categories. Some of these groups can act on hyperbolic spaces. Since this thesis focuses primarily on finite and affine Coxeter groups, we will not go into the details of this category. For more information, interested readers may refer to [Hum90] or [Dav08].

Independent of its category, every Coxeter system (W, S) has a geometric realization as an abstract simplicial complex $\Sigma = \Sigma(W, S)$ that it naturally acts on. The formal definition is as follows:

Definition 2.2.7 (Coxeter complex)**.** Let (W, S) be a Coxeter system of rank $n + 1$. Consider the set $\Sigma = \Sigma(W, S)$ of left-cosets xW_J of the standard parabolic subgroups $W_J := \langle S_J \rangle$, where $J \subseteq I$ and $S_J := \{s_j \in S |\ j \in J\}$, partially ordered by the reverse inclusion order: For subsets $J, K \subseteq I$ and elements $x, y \in W$ we set

$$xW_J \leq yW_K \Leftrightarrow yW_K \subseteq xW_J.$$

This poset Σ is an abstract simplicial complex. We call it the *Coxeter complex of* (W, S). The 0-dimensional elements of Σ, the *vertices*, correspond to the cosets of maximal parabolic subgroups with generating sets $S_J = S \setminus \{s_j\}$. The maximal dimensional simplices of Σ are in bijection with the group elements of W. We call them *alcoves* and denote them by bold lowercase letters, e.g. $\mathbf{c}$ or $\mathbf{x}$, while we denote the corresponding group elements by c or x. Their codimension one faces will be called *panels*, denoted by p, q. Since every panel corresponds to a parabolic subgroup of the form xW_s for some $s \in S$, we can assign a *type* $\tau(p) = s$ to every panel.

Example 2.2.8. The Coxeter group $S_3 = \mathtt{A}_2$ acts on the hexagonal tiling of the blue circle that is depicted in the left picture of Figure 2.3, which illustrates the Coxeter complex of S_3. The six simplicial segments of the circle, formed by intersecting it with the reflection hyperplanes of the triangle, correspond to the six group elements of S_3. The panels bounding the alcove labeled e correspond to the generators s_1 and s_2, coloured as grey and red dots, respectively. As S_3 acts type-preserving on the panels of the Coxeter complex, this allows to determine the types of the remaining panels.

We close this section by giving our notation for two important sets of Coxeter groups. First, we introduce *triangle groups*:

Definition 2.2.9 (Triangle group)**.** Let Δ be the complete labeled graph on three vertices $\{s_1, s_2, s_3\}$ with edge-labeling $p, q, r \in \mathbb{N}_{\geq 2} \cup \{\infty\}$. The associated group defined by the presentation

$$\Delta(p, q, r) := \langle s_1, s_2, s_3 \mid s_1^2, s_2^2, s_3^2, (s_1 s_2)^p, (s_1 s_3)^q, (s_2 s_3)^r \rangle$$

is called *triangle group* $\Delta(p, q, r)$.

For example $W_{\tilde{\mathtt{A}}_2} = \Delta(3,3,3)$ is a triangle group. Notice that $\Delta(p,q,r)$ is infinite if and only if at least one edge-label is ∞ or $\frac{1}{p}+\frac{1}{q}+\frac{1}{r} \leq 1$, since the parameters determine the angles of a triangle as $\frac{\pi}{p}$, $\frac{\pi}{q}$, and $\frac{\pi}{r}$.

Right-angled Coxeter groups, commonly referred to as RACGs, are another notable subclass of Coxeter groups that will appear in Part III below. To prepare for this, we also include the common notation for RACGs here:

Definition 2.2.10 (Right-angled Coxeter group)**.** Let (W,S) be a Coxeter system. If the exponents $m_{i,j}$ for $i \neq j$ are all equal to 2 or ∞, we say that W is a *right-angled Coxeter group (RACG)*. Typically, RACGs are given via their *presentation diagram* (or *defining graph*) $\Lambda = (V,E)$, which is a finite simple graph, such that

$$W(\Lambda) = \langle V(\Lambda) \mid v^2 \text{ for all } v \in V(\Lambda), \text{ and } (vw)^2 \text{ for all } \{v,w\} \in E(\Lambda)\rangle.$$

2.2.2. Roots. Besides this combinatoric perspective on Coxeter groups and complexes, there is also an algebraic approach to certain finite and affine Coxeter groups via their root systems. Here, we will only outline the essential notation. For more details, refer to [Bou02, Chap. 6]. For this, let V be a vector space over $\mathbb{R}$ with dual vector space V^* and denote by $\langle x, y^\vee\rangle$ the evaluation of $y \in V^*$ on $x \in V$.

Definition 2.2.11 (Root system)**.** Let V be a real vector space. A finite subset $\Phi = \{\alpha_1, \cdots, \alpha_n\} \subseteq V$ is called *root system* if the following conditions hold:

- $0 \notin \Phi$ and Φ generates V;
- for all $\alpha \in \Phi$ there exists $\alpha^\vee \in V^*$ with $\langle \alpha, \alpha^\vee\rangle = 2$;
- Φ is invariant under the reflection $s_{\alpha,\alpha^\vee} : x \mapsto x - \langle x, \alpha^\vee\rangle\alpha$;
- for all $\alpha \in \Phi$ it holds $\alpha^\vee(\Phi) \subseteq \mathbb{Z}$.

The elements of Φ are called *roots* and the dimension of V is the *rank* of the root system.

The reflection $s_{\alpha,\alpha^\vee}$ is uniquely determined by α, which justifies the short notion $s_\alpha := s_{\alpha,\alpha^\vee}$. See [Bou02, p. VI.1.1.].
Given two root systems Φ_1 and Φ_2, we can construct another root system $\Phi = \Phi_1 \cup \Phi_2$ such that $\operatorname{span}(\Phi) = \operatorname{span}(\Phi_1) \oplus \operatorname{span}(\Phi_2)$. Root systems that can be decomposed in this manner are called *reducible*, otherwise *irreducible*.
The automorphisms of V that stabilize the root system Φ form a group, and the subgroup generated by the reflections s_α with $\alpha \in \Phi$ is known as the *Weyl group* of the root system. The finite Coxeter groups of types $\mathtt{A}_n, \mathtt{B}_n, \mathtt{C}_n, \mathtt{D}_n, \mathtt{E}_6, \mathtt{E}_7, \mathtt{E}_8, \mathtt{F}_4, \mathtt{G}_2$, and their corresponding affine Coxeter groups are Weyl groups of some root systems.

Definition 2.2.12 (Basis of roots, positive/negative roots)**.** Let Φ be a root system in V. A *root basis* $\Phi^* \subseteq \Phi$ is a basis of V such that every root β can be expressed as an integer linear combination of *base roots* $\alpha \in \Phi^*$ with all coefficients being either non-negative or non-positive. The elements of Φ^* are also referred to as *simple roots*.
Given a root basis Φ^*, we call the roots that can be expressed via Φ^* using non-negative coefficients *positive roots* and denote them by Φ^+. Analogously, the roots with non-positive coefficients are called *negative roots*, denoted as Φ^-.

Note that positivity of roots depends on the choice of a root basis.

Example 2.2.13. Let $V_1 \subseteq \mathbb{R}^3$ be the subspace consisting of all vectors whose coordinates sum to zero. Denote the vectors of canonical standard basis of $\mathbb{R}^3$ by e_i for $i \in [3]$. The set of six vectors $\Phi = \{\mathrm{e}_i - \mathrm{e}_j \mid 1 \leq i, j \leq 3,\ i \neq j\}$ forms a root system for the Coxeter group $S_3 = W_{\mathtt{A}_2}$ of type $\mathtt{A}_2$. A root basis is given by the two vectors $\Phi^* = \{\alpha_1 = \mathrm{e}_1 - \mathrm{e}_2, \alpha_2 = \mathrm{e}_2 - e_3\}$.
On the other hand, consider the Coxeter group $W_{\mathtt{B}_2}$, which has eight elements. Compare Figure A.1. Let $V_2 = \mathbb{R}^2$ be a real vector space with canonical standard basis. Then the set of eight roots $\Phi = \{\pm \mathrm{e}_i,\ \pm e_j \pm e_k |\ i \in [2], 1 \leq j < k \leq 2\}$ is a root system of $W_{\mathtt{B}_2}$. A root basis is given by the two vectors $\Phi^* = \{\alpha_1 = \mathrm{e}_1 - \mathrm{e}_2, \alpha_2 = \mathrm{e}_2\}$.
Notice that the roots of $W_{\mathtt{A}_2}$ all have the same length, whereas the root system of $W_{\mathtt{B}_2}$ contains both short and long roots. The illustrations in Figure 2.4 show these two root systems.

Remark 2.2.14. Given a root basis of a root system Φ, the base roots define a sector of the Coxeter complex through the reflection hyperplanes associated with the reflections s_α. When we identify the generators of the Coxeter group with the reflections defined by the base roots, this sector coincides with the alcove that represents the identity element.

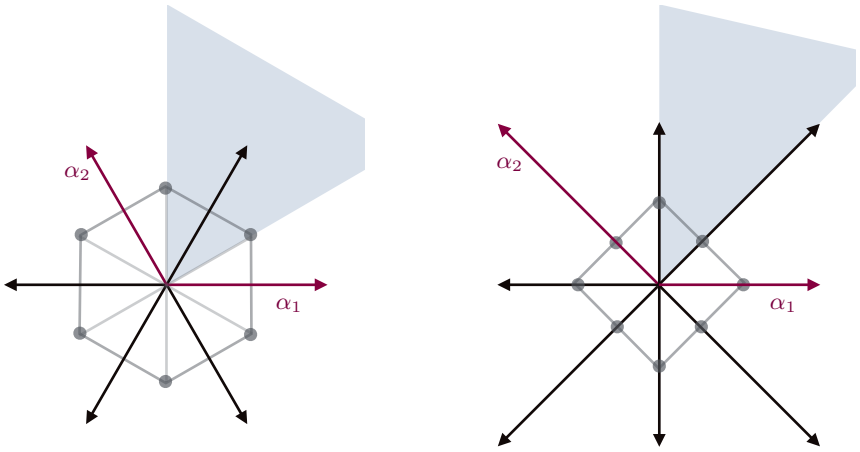

FIGURE 2.4. *On the left:* Root system of $\mathtt{A}_2$. *On the right:* Root system of $\mathtt{B}_2$. The blue cone represents the positive sector defined by the root basis shown in purple.

We close this section by stating our notation on coroots, weights, and coweights in root systems:

Definition 2.2.15 (Coroots, weights and coweights)**.** Let Φ be a root system in V with root basis Φ^*. We denote by $\alpha^\vee = \frac{2\alpha}{\langle \alpha, \alpha \rangle}$ the *coroot* associated with the root $\alpha \in \Phi$. Then $\Phi^\vee = \{\alpha^\vee |\ \alpha \in \Phi\}$ is a root system in V^*, and $(\Phi^*)^\vee := \{\alpha^\vee |\ \alpha \in \Phi^*\}$ is a basis of the dual root system. We denote the coroot lattice by $R^\vee = \oplus_{i=1}^n \mathbb{Z}\alpha_i^\vee \subseteq \mathbb{Z}^n$, and use lower case greek letters such as λ, μ, and ν for its elements. The *fundamental weights* ω_α and *co-weights* $\omega_\alpha^\vee$ are dual bases to $(\Phi^*)^\vee$ and Φ^*. We denote the *weight lattice* by $X := \mathbb{Z}\omega_1 \oplus \cdots \oplus \mathbb{Z}\omega_n$.

2.2.3. Bruhat order. All Coxeter groups come with a partial order structure, the *Bruhat order*, which simultaneously encodes algebraic, geometric, and combinatorial properties. The Bruhat order on Weyl groups was first studied by Verma [Ver68]. However, significant contributions to the concept of Bruhat order on Schubert varieties were made earlier by Ehresmann [Ehr34], and later by Björner, who further developed the notion and whose notation we will follow for this section. Compare [BB06, Section 2].

Definition 2.2.16 (Bruhat order)**.** Let (W, S) be a Coxeter system and $v, w, u \in W$. Denote by $R = \{wsw^{-1} : \ w \in W, \ s \in S\}$ its set of reflections. Write $v \to w$ if there exists $r \in R$ with $v^{-1}w = r$ and $l(v) < l(w)$. Then we say that $u \leq w$ in *Bruhat order* if there exist $u_i \in W$ such that

$$u = u_0 \to u_1 \to \cdots \to u_{k-1} \to u_k = w.$$

We denote intervals in Bruhat order by $[u, w] := \{v \in W |\ u \leq v \leq w\}$ and call them *Bruhat intervals*.

One can show that this definition is equivalent to the following:

Proposition 2.2.17 (Subword property)**.** *Let (W, S) be a Coxeter system and $v, w \in W$. Let $w = s_1 \cdots s_m$ be a reduced expression. Then $v \leq w$ in Bruhat order if and only if there exists a reduced expression $v = s_{v_1} \cdots s_{v_k}$ with $1 \leq v_1 \leq \cdots \leq v_k \leq m$.*

This implies immediately:

Corollary 2.2.18. *Let (W, S) be a Coxeter system and $v, w \in W$. Then $[v, w]$ is finite with* $\mathrm{card}([v, w]) \leq 2^{l(w)}$.

The Bruhat order can be visualized via the *Bruhat graph*:

Definition 2.2.19 (Bruhat graph)**.** Let (W, S) be a Coxeter system and $R = \{wsw^{-1} : w \in W, \ s \in S\}$ its set of reflections. The *Bruhat graph* of W is the directed graph $\mathcal{B}_W = (V, E)$ with $V = \{w : \ w \in W\}$ and $e = (u, w) \in E \Leftrightarrow l(u) < l(w)$ and $w = r(u) = u \cdot r$ for a reflection $r \in R$.

Example 2.2.20. Consider the spherical Coxeter groups $W_{\mathtt{A}_2}$ and $W_{\mathtt{B}_2}$, both generated by two generators denoted s_1 and s_2. Their Bruhat graphs are depicted in Figure 2.5: The nodes of the graphs represent the six and eight group elements of $W_{\mathtt{A}_2}$ and $W_{\mathtt{B}_2}$, respectively. The unique longest elements $w_0 = s_1s_2s_1 = s_2s_1s_2$ in $W_{\mathtt{A}_2}$, and $w_0 = s_1s_2s_1s_2 = s_2s_1s_2s_1$ in $W_{\mathtt{B}_2}$ have no outgoing edges in the Bruhat graph, visualizing that no element of the group is greater in Bruhat order.

2.2.4. Geometry of affine Coxeter complexes. For most of this text, we will restrict to the study of affine Coxeter systems. In this case, the group W has the structure of a semi-direct product $W = T \rtimes W_0$, with a translation group $T \cong \mathbb{Z}^n$ corresponding to the coroot lattice $R^\vee$, and an associated spherical Weyl group W_0. This structure allows us to express a group element $x \in W$ as $x = t^\lambda v$ with $\lambda \in T$ and $v \in W_0$. For notation, we fix:

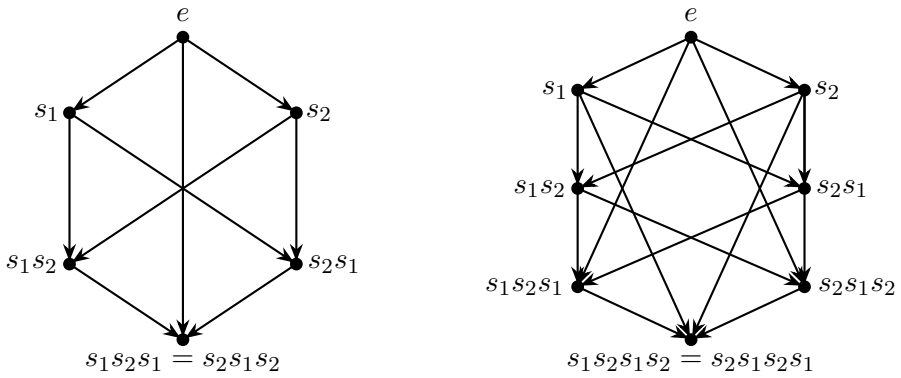

FIGURE 2.5. *On the left:* Bruhat graph of $W_{\mathtt{A}_2}$ *On the right:* Bruhat graph of $W_{\mathtt{B}_2}$.

Definition 2.2.21 (Spherical direction)**.** Let (W, S) be an affine Coxeter system with corresponding spherical Coxeter group W_0 and let $x = t^\lambda w \in W$. Then, we denote by $\mathrm{sph} : W \to W_0$, $x \mapsto \mathrm{sph}(x) = w$ the map that records the *spherical direction* of the group element x.

Definition 2.2.22 (Vertex of an alcove)**.** Let (W, S) be an affine Coxeter system with corresponding spherical Coxeter group W_0 and let $x = t^\lambda w \in W$. Then, we denote by $\mathrm{vtx} : W \to T$, $x \mapsto \mathrm{vtx}(x) = \lambda$ the map that records the *vertex* of the group element x. The vertices of Σ whose stabilizer in W is isomorphic to W_0 are called the *special vertices*.

As already mentioned in Section 2.2.1, affine Coxeter groups act cocompactly on some $\mathbb{R}^n$. More precisely, for an affine Coxeter group W, we can identify Σ with a tiled n-dimensional Euclidean vector space that W acts on. We will refer to the hyperplanes H of this tiling as *walls*. Observe that every reflection r in W fixes a wall H_r in Σ which we call the *reflection hyperplane of* r. For example, see the hyperplane shown in purple in Figure 2.6.

We denote the origin of the vector space V by $v_0 = 0$ and choose the geometric realization of Σ in a way such that v_0 is a special vertex, fixed by all elements in $S_0 = \{s_1, \ldots, s_n\}$, which is the subset of $S = \{s_0, s_1, \ldots, s_n\}$ that generates the spherical Weyl group W_0. The walls of the Coxeter complex Σ through the origin v_0, which is the set of reflection hyperplanes for reflections in W that fix this vertex, are in fact the linear hyperplanes perpendicular to the roots $\alpha \in \Phi$ of the root system associated with W. For the notation, we establish:

Definition 2.2.23 (Reflections and reflection hyperplanes)**.** Let (W, S) be an affine Coxeter system with root system Φ and associated spherical Weyl group (W_0, S_0) with root system Φ_0. We write $H_\alpha := \{x \in V | \langle x, \alpha^\vee \rangle = 0\}$ for the hyperplanes that contain the origin v_0 and call them *fundamental hyperplanes* or *linear hyperplanes*. The corresponding reflections are called *fundamental reflections* and are denoted by r_α.
Furthermore, we consider the affine hyperplanes $H_{\alpha,k} := \{x \in V | \langle x, \alpha^\vee \rangle = k\}$ for each

root $\alpha \in \Phi$, and the two associated half-spaces $H^+_{\alpha,k} = \{x \in V |\ \langle x, \alpha^\vee \rangle \geq k\}$ and $H^-_{\alpha,k} = \{x \in V |\ \langle x, \alpha^\vee \rangle \leq k\}$. We denote by $r_{\alpha,k}$ the reflection along the hyperplane $H_{\alpha,k}$. Sometimes, we also index the associated generator of S_0 (resp. S) by the root perpendicular to their fundamental reflection hyperplane: $S_0 = \{s_{\alpha,0} = s_{\alpha_i} |\ \alpha_i \in \Phi_0\}$, $S = \{s_{\alpha,0} = s_{\alpha_i} |\ \alpha_i \in \Phi\}$.

Notice that this aligns with the notation established in Section 2.2.2. For evaluating coroot lattice points on hyperplanes, we introduce the following brief notion:

Notation 2.2.24 (Hyperplane coordinates of coroot lattice points)**.** Let (W, S) be an affine Coxeter system with root system Φ. Let further $\lambda \in T$ be a coroot lattice point and $\alpha \in \Phi^+$. We denote by $h_\alpha := \langle \lambda, \alpha^\vee \rangle$ the *hyperplane coordinate of λ with respect to the root α*.

When studying geometric constructions in affine Coxeter complexes, we will also utilize the notions of positive and negative cones (cf. [Bou02]):

Definition 2.2.25 (Positive and negative cones)**.** Let (W, S) be an affine Coxeter system with root system Φ and $\Phi^\vee$ the corresponding system of coroots. We denote by $\mathcal{C}^+$ the positive span of all positive simple coroots and refer to it as the *positive cone* of $\Phi^\vee$. Analogously, we denote by $\mathcal{C}^-$ the positive span of all negative simple coroots and call it the *negative cone* of $\Phi^\vee$.

The set of walls $\mathcal{H}_\lambda$ through a special vertex λ divides the space V into $\mathrm{card}(W_0)$ simplicial cones that are of significant interest to us:

Definition 2.2.26 (Weyl chambers)**.** Let (W, S) be an affine Coxeter system with Coxeter complex $\Sigma(W, S)$. Let further $\mathcal{H}_\lambda$ denote the set of reflection hyperplanes that contain the special vertex λ. We call the closures of the connected components $V \setminus \mathcal{H}_\lambda$ *Weyl chambers* and denote the Weyl chambers with cone point the origin v_0 by $\mathcal{C}_v$, indexed by the spherical group element v with $t^0 v \subseteq \mathcal{C}_v$.
We denote the Weyl chamber with cone point at the origin v_0 corresponding to the parallelism class of Weyl chambers that is represented by the identity element $e \in W_0$ by $\mathcal{C}_f$, and call it the *fundamental Weyl chamber*.

Remark 2.2.27. Let (W, S) be an affine Coxeter system with associated affine Coxeter complex Σ and corresponding spherical Weyl group W_0. The set of parallelism classes of rays in Σ form a sphere at the boundary of Σ which we call the *boundary sphere* $\partial\Sigma$. This sphere is also a Coxeter complex, associated with the spherical Weyl group W_0, inheriting its structure from Σ by taking the parallelism classes of hyperplanes as hyperplanes in $\partial\Sigma$ that induce a simplicial tiling of $\partial\Sigma$. The parallelism classes of Weyl chambers in Σ correspond to the maximal dimensional simplices of this tiling, which coincide with the alcoves of the Coxeter complex of the spherical Weyl group W_0. Therefore, we can identify $\partial\Sigma$ with the Coxeter complex $\Sigma_0 = \Sigma(W_0, S_0)$ and sometimes refer to the alcoves of the spherical Coxeter complex associated with an affine Coxeter complex as Weyl chambers too. For an illustration of this connection, see Figure 2.6, where the Weyl chamber $\mathcal{C}_{s_2 s_1}$ corresponds to the alcove $s_2 s_1 \in \partial\Sigma$ in the boundary, which is also highlighted in light blue.

Using this notion, we can introduce our notation for alcoves in affine Coxeter complexes:

Notation 2.2.28 (Fundamental alcove, alcoves)**.** Let (W, S) be an affine Coxeter system with Coxeter complex $\Sigma(W, S)$. The unique alcove of Σ contained in $\mathcal{C}_f$ that has v_0 as a vertex is called *fundamental alcove* and is denoted by $\mathbf{c_f}$. Then, the W action on Σ identifies alcoves in Σ with group elements $w \in W$ as $\mathbf{w} = w\mathbf{c_f}$. We will denote them by bold lowercase letters.

We illustrate this collection of concepts with the following example:

Example 2.2.29. Figure 2.6 shows the affine Coxeter complex of $W_{\tilde{\mathbf{A}}_2}$ with its boundary complex $\partial\Sigma$. The six alcoves adjacent to the origin v_0 are labeled with their corresponding group elements. All hyperplanes of the parallelism class α_2, such as the wall $H_{\alpha_2,1}$ depicted in the image, correspond to the hyperplanes in $\partial\Sigma$ that are highlighted in purple.

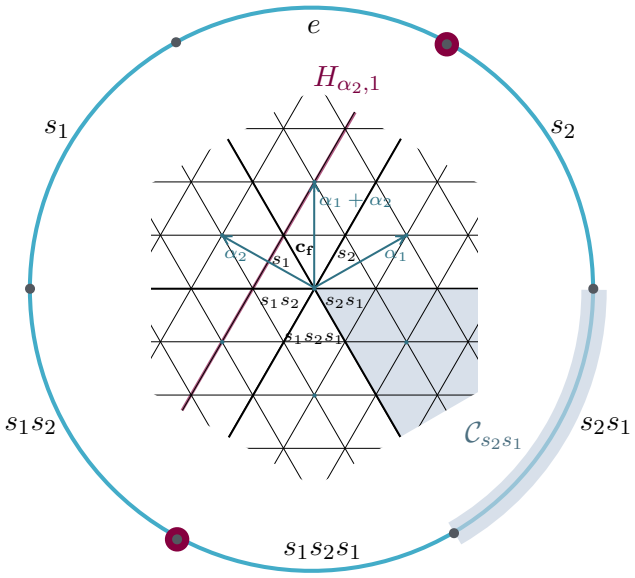

FIGURE 2.6. Affine Coxeter complex of $W_{\tilde{\mathbf{A}}_2}$ with boundary complex $\partial\Sigma$.

Because of the semidirect product structure of an affine Coxeter Group $W = W_0 \rtimes T$ with W_0 a spherical Coxeter group and $T \cong \mathbb{Z}^n$, we can find the tiling of $\mathbb{R}^n$ given by the Weyl chambers with cone point v_0 also at every other coroot lattice point $\mu \in T$. This gives the Coxeter complex Σ a structure similar to infinitely many local copies of $\Sigma(W_0, S_0)$ at every $\mu \in T$. Since we want to make use of this local-to-global-geometric structure below, we introduce the following:

Definition 2.2.30 (Local Weyl chamber)**.** Let (W, S) be an affine Coxeter system with (W_0, S_0) the corresponding spherical Coxeter system. Let $x = t^\mu w \in W$ with $\mu \in T$, $w \in W_0$ and define $h_\alpha(\mu) = \langle \mu, \alpha^\vee \rangle$ for all positive roots $\alpha \in \Phi^+$. Denote by $H^{\mathbf{x}}_{\alpha,h_\alpha(\mu)}$

the half-space determined by the hyperplane $H_{\alpha,h_\alpha(\mu)}$ that contains the alcove $\mathbf{x}$. Then we call the cone

$$\mathcal{C}_{\mu,w} := \bigcap_{\alpha\in\Phi^+} H^{\mathbf{x}}_{\alpha,h_\alpha(\mu)}$$

the *local Weyl chamber at μ with direction w*. Notice that $\mathbf{x}$ is the alcove at the tip of the cone, and μ is the cone point.

Below, we will frequently utilize the parallelity of hyperplanes in affine Coxeter complexes. The following notions will help us to describe our observations more easily:

Definition 2.2.31 (Parallelism class of a hyperplane)**.** Let (W, S) be an affine Coxeter system with root system Φ. Let $H_{\alpha,k}$ be a hyperplane in the associated Coxeter complex Σ perpendicular to a positive, not necessarily simple root $\alpha \in \Phi^+$. We call α the *parallelism* or *root class of $H_{\alpha,k}$*. Sometimes, we also call $H_{\alpha,k}$ an α-hyperplane.

Definition 2.2.32 (i-strip)**.** Let $\Sigma = \Sigma(W, S)$ be the affine Coxeter complex corresponding to the Coxeter system (W, S) and let $\alpha \in \Phi^+$ be a positive root of W. Denote by $H^{\mathbf{c_f}}_{\alpha,0}$ the half-space defined by $H_{\alpha,0}$ that contains the fundamental alcove $\mathbf{c_f}$ and by $H^{\mathbf{c_f}}_{\alpha,i}$ for $i \in \mathbb{Z}$ the half-space corresponding to $H_{\alpha,i}$ that satisfies $H^{\mathbf{c_f}}_{\alpha,i} \subseteq H^{\mathbf{c_f}}_{\alpha,0}$ or $H^{\mathbf{c_f}}_{\alpha,i} \supseteq H^{\mathbf{c_f}}_{\alpha,0}$. Denote the second half-space defined by $H_{\alpha,i}$ by $H^{\neg\mathbf{c_f}}_{\alpha,i}$. Then, we define the *$i$-strip with respect to α* to be

$$\mathcal{S}_{\alpha,i} := H^{\mathbf{c_f}}_{\alpha,i} \cap H^{\neg\mathbf{c_f}}_{\alpha,i+1}.$$

By using half-spaces defined by hyperplanes perpendicular to roots, we can define another convex hull in the Coxeter complex, besides the Euclidean convex hull:

Definition 2.2.33 (Convex hull/Euclidean convex hull)**.** Let (W, S) be an affine Coxeter system and let x, y be two simplices of the associated Coxeter complex $\Sigma = \Sigma(W, S)$. Let further X and Y be two finite subsets of the vector space V underlying Σ. We define the *convex hull in the Coxeter complex* as

$$\mathrm{conv}(x, y) = \bigcap \left\{ H^{\varepsilon}_{\alpha,k} |\ x, y \subseteq H^{\varepsilon}_{\alpha,k},\ \alpha \in \Phi^+, k \in \mathbb{Z} \right\},$$

and the *Euclidean convex hull* as

$$\mathrm{conv}^*(X, Y) = \left\{ \sum_{i=1}^{n} a_i z_i |\ z_i \in X \cup Y,\ \sum_{i=1}^{n} a_i = 1, a_i \geq 0, n \in \mathbb{N} \right\}.$$

2.2.5. Orientations. In this subsection, we introduce orientations of Coxeter complexes, using the Definitions of [GS20, Section 3]. Although orientations can be assigned to all families of Coxeter groups, we will later restrict to orientations defined for affine Coxeter complexes only.

Definition 2.2.34 (Orientation of Σ)**.** Let (W, S) be a Coxeter system with Coxeter complex Σ. An *orientation* ϕ of Σ is a map that assigns to every pair of alcove $\mathbf{c}$ and panel p contained in $\mathbf{c}$ either $+1$ or -1. We say that an alcove $\mathbf{c}$ is *on the positive (resp. negative) side of p* if $\phi(p, \mathbf{c}) = +1$ (resp. $\phi(p, \mathbf{c}) = -1$). An orientation ϕ is called

wall-consistent if for any wall H in Σ and alcoves $\mathbf{c}, \mathbf{d}$ contained in the same half-space defined by H and having panels p, q in H, one has:

$$\phi(p, \mathbf{c}) = +1 \Leftrightarrow \phi(q, \mathbf{d}) = +1.$$

Then, it makes sense to consider the *ϕ-positive* (resp. *ϕ-negative*) side of the wall H. We call ϕ *periodic* if ϕ is wall-consistent and it holds: Let H_1 and H_2 be two parallel walls with corresponding half-spaces $H_1^{\varepsilon_1}$ and $H_2^{\varepsilon_2}$ satisfying $H_1^{\varepsilon_1} \subseteq H_2^{\varepsilon_2}$. Then $H_1^{\varepsilon_1}$ is the ϕ-positive side of H_1 if and only if $H_2^{\varepsilon_2}$ is the ϕ-positive side of H_2.

There are various methods to introduce trivial and natural orientations on Σ. One approach is to assign $+1$ (resp. -1) to every panel of the Coxeter complex, resulting in the *trivial positive (resp. negative) orientation.* Another option is to define orientation based on a specific simplex within the complex:

Definition 2.2.35 (Simplex orientation)**.** Let (W, S) be a Coxeter system with Coxeter complex Σ. Let further b be a simplex in Σ, $\mathbf{c}$ an alcove, and p a panel of $\mathbf{c}$. Define $\phi_b(p, \mathbf{c}) = +1$ if and only if $\mathbf{c}$ and b are on the same side of the wall H containing p or if $b \subseteq H$. The orientation ϕ_b obtained this way is called *simplex orientation towards b.*

For example, we can choose a vertex or an alcove of the Coxeter complex to be the orientation-defining simplex b. The reader interested in further details may refer to [GS20, Section 3]. Throughout this text, we will mainly restrict to two types of orientations of affine Coxeter complexes. The first one is a specific type of (boundary) simplex orientation that implicitly appeared first in the works of Littelmann [Lit94; Lit95] and Gaussent and Littelmann [GL05] on the Littelmann path model:

Definition 2.2.36 (Weyl chamber orientation)**.** Let Σ be the Coxeter complex associated with an affine Coxeter system (W, S) and $\partial\phi_v$ the simplex orientation of the boundary complex $\partial\Sigma$ towards a chamber $v \in \partial\Sigma$. Then, we can assign a wall-consistent orientation to Σ by choosing the side H^ε of a hyperplane H to be the positive (resp. negative) side if and only if ∂H^ε is the positive (resp. negative) side with respect to $\partial\phi_v$. We denote the resulting orientation of Σ by ϕ_v and call it the *Weyl chamber orientation with respect to v.*

Remark 2.2.37. Using the connection between the Coxeter complex Σ and the boundary complex $\partial\Sigma$ for affine Coxeter systems (W, S) that we discussed in Remark 2.2.27, Graeber and Schwer showed in [GS20, Lemma 3.12] that Weyl chamber orientations are wall-consistent and periodic; because of their definition via the boundary complex, they are also referred to as *induced affine orientations* or *orientations at infinity.*
Also, observe that our definition of Weyl chamber orientations is equivalent to the following alternative formulation: The Weyl chamber $v \in \partial\Sigma$ corresponds to a parallelism class of Weyl chambers in Σ. Define the orientation ϕ_v by setting $\phi_v(p, \mathbf{c}) = +1$ if and only if v has a representative cone $\mathcal{C}_v$ in the same half-space defined by the supporting hyperplane H_p of the panel p as the alcove $\mathbf{c}$.

Example 2.2.38. Figure 2.7 illustrates the affine Coxeter complex of the Coxeter group $W_{\tilde{\mathtt{A}}_2}$ equipped with the Weyl chamber orientation ϕ_w induced by $w = s_2 s_1 \in W_0$. Observe that all hyperplanes of a parallelism class, indicated in the figure by violet, green,

and orange colours, are oriented in the same direction: The positive side of a hyperplane H_α, marked with $+$, always faces the half space H_α^ε that contains the Weyl chamber $\mathcal{C}_w$, which is represented by the blue shaded cone. Additionally, Figure 2.7 illustrates the simplex orientation towards $w \in \partial\Sigma$ of the boundary complex $\partial\Sigma$. Observe that the hyperplanes in the boundary that correspond to a parallelism class of walls in Σ marked with the same colour are oriented in the same direction as the affine hyperplanes.

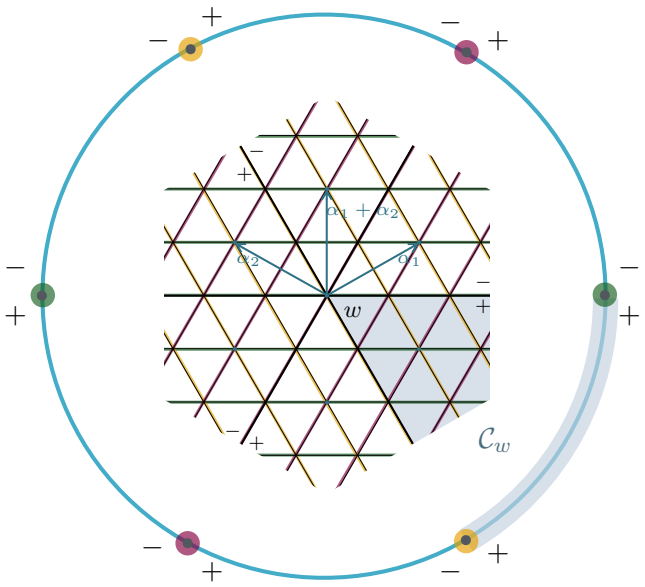

FIGURE 2.7. Affine Coxeter complex of type $\tilde{\mathtt{A}}_2$ with Weyl chamber orientation ϕ_w induced by the chamber $\mathcal{C}_w$, which is highlighted in light blue. The corresponding spherical Coxeter complex $\partial\Sigma$ of type $\mathtt{A}_2$ is oriented by the simplex orientation towards the alcove $w \in \partial\Sigma$. Hyperplanes of the same colour are oriented in the same direction.

The second family of orientations we are interested in is known as *chimney orientations*. Chimneys arise in the context of buildings and were introduced by Rousseau [Rou77; Rou01] as the closure of a geodesic half-line and a geodesic segment with common origin in one single apartment A of an affine building X. While we will restrict to the affine case again, chimneys may also be introduced in non-affine buildings. The interested reader may find a different approach in [CL11]. Although we do not require the full generality of the concepts for buildings for this text, as we are working in a single apartment (i.e., a single Coxeter complex), we will continue in the terminology of buildings throughout this section, following the notion of chimneys introduced by Milicevic, Naqvi, Schwer, and Thomas in [Mil+24], which differs from Rousseu's definition. Readers who may be unfamiliar with buildings can imagine using the same affine Coxeter complex Σ whenever we refer to an apartment A or a building X in the following discussions. The following definitions are taken from [Mil+24, Def. 3.1, 3.7, Def. 3.23].

Definition 2.2.39 (Chimneys and sectors)**.** Let X be an affine building of type (W, S) and A an apartment of X with fixed identification with the vector space V.

Let $\Phi = \{\alpha_1, \cdots, \alpha_n\}$ be the root system. Denote by $\alpha^{k,w}$ the half-apartment of A corresponding to the hyperplane $H_{\alpha,k}$ that contains a subsector of the Weyl chamber $\mathcal{C}_w$. Let $J \subseteq \{1, \ldots, n\}$ and Φ_J the corresponding root system. We call the follwing collection of half-apartments in A the *j-chimney (in A)*:

$$\xi_J := \left\{\alpha^{k,e} | \alpha \in \Phi_J^+, k \leq 0\right\} \cup \left\{\alpha^{k,w_0} | \alpha \in \Phi_J^+, k \geq 1\right\} \cup \left\{\beta^{k,w_0} | \beta \in \Phi^+ \setminus \Phi_J^+, k \in \mathbb{Z}\right\}.$$

For any collection of integers $\{n_\beta \in \mathbb{Z} |\ \beta \in \Phi^+ \setminus \Phi_J^+\}$ we define the corresponding *J-sector* as the subcomplex of A given by

$$S_J(\{n_\beta\}) := \left(\bigcap_{\alpha \in \Phi_J^+} \alpha^{0,e} \cap \alpha^{1,w_0}\right) \cap \left(\bigcap_{\beta \in \Phi^+ \setminus \Phi_J^+} \beta^{n_\beta, w_0}\right).$$

For $y \in W$, the (J,y)*-chimney* $\xi_{J,y}$ is obtained by acting on the J-chimney on the left by y as $\xi_{J,y} := y \cdot \xi_J$. With $y = t^\mu u$ with $\mu \in R^\vee$ and $u \in W_0$, we have

$$\begin{aligned}\xi_{J,y} := &\left\{(u\alpha)^{k+\langle u\alpha, \mu\rangle, u} | \alpha \in \Phi_J^+, k \leq 0\right\} \\ &\cup \left\{(u\alpha)^{k+\langle u\alpha, \mu\rangle, uw_0} | \alpha \in \Phi_J^+, k \geq 1\right\} \cup \left\{(u\beta)^{k, uw_0} | \beta \in \Phi^+ \setminus \Phi_J^+, k \in \mathbb{Z}\right\}.\end{aligned}$$

Analogously we define the (J,y)*-sector* $S_{J,y}(\{n_\beta\}) := y \cdot S_J(\{n_\beta\})$ for all $y = t^\mu u \in W$ and any set $\{n_\beta \in \mathbb{Z} |\ \beta \in \Phi^+ \setminus \Phi_J^+\}$ as

$$S_{J,y}(\{n_\beta\}) := \left(\bigcap_{\alpha \in \Phi_J^+} (u\alpha)^{\langle u\alpha, \mu\rangle, u} \cap (u\alpha)^{1+\langle u\alpha, \mu\rangle, uw_0}\right) \cap \left(\bigcap_{\beta \in \Phi^+ \setminus \Phi_J^+} (u\beta)^{n_\beta + \langle u\beta, \mu\rangle, uw_0}\right).$$

One can view a J-sector as a representative of the J-chimney ξ_J within the apartment A, while ξ_J can be interpreted as a direction at infinity of the building X. Having this, we can introduce chimney-induced orientations.

Definition 2.2.40 (Chimney-induced orientation)**.** Let X be an affine building of type (W,S), A an apartment of X with fixed identification with the vector space V, and let $J \subseteq \{1, \ldots, n\}$, $y \in W$. Let further $\mathbf{c}$ be an alcove of A and p a panel of $\mathbf{c}$ with supporting hyperplane H. The *orientation induced by the* (J,y)*-chimney*, $\phi_{J,y}$ is defined as $\phi_{J,y}(\mathbf{c}, p) = +1$ if the half-apartment determined by H which contains $\mathbf{c}$ is not an element of the (J,y)-chimney; else $\phi_{J,y}(\mathbf{c}, p) = -1$.

We can give an alternative formulation of Definition 2.2.40 in terms of (J,y)-sectors: For this, observe that every half-apartment of the set $\{\alpha^{k,e} |\ \alpha \in \Phi_J^+,\ k \leq 0\}$ contains the sector-defining half-apartment $\alpha^{0,e}$. Similarly, every half-apartment of the set $\{\alpha^{k,w_0} |\ \alpha \in \Phi_J^+,\ k \geq 1\}$ contains the sector-defining half-apartment α^{1,w_0}. For the half-apartments $\{\beta^{k,w_0} |\ \beta \in \Phi^+ \setminus \Phi_J^+,\ k \in \mathbb{Z}\}$, one of the following two cases applies: Either they contain the (J,y)-sector, or they intersect with it in infinitely many alcoves. In summary, all half-apartments within the (J,y)-chimney have a specific, non-empty intersection with every (J,y)-sector:

Lemma 2.2.41. *Let $J \subseteq \{1, \dots, n\}$, $y \in W$. Let $\mathbf{c}$ be an alcove and p a panel of $\mathbf{c}$ with supporting hyperplane H. Let $\phi_{J,y}$ be an orientation of Σ induced by the (J, y)-chimney. Then $\phi_{J,y}(p, c) = +1$ if and only if the half-apartment determined by H which contains $\mathbf{c}$ has empty or finite intersection with the (J, y)-sectors and does not contain the sector.*

Notice that the orientation does not depend on the choice of sector for a given chimney and that chimney-induced orientations are always wall consistent (see [Mil+24, Lemma 3.24]).

We conclude this section by presenting an example of a chimney orientation:

Example 2.2.42. Let $(W_{\tilde{\mathtt{A}}_2}, S)$ be a Coxeter system of type $\tilde{\mathtt{A}}_2$ with root system Φ and root basis $\Phi^* = \{\alpha_1, \alpha_2\}$. Consider the group element $y = t^\lambda e$ with $\lambda = -\alpha_1^\vee$ and the (J, y)-chimney with $J = \{1\}$, which implies $\Phi_J = \{\alpha_1\}$. Figure 2.8 illustrates the Coxeter complex of $W_{\tilde{\mathtt{A}}_2}$ with chimney-orientation $\phi_{J,y}$. The chimney is represented by the (J, y)-sector $S_{J,y}$ which is coloured in purple and is bounded by the hyperplanes $H_{\alpha_1,-2}$ and $H_{\alpha_1,-1}$. Notice that $\phi_{J,y}$ is not periodic: All hyperplanes of the parallelism class α_2 as well as those of the parallelism class $\alpha_1 + \alpha_2$ are oriented the same way as shown for the fundamental hyperplanes in Figure 2.8. However, for hyperplanes of the parallelism class α_1, the orange hyperplanes are oriented in the opposite direction compared to the green hyperplanes.

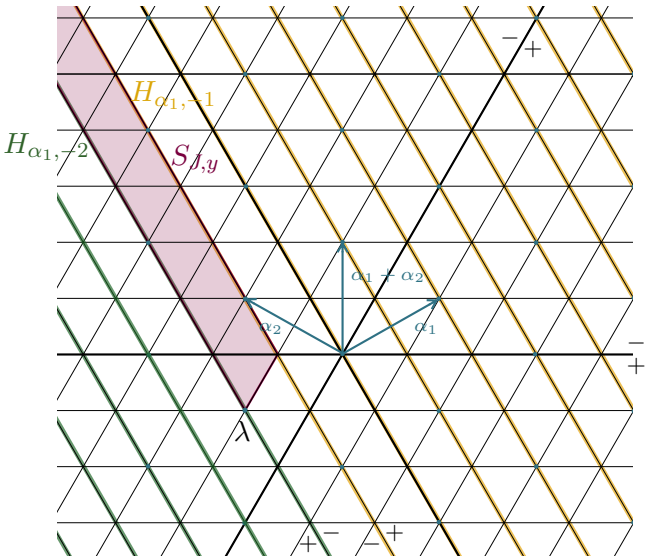

FIGURE 2.8. Affine Coxeter complex of type $\tilde{\mathtt{A}}_2$ with (J, y)-chimney orientation for $\Phi_J = \{\alpha_1\}$ and $y = t^\lambda e$. A sector $S_{J,y}$ representing the chimney is shown in purple.

Part II

Combinatorics of folded galleries for Coxeter shadows

CHAPTER 3

Folding patterns for Coxeter shadows

Sections 3.1, 3.2.1 and 3.3 of this chapter are based on the author's article [Rei24]. Our goal is to combinatorially characterize the options of folding a minimal gallery in an affine Coxeter complex positively with respect to a given Weyl chamber orientation of the complex. For this, we will introduce the notion of *folding patterns* that represent these options. Furthermore, we will characterize all applicable folding patterns of a given minimal gallery by drawing a connection between the gallery's end alcove, the Weyl chamber of the affine Coxeter complex in which that gallery ends, and the Bruhat moment graph of the associated spherical Coxeter group.

In Section 3.1, we introduce combinatorial galleries in Coxeter complexes in Section 3.1.1 and prove some technical properties of galleries in affine Coxeter complexes in Section 3.1.2. We study folded galleries in Section 3.2. Therefore, we introduce our notation and explain the technique on folding galleries in Section 3.2.1. In Section 3.2.2, we recall the notion of Coxeter shadows as given in [GS20]. Furthermore, we examine a translation property and the symmetry of Coxeter shadows in relation to diagram automorphisms. We also establish a connection between Coxeter shadows with respect to Weyl chamber and chimney-induced orientations. In the final Section 3.3, we study relations between Bruhat moment graphs and folding patterns. We establish a connection between folding patterns with respect to Weyl chamber orientations and the Bruhat moment graph of the associated spherical Weyl group in Section 3.3.1. Moreover, we construct the set of group elements such that for every element, there exists a minimal gallery ending in the alcove corresponding to that element, to which the folding pattern can be applied. We conclude by showing a link between the Bruhat moment graph and the spherical direction of the end alcove of a folded gallery in Section 3.3.2.

3.1. Minimal galleries

In this section, we establish our notation for galleries in 3.1.1, distinguishing between two closely related notions and following the notion used in [MST15]. Observe that our perception is slightly different from the more general one used in [GL05], where the concept of folded galleries appeared earlier. In Section 3.1.2, we derive the number of crossed hyperplanes of a given parallelism class for minimal galleries in Lemma 3.1.11. Furthermore, we characterize minimal galleries by the directions of their hyperplane crossings with respect to Weyl chamber orientations, as shown in Lemma 3.1.14, and the position of their end alcove, as discussed in Lemma 3.1.16.

3.1.1. Notion and notation. We begin with our definitions of galleries.

Definition 3.1.1 (Vertex-to-vertex gallery)**.** A *vertex-to-vertex gallery* in Σ is a sequence

$$\gamma = (\lambda_0, \mathbf{c}_0, p_1, \mathbf{c}_1, \cdots, p_n, \mathbf{c}_n, \lambda_n)$$

of vertices $\lambda_0, \lambda_n \in T$, alcoves $\mathbf{c}_i$, and panels p_i with $p_i \in \mathbf{c}_{i-1}$, $p_i \in \mathbf{c}_i$, $\lambda_0 \in \mathbf{c}_0$, and $\lambda_n \in \mathbf{c}_n$.

Definition 3.1.2 (Alcove-to-alcove gallery)**.** An *alcove-to-alcove gallery* in Σ is a sequence

$$\gamma = (\mathbf{c}_0, p_1, \mathbf{c}_1, \cdots, p_n, \mathbf{c}_n)$$

of alcoves $\mathbf{c}_i$ and panels p_i with $p_i \in \mathbf{c}_{i-1}$ and $p_i \in \mathbf{c}_i$.

Definition 3.1.3 (Length and minimality of galleries)**.** We define the *length* $\ell(\gamma)$ of an alcove-to-alcove gallery $\gamma = (\mathbf{c}_0, p_1, \mathbf{c}_1, \cdots, p_n, \mathbf{c}_n)$ or a vertex-to-vertex gallery $\gamma = (\lambda_0, \mathbf{c}_0, p_1, \mathbf{c}_1, \cdots, p_n, \mathbf{c}_n, \lambda_n)$ to be $n+1$, which equals the number of alcoves contained in γ, counted with multiplicity. We say that a gallery is *minimal* if there is no shorter gallery with start alcove $\mathbf{c}_0$ and end alcove $\mathbf{c}_n$, resp. start vertex λ_0 and end vertex λ_n.

The length function for galleries defines a natural metric on the set of alcoves of a Coxeter complex. For two alcoves $\mathbf{c}_1$ and $\mathbf{c}_2$, we define the distance $\mathrm{d}(\mathbf{c}_1, \mathbf{c}_2)$ as the length of a minimal gallery that starts in $\mathbf{c}_1$ and ends in $\mathbf{c}_2$.

Remark 3.1.4 (Simplex galleries)**.** One can easily generalize these definitions to *simplex-to-simplex galleries* by taking an alcove-to-alcove gallery and choosing simplices $\mathbf{s}_0 \subseteq \mathbf{c}_0$ and $\mathbf{s}_n \subseteq \mathbf{c}_n$ as the start and end simplices of the gallery. In particular, this allows the construction of alcove-to-vertex and vertex-to-alcove galleries.

Given an alcove-to-alcove gallery, there is a canonical way of transforming it into an alcove-to-vertex or a vertex-to-vertex gallery, and vice versa. Our notion for this procedure is inspired by music theory and was introduced in [MST15].

Definition 3.1.5 (Extension and truncation of galleries)**.** Let $\gamma = (\mathbf{c}_0, p_1, \mathbf{c}_1, \cdots, p_n, \mathbf{c}_n)$ be a minimal alcove-to-alcove gallery with $c_0 = t^{\lambda_0} v$ and $c_n = t^{\lambda_n} w$. We define the associated alcove-to-vertex gallery $\gamma^\sharp$ as

$$\gamma^\sharp = (\mathbf{c}_0, p_1, \mathbf{c}_1, p_2, \mathbf{c}_2, \ldots, p_n, \mathbf{c}_n, \lambda_n).$$

Also, we define the associated vertex-to-vertex gallery $\gamma^{\sharp\sharp}$ as

$$\gamma^{\sharp\sharp} = (\lambda_0, \mathbf{c}_0, p_1, \mathbf{c}_1, p_2, \mathbf{c}_2, \ldots, p_n, \mathbf{c}_n, \lambda_n).$$

For a vertex-to-vertex gallery $\gamma = (\lambda_0, \mathbf{c}_0, p_1, \mathbf{c}_1, \cdots, p_n, \mathbf{c}_n, \lambda_n)$ we define the associated vertex-to-alcove gallery $\gamma^\flat$ as

$$\gamma^\flat = (\lambda_0, \mathbf{c}_0, p_1, \mathbf{c}_1, p_2, \mathbf{c}_2, \ldots, p_n, \mathbf{c}_n).$$

Furthermore, we define the associated alcove-to-alcove gallery $\gamma^{\flat\flat}$ as

$$\gamma^{\flat\flat} = (\mathbf{c}_0, p_1, \mathbf{c}_1, p_2, \mathbf{c}_2, \ldots, p_n, \mathbf{c}_n).$$

Note that $(\gamma^{\sharp\sharp})^{\flat\flat} = \gamma$ for every alcove-to-alcove gallery γ, and whilst γ is a vertex-to-vertex gallery, it holds $(\gamma^{\flat\flat})^{\sharp\sharp} = \gamma$.

Often, we do not require all the information on the alcoves and panels a gallery passes through; instead, we only require knowledge of its starting and/or ending alcoves or vertices. For this purpose we denote a gallery $\gamma = (\mathbf{c}_0 = \mathbf{x}, p_1, \mathbf{c}_1, \dots, p_n\mathbf{c}_n = \mathbf{y})$ abbreviatory by $\gamma : \mathbf{x} \rightsquigarrow \mathbf{y}$, and write $\tilde{\gamma} : \lambda_0 \rightsquigarrow \lambda_n$ for a gallery $\tilde{\gamma} = (\lambda_0, \mathbf{c}_0, p_1, \mathbf{c}_1, \dots, p_n\mathbf{c}_n, \lambda_n)$. In some cases, we are only interested in the coroot lattice point of the end alcove of an alcove-to-alcove gallery or the final vertex. Analogous to Definition 2.2.22, we use $\mathrm{vtx}(\gamma)$ to indicate the end vertex or the vertex of the end alcove of a given gallery γ.
It is important to note that we do not require $\mathbf{c}_i \neq \mathbf{c}_{i-1}\ \forall i \in \{1, \dots, n\}$, so that $\mathbf{c}_i = \mathbf{c}_{i-1}$ is explicitly allowed. We will call such galleries *stammering*, and notice that they are not minimal. Since a non-stammering alcove-to-alcove (resp. vertex-to-vertex) gallery γ is uniquely determined by its first alcove and its panels (resp. and the first and last vertex), it is meaningful to introduce the *type* of a gallery:

Definition 3.1.6 (Type of a gallery)**.** Let γ be a gallery. We define the *type of* γ as the word

$$\tau(\gamma) := \tau(p_1) \cdots \tau(p_n) = s_{p_1} \cdots s_{p_n}$$

in S, where p_i denotes the i-th panel of γ.

Notice that one can also introduce types for stammering galleries, but that they do not give a unique description: Multiple stammering galleries may have the same type. To deal with this, sometimes the notion of a *decorated type* is used, marking (types of) panels between identical alcoves. For further details, see [GS20, Def. 4.7].

We collect some basic properties of the types of galleries in the following proposition. A proof of these results can be found in [GS20, Section 4].

Proposition 3.1.7. *Let (W, S) be a Coxeter system. Fix an alcove $\mathbf{c} \in \Sigma = \Sigma(W, S)$. It holds*

(i) Words in S are in bijection with the unfolded galleries starting in $\mathbf{c}$.

(ii) Reduced expressions in S are in bijection with minimal galleries starting in $\mathbf{c}$.

(iii) Decorated words are in bijection with all galleries starting in $\mathbf{c}$.

This result allows us to represent all group elements of W by minimal galleries, although not uniquely in general. A question that arises when considering the non-uniqueness of minimal galleries is which alcoves can be contained in minimal galleries between two alcoves (or vertices). Recall from Definition 2.2.33 that $\mathrm{conv}(\cdot)$ denotes the convex hull in the Coxeter complex here.

Proposition 3.1.8. *Let (W, S) be a Coxeter system with Coxeter complex $\Sigma(W, S)$. Fix three alcoves $\mathbf{a}, \mathbf{c}, \mathbf{d} \in \Sigma$. Then there exists a minimal gallery $\gamma : \mathbf{c} \rightsquigarrow \mathbf{d}$ with $\mathbf{a} \in \gamma$ if and only if $\mathbf{a} \in \mathrm{conv}(\mathbf{c}, \mathbf{d})$.*

PROOF. First, let $\gamma : \mathbf{c} \rightsquigarrow \mathbf{d}$ be a minimal gallery with $\mathbf{a} \in \gamma$. According to [Bro89, Chap. I., Prop. 4], γ crosses each hyperplane that separates $\mathbf{c}$ and $\mathbf{d}$ exactly once. We denote this set of walls by $\mathcal{H}(\mathbf{c}, \mathbf{d})$. This implies that $\mathbf{a}$ is separated from $\mathbf{c}$ and from $\mathbf{d}$ by walls in $\mathcal{H}(\mathbf{c}, \mathbf{d})$. Let $H^{\varepsilon}_{\alpha,k}$ be a half-space defined by $H_{\alpha,k}$ that contains $\mathbf{c}$ and $\mathbf{d}$, where $\alpha \in \Phi$ is a positive root and $k \in \mathbb{Z}$. Observe that $H_{\alpha,k} \notin \mathcal{H}(\mathbf{c}, \mathbf{d})$. For any wall $H_{\alpha,l} \in \mathcal{H}(\mathbf{c}, \mathbf{d})$, it follows $H_{\alpha,l} \subseteq H^{\varepsilon}_{\alpha,k}$. This shows that $\mathbf{a}$ is contained in every half-space that contains $\mathbf{c}$ and $\mathbf{d}$, and thus $\mathbf{a} \in \mathrm{conv}(\mathbf{c}, \mathbf{d})$.
Conversely, let $\mathbf{a} \in \mathrm{conv}(\mathbf{c}, \mathbf{d})$. Then, $\mathbf{a}$ is contained in every half-space containing $\mathbf{c}$ and $\mathbf{d}$. If now $H_{\alpha,k}$ is a hyperplane that either separates $\mathbf{c}$ and $\mathbf{a}$ or $\mathbf{a}$ and $\mathbf{d}$, it holds $H_{\alpha,k} \in \mathcal{H}(\mathbf{c}, \mathbf{d})$. Again, referring to [Bro89, Chap. I., Prop. 4], which states that a minimal gallery crosses exactly once each hyperplane that separates its start and end alcove once, we deduce that the set of hyperplanes crossed by a minimal gallery $\gamma_1 : \mathbf{c} \rightsquigarrow \mathbf{a}$ or $\gamma_2 : \mathbf{a} \rightsquigarrow \mathbf{d}$ is a subset of $\mathcal{H}(\mathbf{c}, \mathbf{d})$, because $\mathcal{H}(\mathbf{c}, \mathbf{a}) \subseteq \mathcal{H}(\mathbf{c}, \mathbf{d})$, resp. $\mathcal{H}(\mathbf{a}, \mathbf{d}) \subseteq \mathcal{H}(\mathbf{c}, \mathbf{d})$. Therefore, we can extend the galleries γ_1 or γ_2 to form a minimal gallery $\gamma = \gamma' * \gamma_1$ or $\gamma = \gamma_2 * \gamma''$, which crosses exactly the walls in $\mathcal{H}(\mathbf{c}, \mathbf{d})$. This shows that $\mathbf{a} \in \gamma$ for a minimal gallery $\gamma : \mathbf{c} \rightsquigarrow \mathbf{d}$. □

Since the type τ of a gallery is a word in S and concatenation of words gives words again, we can also define concatenation of galleries:

Definition 3.1.9 (Concatenation of galleries)**.** Let $\gamma_1 = (\mathbf{c}_{0,1}, p_{1,1}, \mathbf{c}_{1,1}, \cdots, p_{n,1}, \mathbf{c}_{n,1})$ and $\gamma_2 = (\mathbf{c}_{0,2}, p_{1,2}, \mathbf{c}_{1,2}, \cdots, p_{m,2}, \mathbf{c}_{m,2})$ be galleries in Σ with $\tau(\gamma_1) = w$ in S. We define the *concatenation* $\tilde{\gamma} := \gamma_2 * \gamma_1$ of γ_1 and γ_2 as:

$$\tilde{\gamma} = (\mathbf{c}_{0,1}, p_{1,1}, \mathbf{c}_{1,1}, \cdots, p_{n,1}, \mathbf{c}_{n,1}, w.\mathbf{c}_{0,2}, w.p_{1,2}, w.\mathbf{c}_{1,2}, \cdots, w.p_{m,2}, w.\mathbf{c}_{m,2}).$$

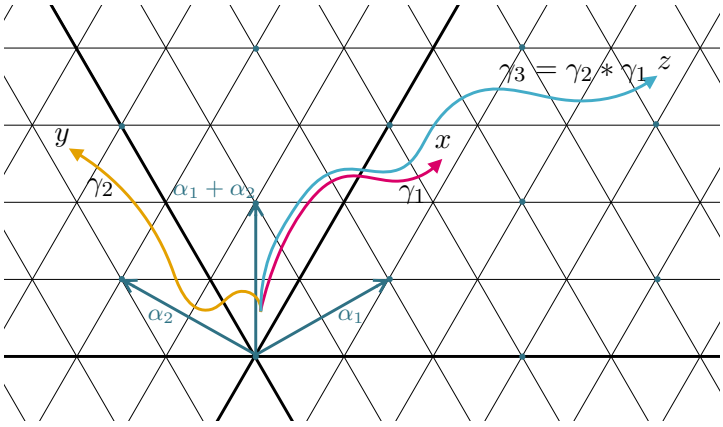

FIGURE 3.1. Minimal alcove-to-alcove galleries γ_1, γ_2, and $\gamma_3 = \gamma_2 * \gamma_1$ in a Coxeter complex of the group $W_{\tilde{\mathbf{A}}_2}$

Example 3.1.10. Consider the minimal galleries $\gamma_1 = (\mathbf{c_f}, p_{1,1}, \mathbf{c}_{1,1}, \cdots, p_{n,1}, \mathbf{c}_{n,1} = \mathbf{x})$ and $\gamma_2 = (\mathbf{c_f}, p_{1,2}, \mathbf{c}_{1,2}, \cdots, p_{n,2}, \mathbf{c}_{n,2} = \mathbf{y})$. An illustration of the galleries is given in Figure 3.1. It holds $\tau(\gamma_1) = s_0 s_2 s_1 s_0 s_1 s_2 =: w$ and $\tau(\gamma_2) = s_1 s_0 s_1 s_2 s_0 s_1$. The concatenated gallery

$$\gamma_3 = \gamma_2 * \gamma_1 = (\mathbf{c_f}, p_{1,1}, \mathbf{c}_{1,1}, \cdots, p_{n,1}, \mathbf{x}, w.\mathbf{c_f}, w.p_{1,2}, w.\mathbf{c}_{1,2}, \cdots, w.p_{n,2}, w.\mathbf{y} = \mathbf{z})$$

has the type $\tau(\gamma_3) = s_0s_2s_1s_0s_1s_2s_1s_0s_1s_2s_0s_1$. Observe that $\tau(\gamma_3)$ is a reduced expression for z and that γ_3 is a minimal gallery.

3.1.2. Crossings of minimal galleries. In the next lemmata, we will study two properties of minimal galleries $\gamma : \mathbf{c_f} \rightsquigarrow \mathbf{x} = t^\lambda \mathbf{w}$ in affine Coxeter systems: The number of crossed hyperplanes of a given parallelism class and, given a periodic orientation of the Coxeter complex, the direction of these crossings.

Observe that the number of crossed α-hyperplanes only depends on three ingredients: The height $h_\alpha(\lambda) = \langle \lambda, \alpha^\vee \rangle$ of the coroot coordinate λ of x over the root α, the spherical direction $\mathrm{sph}(x) = w$ of the element, and the Weyl chamber containing x (which is implicitly given by the first two bits of information). Given this, a short distinction of cases enables us to determine the number of crossed hyperplanes of a given parallelism class. See also Lemma 4.1.7, where we discuss this property for a special kind of galleries.

Lemma 3.1.11 (Numbers of crossings of minimal galleries)**.** *Let (W, S) be an affine Coxeter system and let $x = t^\lambda w \in \mathcal{C}_v$ with $v \in W_0$. Let further $\gamma : \mathbf{c_f} \rightsquigarrow \mathbf{x}$ be a minimal gallery. Denote by $M(x, \alpha)$ the number of α-hyperplanes crossed by γ and write $h_\alpha(\lambda) := \langle \lambda, \alpha^\vee \rangle$ for a positive root α. It holds:*

$$M(x,\alpha) = \begin{cases} h_\alpha(\lambda) - 1, & \text{if } \mathbf{c_f} \text{ and } \mathbf{v} \text{ are separated from } \mathbf{w} \text{ by } H_{\alpha,0}, \\ h_\alpha(\lambda), & \text{if } \mathbf{c_f}, \mathbf{v}, \mathbf{w} \text{ are in a common half-space defined by } H_{\alpha,0}, \\ |h_\alpha(\lambda)|, & \text{if } \mathbf{c_f} \text{ and } \mathbf{w} \text{ are separated from } \mathbf{v} \text{ by } H_{\alpha,0}, \\ |h_\alpha(\lambda)| + 1, & \text{if } \mathbf{v} \text{ and } \mathbf{w} \text{ are separated from } \mathbf{c_f} \text{ by } H_{\alpha,0}. \end{cases}$$

Proof. First, observe that every minimal gallery of $\gamma : \mathbf{c_f} \rightsquigarrow \mathbf{x}$ is crossing all α-hyperplanes that separate $\mathbf{c_f}$ and λ.

We distinguish two cases: If $\mathbf{c_f}$ and $\mathbf{v}$ are contained within a common half-space defined by $H_{\alpha,0}$, we find that $h_\alpha(\lambda) \geq 0$. Consequently, $\mathbf{c_f}$ and λ are separated by the α-hyperplanes $\{H_{\alpha,i} |\ i \in \{1, \dots, h_\alpha(\lambda) - 1\}\}$, but not the hyperplane $H_{\alpha,0}$. Now, if $\mathbf{c_f}$ is separated from $\mathbf{w}$ by $H_{\alpha,0}$, then due to the semidirect product structure of W, it follows that $t^\lambda \mathbf{c_f}$ is also separated from $t^\lambda \mathbf{w}$ by $H_{\alpha,h_\alpha(\lambda)}$. This implies $h_\alpha(\lambda) > 0$, and $\mathbf{c_f}$ and $\mathbf{x}$ are separated by the $h_\alpha(\lambda) - 1$ α-hyperplanes $\{H_{\alpha,i} |\ i \in \{1, \dots, h_\alpha - 1\}\}$. Moreover, if $\mathbf{c_f}$ is not separated from $\mathbf{w}$ by $H_{\alpha,0}$, then it follows, again due to the semidirect product structure of W, that $t^\lambda \mathbf{c_f}$ is not separated from $t^\lambda \mathbf{w}$ by $H_{\alpha,h_\alpha(\lambda)}$. This implies $h_\alpha(\lambda) \geq 0$ and $\mathbf{c_f}$ and $\mathbf{x}$ are also separated by the wall $H_{\alpha,h_\alpha(\lambda)}$. Therefore, the alcoves are separated by the $h_\alpha(\lambda)$ α-hyperplanes $\{H_{\alpha,i} |\ i \in \{1, \dots, h_\alpha\}\}$.

For the second case, consider that $\mathbf{c_f}$ and $\mathbf{v}$ are separated by $H_{\alpha,0}$. It follows $h_\alpha(\lambda) \leq 0$. Therefore, $\mathbf{c_f}$ and λ are separated by the α-hyperplanes $\{H_{\alpha,i} |\ i \in \{0, \dots, |h_\alpha| - 1\}\}$. As above, observe that if $\mathbf{c_f}$ is separated from $\mathbf{w}$ by $H_{\alpha,0}$, the semidirect product structure of W indicates that $t^\lambda \mathbf{c_f}$ is also separated from $t^\lambda \mathbf{w}$ by $H_{\alpha,h_\alpha(\lambda)}$. This leads to $h_\alpha(\lambda) < 0$, and $\mathbf{c_f}$ and $\mathbf{x}$ are also separated by the wall $H_{\alpha,h_\alpha(\lambda)}$. As a result, the alcoves are separated by the $|h_\alpha(\lambda)| + 1$ α-hyperplanes $\{H_{\alpha,i} |\ i \in \{0, \dots, |h_\alpha|\}\}$. And if $\mathbf{c_f}$ is not separated from $\mathbf{w}$ by $H_{\alpha,0}$, it follows from the semidirect product structure of W that $t^\lambda \mathbf{c_f}$ is also not separated from $t^\lambda \mathbf{w}$ by $H_{\alpha,h_\alpha(\lambda)}$. Hence, the alcoves are separated by the $h_\alpha(\lambda)$ α-hyperplanes $\{H_{\alpha,i} |\ i \in \{0, \dots, |h_\alpha| - 1\}\}$. □

Example 3.1.12. Consider again the minimal galleries γ_2 and γ_3 as depicted in Figure 3.1. The gallery γ_2 ends in $\mathbf{y} = t^\lambda \mathbf{u} \subseteq \mathcal{C}_w$ with $u = s_1 s_2$ and $w = s_1$. We have

$$\begin{aligned} h_{\alpha_1}(\lambda) &= \langle \lambda, \alpha_1^\vee \rangle = 0; \\ h_{\alpha_2}(\lambda) &= \langle \lambda, \alpha_2^\vee \rangle = 3; \\ h_{\alpha_1+\alpha_2}(\lambda) &= \langle \lambda, (\alpha_1+\alpha_2)^\vee \rangle = 3. \end{aligned}$$

Since $\mathbf{c_f}$ is separated from $\mathbf{u}$ and $\mathbf{w}$ by $H_{\alpha_1,0}$, it follows with Lemma 3.1.11 that γ_2 crosses $|h_{\alpha_1}(\lambda)| + 1 = 1$ α_1-hyperplanes. Additionally, since $\mathbf{c_f}$, $\mathbf{u}$ and $\mathbf{w}$ are not separated by $H_{\alpha_2,0}$, it follows with Lemma 3.1.11 that γ_2 crosses $h_{\alpha_2}(\lambda) = 3$ α_2-hyperplanes. Furthermore, since $\mathbf{c_f}$ and $\mathbf{w}$ are separated from $\mathbf{u}$ by the hyperplane $H_{\alpha_1+\alpha_2,0}$, Lemma 3.1.11 shows that the gallery crosses $h_{\alpha_1+\alpha_2}(\lambda) - 1 = 2$ hyperplanes of class $\alpha_1 + \alpha_2$.
The gallery γ_3 ends in $\mathbf{z} = t^\lambda \mathbf{c_f} \subseteq \mathcal{C}_v$. We have

$$\begin{aligned} h_{\alpha_1}(\lambda) &= \langle \lambda, \alpha_1^\vee \rangle = 6; \\ h_{\alpha_2}(\lambda) &= \langle \lambda, \alpha_2^\vee \rangle = -3; \\ h_{\alpha_1+\alpha_2}(\lambda) &= \langle \lambda, (\alpha_1+\alpha_2)^\vee \rangle = 3. \end{aligned}$$

Since $\mathbf{c_f}$ is separated from $\mathbf{v}$ by $H_{\alpha_2,0}$, it follows with Lemma 3.1.11 that γ_3 crosses $|h_{\alpha_2}(\lambda)| = 3$ α_2-hyperplanes. And because $\mathbf{c_f}$ and $\mathbf{v}$ are not separated by the hyperplanes $H_{\alpha_1+\alpha_2,0}$ and $H_{\alpha_1,0}$, Lemma 3.1.11 shows that the gallery crosses $h_{\alpha_1+\alpha_2}(\lambda) = 3$ hyperplanes of class $\alpha_1 + \alpha_2$ and $h_{\alpha_1}(\lambda) = 6$ hyperplanes of class α_1. Observe further that the number of crossed hyperplanes is the same for all minimal galleries starting in $\mathbf{c_f}$ and ending in $\mathbf{z}$. For example, see the minimal gallery γ depicted in Figure 3.3.

Next, assume that the Coxeter complex has a Weyl chamber orientation. We will now determine whether a given gallery is minimal by analysing the crossing directions of the gallery. To do this, we introduce first:

Definition 3.1.13 (Positive/negative crossing)**.** Let (W, S) be a Coxeter system, and let the associated Coxeter complex be equipped with an orientation ϕ. Consider a gallery γ crossing a hyperplane H at the panel p_i from $\mathbf{c}_{i-1}$ to $\mathbf{c}_i$. We say, that the crossing of H at p_i is a *positive* (resp. *negative*) *crossing* or *in positive (negative) direction* if $\phi(p_i, \mathbf{c}_{i-1}) = +1$ (resp. $\phi(p_i, \mathbf{c}_{i-1}) = -1$).

Lemma 3.1.14. *Let (W, S) be an affine Coxeter system and $x \in W$, $x = t^\lambda w$ with $w \in W_0$ and $\lambda \in T$. Let $\phi = \phi_v$ be a Weyl chamber orientation of the Coxeter complex $\Sigma = \Sigma(W, S)$ with respect to the chamber $v \in \partial\Sigma$. Then $\gamma : \mathbf{c_f} \rightsquigarrow \mathbf{x}$ is a minimal gallery if and only if every positive root $\alpha \in \Phi^+$ satisfies one of the following three conditions:*

(1) $\langle \lambda, \alpha^\vee \rangle \neq 0$ and all crossings of hyperplanes of class α are either positive or all negative;

(2) $\langle \lambda, \alpha^\vee \rangle = 0$, the alcoves $\mathbf{c_f}$ and $\mathbf{w}$ are not separated by $H_{\alpha,0}$, and γ crosses no α-hyperplane;

(3) $\langle \lambda, \alpha^\vee \rangle = 0$, the alcoves $\mathbf{c_f}$ and $\mathbf{w}$ are separated by $H_{\alpha,0}$, and γ crosses one single α-hyperplane once.

PROOF. Suppose first that $\gamma : \mathbf{c_f} \rightsquigarrow \mathbf{x}$ is minimal. Then it follows from [Bro89, I. 4D, Prop. 4] that every hyperplane crossed by γ is crossed only once, and the set of crossed hyperplanes is the set of hyperplanes separating $\mathbf{c_f}$ and $\mathbf{x}$. We distinguish two cases:
Case 1: $\langle \lambda, \alpha^\vee \rangle = 0$. It follows that $x \in \mathcal{S}_{\alpha,0}$ if $\mathbf{c_f}$ and $\mathbf{w}$ are not separated by $H_{\alpha,0}$, and that $x \in \mathcal{S}_{\alpha,-1}$, if $\mathbf{c_f}$ and $\mathbf{w}$ are separated by $H_{\alpha,0}$. If $x \in \mathcal{S}_{\alpha,0}$, then γ does not cross an α-hyperplane, since $\mathbf{c_f}$ is also contained in the 0-strip with respect to α. Hence every minimal gallery $\gamma : \mathbf{c_f} \rightsquigarrow \mathbf{x}$ satisfies $\gamma \subseteq \mathcal{S}_{\alpha,0}$ and case (2) of the assertion. If $x \in \mathcal{S}_{\alpha,-1}$, then γ has to cross $H_{\alpha,0}$ that separates $\mathbf{c_f} \in \mathcal{S}_{\alpha_i,0}$ and x. However, then γ cannot cross another α-hyperplane without exiting the strip $\mathcal{S}_{\alpha,0}$; and with $x \in \mathcal{S}_{\alpha,0}$ it has to end in the strip and therefore has to enter it again, which contradicts the minimality of γ. In particular, the crossing of the hyperplane $H_{\alpha,0}$ is the only crossing of an α-hyperplane that such a minimal gallery does, hence case (3) of the assertion.
Case 2: $\langle \lambda, \alpha_i^\vee \rangle \neq 0$. First, observe that $\mathbf{c_f}$ and $\mathbf{x}$ are separated by at least one hyperplane of class α, hence γ has to cross α-hyperplanes. Now it follows from the periodicity of ϕ that crossings of γ are either all positive or all negative: Suppose γ crosses not all α-hyperplanes in the same direction, that is, one hyperplane H_1 is crossed positively and another hyperplane H_2 (with $H_1 = H_2$ not forbidden) is crossed negatively. Since $\mathbf{x}$ is on the ε-side and $\mathbf{c_f}$ on the $-\varepsilon$-side of all α-hyperplanes separating them, this implies that γ is either crossing a hyperplane not separating $\mathbf{c_f}$ and $\mathbf{x}$, or crossing one of them more than once, both items contradicting the minimality of the gallery.
To prove the converse, let γ be a gallery that satisfies one of the stated conditions for every choice of positive root $\alpha \in \Phi^+$. We prove via contradiction that this gallery is minimal by showing that a non-minimal gallery fails all three of the stated conditions for at least one root α_i. Suppose γ is not minimal. Then γ crosses at least one hyperplane $H_{\alpha,k}$ with $k \in \mathbb{Z}$ more than once. Since ϕ is wall-consistent, a multiple crossed hyperplane is crossed at least once each in the positive and the negative direction. It follows immediately that γ fails the condition of crossings of α-hyperplanes being all positive or all negative for $\langle \lambda, \alpha^\vee \rangle \neq 0$, hence not case (1) of the assertion. However, γ also fails the conditions of not crossing an α-hyperplane, hence not case (2), or only crossing a single α-hyperplane once, hence also not case (3). This is a contradiction, hence γ has to be minimal. □

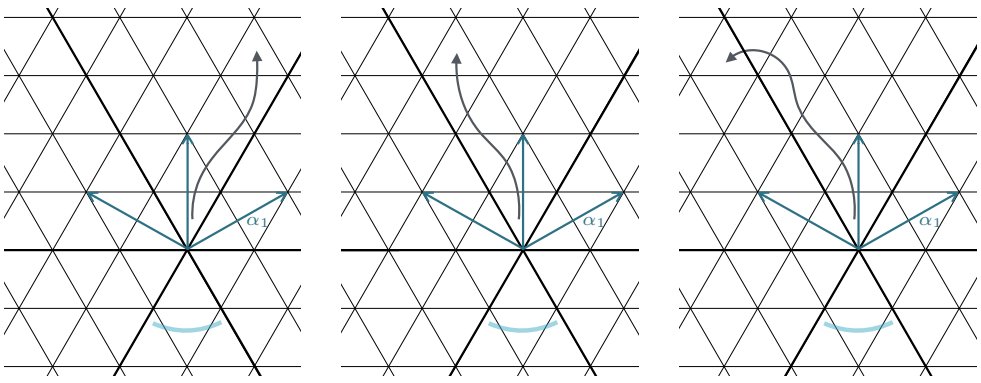

FIGURE 3.2. Examples of minimal galleries satisfying the three conditions of Lemma 3.1.14 with respect to the root α_1. The blue arc indicates the orientation defining Weyl chamber.

Example 3.1.15. Figure 3.2 shows examples of the three possible situations of crossings discussed in Lemma 3.1.14. The picture on the left shows a gallery ending in $x = t^\lambda w$ with $\langle \lambda, \alpha_1^\vee \rangle = 3$. It crosses two α_1-hyperplanes, with the second and the fourth panels. Both crossings are in the same direction.
The picture in the middle shows a minimal gallery ending in $x = t^\lambda w$ with $\langle \lambda, \alpha_1^\vee \rangle = 0$ and $\mathbf{w} \subseteq H^{\mathbf{c_f}}_{\alpha_1,0}$. That is $\gamma \subseteq \mathcal{S}_{\alpha_1,0}$, hence γ crosses no α_1-hyperplane.
The picture on the right shows a minimal gallery ending in $x = t^\lambda w$ with $\langle \lambda, \alpha_1^\vee \rangle = 0$ and $\mathbf{w} \nsubseteq H^{\mathbf{c_f}}_{\alpha_1,0}$. The gallery crosses $H_{\alpha_1,0}$ and no other α_1-hyperplane.

We now want to study the directions of crossings with respect to a given Weyl chamber orientation in more detail. Given $\lambda \in T$ and $\alpha \in \Phi^+$, observe that $\operatorname{sgn}(\langle \lambda, \alpha^\vee \rangle)$ only depends on the spherical Weyl chamber $\mathcal{C}_w$ which contains the lattice point λ. Hence, the direction of crossing α-hyperplanes with respect to a Weyl chamber orientation is the same for all minimal galleries in this chamber and can be deduced by checking if $\mathbf{w}$ is on the same side of $\mathcal{H}_{\alpha,0}$ as $\mathbf{c_f}$. We will discuss this in the following lemma.

Lemma 3.1.16 (Crossing directions of minimal galleries)**.** *Let (W, S) be an affine Coxeter system with corresponding spherical group W_0. Denote by $\Sigma = \Sigma(W, S)$ its Coxeter complex and let $\phi = \phi_w$ be the Weyl chamber orientation of Σ with respect to $w \in W_0$. Let further $\partial\phi_w$ be the alcove orientation of the spherical Coxeter complex $\partial\Sigma$ that induces ϕ_w. Then one has for all $v \in W_0$, $x \in \mathcal{C}_v$, and every minimal gallery $\gamma : \mathbf{c_f} \rightsquigarrow \mathbf{x}$ that crosses a hyperplane H: γ crosses H in Σ positively with respect to ϕ_w if and only if v is on the $\partial\phi_w$-negative side of the hyperplane ∂H in $\partial\Sigma$.*

Proof. Recall that since γ is minimal, no hyperplane is crossed more than once by the gallery, and it is reasonable to talk about *the* crossing of the hyperplane.
First, let $H_{\alpha,k}$ with $\alpha \in \Phi^+$, $k \in \mathbb{Z}$ be a hyperplane γ crosses in ϕ_w-positive direction in Σ. It follows that $x \in H^-_{\alpha,k}$, and with Lemma 3.1.14, condition (1) or (3), also $x \in H^-_{\alpha,0}$. Since $\mathcal{C}_v$ is bounded by $H_{\beta,0}$ for suitable $\beta \in \Phi^+$, it holds either $\mathcal{C}_v \subseteq H^+_{\alpha,0}$ or $\mathcal{C}_v \subseteq H^-_{\alpha,0}$. But we have seen that $x \in H^-_{\alpha,0}$, and with $x \in \mathcal{C}_v$ it follows $\mathcal{C}_v \subseteq H^-_{\alpha,0}$. With $\mathbf{v} \subseteq \mathcal{C}_v$, the claim now follows from the definition of induced spherical orientation on $\partial\Sigma$.
On the other hand, if v is on the $\partial\phi_w$-negative side of a hyperplane ∂H in $\partial\Sigma$, it follows from the definition of induced affine orientation that $\mathcal{C}_v \subseteq H^-_{\alpha,0}$, with α the parallelism class of the hyperplanes in Σ that belong to the hyperplane ∂H in the boundary. Since $x \in \mathcal{C}_v$, it holds $x \in H^-_{\alpha,0}$. Furthermore, since γ is minimal, with Lemma 3.1.14, case (1) or (3), we further have $x \in H^-_{\alpha,k}$ for all α-hyperplanes in Σ that γ crosses. □

See Figure 3.3 for an example. The result of Lemma 3.1.16 also applies to minimal galleries not starting in the fundamental alcove:

Corollary 3.1.17. *Let (W, S) be an affine Coxeter system with corresponding spherical group W_0. Denote by $\Sigma = \Sigma(W, S)$ its Coxeter complex and let $\phi = \phi_w$ be the Weyl chamber orientation of Σ with $w \in W_0$. Let further $\partial\phi_w$ be the alcove orientation of the spherical Coxeter complex $\partial\Sigma$ that induces ϕ_w. Then one has for all $u, v \in W_0$, $y = t^\mu u \in W$, $x \in \mathcal{C}_{\mu,v}$ and every minimal gallery $\gamma : \mathbf{y} \rightsquigarrow \mathbf{x}$ that crosses a hyperplane H:*

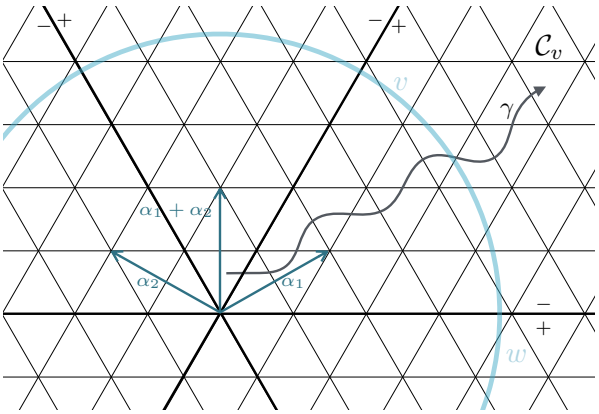

FIGURE 3.3. Visualization of Lemma 3.1.16. The light blue circle indicates the boundary sphere $\partial\Sigma$. The depicted gallery γ ends in $\mathcal{C}_v$. Since $v \in \partial\Sigma$ is on the $\partial\phi_w$-negative side of the horizontal hyperplane ∂H, crossings of horizontal hyperplanes of γ in Σ are positive. Since ∂v is on the $\partial\phi_w$-positive side of the boundary hyperplane corresponding to hyperplanes in Σ perpendicular to α_1, all crossings of α_1-hyperplanes of γ are ϕ_w-negative.

The crossing is ϕ_w-positive if and only if v is on the $\partial\phi_w$-negative side of the hyperplane ∂H in $\partial\Sigma$.

PROOF. Let $\gamma : \mathbf{y} \rightsquigarrow \mathbf{x}$ be a minimal gallery of type $s_{\gamma_1} s_{\gamma_2} \cdots s_{\gamma_n}$ and $\mathcal{H}_\gamma$ the set of crossed hyperplanes. Assume that $y = t^0 u$, that is, one vertex of the alcove $\mathbf{y}$ is the origin. Then $x \in \mathcal{C}_{0,v} = \mathcal{C}_v$. Let $\gamma_y : \mathbf{c_f} \rightsquigarrow \mathbf{y}$ be a minimal gallery with corresponding word $y = s_{y_1} s_{y_2} \cdots s_{y_m}$ and set of crossed hyperplanes $\mathcal{H}_y$. We distinguish two cases:
Case 1: $\mathcal{H}_y \cap \mathcal{H}_\gamma = \emptyset$. Then the concatenation $\gamma' := \gamma * \gamma_y : \mathbf{c_f} \rightsquigarrow \mathbf{x}$ is a minimal gallery. Application of Lemma 3.1.16 proves the assertion.
Case 2: $\mathcal{H}_y \cap \mathcal{H}_\gamma \neq \emptyset$. Then the concatenation $\gamma' := \gamma * \gamma_y : \mathbf{c_f} \rightsquigarrow \mathbf{x}$ is not a minimal gallery. We observe: For a hyperplane H, the following two assertions hold:

- $H \in \mathcal{H}_y$ if and only if $\mathbf{c_f}$ and $\mathbf{y}$ are on different sides of H and H contains the origin;
- $H \in \mathcal{H}_\gamma$ if $\mathbf{y}$ and $\mathbf{v}$ are on different sides of H; with equivalence if H contains the origin.

Hence for $H \in \mathcal{H}_y \cap \mathcal{H}_\gamma$, we have that $\mathbf{c_f}$ and $\mathbf{v}$ are on one side and $\mathbf{y}$ is on the other side of H. Furthermore, for hyperplanes H with $H \in \mathcal{H}_\gamma$ and $H \notin \mathcal{H}_y$ containing the origin, we have that $\mathbf{c_f}$ and $\mathbf{y}$ are together on one side of H and $\mathbf{v}$ is on the other side of H. Given this, let now H be a hyperplane crossed by γ. We consider the two possible situations:
Case 2A: $H \in \mathcal{H}_y \cap \mathcal{H}_\gamma$. Then H is crossed twice by γ', once in every concatenated part. With our observations from above and the periodicity of the orientation ϕ_w, this gives us that γ is crossing H ϕ_w-positively if and only if γ_y crosses H ϕ_w-negatively. With Lemma 3.1.16 this is equivalent to $\mathrm{sph}(y) = u$ being on the $\partial\phi_w$-positive side of ∂H in

$\partial\Sigma$. Moreover, as noted above, this holds if and only if v is on the $\partial\phi_w$ negative side of ∂H in $\partial\Sigma$, hence the claim.
Case 2B: $H \in \mathcal{H}_\gamma$ and $H \notin \mathcal{H}_y$. It follows from our observation above on $\mathbf{c_f}$ and $\mathbf{y}$ being on the same side of H, that a minimal gallery $\tilde{\gamma} : \mathbf{c_f} \rightsquigarrow \mathbf{x}$ crosses H in the same direction as γ. Hence γ crosses H ϕ_w-positively if and only if $\tilde{\gamma}$ crosses H ϕ_w-negatively. Application of Lemma 3.1.16 to $\tilde{\gamma}$ gives: $\tilde{\gamma}$ crosses H ϕ_w-positively if and only if v is on the $\partial\phi_w$ negative side of ∂H in $\partial\Sigma$. This proves the assertion.
To see now that this also holds for $y = t^\mu u$ with $\mu \neq 0$, let $\gamma_t : \mathbf{y} \rightsquigarrow t^0\mathbf{u}$ be a minimal gallery and consider $\gamma'' := \gamma * \gamma_t = t^{-\mu}(\gamma)$. Since ϕ_w is periodic, γ'' crosses all hyperplanes in the γ-part in the same direction as γ. The application of the results above to this part proves the claim. □

From Lemma 3.1.16 it follows that all minimal galleries with end alcoves in a common Weyl chamber show the same behavior in terms of crossing directions of parallel hyperplanes with respect to a Weyl chamber orientation ϕ_w. This will be crucial when it comes to positively folding these galleries, as we will see in the next section and Theorem 3.3.3 below.

3.2. Folded galleries and Coxeter shadows

In this section, we present our notation of folds and their positivity in Section 3.2.1. We introduce Coxeter shadows with respect to different orientations in Section 3.2.2, where we also discuss some fundamental properties.

3.2.1. Folds. We now introduce folded galleries. Although stated for alcove-to-alcove galleries here, notice that all definitions of this subsection also apply to alcove-to-vertex and vertex-to-vertex galleries.

Definition 3.2.1 (Folded gallery)**.** Let $\gamma = (\mathbf{c}_0, p_1, \mathbf{c}_1, \cdots, p_n, \mathbf{c}_n)$ be a gallery. If $\mathbf{c}_i = \mathbf{c}_{i-1}$ for some i, we say that the gallery is *stammering* and *folded at the panel* p_i, otherwise, we call it *unfolded*.

When considering only the end alcove, folding a gallery γ at a panel p_i is equivalent to deleting the letter $\tau(p_i) = s_{p_i}$ from the word for γ. But notice that every folded gallery γ', obtained from an unfolded gallery γ, satisfies: $\tau(\gamma') = \tau(\gamma)$. Geometrically, folding a gallery γ at a panel p_i reflects the remaining part of the gallery $\gamma_r := (\mathbf{c}_i, p_{i+1}, \cdots, p_n, \mathbf{c}_n)$ at the hyperplane H containing the panel p_i. The following definition of an explicit (un-)folding of a gallery is taken from [GS20, Def. 4.15] and states this more precisely:

Definition 3.2.2 ((Un-)Folding a gallery)**.** Let $\gamma = (\mathbf{c}_0, p_1, \mathbf{c}_1, \ldots, p_n, \mathbf{c}_n)$ be a gallery and denote by r_i the reflection across the wall H_{p_i} spanned by the panel p_i. Then we call

$$\gamma^i := (\mathbf{c}_0, p_1, \mathbf{c}_1, \ldots, p_i, r_i\mathbf{c}_i, r_ip_{i+1}, r_i\mathbf{c}_{i+1}, \ldots, r_ip_n, r_i\mathbf{c}_n)$$

a *(un-)folding of γ at the panel p_i*.

We want to study folded galleries in relation to orientations of Σ:

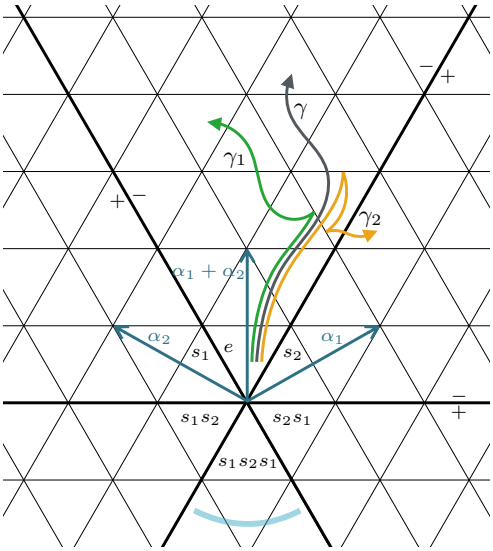

FIGURE 3.4. Folded galleries.

Definition 3.2.3 (Positive/negative folds)**.** Let ϕ be an orientation of the Coxeter complex Σ and $\gamma = (\mathbf{c}_0, p_1, \dots, p_n, \mathbf{c}_n)$ be a gallery in Σ. We say, that γ is *positively* (resp. *negatively*) *folded with respect to the orientation* ϕ *at the panel* p_i if $\mathbf{c}_i = \mathbf{c}_{i-1}$ and $\phi(p_i, \mathbf{c}_i) = +1$ (resp. $\phi(p_i, \mathbf{c}_i) = -1$). We say further, that γ is *positively* (resp. *negatively*) *folded with respect to the orientation* ϕ if for all $i \in \{1, \dots, n\}$ either $\mathbf{c}_i \neq \mathbf{c}_{i-1}$, that is γ is unfolded, or $\mathbf{c}_i = \mathbf{c}_{i-1}$ and $\phi(p_i, \mathbf{c}_i) = +1$ (resp. $\phi(p_i, \mathbf{c}_i) = -1$).

Note that it is possible to fold a gallery at several panels simultaneously and that foldings commute: $\left(\gamma^i\right)^j = \left(\gamma^j\right)^i$ and $\left(\gamma^i\right)^i = \gamma$. This was proven in [GS20, Lemma 4.17]. Denote the set of indices of panels, where γ has a fold in, by $F(\gamma)$. Since reflections are type preserving on Σ, it holds $\tau(\gamma) = \tau(\gamma^i)$. Depending on whether γ was already folded at the panel p_i, the *number of folds* $|F(\gamma)|$ of the gallery γ increases or decreases by one for each folding. Given this, it is reasonable to introduce notation for galleries of the same type being folded onto each other: We will denote $\gamma \rightharpoonup \mu$ for $\mu = \gamma^I$ with index set $I \subseteq \{1, \dots, n\} \setminus F(\gamma)$. If in this notation the gallery γ is folded positively with respect to a given orientation ϕ, we represent this by labeling the arrow with ϕ, written as $\gamma \overset{\phi}{\rightharpoonup} \mu$.

Example 3.2.4. Figure 3.4 shows two galleries γ_1 and γ_2 obtained by folding the grey gallery γ. γ_1 is folded once at the fourth panel. With respect to the Weyl chamber orientation defined by $s_1 s_2 s_1 = w_0 \in \partial\Sigma$, this fold is positive, since the repeated alcove is on the positive side of the α_1-hyperplane containing the fourth panel. γ_2 is folded twice at the fifth and sixth panels. The fold at the fifth panel is positive with respect to ϕ_{w_0}, but the second fold is negative: The repeated sixth and seventh alcove of γ_2 is on the negative side of the α_1-hyperplane containing the sixth panel. Hence γ_2 is not positively folded with respect to ϕ_{w_0}.

The positivity of a fold with respect to a Weyl chamber orientation ϕ_w only depends on the parallelism class of the hyperplane the folds panel is contained in. With our

results from Lemma 3.1.16 above, that galleries ending in the same Weyl chamber cross parallel hyperplanes in the same crossing direction, we conclude that the set of hyperplane classes these galleries can be folded in positively must coincide. Hence we introduce the following:

Definition 3.2.5 ((Positive) Folding pattern)**.** Let γ be a gallery that is obtained from a minimal gallery by performing n folds. If the i-th fold, counted with a rising index number, is in a panel that has a supporting hyperplane in the parallelism class α_j for a positive root α_j, then we call the n-tuple $(\alpha_{j,i})_{i\in[n]}$ the *folding pattern* of the gallery γ. If the Coxeter complex $\Sigma = \Sigma(W, S)$ is equipped with a periodic orientation ϕ and all foldings in a folding pattern $(\alpha_{j,i})_{i\in[n]}$ are positive with respect to ϕ, we call this a *ϕ-positive folding pattern.*

Remark 3.2.6. Sometimes we refer to folding patterns as a sequence of folds within fixed parallelism classes of hyperplanes without specifying a gallery. In this case, we say that a pattern $(\alpha_{j,i})_{i\in[n]}$ *applies to a minimal gallery*, if the minimal gallery can be folded such that the folded gallery has the folding pattern $(\alpha_{j,i})_{i\in[n]}$. Note that, as a consequence, it might be impossible to apply a fixed folding pattern to a minimal gallery, because, e.g., the gallery is too short. If a folding pattern applies to a minimal gallery, restricting to periodic orientations of Σ when defining positive folding patterns allows the application of a pattern to arbitrary crossed hyperplanes of the given parallelism class for a fixed gallery γ while keeping the positivity.

3.2.2. Coxeter Shadows. The concept of Coxeter shadows was first introduced by Graeber and Schwer in their article [GS20]. For our work, we will adopt their definition and present it below. To clarify the notion of Coxeter shadows, we first need to introduce braid-invariant orientations. These orientations are motivated by the work of Matsumoto [Mat64] and Tits [Tit69], who proved in the 1960s that different reduced expressions for a given element $x \in W$ can be transformed into each other through a sequence of braid moves. Therefore, it is desirable to have compatibility between positively folding a gallery with respect to an orientation and modifying the gallery by braid moves on the underlying word while keeping the folds positioned at the same panel indices. Braid-invariant orientations, as introduced in [GS20], fulfill this requirement.

Definition 3.2.7 (Braid-invariant orientation)**.** Let Σ be a Coxeter complex and ϕ an orientation of Σ. We say, that ϕ is *braid-invariant* if for every two braid equivalent words v, w in S with corresponding galleries γ and γ' and every $x \in W$ one has $\gamma \xrightarrow{\phi} \gamma_x$ if and only if $\gamma' \xrightarrow{\phi} \gamma_x$.

Thus, for a braid-invariant orientation we introduce the simple notation $x \xrightarrow{\phi} y$ for $x, y \in W$ to express that there exists a minimal gallery $\gamma_x : \mathbf{c_f} \rightsquigarrow \mathbf{x}$ which can be ϕ-positively folded onto a gallery $\gamma_y : \mathbf{c_f} \rightsquigarrow \mathbf{y}$ corresponding to a word for y.
In general, orientations are not braid-invariant. However, it can be shown that the Weyl chamber orientations introduced in Definition 2.2.36 above are indeed braid-invariant. For a proof, refer to [GS20, Prop. 5.4].

With this, we are ready to give the definition of Coxeter shadows, following [GS20].

Definition 3.2.8 (Coxeter shadow)**.** Let (W, S) be a Coxeter system with Coxeter complex $\Sigma(W, S)$ and ϕ an orientation of Σ. We define the *Coxeter shadow* of a word w in S with respect to ϕ as

$$\mathrm{Sh}_\phi(w) := \left\{ y \in W |\ \gamma_w \overset{\phi}{\rightharpoonup} \gamma_y \right\},$$

where γ_w denotes the gallery associated to the word w and $\gamma_y : \mathbf{c_f} \rightsquigarrow \mathbf{y}$.
If ϕ is braid-invariant, we define $\mathrm{Sh}_\phi(x) := \mathrm{Sh}_\phi(w)$ for any choice of a reduced expression w for $x \in W$.

There is an interesting connection between Coxeter shadows and Bruhat order (see Section 2.2.3) that follows from the subword property (see Proposition 2.2.17) and allows us to use Coxeter shadows to describe intervals of the form $[1, x]$ in Bruhat order. A proof of this result can be found in [GS20, Prop. 6.8].

Proposition 3.2.9. *Let (W, S) be a Coxeter system and $x, y \in W$. Denote by $\phi_{\mathbf{c_f}}$ the alcove orientation towards the fundamental alcove, and by ϕ_+ the trivial positive orientation. Then one has*

$$x \geq y \Leftrightarrow x \overset{\phi_{\mathbf{c_f}}}{\rightharpoonup} y \Leftrightarrow x \overset{\phi_+}{\rightharpoonup} y.$$

In particular, $\mathrm{Sh}_{\phi_{\mathbf{c_f}}}(x) = \mathrm{Sh}_{\phi_+}(x) = [1, x]$.

Open question 3.2.10. One can also use Coxeter shadows to describe other intervals $[x, y]$ in Bruhat order (cf. [GS20, Remark 6.10]). For this, consider $\mathrm{Sh}_{\phi_+}(y)$ and derive all elements represented by alcoves $\mathbf{z} \in \mathrm{Sh}_{\phi_+}(y)$, such that a minimal gallery $\gamma : \mathbf{c_f} \rightsquigarrow \mathbf{z}$ can be folded onto $\mathbf{x}$. Motivated by these results, it is an open question to describe connections between Coxeter shadows and other order relations.

One natural modification of the notion of Coxeter shadows is to consider vertex-to-vertex galleries instead of galleries ending in an alcove. For this, we introduce:

Definition 3.2.11 (Vertex shadow)**.** Let (W, S) be a Coxeter system with Coxeter complex $\Sigma(W, S)$ and ϕ a braid-invariant orientation of Σ. Let $x \in W$, $\lambda \in \Sigma$ a vertex, and $\gamma = (0, \mathbf{c_f}, p_1, \mathbf{c}_1, \ldots, p_n, \mathbf{c}_n, \lambda)$ a minimal vertex-to-vertex gallery. We define the *vertex shadow* of x as the set

$$\mathrm{Sh}^{\mathrm{vtx}}_\phi(x) := \left\{ \mathrm{vtx}(y) \in W |\ \gamma_x \overset{\phi}{\rightharpoonup} \gamma_y \right\},$$

where $\gamma_x : \mathbf{c_f} \rightsquigarrow \mathbf{x}$ denotes a minimal alcove-to-alcove gallery and $\gamma_y : \mathbf{c_f} \rightsquigarrow \mathbf{y}$ is an alcove-to-alcove gallery. We further define the *vertex shadow* of the vertex λ with respect to ϕ as

$$\mathrm{Sh}^{\mathrm{vtx}}_\phi(\lambda) := \left\{ \mu \in \Sigma |\ \exists \gamma_\mu \text{ with } \mathrm{vtx}(\gamma_\mu) = \mu,\ \tau(\gamma_\mu) = \tau(\gamma_\lambda) \text{ and } \gamma_\lambda \overset{\phi}{\rightharpoonup} \gamma_\mu \right\},$$

where γ_μ denotes a vertex-to-vertex gallery $\gamma_\mu : 0 \rightsquigarrow \mu$.

Remark 3.2.12. Given $\mathrm{Sh}_\phi(x)$ and the set of galleries $\gamma_y : \mathbf{c_f} \rightsquigarrow \mathbf{y}$ for $y \in \mathrm{Sh}_\phi(x)$ constructed to obtain the shadow for $x = t^\lambda w \in W$ and an orientation ϕ, it is straightforward to obtain the vertex shadow $\mathrm{Sh}^{\mathrm{vtx}}_\phi(\lambda)$. This can be achieved by considering the canonically associated alcove-to-vertex galleries $\gamma_y^\sharp$ and collecting their end vertices.

From this observation, the next lemma follows immediately.

Lemma 3.2.13. *Let (W,S) be a Coxeter system with Coxeter complex $\Sigma(W,S)$ and ϕ a braid-invariant orientation of Σ. Let further $x = t^\lambda w$, $y = t^\lambda v \in W$. Then $\mathrm{Sh}_\phi^{\mathrm{vtx}}(x) = \mathrm{Sh}_\phi^{\mathrm{vtx}}(y)$.*

PROOF. Notice that the sets $\mathcal{H}_x$ and $\mathcal{H}_y$ of hyperplanes crossed by minimal galleries $\gamma_x : \mathbf{c_f} \rightsquigarrow \mathbf{x}$ and $\gamma_y : \mathbf{c_f} \rightsquigarrow \mathbf{y}$ only differ in hyperplanes containing λ. Furthermore, observe that points on a hyperplane are fixed under the reflection along this hyperplane. Now recall that folding a gallery at a panel p is reflecting the remaining part of the gallery along the supporting hyperplane of p. Together, this proves the assertion. □

We include a well-known observation on the geometry of vertex shadows here that follows from the theory of galleries in affine buildings:

Lemma 3.2.14. *Let (W,S) be an affine Coxeter system with associated spherical Weyl group W_0. Furthermore, let the corresponding Coxeter complex be equipped with an orientation ϕ. Fix $\lambda \in T$. Then $\mathrm{Sh}_\phi^{\mathrm{vtx}}(\lambda) \subseteq \mathrm{conv}^*(W_0.\lambda)$, where conv^* denotes the Euclidean convex hull.*

PROOF. This follows from [Hit10, Prop. 3.2] with the observation that every affine Coxeter complex is an apartment in a thick affine building. □

We visualize a shadow $\mathrm{Sh}_\phi(x)$, resp. $\mathrm{Sh}_\phi^{\mathrm{vtx}}(\lambda)$, as the set of end alcoves $\mathbf{y}$ (resp. end vertices) of galleries that can be obtained by positively folding a minimal gallery $\gamma_x : \mathbf{c_f} \rightsquigarrow \mathbf{x}$, resp. $\gamma_\lambda : 0 \rightsquigarrow \lambda$.

Example 3.2.15. Consider $x_1 = t^\lambda s_2 \in W_{\tilde{\mathbf{A}}_2}$ with $\lambda = 2\alpha_1 + 2\alpha_2$ that we already studied as the end alcove of the minimal gallery presented in Figure 3.4, and $x_2 = t^\lambda s_1 s_2$. With respect to the Weyl chamber orientation ϕ_{w_0} induced by $w_0 \in W_0$, the corresponding Coxeter shadows are illustrated in Figure 3.5. We observe that both Coxeter shadows appear as subsets of the Bruhat interval $[1, x_1]$ and $[1, x_2]$, respectively, which equals the Coxeter shadow with respect to the trivial positive orientation.
To compute the vertex shadow $\mathrm{Sh}_{\phi_{w_0}}(\lambda)$, following Definition 3.2.11, we have two options: Either we consider the gallery $\gamma^\sharp : \mathbf{c_f} \rightsquigarrow \lambda$ and compute the set of end vertices of ϕ_{w_0}-positively folded galleries. Alternatively, we can apply the vertex operator to all alcoves $\mathbf{y} \in \mathrm{Sh}_{\phi_{w_0}}(x_1)$. Invoking Lemma 3.2.13, we could also use $\mathrm{Sh}_{\phi_{w_0}}(x_2)$ for the second option. The set of coroot lattice points obtained both ways is the same and is illustrated as black dots in the pictures of Figure 3.5.

Open question 3.2.16. As stated here, Coxeter shadows are introduced for arbitrary Coxeter groups, but to date, they have not been studied in hyperbolic Coxeter groups. For this, it is necessary to implement the concept of braid-invariance for orientations of hyperbolic Coxeter complexes, which is open.

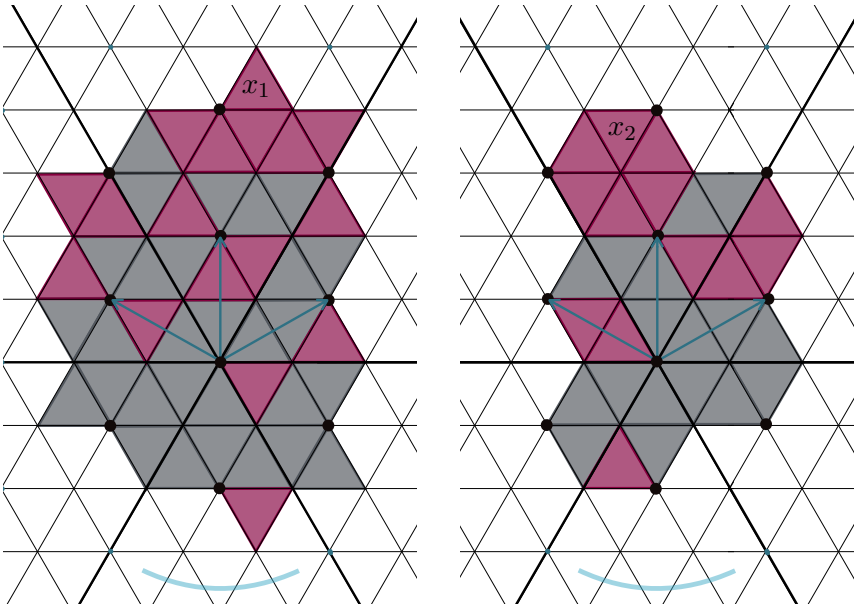

FIGURE 3.5. Coxeter shadows with respect to the Weyl chamber orientation ϕ_{w_0} of the group elements x_1 on the left and x_2 on the right. The direction of the Weyl chamber defining the orientation is indicated by the light blue arc. The elements of the shadow are highlighted as purple alcoves. The vertex shadows $\mathrm{Sh}^{\mathrm{vtx}}_{\phi_{w_0}(x_1)}$ and $\mathrm{Sh}^{\mathrm{vtx}}_{\phi_{w_0}(x_2)}$ coincide and are shown as black dots. The Bruhat intervals $[1, x_1]$ on the left, respective $[1, x_2]$ on the right are illustrated as grey and purple alcoves.

We continue with three observations on Coxeter shadows: one addressing a translation property, one considering their symmetries, and one developing a connection between shadows with respect to different orientations.

Translation of Coxeter shadows. In the following, let (W, S) be an affine Coxeter system and let the corresponding Coxeter complex $\Sigma = \Sigma(W, S)$ be equipped with a periodic orientation ϕ. We start with an example.

Example 3.2.17. Let $W = W_{\tilde{\mathtt{A}}_2}$ and let the Coxeter complex Σ be equipped with the Weyl chamber orientation ϕ_{w_0} induced by $w_0 \in W_0$. Figure 3.6 shows the Coxeter shadows of the three group elements $x_1, x_2, x_3 \in W$. Observe that a translation of the Coxeter shadow of $x_1 = t^{\lambda} s_2$ with $\lambda = 2\alpha_1^\vee + 2\alpha_2^\vee$ is contained in the two other Coxeter shadows. For $x_2 = t^{\mu} s_2$ with $\mu = 3\alpha_1^\vee + 3\alpha_2^\vee$, we observe $t^{\alpha_1^\vee} t^{\alpha_2^\vee}(\mathrm{Sh}_{\phi_{w_0}}(x_1)) \subseteq \mathrm{Sh}_{\phi_{w_0}}(x_2)$. For $x_3 = t^{\xi} s_2$ with $\xi = 4\alpha_1^\vee + 3\alpha_2^\vee$, we observe $t^{2\alpha_1^\vee} t^{\alpha_2^\vee}(\mathrm{Sh}_{\phi_{w_0}}(x_1)) \subseteq \mathrm{Sh}_{\phi_{w_0}}(x_3)$. Furthermore, notice that no translation of $\mathrm{Sh}_{\phi_{w_0}}(x_2)$ is contained in $\mathrm{Sh}_{\phi_{w_0}}(x_3)$.

The following proposition describes our observations from Example 3.2.17.

Proposition 3.2.18 (Translation of Coxeter Shadows)**.** *Let (W, S) be an affine Coxeter system and let the corresponding Coxeter complex $\Sigma = \Sigma(W, S)$ be equipped with a periodic orientation ϕ. Let $x \in W$, and $w_x = w_y w_z$ be a reduced expression for x, such*

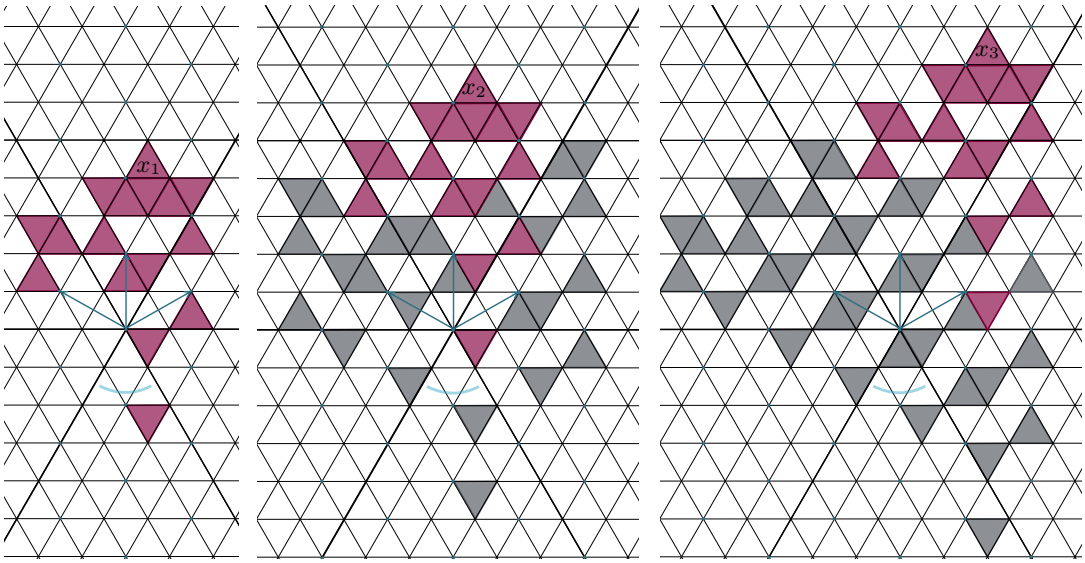

FIGURE 3.6. Coxeter shadows of $x_1, x_2, x_3 \in W_{\tilde{\mathbf{A}}_2}$ with respect to the Weyl chamber orientation ϕ_{w_0}. The orientation defining Weyl chamber is indicated by the light blue arc. A translation of the set of alcoves of $\mathrm{Sh}_{\phi_{w_0}}(x_1)$ is contained in $\mathrm{Sh}_{\phi_{w_0}}(x_2)$ and $\mathrm{Sh}_{\phi_{w_0}}(x_3)$. The corresponding alcoves are marked purple.

that w_y is a reduced expression for the translation $y = t^\lambda$ with $\lambda \in T$, and w_z a reduced expression for $z \in W$. Then $y(\mathrm{Sh}_\phi(z)) \subseteq \mathrm{Sh}_\phi(x)$.

PROOF. Let $a \in \mathrm{Sh}_\phi(z)$. Then we find a minimal gallery $\gamma_z : \mathbf{c_f} \rightsquigarrow \mathbf{z}$ that can be ϕ-positively folded onto a gallery $\gamma_a : \mathbf{c_f} \rightsquigarrow \mathbf{a}$. Now let $\gamma_y : \mathbf{c_f} \rightsquigarrow \mathbf{y}$ be a minimal gallery of type w_y. Since $w_x = w_y w_z$ is reduced, the concatenation $\gamma := \gamma_z * \gamma_y$ is also a minimal gallery with $\gamma : \mathbf{c_f} \rightsquigarrow \mathbf{b}$. With Definition 3.1.9 follows $b = yz = x$. Moreover, since ϕ is periodic, the folds in the panels of γ_z are also positive in γ. In other words, the concatenation $\gamma' := \gamma_a * \gamma_y$ with $\gamma' : \mathbf{c_f} \rightsquigarrow y.\mathbf{a}$ is ϕ-positively folded. Hence $y.\mathbf{a} \in \mathrm{Sh}_\phi(x)$. □

Coxeter shadows and diagram automorphisms. Now let $\Sigma(W, S)$ be equipped with a Weyl chamber orientation ϕ_w induced by the chamber $w \in \partial\Sigma$.
It follows from the poset theoretic definition of Σ (cf. [AB08, Section 1.5.1]) that the Coxeter complex has reflection symmetries with respect to its hyperplanes. However, Σ has even more symmetries, and we can describe some in terms of *diagram automorphisms* (cf. [Dav08, Def. 9.1.6]).

Definition 3.2.19. Let (W, S) be a Coxeter system. An automorphism $f : W \to W$ with $f(S) = S$ is called *diagram automorphism*. We denote by $\mathrm{Aut}(\Gamma_W)$ the group of diagram automorphisms of W.

A diagram automorphism is a permutation of the generators S that is induced by an automorphism of the underlying Coxeter diagram Γ_W. It is determined by $f|_S$: For any

group element $w \in W$, choose a reduced expression $w = (s_{w_1} \cdots s_{w_n})$ and compute the image under f as $f(w) = f(s_{w_1} \cdots s_{w_n}) = f(s_{w_1}) \cdots f(s_{w_n})$. Note, that f preserves the Coxeter matrix: $m(s,t) = m(f(s), f(t)) \quad \forall s, t \in S$.

We want to study Coxeter shadows under the application of diagram automorphisms. To prepare for this, we need to prove the following two lemmas.

Lemma 3.2.20. *Let (W,S) be a Coxeter system with Coxeter complex $\Sigma = \Sigma(W,S)$ and $f : W \to W$ a diagram automorphism of W. Then f maps galleries in Σ onto galleries in $f(\Sigma)$.*

PROOF. We show that for two adjacent alcoves $\mathbf{c}, \mathbf{d}$ with common panel p the images $f(\mathbf{c})$ and $f(\mathbf{d})$ are adjacent along the panel $f(p)$ after applying f:
Since $\mathbf{c}$ and $\mathbf{d}$ are adjacent, we find $s_i \in S$ such that $\mathbf{c} = \mathbf{d} \cdot s_i$. Because f is a diagram automorphism, we have $f(\mathbf{c}) = f(\mathbf{d} \cdot s_i) = f(\mathbf{d}) \cdot f(s_i)$ with $f(s_i) \in S$. This proves that $f(\mathbf{c})$ and $f(\mathbf{d})$ are again adjacent with common panel $f(p)$ of type $f(s_i)$. □

For affine Coxeter groups of type $\tilde{\mathtt{A}}$, we have:

Lemma 3.2.21. *Let (W,S) be an affine Coxeter system of type $\tilde{\mathtt{A}}$, and let the Coxeter complex $\Sigma = \Sigma(W,S)$ be oriented by the Weyl chamber orientation ϕ_w. Denote by W_0 the associated spherical Weyl group. Then $\mathrm{Aut}(\Gamma_W)$ acts on the set of chamber-induced orientations of $\partial\Sigma$, i.e., $\mathrm{Aut}(\Gamma_W) \curvearrowright W_0$, via $f.\phi_w := \phi_{f(w)}$.*

PROOF. For $S = \{s_1, \ldots, s_n\}$, recall that Γ_W is a circle, and it has the symmetry group of a regular n-gon, which is $\mathtt{A}_{n-1}$ (compare Figure A.2). This implies that $\mathrm{Aut}(\Gamma_W) \cong W_0$. Let now $f \in \mathrm{Aut}(\Gamma_W)$. Then f induces an isometry φ of the Coxeter complex Σ, which, in turn, induces an isometry $\varphi_\partial : \partial\Sigma \to \partial\Sigma$. For $v \in \partial\Sigma$, it holds $\varphi_\partial(v) = w \in \partial\Sigma$. Remember that we can identify W_0 and $\partial\Sigma$. Regarding the isometry φ, let us consider $v, w \in \partial\Sigma$ with minimal expressions $v = s_{v_1} \cdots s_{v_n}$ and $w = s_{w_1} \cdots s_{w_m}$. Then $v \cdot w = u \in \partial\Sigma$ and $s_{v_1} \cdots s_{v_n} \cdot s_{w_1} \cdots s_{w_m}$ is a word for u. Furthermore, it holds $\varphi_\partial(v \cdot w) = \varphi_\partial((s_{v_1} \cdots s_{v_n}) \cdot (s_{w_1} \cdots s_{w_m})) = \varphi_\partial(s_{v_1} \cdots s_{v_n} \cdot s_{w_1} \cdots s_{w_m}) = \varphi_\partial(s_{v_1}) \cdots \varphi_\partial(s_{v_n}) \cdot \varphi_\partial(s_{w_1}) \cdots \varphi_\partial(s_{w_m}) = \varphi_\partial(u)$. This shows that φ acts on the set of Weyl chamber orientations via $\varphi.\phi_v = \phi_{\varphi(v)}$. □

Lemma 3.2.21 implies that the orientation ϕ_w of Σ is preserved:

Corollary 3.2.22. *Let ϕ_w be a Weyl chamber orientation of the affine Coxeter complex $\Sigma(W_{\tilde{\mathtt{A}}_n}, S)$. Let further f be a diagram automorphism of $\Gamma_{W_{\tilde{\mathtt{A}}_n}}$, and let $\phi_{f(w)}$ be the Weyl chamber orientation of Σ induced by $f(w) \in \partial\Sigma$. For all alcoves $\mathbf{c} \in \Sigma$ with panels $p \subseteq \mathbf{c}$, the following holds: If $\phi_w(p, \mathbf{c}) = +1$, then $\phi_{f(w)}(f(p), f(\mathbf{c})) = +1$.*

We are now ready to present our findings on the behavior of Coxeter shadows when applying diagram automorphisms.

Proposition 3.2.23. *Let (W,S) be an affine Coxeter system of type $\tilde{\mathtt{A}}$. Let $x \in W$ and ϕ_w be an orientation of $\Sigma = \Sigma(W,S)$ induced by $w \in \partial\Sigma$. Also, let $f : W \to W$ be a diagram automorphism. Then we have the following equality:*

$$f\left(\mathrm{Sh}_{\phi_w}(x)\right) = \mathrm{Sh}_{\phi_{f(w)}}\left(f(x)\right).$$

In particular, it holds $f\left(\mathrm{Sh}_{\phi_w}(x)\right) = \mathrm{Sh}_{\phi_w}\left(f(x)\right)$ if f fixes $w \in \partial\Sigma$.

Proof. First, let $\mathbf{z} \in f\left(\mathrm{Sh}_{\phi_w}(x)\right)$. Then we find $\mathbf{y} \in \mathrm{Sh}_{\phi_w}(x)$ and a corresponding ϕ_w-positively folded gallery $\gamma_y : \mathbf{c_f} \rightsquigarrow \mathbf{y}$ obtained from a minimal gallery $\gamma_x : \mathbf{c_f} \rightsquigarrow \mathbf{x}$ with $\gamma_x \overset{\phi_w}{\rightharpoonup} \gamma_y$, such that $\mathbf{z} = f(\mathbf{y})$. Let $\tau(\gamma_x) = s_1 \cdots s_n$ and $\hat{\tau}(\gamma_y) = s_1 \cdots s_{i-1}\hat{s}_i s_{i+1} \cdots s_n$. If γ_y has multiple folds, apply the following arguments to all folds. Since $\mathbf{y}$ and $\mathbf{z}$ are uniquely determined by the decorated type of γ_y, and f is an automorphism, we have

$$z = f(s_1 \cdots s_{i-1}\hat{s}_i s_{i+1} \cdots s_n) = f(s_1)f(s_2)\cdots f(s_{i-1})f(\hat{s}_i)f(s_{i+1})\cdots f(s_n).$$

This word corresponds to a gallery γ_z that can be obtained from the gallery $\gamma_{f(x)} : \mathbf{c_f} \rightsquigarrow f(\mathbf{x})$ with $\tau(\gamma_{f(x)}) = f(s_1)\cdots f(s_n)$ by folding at the panel p_i. Invoking Lemma 3.2.21 shows that the fold at the panel p_i is positive with respect to the Weyl chamber orientation $\phi_{f(w)}$, hence $\mathbf{z} \in \mathrm{Sh}_{\phi_{f(w)}}(f(x))$.

On the other hand, let $\mathbf{z} \in \mathrm{Sh}_{\phi_{f(w)}}\left(f(x)\right)$. Then we find a minimal gallery $\gamma_{f(x)} : \mathbf{c_f} \rightsquigarrow f(\mathbf{x})$ that can be positively folded onto a gallery $\gamma_z : \mathbf{c_f} \rightsquigarrow \mathbf{z}$ with respect to $\phi_{f(w)}$. If γ_z has multiple folds, apply the following arguments to all folds. For the type of $\gamma_{f(x)}$ it holds $\tau\left(\gamma_{f(x)}\right) = f(x) = f(s_1 \cdots s_n) = f(s_1)\cdots f(s_n)$. The factorization is permissible, since f is a diagram automorphism. By definition of the Coxeter shadow, γ_z has the same type and the decorated type

$$\hat{\tau}(\gamma_z) = f(s_1)\cdots f(s_{i-1})f(\hat{s}_i)f(s_{i+1})\cdots f(s_n) = f(s_1 \cdots s_{i-1}\hat{s}_i s_{i+1} \cdots s_n).$$

Hence the type of γ_z is the f-image of the type of a gallery $\gamma_y : \mathbf{c_f} \rightsquigarrow \mathbf{y}$ with $\hat{\tau}(\gamma_y) = s_1 \cdots s_{i-1}\hat{s}_i s_{i+1} \cdots s_n$ and $\tau(\gamma_y) = s_1 \cdots s_n = x$. Furthermore, γ_y can be obtained from $\gamma_x : \mathbf{c_f} \rightsquigarrow \mathbf{x}$ with $\tau(\gamma_x) = s_1 \cdots s_n$ by folding at the panel p_i. Since the fold in γ_z was $\phi_{f(w)}$-positiv, Lemma 3.2.21 ensures that the fold in γ_y is positiv with respect to ϕ_w. This implies $\gamma_x \overset{\phi_w}{\rightharpoonup} \gamma_y$ and $\mathbf{y} \in \mathrm{Sh}_{\phi_w}(x)$. It follows $\mathbf{z} \in f\left(\mathrm{Sh}_{\phi_w}(x)\right)$. □

Example 3.2.24. Consider $W_{\tilde{\mathtt{A}}_2}$ with $S = \{s_1, s_2, s_0\}$ and fix the Weyl chamber $w = s_2 \in W_0$. Let $f : W_{\tilde{\mathtt{A}}_2} \to W_{\tilde{\mathtt{A}}_2}$ be the diagram automorphism defined by $f(s_1) = s_2$, $f(s_2) = s_1$ and $f(s_0) = s_0$. Compare also Figure A.2 for the Coxeter diagram of $W_{\tilde{\mathtt{A}}_2}$. Consider $x = s_1 s_2 s_0 s_2 s_1 s_2 s_0 s_2$. The left picture of Figure 3.7 shows a minimal gallery $\gamma_x : \mathbf{c_f} \rightsquigarrow \mathbf{x}$ and $\mathrm{Sh}_{\phi_w}(x)$ with respect to the orientation induced by the Weyl chamber w. Applying the diagram automorphism f to $\Sigma(W,S)$, its boundary complex $\partial\Sigma$, and $\mathrm{Sh}_{\phi_w}(x)$ leads to the set of alcoves shown in the picture on the right. This is the same set of alcoves as obtained by applying f to x, obtaining $f(x) = s_2 s_1 s_0 s_1 s_2 s_1 s_0 s_1$, and to w, obtaining $f(w) = s_1$, and computing the shadow $\mathrm{Sh}_{\phi_{f(w)}}(f(x))$ with respect to the (different) orientation induced by the Weyl chamber $f(w)$.

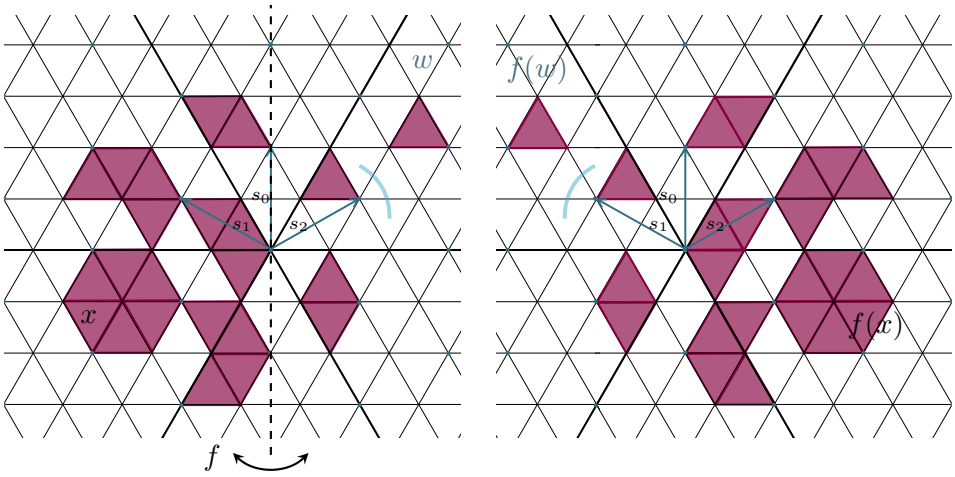

FIGURE 3.7. Illustration of the symmetry of a Coxeter shadows in $W_{\tilde{\mathbf{A}}_2}$ under the diagram automorphism $f : W \to W$. The blue arc indicates the orientation defining Weyl chamber. *On the left:* $\mathrm{Sh}_{\phi_w}(x)$. *On the right:* $f(\mathrm{Sh}_{\phi_w}(x)) = \mathrm{Sh}_{f(\phi_w)}(f(x))$.

Relation between chimney and Weyl chamber shadows. We conclude this section with a connection between Coxeter shadows with respect to Weyl chamber orientations and chimney-induced orientations. Notice that it was shown in [Mil+24, Prop. 3.28] that chimney-induced orientations are braid-invariant, which ensures that Coxeter shadows $\mathrm{Sh}(x)$ for group elements x are well-defined with respect to these orientations.
We begin by defining our notation for these Coxeter shadows, which we adopt from [Mil+24, Def. 3.29], where the authors introduced shadows with respect to chimney orientations in a more general setting.

Notation 3.2.25 (Chimney shadows)**.** Let (W, S) be an affine Coxeter system. Let $J \subseteq \{1, \dots, n\}$ and $x, y \in W$. We denote the Coxeter shadow of x with respect to the (J, y)-orientation by $\mathrm{Sh}_{J,y}(x)$. We will also refer to $\mathrm{Sh}_{J,y}(x)$ as the (J, y)-*chimney shadow*. Note that with the amalgamations explained in Definition 3.2.11 and Remark 3.2.12, it is also possible to study (J, y)-chimney shadows of vertices.

Remark 3.2.26. Chimney shadows are closely linked to the study of affine buildings. One can show that the chimney shadow of an element $x \in W$ for an affine Coxeter system (W, S) is the image of a chimney retraction applied to the pre-image of a retraction centered at $\mathbf{c_f}$ in a thick affine building. In a different context, this observation already appeared in [Hit10] and was later explored in more detail in [Mil+24].

We continue with an example of chimney shadows.

Example 3.2.27. Consider $x, y \in W_{\tilde{\mathbf{A}}_2}$ where $x = t^{\lambda}e$ and $\lambda = 3\alpha_1^\vee + 3\alpha_2^\vee$. Let $y = t^{\mu}e$ with $\mu = 2\alpha_2^\vee - 3\alpha_1^\vee$ and $z = t^{\nu}e$ with $\nu = \alpha_1^\vee + \alpha_2^\vee$. Let $J = 1$, and therefore $\Phi_J = \{\alpha_1\}$. The left picture of Figure 3.8 illustrates $\mathrm{Sh}_{1,y}(x)$ and $\mathrm{Sh}_{\phi_w}(x)$ for $w = s_2 s_1$. Observe that the sector $(1, y)$ does not intersect the polytope in Σ defined by the Weyl orbit $W_0.\lambda$

and that the polytope and the sector can be separated by the wall $H_{\alpha_1,-7}$. Furthermore, notice that both shadows coincide.
The right picture of Figure 3.8 illustrates $\mathrm{Sh}_{1,z}(x)$ and $\mathrm{Sh}_{\phi_w}(x)$ for $w = s_2s_1$. In this case, the sector $(1, z)$ is located near $\mathbf{c_f}$ and intersects $\mathrm{conv}(W_0.\lambda)$. Here, we can see that $\mathrm{Sh}_{1,z}(x) \subsetneq \mathrm{Sh}_{\phi_w}(x)$. The set of alcoves missing from $\mathrm{Sh}_{1,z}(x)$ is contained within a cone that is cut off from $\mathrm{Sh}_{\phi_w}(x)$.

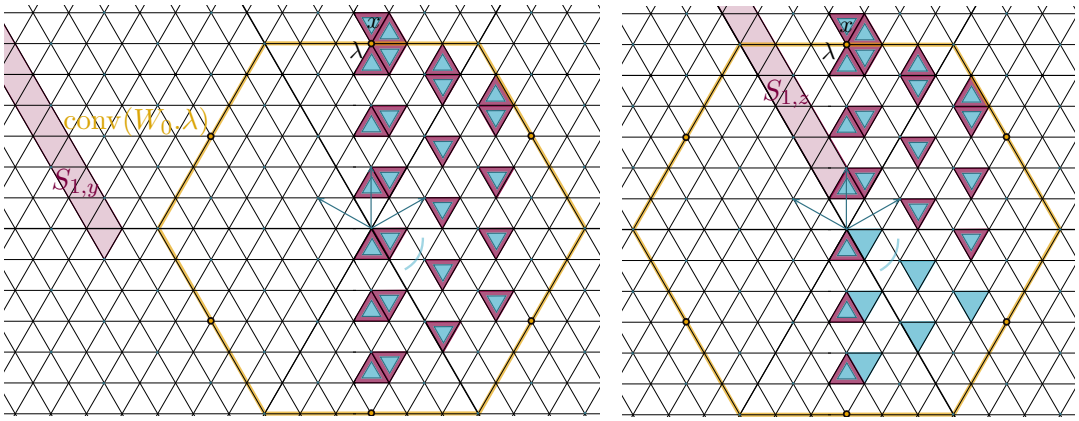

FIGURE 3.8. Coxeter shadows of $x = t^\lambda e$ with respect to chimney orientations (purple) and Weyl chamber orientations (blue). The orientation defining chimneys are illustrated as purple sectors $S_{1,y}$ and $S_{1,z}$ and the orientation defining Weyl chambers are indicated by the blue arc. The orange polytope illustrates the convex hull of the orbit $W_0.\lambda$.

Motivated by our observations in Example 3.2.27, we now prove that shadows with respect to Weyl chamber orientations are exceptional instances of chimney shadows, where the sectors are positioned *far away* from the gallery.

Proposition 3.2.28. *Let (W, S) be an affine Coxeter system. Let $J \subseteq \{1, \dots, n\}$ and $x, y \in W$ with $x = t^\lambda w$. Then $\mathrm{Sh}_{J,y}(x) = \mathrm{Sh}_{\phi_v}(x)$ for a Weyl chamber $v \in \partial\Sigma$, if the following two conditions hold:*

(i) For all positive roots $\alpha \in \Phi_J$, the (J, y)-sector can be strictly separated from the convex hull of the Weyl group orbit $\mathrm{conv}(W_0.\lambda)$ by a wall $H_{\alpha,k}$;

(ii) and for all positive roots $\alpha \in \Phi^+ \setminus \Phi_J$, the (J, y)-sector intersects the convex hull of the Weyl group orbit $\mathrm{conv}(W_0.\lambda)$ in a finite or empty set of alcoves.

Notice that $\mathrm{conv}(\cdot)$ denotes the convex hull in the Coxeter complex here.

PROOF. Let $\gamma_x : \mathbf{c_f} \rightsquigarrow \mathbf{x}$ be a minimal gallery and denote the (J, y)-sector by $\mathcal{J}$. Denote further $h_\alpha(\lambda) = \langle \lambda, \alpha^\vee \rangle$. Recall that we observed in Lemma 3.2.14 that for every orientation ϕ it holds $\mathrm{Sh}^{\mathrm{vtx}}_\phi(x) \subseteq \mathrm{conv}^*(W_0.\lambda)$. Here, $\mathrm{conv}^*(\cdot)$ denotes the Euclidean convex hull. This implies $\mathrm{Sh}^{\mathrm{vtx}}_\phi(x) \subseteq \mathrm{conv}(W_0.\lambda)$ and $\mathrm{Sh}_\phi(x) \subseteq \bigcap_{\alpha\in\Phi} H_{\alpha,h_\alpha(\lambda)+1} =: \mathcal{P}$. Denote by $\mathcal{H}$ the set of hyperplanes H with $H \cap \mathcal{P} \neq \emptyset$. Observe that all hyperplanes crossed by γ_x and galleries obtained by folding γ_x are contained in $\mathcal{H}$.

For $\alpha \in \Phi_J$, let $H_{\alpha,k}$ be a strictly separating hyperplane between $\mathcal{J}$ and $\mathrm{conv}(W_0.\lambda)$. Notice that $H_{\alpha,k}$ also separates $\mathcal{J}$ and $\mathcal{P}$, and that the side of $H_{\alpha,k}$ towards the halfspace $H^{\varepsilon}_{\alpha,k}$ with $\mathcal{P} \subseteq H^{\varepsilon}_{\alpha,k}$ is the $\phi_{J,y}$-positive side of $H_{\alpha,k}$. Now observe that for all $H_\alpha \in \mathcal{H}$ it holds $H_\alpha \subseteq H^{\varepsilon}_{\alpha,k}$. For all these hyperplanes, the side towards the half-space containing $\mathcal{J}$ is the negative side with respect to $\phi_{J,y}$.
For $\alpha \in \Phi^+ \setminus \Phi_J$, we find a wall $H_{\alpha,j}$ with $\mathcal{P} \subseteq H^{\varepsilon}_{\alpha,j}$ and $\mathcal{J} \cap H^{\varepsilon}_{\alpha}$ is empty or a finite set of alcoves. Let now $H_\alpha \in \mathcal{H}$. Then $H_\alpha \subseteq H^{\varepsilon}_{\alpha,j}$. Denote $H^{\varepsilon'}_{\alpha}$ for the half-space satisfying $H^{\varepsilon'}_{\alpha} \subseteq H^{\varepsilon}_{\alpha,j}$. Then the side of H_α towards the half-space $H^{\varepsilon'}_{\alpha}$ with $\mathcal{J} \cap H^{\varepsilon'}_{\alpha}$ being an empty or finite set of alcoves is the $\phi_{J,y}$-positive side of H_α.
Together, this shows that $\phi_{J,y}$ is periodic on the hyperplanes $\mathcal{H}$.
Now fix a coroot lattice point $\eta \in \mathcal{P}$ and let $H_{\alpha_1}, \dots, H_{\alpha_k}$ be the hyperplanes for the positive roots $\alpha_i \in \Phi^+$ containing η. It holds $H_{\alpha_1}, \dots, H_{\alpha_k} \in \mathcal{H}$. Denote by $H^+_{\alpha_i}$ the halfspaces towards the $\phi_{J,y}$-positive sides. The intersection $\bigcap_{i\in[k]} H^+_{\alpha_i}$ then defines a local Weyl chamber $\mathcal{C}_{\eta,v}$ with $\mathcal{J} \cap \mathcal{C}_{\eta,v}$ empty or finite. Since $\phi_{J,y}$ is periodic on $\mathcal{H}$, the Weyl chamber $v \in \partial\Sigma$ represented by $\mathcal{C}_{\eta,v}$ is the same for all $\eta \in \mathcal{P}$. It follows, that $\phi_{J,y} = \phi_v$ on $\mathcal{H}$, where ϕ_v denotes the Weyl chamber orientation induced by $v \in \partial\Sigma$. Since the shadow of x only depends on the orientation of the hyperplanes in $\mathcal{H}$, it follows the claim. □

Open question 3.2.29. As in Example 3.2.27, we observed that chimney shadows, which do not meet the assumptions of Proposition 3.2.28, are subsets of the Weyl chamber shadows with missing alcoves contained in a cone that is *cut off* from the shadow. It remains open question to describe these cones in relation to the chimney. Additionally, it would be interesting to precisely describe how the orientations of the hyperplanes change as a sector moves from being far away from the gallery to being closer to it.
Recall further, that every (J, y)-chimney ξ that is represented by a sector containing more than one alcove (and thus, containing infinitely many, cf. [Mil+24, Lemma 3.10]) is represented by sectors bounded by two adjacent hyperplanes of the same parallelism class. Since this parallelism class corresponds to a panel in the boundary complex $\partial\Sigma$, which lies within certain Weyl chambers, it might be worthwhile to study the chimney orientation $\phi_{J,y}$ in relation to these Weyl chamber orientations of Σ.

3.3. Connection to moment graphs

In this section, we point out two connections between the Bruhat moment graph of the spherical Weyl group W_0 associated with an affine Coxeter group W and the ϕ-positive folding patterns in W for a Weyl chamber orientation ϕ_w. We start by giving a general definition of a moment graph, following [Fie16]:

Definition 3.3.1 (Moment graph)**.** Let $\Lambda = \mathbb{Z}^r$ be a lattice. A moment graph $\mathcal{G}$ over Λ is a labeled simple directed graph $\mathcal{G} = (V, E)$ with vertices V, directed edges E, and labeling map $f_{\mathcal{G}} : E \to \Lambda \setminus \{0\}$.

The moment graphs that are important to us are the moment graphs obtained from Bruhat graphs. Refer to Definition 2.2.16 in Section 2.2.3 for our notion and notation. We already noted above in Proposition 3.2.9 that the Bruhat order has a geometric interpretation via galleries: For group elements $x, y \in W$ it holds $y \leq x$ in Bruhat order

if and only if a minimal gallery $\gamma_x : \mathbf{c_f} \rightsquigarrow \mathbf{x}$ can be folded onto a gallery $\gamma_y : \mathbf{c_f} \rightsquigarrow \mathbf{y}$ of the same type. We will prove another connection between Bruhat graphs and positive folding patterns of galleries below.

Since there is a 1-on-1 correspondence between reflections in W_0 and the positive roots of the affine Coxeter group W, each reflection r corresponds to one parallelism class of hyperplanes in the affine Coxeter group. Therefore, we can index the reflections with their affiliated positive root in W and obtain a moment graph:

Definition 3.3.2 (Bruhat moment graph)**.** Let (W_0, S_0) be a spherical Coxeter system with root system Φ and Φ^+ the set of positive roots. Recall, that we denote by $X := \mathbb{Z}\omega_1 \oplus \cdots \oplus \mathbb{Z}\omega_n$ the weight lattice. The labeled graph $\mathcal{G}_{W_0} = (V, E, \Phi^+)$ with vertex set $V = \{w : \ w \in W_0\}$ and edges $e = (u, w) \in E$ if and only if $l(u) < l(w)$ and $w = r_{\alpha_i}(u)$ for a reflection $r_{\alpha_i} \in R$ with $\alpha_i \in \Phi^+$ a positive root in W_0 is called the *Bruhat moment graph*. We set $f_{\mathcal{G}_{W_0}}(e = (u, w)) = \alpha_i$.

For example, the picture on the right of Figure 1.1 depicts the Bruhat moment graph of the Coxeter group of type $\mathtt{A}_2$.

3.3.1. Folding patterns and moment graphs. We can now present the main result of this chapter: The Bruhat graph encodes adjacency relations via reflections of group elements in W_0, and the labeling of the Bruhat moment graph gives the parallelism classes of the hyperplanes corresponding to these reflections. Because of the semidirect product structure of affine Coxeter groups, the reflections in W_0 encoded in the Bruhat graph each represent a class of reflections in parallel hyperplanes in the associated affine group W. For periodic orientations of its Coxeter complex Σ, it then suffices to study a single representative of a hyperplane class to understand the positivity of foldings in affine Coxeter groups, hence a Bruhat moment graph. This leads to the following connection:

Theorem 3.3.3 (Positive folding patterns and moment graph)**.** *Let (W, S) be an affine Coxeter system and W_0 the corresponding spherical Coxeter group with moment graph $\mathcal{G}_{W_0} = (V, E, \Phi^+_{W_0})$. Denote by Σ the affine Coxeter complex corresponding to (W, S) and let ϕ_{w_0} be the Weyl chamber orientation on Σ with $w_0 \in W_0$ the unique longest element. Let $x \in \mathcal{C}_v$ and $\gamma : \mathbf{c_f} \rightsquigarrow \mathbf{x}$ be a minimal gallery. Then $(\alpha_{j,i})_{i\in[n]}$ is a positive folding pattern for γ if and only if $(\alpha_{j,1}, \alpha_{j,2}, \ldots, \alpha_{j,n})$ is the label index sequence of a directed path in $\mathcal{G}_{W_0}$ starting in the vertex v.*

Before we present the proof, we first obtain a well-known result about the maximum number of positive folds of a minimal gallery with respect to a Weyl chamber orientation from this (cf. [GS20, Prop. 4.24]):

Corollary 3.3.4. *Let (W, S) be an affine Coxeter system and W_0 the corresponding spherical Coxeter group with unique longest element $w_0 \in W_0$. Let further γ be a gallery that is obtained by positively folding a minimal gallery with respect to the Weyl chamber orientation ϕ_{w_0}. Then one has for the number of folds $|F(\gamma)|$:*

$$|F(\gamma)| \leq l(w_0),$$

where l denotes the word length of an element in W_0.

PROOF. This follows immediately from Theorem 3.3.3 since no directed path in the Bruhat moment graph is longer than $l(w_0)$. □

Next, we will describe a connection between directed edges in the moment graph and the Weyl chamber orientation ϕ_{w_0} for $w_0 \in W_0$. This serves as a preparation for the proof of Theorem 3.3.3:

Lemma 3.3.5 (Bruhat moment graph and ϕ_{w_0})**.** *Let $\mathcal{G}_{W_0}$ be the moment graph corresponding to the spherical Coxeter group W_0 and affine Coxeter system (W, S), and let $u, w \in W_0$. Denote by $\partial\Sigma$ the Coxeter complex associated with W_0 in the boundary of Σ and by $\partial\phi_{w_0}$ the Weyl chamber orientation of $\partial\Sigma$ induced by the unique longest element $w_0 \in W_0$. Then there exists a directed edge $e = (u, w) \in \mathcal{G}_{W_0}$ if and only if the Weyl chamber $u \subseteq \partial\Sigma$ is on the $\partial\phi_{w_0}$-negative side and $w \subseteq \partial\Sigma$ is on the $\partial\phi_{w_0}$-positive side of the reflection hyperplane H_r with $w = r(u) = u \cdot r$, $r \in R$.*

PROOF. First, let $e = (u, w) \in \mathcal{G}_{W_0}$ be a directed edge from u to w in the moment graph of W_0. It follows that $w = u \cdot r$ for a reflection $r \in R$ and $l(u) < l(w)$. Observe with [Hum90, Section 1.8], that

$$\begin{aligned} l(u) < l(w) &\Leftrightarrow -l(u) > -l(w) \Leftrightarrow l(w_0) - l(u) > l(w_0) - l(w) \Leftrightarrow l(u^{-1}w_0) > l(w^{-1}w_0) \\ &\Leftrightarrow \mathrm{d}(u, w_0) > \mathrm{d}(w, w_0). \end{aligned}$$

Let ∂H_r be the hyperplane in the Coxeter complex $\partial\Sigma$ corresponding to r. The chambers u and w lie on opposite sides of ∂H_r and it follows from the definition of ϕ_{w_0} that w_0 is on the ϕ_{w_0}-positive side of ∂H_r. Hence, if $w = w_0$, w is on the ϕ_{w_0}-positive side of ∂H_r and there is nothing more to show. If $w \neq w_0$, we show that w is on the ϕ_{w_0}-positive side of ∂H_r via contradiction. Suppose that w is on the ϕ_{w_0}-negative side of $\partial\mathcal{H}_r$. Then u is on the ϕ_{w_0}-positive side of ∂H_r. And since w_0 is on the ϕ_{w_0}-positive side of all hyperplanes in $\partial\Sigma$, this implies $\mathrm{d}(u, w_0) < \mathrm{d}(w, w_0)$, because: Let $\gamma : w_0 \rightsquigarrow w$ be a minimal gallery in $\partial\Sigma$. Then we have $\ell(\gamma) = \mathrm{d}(w, w_0)$. Since ∂H_r separates w_0 and w, γ crosses ∂H_r with a panel p. Now fold γ at p to obtain the gallery γ'. Then γ' is stuttering, hence not minimal, and fully contained in the half-space defined by ∂H_r that contains w_0 and, since $w = u \cdot r$, $\gamma' : w_0 \rightsquigarrow u$. But then we can shorten γ' to obtain a minimal gallery $\gamma'' : w_0 \rightsquigarrow u$ with $\ell(\gamma'') < \ell(\gamma') = \ell(\gamma)$. With $\mathrm{d}(u, w_0) = \ell(\gamma'')$ follows the claim: $\mathrm{d}(u, w_0) < \mathrm{d}(w, w_0)$. But this is a contradiction. Hence w is on the ϕ_{w_0}-positive and u on the ϕ_{w_0}-negative side of ∂H_r.
To prove the converse, let u be on the ϕ_{w_0}-negative and w be on the ϕ_{w_0}-positive side of the hyperplane ∂H_r with $w = u \cdot r$ and $r \in R$. Then surely (u, w) or (w, u) is an edge of the moment graph $\mathcal{G}_{W_0}$, depending on whether $l(u) < l(w)$ or $l(w) < l(u)$. Since w is on the ϕ_{w_0}-positive side of the hyperplane ∂H_r, it follows from the definition of the orientation $\partial\phi_{w_0}$ that w and w_0 lie on the same side of the hyperplane ∂H_r. Because ∂H_r separates w and u, we see with the same argumentation as above that $\mathrm{d}(w, w_0) < \mathrm{d}(u, w_0)$. And with this, we have with [Hum90, Section 1.8] again:

$$\mathrm{d}(w, w_0) < \mathrm{d}(u, w_0) \Leftrightarrow l(u) < l(w).$$

Hence, $(u, w) \in \mathcal{G}_{W_0}$. □

With this, we are ready to prove Theorem 3.3.3:

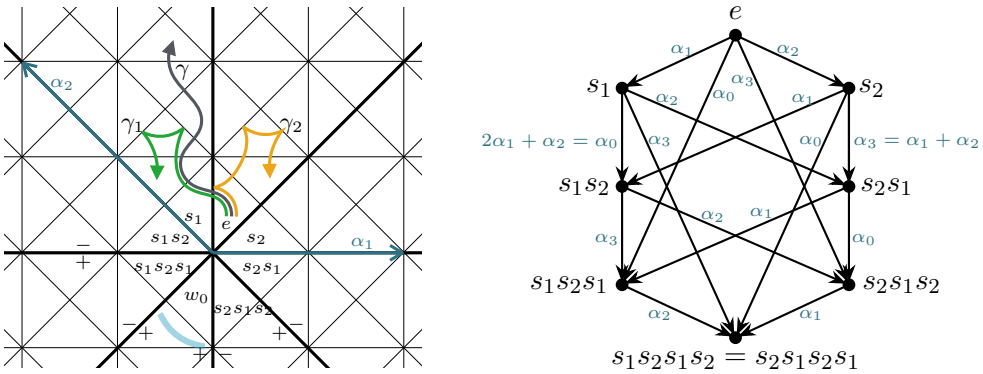

FIGURE 3.9. *On the left:* Coxeter complex of $\widetilde{\mathtt{B}}_2$ with folded galleries. *On the right:* Bruhat moment graph of $\mathtt{B}_2$.

PROOF OF THEOREM 3.3.3. First, let $(\alpha_{j,i})_{i\in[n]}$ be a positive folding pattern for γ. Suppose, $(\alpha_{j,i})_{i\in[n]}$ is not a label index sequence of a directed path in $\mathcal{G}_{W_0}$ starting in v. Then we find an index j,k with $k\in\{1,\dots,n\}$, such that $(\alpha_{j,1},\dots,\alpha_{j,k-1})$ is an index sequence of a directed path $\xi=(v,\dots,u)$ in $\mathcal{G}_{W_0}$ with v,u vertices, and $(\alpha_{j,1},\dots,\alpha_{j,k})$ is not. Consider the gallery γ' which is obtained from γ by application of the folding pattern $(\alpha_{j,i})_{i\in[k-1]}$ to a feasible choice of panels, such that γ' crosses at least one hyperplane of class $\alpha_{j,k}$ in the remaining unfolded part behind the last fold. If we can not find such a gallery, the folding pattern $(\alpha_{j,i})_{i\in[k]}$ does not apply to γ, and since the pattern $(\alpha_{j,i})_{i\in[k-1]}$ corresponded to a directed path in the graph $\mathcal{G}_{W_0}$ starting in v there is nothing to show. So we find such a gallery γ'. Denote the unfolded remaining part of the gallery γ' by $\gamma'_r:\mathbf{y}\rightsquigarrow\mathbf{z}$ with $y=t^\mu w$ and $z=t^\nu w'$. Since γ'_r is minimal and assumed to cross at least one hyperplane $H_{\alpha_{i,k},h}$ with $\alpha_{i,k}$ the next element in the positive folding pattern for γ, we know that $\mathbf{z}$ satisfies $\mathbf{z}\subseteq H^-_{\alpha_{i,k},h}$ with respect to the orientation ϕ_{w_0}. Hence we conclude with Corollary 3.1.17 that $\mathbf{z}\subseteq\mathcal{C}_{\mu,u'}$ with u' on the $\partial\phi_{w_0}$-negative side of the hyperplane $\partial H_{\alpha_{i,k},h}$ in $\partial\Sigma$. Then Lemma 3.3.5 shows that there is a directed edge e labeled $\alpha_{i,k}$ leaving the node u in the moment graph. So we can prolong the directed path ξ above with e such that the label index sequence $(\alpha_{i,1},\dots,\alpha_{i,k})$ does correspond to a directed path in the moment graph $\mathcal{G}_{W_0}$.
To prove the converse, let $(\alpha_{v_1},\alpha_{v_2},\dots,\alpha_{v_n})$ be the label index sequence of a directed path in $\mathcal{G}_{W_0}$ starting in the node labeled v. Then v is on the $\partial\phi_{w_0}$-negative side of the hyperplanes $\partial H_{\alpha_{v_i}}$ for $i\in\{1,\dots,n\}$. It follows from Lemma 3.1.16 that for a minimal gallery $\gamma\subseteq\mathcal{C}_v$ it holds: If γ crosses a corresponding hyperplane $H_{\alpha_{v_i},k}$ with $i\in\{1,\dots,n\}$ and $k\in\mathbb{Z}$ in Σ, then γ crosses this hyperplane from the ϕ_{w_0}-positive to the ϕ_{w_0}-negative side. Hence, we can fold the gallery γ with positive folding pattern $(\alpha_{v_1},\alpha_{v_2},\cdots\alpha_{v_n})$. □

Example 3.3.6. Figure 3.9 visualises Theorem 3.3.3. The grey unfolded minimal gallery γ on the left ends in $\mathcal{C}_{s_1}$. The galleries γ_1 and γ_2 are obtained from γ by folding it at the fourth and fifth, or the first, fourth, and fifth panels, respectively. Let ϕ_{w_0} be the Weyl chamber orientation defined by ∂w_0, marked with a light blue arc. With respect to ϕ_{w_0}, γ_1 is positively folded with folding pattern (α_0,α_2). This corresponds to the label sequence of a directed path in $\mathcal{G}_{\mathtt{B}_2}$ starting in the node s_1. The gallery γ_2 is folded with

folding pattern $(\alpha_1, \alpha_2, \alpha_0)$ as is obtained from γ_1 by adding the fold in the first panel. We read off from the moment graph $\mathcal{G}_{\mathtt{B}_2}$ depicted on the right of Figure 3.9 that this folding pattern does not correspond to a label sequence of a directed path in the graph starting in s_1. The gallery γ_2 is not positively folded with respect to ϕ_{w_0}, since the first fold is not positive. This also shows that when a new fold is added to a folded gallery before the existing folds, the positivity of these folds may be reversed.

With a modification of the moment graph, the results of Lemma 3.3.5 and Theorem 3.3.3 can be generalized to Weyl chamber orientations ϕ_w with $w \neq w_0$. Recall that in a Bruhat moment graph, directed paths correspond to minimal words in W_0 with the labels of the used edges giving the parallelism classes of the hyperplanes a gallery corresponding to this word is crossing.
Now imagine a minimal gallery in W_0 starting in $v \neq e$. Then, the end alcove of the longest minimal galleries will not be w_0, but the alcove w maximizing $\mathrm{d}(v, w)$. To represent this translation in folding patterns, we shift the labels of a Bruhat moment graph and obtain a modified moment graph:

Definition 3.3.7 (Modified moment graph)**.** Let $\mathcal{G}_{W_0} = (V, E, \Phi^+_{W_0})$ be a Bruhat moment graph with labels $f_{\mathcal{G}_{W_0}}(e = (u, w)) = \alpha_i$. Now let $\varphi : V \to V$ be a bijection on the set of vertex labels and $\psi : f_{\mathcal{G}_{W_0}}(E) \to f_{\mathcal{G}^{mod}_{W_0}}(E)$ a bijection on the set of edge labels, such that it holds:

$$\begin{aligned}
\{u, w\} \in E(\mathcal{G}_{W_0}) &\Leftrightarrow \{\varphi(u), \varphi(w)\} \in E(\mathcal{G}^{mod}_{W_0}) \text{ as undirected edges,}\\
(u, w) \in E(\mathcal{G}_{W_0}) &\Rightarrow (\varphi(u'), \varphi(w')) \in E(\mathcal{G}^{mod}_{W_0}) \text{ with } \varphi(u') = u, \varphi(w') = w,\\
f_{\mathcal{G}_{W_0}}(e = \{u, w\}) = \alpha_i &\Leftrightarrow f_{\mathcal{G}^{mod}_{W_0}}(\psi(e) = \{\varphi(u), \varphi(w)\}) = \alpha_i \text{ as undirected edges;}
\end{aligned}$$

That is, the labels of the Bruhat moment graphs are rotated. Let v be the vertex in the modified graph with no ingoing edges. Then we call the labeled graph $\mathcal{G}^{mod}_{W_0} = (\varphi(V), E)$ with edge labels $f_{\mathcal{G}^{mod}_{W_0}}(\psi(e) = (\varphi(u), \varphi(w))) = \alpha_j \in \Phi^+$ *modified moment graph with minimal element* v.

Analogous to Lemma 3.3.5, we draw a connection between a modified moment graph and ϕ_v:

Lemma 3.3.8 (Modified moment graph and ϕ_v)**.** *Let $\mathcal{G}^{mod}_{W_0}$ be the modified moment graph corresponding to a spherical Coxeter group W_0 with minimal element vw_0. Let (W, S) be the affine Coxeter system associated with W_0 with Coxeter complex $\Sigma = \Sigma(W, S)$ and let $u, w \in W_0$. Denote by $\partial\Sigma$ the Coxeter complex associated with W_0 in the boundary of Σ and by $\partial\phi_v$ the Weyl chamber orientation of $\partial\Sigma$ induced by $v \in W_0$. Then there is a directed edge $e = (u, w) \in \mathcal{G}^{mod}_{W_0}$ if and only if the Weyl chamber $u \subseteq \partial\Sigma$ is on the $\partial\phi_v$-negative side and $w \subseteq \partial\Sigma$ is on the $\partial\phi_v$-positive side of the reflection hyperplane H_r with $w = r(u) = u \cdot r$, $r \in R$.*

Proof. Notice that it follows from Definition 3.3.7 of a modified moment graph, that (undirected) incidences between vertices and their corresponding edge labels are preserved as in a Bruhat moment graph. Hence we have a directed edge $e = (u, w)$ or

$e = (w, u)$ in a modified moment graph $\mathcal{G}_{W_0}^{mod}$ with minimal element vw_0 if and only if u can be reflected onto w with $w = r(u) = u \cdot r,\ r \in R$. Observe also that this edge is labeled α_i if and only if the reflection hyperplane H_r is in class α_i. Recall further that we have a directed edge $e = (u, w)$ in a moment graph if and only if $\mathrm{d}(e, u) < \mathrm{d}(e, w)$ (resp. $\mathrm{d}(u, w_0) > \mathrm{d}(w, w_0)$) and $w = r(u)$ for a reflection $r \in R$. Since in $\mathcal{G}_{W_0}^{mod}$ the vertex label vw_0 is mapped onto the vertex e in $\mathcal{G}_{W_0}$, and (undirected) incidences of vertices and edge directions are kept, we have that $\mathrm{d}(u, v) < \mathrm{d}(w, v)$ and $w = r(u)$ if and only if $e = (u, w)$ is a directed edge in $\mathcal{G}_{W_0}^{mod}$ with minimal element vw_0.
Together with the observations above on distances in W_0 and the fact that v is on the $\partial\phi_v$-positive side of all hyperplanes in $\partial\Sigma$, the first direction of the proof follows by the same argument as given in the proof of Lemma 3.3.5. Exchange w_0 by v.
To prove the converse, let u be on the ϕ_v-negative and w be on the ϕ_v-positive side of the hyperplane ∂H_r with $w = u \cdot r$ and $r \in R$. Then (u, w) or (w, u) is an edge of $\mathcal{G}_{W_0}^{mod}$. Since v is on the ϕ_v-positive side of all hyperplanes in $\partial\Sigma$ and w is on the ϕ_v-positive side of the hyperplane ∂H_r, it follows from the definition of the orientation $\partial\phi_v$ that w and v lie on the same side of the hyperplane ∂H_r and u and v are separated by H_r. It follows that $\mathrm{d}(u, v) > \mathrm{d}(w, v)$. But this implies that the edge is directed towards w, hence $(u, w) \in E(\mathcal{G}_{W_0}^{mod})$. □

With this, we can generalize Theorem 3.3.3 and state our main result of this chapter:

Theorem 3.3.9 (Positive folding patterns and modified moment graph)**.** *Let (W, S) be an affine Coxeter system and W_0 the corresponding spherical Coxeter group with modified moment graph $\mathcal{G}_{W_0}^{mod} = (V, E, \Phi_{W_0}^+)$ with minimal element ww_0. Denote by Σ the affine Coxeter complex corresponding to (W, S), and let ϕ_w be the Weyl chamber orientation on Σ with defining element $w \in W_0$. Let $x \in \mathcal{C}_v$ and $\gamma : \mathbf{c_f} \rightsquigarrow \mathbf{x}$ be a minimal gallery. Then $(\alpha_{j,i})_{i\in[n]}$ is a ϕ_v-positive folding pattern for γ if and only if $(\alpha_{j,1}, \alpha_{j,2}, \ldots, \alpha_{j,n})$ is the label index sequence of a directed path in $\mathcal{G}_{W_0}^{mod}$ starting in the vertex v.*

Proof. Use the same argumentation as in the proof of Theorem 3.3.3, replacing $\mathcal{G}_{W_0}$ with $\mathcal{G}_{W_0}^{mod}$, the orientation ϕ_{w_0} with ϕ_w, and Lemma 3.3.5 with Lemma 3.3.8. □

Remark 3.3.10. With our construction of paths in the (modified) Bruhat moment graph, we recover and generalize a construction of alcove paths presented by Guilhot and Parkinson in [GP19, Lemma 6.2] for type $\widetilde{\mathtt{G}}_2$. This construction was utilized by the authors as a technical tool to prove Lusztig's conjectures regarding the structure of Hecke algebras with unequal parameters for type $\widetilde{\mathtt{G}}_2$ [Lus03]. Specifically, the alcove path they constructed corresponds to the vertex sequence of a directed path starting from the vertex v in $\mathcal{G}_{W_0}^{mod}$.

Recall that, in general, not all ϕ_v-positive folding patterns for a gallery γ can be applied to it, e.g., because the gallery is too short. Therefore, we introduce the sets $\mathcal{X}(\mathcal{C}_v, \phi_w, (\alpha_{j,i})_{i\in[n]}) \subseteq \Sigma(W, S)$ of alcoves $\mathbf{x} \in \mathcal{C}_v$ that allow for the application of a ϕ_w-positive folding pattern $(\alpha_{j,i})_{i\in[n]}$ to a minimal gallery ending in $\mathbf{x}$. It is then a natural question to also ask for the intersection set, that is, the set of all alcoves in a common Weyl chamber, satisfying that every ϕ_w-positive folding pattern can be realized in a folding of a gallery ending in these alcoves.

Definition 3.3.11. Let (W, S) be an affine Coxeter system and let its Coxeter complex $\Sigma(W, S)$ be equipped with a Weyl chamber orientation ϕ_w. Let further $\mathcal{C}_v$ be a Weyl chamber of $\Sigma(W, S)$. We define the set $\mathcal{X}(\mathcal{C}_v, \phi_w)$ of alcoves $\mathbf{x}$ of $\mathcal{C}_v$, for which every ϕ_w-positive folding pattern obtained from the modified Bruhat moment graph $\mathcal{G}_{W_0}^{mod}$ starting in the vertex v can be realized for at least one minimal gallery $\gamma : \mathbf{c_f} \rightsquigarrow \mathbf{x}$ as:

$$\mathcal{X}(\mathcal{C}_v, \phi_w) := \bigcap_{(\alpha_{j,i})_{i\in[n]}} \mathcal{X}(\mathcal{C}_v, \phi_w, (\alpha_{j,i})_{i\in[n]}).$$

Here, $\mathcal{X}(\mathcal{C}_v, \phi_w, (\alpha_{j,i})_{i\in[n]})$ denotes the set of alcoves $\mathbf{x} \in \Sigma(W, S)$, satisfying that for the folding pattern $(\alpha_{j,i})_{i\in[n]}$ obtained from $\mathcal{G}_{W_0}^{mod}$ starting in the vertex v there exists a minimal gallery $\gamma : \mathbf{c_f} \rightsquigarrow \mathbf{x}$ such that γ can be folded following this pattern.

Remark 3.3.12. Observe that, restricting to folding patterns associated with directed paths in $\mathcal{G}_{W_0}^{mod}$ starting in the node labeled v, is not a restriction when defining the sets $\mathcal{X}(\mathcal{C}_v, \phi_w, (a_{j,i})_{i\in[n]})$: It follows from Theorem 3.3.9 that folding patterns not associated with such paths cannot be applied to minimal galleries ending in $\mathcal{C}_v$, hence the defined alcove sets would be empty.
Observe further, that if $(a_{j,i})_{i\in[n]}$ is a ϕ_w-positive folding pattern that continues the ϕ_w-positive folding pattern $(a_{j,i'})_{i'\in[n']}$, then $\mathcal{X}(\mathcal{C}_v, \phi_w, (a_{j,i})_{i\in[n]}) \subseteq \mathcal{X}(\mathcal{C}_v, \phi_w, (a_{j,i'})_{i'\in[n']})$.

Below, we present a naive construction of a set of alcoves in $\mathcal{X}(\mathcal{C}_v, \phi_w)$. For this, we need a modified notion of shrunken Weyl chambers as introduced in [Gör+06, Def. 7.2.1]:

Definition 3.3.13 (Shrunken Weyl chamber)**.** Denote by $\omega_i^\vee$ the fundamental coweight corresponding to a positive simple root α_i. Let $k \in \mathbb{N}$. We define the *k-shrunken Weyl chamber* $\tilde{\mathcal{C}}_w \subset \mathcal{C}_w$ as

$$\tilde{\mathcal{C}}_{w,k} = \mathcal{C}_w + k \cdot \sum_{i:\ w\alpha_i>0} w\omega_i^\vee.$$

The k-shrunken Weyl chamber contains all the alcoves from $\mathcal{C}_w$ that do not lie between the hyperplanes $H_{w\alpha,0}$ and $H_{w\alpha,k}$ for positive simple roots α.

Proposition 3.3.14 (Naive subset of $\mathcal{X}(\mathcal{C}_v, \phi_w)$)**.** *Let (W, S) be an affine Coxeter system and its Coxeter complex $\Sigma(W, S)$ be equipped with a Weyl chamber orientation ϕ_w. Let further $\mathcal{C}_v$ be a Weyl chamber of $\Sigma(W, S)$ and l_p the length of a longest directed path in $\mathcal{G}_{W_0}^{mod}$ starting in the node labeled v. If $\mathbf{x} \subseteq \tilde{\mathcal{C}}_{w,l_p}$, then every ϕ_w-positive folding pattern corresponding to a directed path in $\mathcal{G}_{W_0}^{mod}$ starting in v can be realized in a folding of a minimal gallery $\gamma : \mathbf{c_f} \rightsquigarrow \mathbf{x}$.*

Proof. We prove the claim for $\mathcal{C}_v = \mathcal{C}_f$. To see the proof for $\mathcal{C}_v \neq \mathcal{C}_f$, follow the same arguments and apply v to the roots and cones.
Denote by $\rho := \frac{1}{2}\sum_{\alpha\in\Phi^+} \alpha$ the half sum of positive roots. Observe, that a minimal gallery $\tau : \mathbf{w_0} \rightsquigarrow \mathbf{c_f}$ crosses a single hyperplane of every parallelism class. Observe further, that $\gamma_t : \mathbf{c_f} \rightsquigarrow t^\rho\mathbf{w_0}$ is minimal, ends in the alcove at the tip of $\tilde{\mathcal{C}}_f$, and that the concatenation $\tau * \gamma_t : \mathbf{c_f} \rightsquigarrow t^\rho\mathbf{c_f}$ crosses at least one hyperplane of every parallelism class. Compare [MST15, Sec. 6.2]. Now let $\mathbf{x} \subseteq \tilde{\mathcal{C}}_{f,l_p}$. Then every minimal gallery

$\gamma : \mathbf{c_f} \rightsquigarrow \mathbf{x}$ also crosses all hyperplanes a minimal gallery $\gamma_{x,t} : \mathbf{c_f} \rightsquigarrow t^{l_p \cdot \rho}\mathbf{w_0}$ crosses. In particular, every minimal gallery γ crosses at least l_p hyperplanes of every parallelism class. With this, one can construct a folded gallery for every ϕ_w-postive folding pattern $(\alpha_{j,i})_{i\in[n]}$ obtained from $\mathcal{G}^{mod}_{W_0}$ starting in the node e out of γ as follows: Let H_1 be the first hyperplane of class $\alpha_{j,1}$ that γ crosses, and denote the corresponding reflection by r_1. Fold γ at its panel contained in H_1. Then, the remaining part of γ is reflected by r_1 and the parallelism classes of the hyperplanes γ crosses in this reflected part may change. But, since γ crosses l_p hyperplanes of every parallelism class and the mapping of hyperplane classes under reflections is bijective, the remaining reflected part of γ crosses at least $l_p - 1$ hyperplanes of every parallelism class. Hence, find the first hyperplane H_2 of class $\alpha_{j,2}$ γ crosses in this remaining part and fold the gallery again at its panel contained in H_2. With the same argument as above we see, that we find a gallery γ such that the remaining part of the gallery behind these two folds crosses at least $l_p - 2$ hyperplanes of every parallelism class. Repeat the construction for the remaining elements of the folding pattern $(\alpha_{j,i})_{i\in[n]}$. The claim then follows by proving that $l_p \geq n$, which follows immediately from the construction of l_p and Theorem 3.3.9. □

Example 3.3.15 demonstrates that the set constructed this way is a proper subset of $\mathcal{X}(\mathcal{C}_w, \phi_v)$. We also give an example of how to construct the exact set $\mathcal{X}(\mathcal{C}_w, \phi_v)$.

Example 3.3.15. Consider $W_{\tilde{\mathbf{A}}_2}$ with generating set $S = \{s_0, s_1, s_2\}$ and positive roots $\Phi^+ = \{\alpha_1, \alpha_2, \alpha_1 + \alpha_2\}$. Let the Coxeter complex $\Sigma = \Sigma(W, S)$ be equipped with the Weyl chamber orientation ϕ_{w_0}. We want to determine all $\mathbf{x} \subseteq \mathcal{C}_f$, such that for every ϕ_{w_0}-positive folding pattern we find a minimal gallery $\gamma : \mathbf{c_f} \rightsquigarrow \mathbf{x}$, to which the pattern can be applied. With Theorem 3.3.9, we read off the longest ϕ_{w_0}-positive folding patterns from the Bruhat moment graph: $(\alpha_1, \alpha_2, \alpha_1)$, $(\alpha_1, \alpha_1+\alpha_2, \alpha_2)$, $(\alpha_2, \alpha_1, \alpha_2)$, $(\alpha_2, \alpha_1+\alpha_2, \alpha_1)$. Compare Figure 1.1. Observe that a reflection in a fundamental hyperplane $H_{\alpha_i,0}$ of class α_i maps the other two positive roots onto each other. This implies that by applying a reflection across a hyperplane of class α_i onto a gallery when folding it in a panel contained in this hyperplane, the hyperplane classes α_j of the hyperplanes crossed after this fold swap for $j \neq i$, and stay fixed for $j = i$. It follows, that a gallery $\gamma : \mathbf{c_f} \rightsquigarrow \mathbf{x}$ must cross hyperplanes of classes $(\alpha_1, r_{\alpha_1}(\alpha_1 + \alpha_2), r_{\alpha_1}(r_{\alpha_1+\alpha_2}(\alpha_2))) = (\alpha_1, \alpha_2, \alpha_1)$ such that we can apply the folding pattern $(\alpha_1, \alpha_1 + \alpha_2, \alpha_2)$. For the folding pattern $(\alpha_1, \alpha_2, \alpha_1)$ we derive, that the gallery must cross hyperplanes of classes $(\alpha_1, \alpha_1+\alpha_2, \alpha_2)$; for the pattern $(\alpha_2, \alpha_1, \alpha_2)$ we derive the hyperplane class sequence $(\alpha_2, \alpha_1 + \alpha_2, \alpha_1)$; and for the pattern $(\alpha_2, \alpha_1 + \alpha_2, \alpha_1)$ we obtain $(\alpha_2, \alpha_1, \alpha_2)$. Together, it follows that for alcoves $\mathbf{x}$ satisfying $\mathbf{x} \subseteq H^+_{\alpha_1,2} \cap H^+_{\alpha_2,2} \cap H^+_{\alpha_1+\alpha_2,1} = H^+_{\alpha_1,2} \cap H^+_{\alpha_2,2}$ all four folding patterns mentioned above can be applied to a minimal gallery $\gamma : \mathbf{c_f} \rightsquigarrow \mathbf{x}$. We note that $\tilde{\mathcal{C}}_{f,3} \subset H^+_{\alpha_1,2} \cap H^+_{\alpha_2,2} = \mathcal{X}(\mathcal{C}_f, \phi_{w_0})$. Figure 3.10 visualizes this set of alcoves.

Open question 3.3.16. As observed in Example 3.3.15, the naive construction presented in Proposition 3.3.14 only provides a proper subset of $\mathcal{X}(\mathcal{C}_v, \phi_w)$. It remains to give a sharp (geometric) description. Furthermore, it could be interesting to study $\mathcal{X}(\mathcal{C}_v, \phi)$ with respect to other types of orientations ϕ.

3.3.2. Moment graphs and spherical directions. We will now present a second connection between folded galleries and Bruhat moment graphs: Folding a gallery not

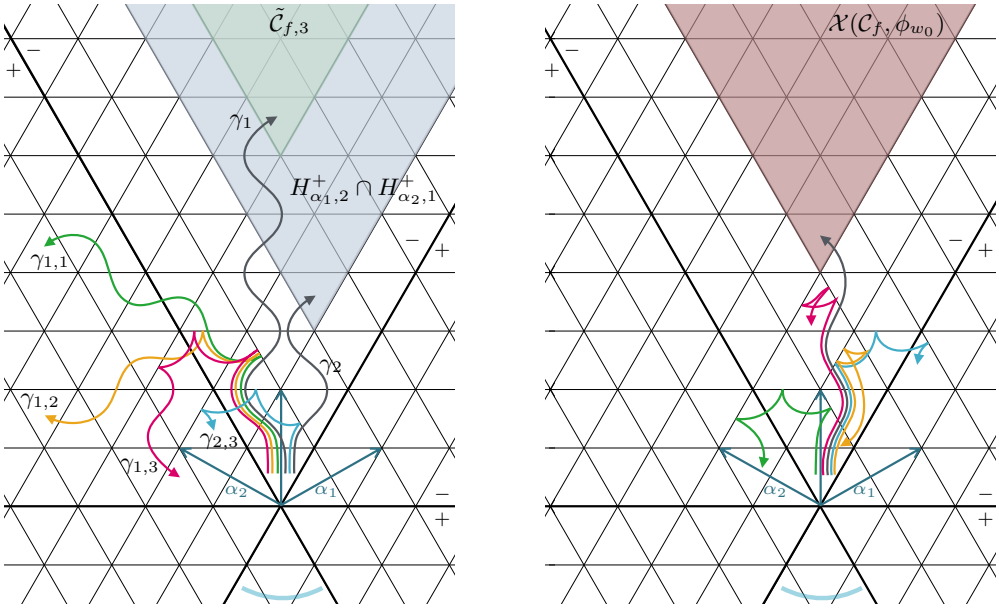

FIGURE 3.10. Visualization of Proposition 3.3.14. The light blue arc indicates the orientation defining Weyl chamber ∂w_0. The green cone in the picture on the left depicts the naive set constructed in Proposition 3.3.14, and the three i-folded galleries $\gamma_{1,i}$ obtained from the minimal gallery γ_1, illustrate the folding procedure presented there for the folding pattern $(\alpha_1, \alpha_1 + \alpha_2, \alpha_2)$. The blue cone depicts $\mathcal{X}(\mathcal{C}_f, \phi_{w_0}, (\alpha_1, \alpha_1 + \alpha_2, \alpha_2))$ as computed in Example 3.3.15. The galleries γ_2 and $\gamma_{2,3}$ give an example of how to apply the pattern there. The brown cone in the picture on the right shows $\mathcal{X}(\mathcal{C}_f, \phi_{w_0})$. The pink, green, orange, and blue galleries are obtained from the grey gallery by ϕ_{w_0}-positive folding, using all feasible folding patterns $(\alpha_1, \alpha_2, \alpha_1)$, $(\alpha_1, \alpha_1 + \alpha_2, \alpha_2)$, $(\alpha_2, \alpha_1, \alpha_2)$, and $(\alpha_2, \alpha_1 + \alpha_2, \alpha_1)$, respectively.

only affects the directions of crossing hyperplanes in a way that is encoded by $\mathcal{G}_{W_0}$, but it also changes the spherical direction of the end alcove of a gallery. These changes follow a structure that is encoded in an undirected version of a Bruhat moment graph, which we introduce as follows:

Definition 3.3.17 (Undirected moment graph)**.** Let $\mathcal{G}_{W_0} = (V, E)$ with vertex set $V = \{w : \ w \in W_0\}$ and edges $e = (u, w) \in E$ if and only if $l(u) < l(w)$ and $w = r_{\alpha_i}(u)$ for a reflection $r_{\alpha_i} \in R$ with $\alpha_i \in \Phi^+$ a positive root in W_0 be the Bruhat moment graph corresponding to a spherical Coxeter system (W_0, S_0). Consider the undirected graph $\mathcal{G}^{un}_{W_0} = (V_{un}, E_{un})$ obtained from $\mathcal{G}_{W_0} = (V, E)$ by replacing every directed edge with an undirected edge between the same vertices and keeping the labels. Then we call this graph the *undirected moment graph of* W_0.

Observe that an undirected moment graph keeps the geometric information of a Bruhat moment graph on the adjacency of alcoves with given spherical direction in the corresponding affine Coxeter group, and also gives the information on the parallelism class

a panel (resp. a hyperplane) in between two such alcoves has. However, the ordering information on the length of the group elements in W_0 is lost.

Theorem 3.3.18 (Undirected moment graph and end alcoves of folded galleries)**.** *Let (W, S) be an affine Coxeter system with (W_0, S_0) the associated spherical system and let $\gamma : \mathbf{c_f} \rightsquigarrow t^\lambda \mathbf{v}$ be a minimal alcove-to-alcove gallery in the affine Coxeter complex oriented by a Weyl chamber orientation ϕ_w. Let further $(\alpha_{j,i})_{i\in[n]}$ be a ϕ_w-positive folding pattern that can be applied to γ.*
Consider the path in the undirected moment graph $\mathcal{G}^{un}_{W_0}$ associated with W_0 with label sequence $(\alpha_{j,1}, \ldots, \alpha_{j,n})$ starting in the vertex v. Then the end vertex of the path coincides with the spherical direction of the end alcove of every gallery γ' that is obtained from γ by folding it with the folding pattern $(\alpha_{j,i})_{i\in[n]}$.

Proof. First, note that each vertex v of an undirected moment graph $\mathcal{G}^{un}_{W_0}$ has a degree of $\deg(v) = \left|\Phi^+_{W_0}\right|$ and is adjacent to an edge labeled α for every $\alpha \in \Phi^+_{W_0}$. Therefore, every folding pattern can be realised uniquely as the label sequence of an undirected path starting in any vertex of this graph.
Furthermore, recall that folding a gallery with end alcove $t^\lambda \mathbf{v}$ at a panel contained within a hyperplane of class α is applying a reflection r_α with reflection hyperplane in class α to the end alcove. For this holds:

$$r_\alpha(t^\lambda v) = t^{r_\alpha(\lambda)} r_{\alpha,W_0}(v),$$

where r_{α,W_0} denotes the reflection with reflection hyperplane in class α in W_0. According to Definition 2.2.19, we have that $r_{\alpha,W_0}(v) =: u$ is the vertex adjacent to v in the undirected moment graph along the edge labeled α.
These two observations together show that the end vertex of the path in $\mathcal{G}^{un}_{W_0}$ starting in v with label sequence $(\alpha_{i_1}, \alpha_{i_2}, \ldots, \alpha_{i_n})$ coincides with the spherical direction of the end alcove of a folded gallery γ' obtained by folding γ following the folding pattern $(\alpha_{j,i})_{i\in[n]}$. □

Open question 3.3.19. It is an open question to investigate potential connections between the folding patterns of galleries in relation to other orientations of the Coxeter complex and different order relations of the group. The concept of folding patterns, as introduced in Definition 3.2.5, only provides information about the parallelism class of the hyperplanes involved in the folds. While this is useful for periodic orientations, it requires modification for non-periodic orientations. In such cases, it is necessary to develop a notion of folding patterns that incorporates information about the height of the hyperplanes where the folds occur. Jacinta Torres and the author are currently exploring this question.

CHAPTER 4

Umbrae of Coxeter shadows

In this chapter, our goal is to provide an explicit description of the alcoves contained within the Coxeter shadow of a group element x. We will not investigate this topic in full generality; instead, we will focus on Weyl chamber orientations of affine Coxeter complexes and group elements $x = t^\lambda w$, where λ is a regular coroot and w is a specific spherical direction, such that x represents the so-called gate of λ. With the results obtained from these restrictions, we can describe a significant subset of the Coxeter shadow for arbitrary group elements in affine Coxeter groups with respect to Weyl chamber orientations.

In Section 4.1 we introduce the concept of gates of coroot lattice points. We will derive gates of regular coroot lattice points and examine some properties of their corresponding gate galleries. Section 4.2 introduces (generalized) root operators, which are the combinatorial tools used to manipulate folded galleries for our main results. We will further note some fundamental properties and illustrate them with an example. In Section 4.3 we introduce the notion of folding pattern polytopes in Section 4.3.1. Our main result, Theorem 4.3.12, is presented in Section 4.3.2 and addresses how to construct the entire Coxeter shadow of group elements in gate position using folding pattern polytopes. We will also explore an example related to this construction. In the final Section 4.4, we utilize the results from the previous sections to compute a subset of the Coxeter shadow in Theorem 4.4.4. Additionally, we draw a connection between folding pattern polytopes and vertex shadows. We will also examine examples and propose open questions for further investigation.

4.1. Gates and gate galleries

Recall that we denote by $\mathrm{d}(\mathbf{c}_1, \mathbf{c}_2)$ the distance of two alcoves $\mathbf{c}_1$ and $\mathbf{c}_2$, which equals the length of a minimal alcove-to-alcove gallery $\gamma : \mathbf{c}_1 \rightsquigarrow \mathbf{c}_2$. One can show that for any $\lambda \in T$ and any alcove $\mathbf{c}$ there exists a unique alcove $\mathbf{d} \in \mathrm{star}(\lambda)$ that has minimal distance to $\mathbf{d}$ with respect to this function. A proof of this is found in [AB08, Section 5.1]. This observation allows the following definition, which we have adapted from [MST23]:

Definition 4.1.1 (Gate of λ)**.** Let $\lambda \in T$ be a coroot lattice point. The *gate of* λ is the unique alcove in $\mathrm{star}(\lambda)$ that has minimal distance to $\mathbf{c_f}$. We denote the gate of λ by $\mathbf{a}_\lambda$.

The next lemmas describe gates of regular and irregular coroot lattice points:

Lemma 4.1.2 (Gates of regular λ)**.** *Let $\lambda \in \mathcal{C}_w$ be a regular coroot lattice point. Then $\mathbf{a}_\lambda = t^\lambda w w_0$.*

PROOF. Observe first, that for $\mu \in T$ with $h_\alpha(\mu) = 1\ \forall \alpha \in \Phi^*$ it holds $\mathbf{a}_\mu = t^\mu w_0$. This is, because $\mathbf{a}_\mu$ is the reflection of $\mathbf{c_f}$ along the adjacent hyperplane $H_{\alpha_{0,1}}$, $\mathrm{d}(\mathbf{c_f}, t^\mu w_0) = 1$, and $\mathrm{d}(\mathbf{c_f}, t^\mu w) > 1\ \forall w \neq w_0$. It follows with the action of S on the Coxeter complex, that $\mathbf{a}_{w\mu} = t^\mu w w_0$ for $w \in S$. For arbitrary $\lambda \in T$, observe that every hyperplane separating $\mathbf{c_f}$ and $t^\lambda w w_0$ also separates $\mathbf{c_f}$ and $t^\lambda u$ for $u \neq w w_0$. The claim then follows by invoking [MST23, Lemma 4.2]. □

For irregular $\lambda \in T$, the gate of λ depends on the fundamental walls that contain the coroot lattice point, which makes the computation of $\mathbf{a}_\lambda$ more complicated. To demonstrate this, we include a result for two-dimensional Coxeter complexes here. However, we will restrict to regular coroot lattice points throughout most parts of this chapter.

Lemma 4.1.3 (Gates of irregular λ in dimension 2)**.** *Let $\Sigma = \Sigma(W, S)$ be a twodimensional Coxeter complex and $\lambda \in T$ with $0 \neq \lambda \in \mathcal{C}_v \cap \mathcal{C}_w$. Let further $\mathrm{d}(\mathbf{v}, \mathbf{c_f}) < \mathrm{d}(\mathbf{w}, \mathbf{c_f})$. Then $\mathbf{a}_\lambda = t^\lambda w w_0$.*

PROOF. Observe first, that $0 \neq \lambda \in \mathcal{C}_v \cap \mathcal{C}_w$ implies that the two Weyl chambers $\mathcal{C}_v$ and $\mathcal{C}_w$ are adjacent, and therefore $\mathbf{v}$ and $\mathbf{w}$ are adjacent as well. It then follows $\mathrm{d}(\mathbf{v}, \mathbf{c_f}) \neq \mathrm{d}(\mathbf{w}, \mathbf{c_f})$ and we see that the assumption $\mathrm{d}(\mathbf{v}, \mathbf{c_f}) < \mathrm{d}(\mathbf{w}, \mathbf{c_f})$ is no restriction. We denote the hyperplane separating $\mathcal{C}_v$ and $\mathcal{C}_w$ and $\mathbf{v}$ and $\mathbf{w}$ by $H_{\alpha,0}$. Let $t^\lambda u$ with $u \neq w w_0$ be an alcove with vertex λ. We need to prove that $\mathrm{d}(\mathbf{c_f}, \mathbf{w w_0}) < \mathrm{d}(\mathbf{c_f}, \mathbf{u})$.
Assume first $\lambda \in \mathcal{C}_f$. This implies $v = e$ and $\ell(w) = 1$. Since $u \neq w w_0$, the alcoves $t^\lambda \mathbf{u}$ and $t^\lambda \mathbf{w w_0}$ are separated by a set of hyperplanes. If the wall $H_{\alpha,0}$ is separating $t^\lambda \mathbf{u}$ and $t^\lambda \mathbf{w w_0}$, observe that $\mathrm{d}(\mathbf{v}, \mathbf{c_f}) < \mathrm{d}(\mathbf{w}, \mathbf{c_f})$ implies that $\mathbf{c_f}$ and $\mathbf{v}$ are contained in a common half-space defined by $H_{\alpha,0}$ and $\mathbf{c_f}$ and $\mathbf{w}$ are separated by $H_{\alpha,0}$. This implies, since also $t^\lambda \mathbf{u}$ and $t^\lambda \mathbf{w w_0}$ are separated by $H_{\alpha,0}$, that $t^\lambda \mathbf{c_f}$ and $t^\lambda \mathbf{w w_0}$ are contained in a common half-space. As well, because of the semidirect product structure of W, $\mathbf{c_f}$ and $t^\lambda \mathbf{c_f}$ are in a common half-space defined by $H_{\alpha,0}$ and, hence $\mathbf{c_f}$ and $t^\lambda \mathbf{w w_0}$ are contained in a common half-space defined by $H_{\alpha,0}$ too. This shows $\mathrm{d}(\mathbf{c_f}, t^\lambda \mathbf{w w_0}) < \mathrm{d}(\mathbf{c_f}, t^\lambda \mathbf{u})$.
If the wall $H_{\alpha,0}$ is not separating $t^\lambda \mathbf{u}$ and $t^\lambda \mathbf{w w_0}$, observe that $t^\lambda \mathbf{c_f}, t^\lambda \mathbf{u}, t^\lambda \mathbf{w_0}, \mathbf{w}$ are contained in a common half-space defined by $H_{\alpha,0}$. Again, invoking the semidirect product structure of W, this implies that $\mathbf{c_f}, \mathbf{u}$, and $\mathbf{w w_0}$ are contained in a common half-space defined by $H_{\alpha,0}$ as well. We conclude two insights from this: First, with the fact, that the alcove $\mathbf{c_f}$ has a panel that is contained in the wall $H_{\alpha,0}$, it follows $\mathrm{d}(\mathbf{c_f}, \mathbf{u}) \neq \mathrm{d}(\mathbf{c_f}, \mathbf{w w_0})$ from this. Second, since $\mathbf{u}$ is in a common half-space defined by $H_{\alpha,0}$ with $\mathbf{c_f}$, it follows $\mathbf{u} \neq \mathbf{w_0}$. This implies $\mathrm{d}(\mathbf{c_f}, \mathbf{u}) \leq \ell(w_0) - 1$. Because $\ell(w) = 1$, it follows $\ell(w w_0) = \ell(w_0) - 1$. Combining this with $\mathrm{d}(\mathbf{c_f}, \mathbf{u}) \neq \mathrm{d}(\mathbf{c_f}, \mathbf{w w_0})$ gives $\mathrm{d}(\mathbf{c_f}, \mathbf{u}) < \mathrm{d}(\mathbf{c_f}, \mathbf{w w_0})$.
Now, consider a hyperplane $H_{\beta,k}$ that separates $t^\lambda \mathbf{u}$ and $t^\lambda \mathbf{w w_0}$ and observe the following two facts on this: First, since $\lambda \neq 0$, the wall $H_{\beta,k}$ separates $\mathbf{c_f}$ and $t^\lambda \mathbf{c_f}$. Second, it follows from the semidirect product structure of W that $H_{\beta,0}$ separates $\mathbf{u}$ and $\mathbf{w w_0}$. Together, this implies that $t^\lambda \mathbf{u}$ and $\mathbf{c_f}$ are separated by $H_{\beta,k}$, but $t^\lambda \mathbf{w w_0}$ and $\mathbf{c_f}$ are not separated by $H_{\beta,k}$. This proves $\mathrm{d}(\mathbf{c_f}, t^\lambda \mathbf{w w_0}) < \mathrm{d}(\mathbf{c_f}, t^\lambda \mathbf{u})$.
For $\lambda \neq \mathcal{C}_f$, use the argumentation above for $v^{-1}\lambda \in \mathcal{C}_f$. Then act with v again to prove the claim. □

Open question 4.1.4. Generalize Lemma 4.1.3 to Coxeter complexes of higher dimension.

Definition 4.1.5 (Gate gallery)**.** Let $\lambda \in T$ be a coroot lattice point and $\mathbf{a}_\lambda$ the gate of λ. Then we call a gallery $\gamma : \mathbf{c_f} \rightsquigarrow \mathbf{a}_\lambda$ a *gate gallery of* λ.

Note that the gate of λ is unique, but a gate gallery of λ, in general, is not.

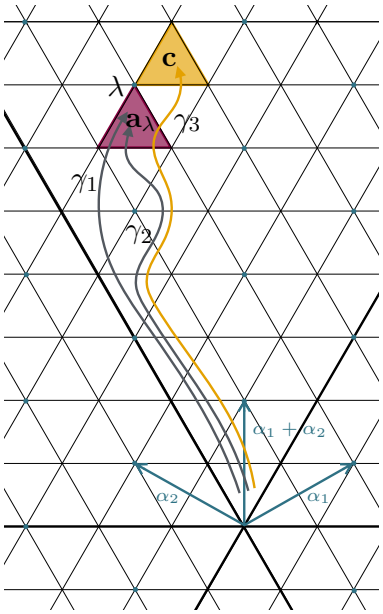

FIGURE 4.1. Two minimal galleries γ_1 and γ_2 ending in the gate $\mathbf{a}_\lambda$ of the coroot lattice point λ. Shown in orange is a third minimal gallery ending in $\mathbf{c}$ at the vertex λ.

Example 4.1.6. Figure 4.1 shows two minimal gate galleries γ_1 and γ_2 for the coroot lattice point λ. They both end in the same alcove $\mathbf{a}_\lambda$ shown in red, which is the gate of λ. This demonstrates that minimal gate galleries are not unique. Observe that the alcove $\mathbf{c}$ also contains the vertex λ. But because the minimal gallery $\gamma_3 : \mathbf{c_f} \rightsquigarrow \mathbf{c}$ is longer than γ_1 and γ_2, $\mathbf{c}$ is not the gate of λ.

There is the following simple connection between the numbers of crossed hyperplanes of a given parallelism class of a minimal gate gallery of λ and the coordinates of the coroot lattice point λ:

Lemma 4.1.7 (Numbers of crossings of minimal gate galleries)**.** *Let $\lambda \in T$ and $\mathbf{a}_\lambda$ the gate of λ. Let further $\gamma : \mathbf{c_f} \rightsquigarrow \mathbf{a}_\lambda$ be a minimal gallery. Denote by $M(\lambda, \alpha)$ the number of α-hyperplanes crossed by γ and write $h_\alpha(\lambda) := \langle \lambda, \alpha^\vee \rangle$. Then:*

$$M(\lambda, \alpha) = \begin{cases} h_\alpha(\lambda) - 1, & \text{if } h_\alpha(\lambda) > 0 \\ |h_\alpha(\lambda)|, & \text{if } h_\alpha(\lambda) \leq 0. \end{cases}$$

PROOF. Recall first that a minimal gate gallery of λ is crossing all α-hyperplanes that are separating $\mathbf{c_f}$ and λ. If now $h_\alpha(\lambda) > 0$, both λ and $\mathbf{c_f}$ are contained in a common half-space defined by $H_{\alpha,0}$. Therefore, the minimal gallery γ is crossing the hyperplanes $\{H_{\alpha,i}|\ i \in \{1,\dots,h_\alpha - 1\}\}$, but not the hyperplane $H_{\alpha,0}$. It follows $M(\lambda,\alpha) = h_\alpha(\lambda) - 1$. If $h_\alpha(\lambda) < 0$, $\mathbf{c_f}$ and λ are contained in different half-spaces defined by $H_{\alpha,0}$. Hence, γ is crossing the hyperplanes $\{H_{\alpha,i}|\ i \in \{0,1,\dots,h_\alpha(\lambda) - 1\}\}$ and $M(\lambda,\alpha) = h_\alpha(\lambda)$. If $h_\alpha(\lambda) = 0$, there exist alcoves $t^\lambda w$ with $w \in W_0$ in both halfspaces defined by $H_{\alpha,0}$. This implies that the minimal gate gallery γ is not crossing $H_{\alpha,0}$, hence it is crossing no α-hyperplane, and it holds $M(\lambda,\alpha) = 0$. □

4.2. Root operators

In this section, we establish our notation for generalized root operators associated with positive (not necessarily simple) roots and record some of their properties. For our definition, we follow [GL05, Section 6], and consider vertex-to-vertex galleries $\gamma' : 0 \rightsquigarrow \lambda$ with $\lambda \in T$. We assume that λ is regular to exclude degenerated vertex-to-vertex galleries. Note that when we obtain our vertex-to-vertex galleries from alcove-to-alcove galleries $\gamma : \mathbf{c_f} \rightsquigarrow \mathbf{x}$ with $\mathbf{x} \in \tilde{\mathcal{C}}_w$ as $\gamma^{\sharp\sharp}$, they will also be nondegenerate.

Notation 4.2.1. Let $\lambda \in T$ be regular and let $\gamma' : 0 \rightsquigarrow \lambda$ be a minimal vertex-to-vertex gallery. Let further $\gamma : 0 \rightsquigarrow \nu$ be a (folded) vertex-to-vertex gallery with $\tau(\gamma) = \tau(\gamma')$. Let $\alpha \in \Phi^+$ be a positive root. Define $m = m(\gamma,\alpha) \in \mathbb{Z}$ to be minimal such that there exists a panel or vertex $p \in \gamma$ with $p \subseteq H_{\alpha,m}$. Define $M = M(\gamma,\alpha) \in \mathbb{Z}$ to be maximal such that there exists a panel or vertex $p \in \gamma$ with $p \subseteq H_{\alpha,M}$.

(I) If $M \geq 2$, let $k = k(\gamma,\alpha,\mathrm{I})$ be minimal with $p_k \subseteq H_{\alpha,M}$ and let $j = j(\gamma,\alpha,\mathrm{I})$ be maximal such that $0 \leq j \leq k$ and $p_j \subseteq H_{\alpha,M-1}$.

(II) If $M \geq \langle \nu, \alpha^\vee \rangle - 1$, let $j = j(\gamma,\alpha,\mathrm{II})$ be maximal with $p_j \subseteq H_{\alpha,M}$ and let $k = k(\gamma,\alpha,\mathrm{II})$ be minimal with $j \leq k \leq n+1$ and $p_k \subseteq H_{\alpha_i,M-1}$.

Notice that the two cases (I) and (II) do not exclude each other.

Definition 4.2.2. We define the root operators e_α and f_α for (I) and (II):

(I) $M \geq 2$: In this case, we define the vertex-to-vertex gallery $e_\alpha(\gamma)$ to be

$$e_\alpha(\gamma) = (0, \mathbf{c'_0}, p'_1, \mathbf{c'_1}, \dots, \mathbf{c'_n}, \mu')$$

with

$$\mathbf{c'_i} = \begin{cases} \mathbf{c_i} & \text{for } i \leq j-1, \\ r_{\alpha,M-1}(\mathbf{c_i}) & \text{for } j \leq i \leq k-1, \\ t^{-\alpha^\vee}(\mathbf{c_i}) & \text{for } i \geq k. \end{cases}$$

(II) $M \geq \langle \nu, \alpha^\vee \rangle + 1$: In this case, we define the vertex-to-vertex gallery $f_\alpha(\gamma)$ to be

$$f_\alpha(\gamma) = (0, \mathbf{c'_0}, p'_1, \mathbf{c'_1}, \dots, \mathbf{c'_n}, \mu')$$

with

$$\mathbf{c_i'} = \begin{cases} \mathbf{c_i} & \text{for } i \leq j-1, \\ r_{\alpha,M}(\mathbf{c_i}) & \text{for } j \leq i \leq k-1, \\ t^{\alpha^\vee}(\mathbf{c_i}) & \text{for } i \geq k. \end{cases}$$

Remark 4.2.3.

- Notice that we explicitly allowed $\gamma = \gamma'$ in Definition 4.2.2 above. This allows us to use the root operator e_α to create a folded gallery $e_\alpha(\gamma')$ if γ' crosses a hyperplane of parallelism class α. By construction, this fold will be along the hyperplane $H_{\alpha,M-1}$.
- For $M = \langle \nu, \alpha^\vee \rangle + 1$, application of f_α to the gallery will erase the fold in the hyperplane $H_{\alpha,M}$, such that $f_\alpha(\gamma)$ has one fold less compared to γ'.
- For the iterative application of a root operator e_α, resp. f_α, to a gallery $e_\alpha(\gamma)$, resp. $f_\alpha(\gamma)$, we abbreviate notation to $e_\alpha^2(\gamma)$, resp. $f_\alpha^2(\gamma)$. For the k-fold application, we write $e_\alpha^k(\gamma)$, resp. $f_\alpha^k(\gamma)$.
- We can apply generalized root operators also to an alcove-to-alcove gallery γ by applying them to the canonical associated vertex-to-vertex gallery $\gamma^{\sharp\sharp}$.
- Although all our vertex-to-vertex galleries have vertices inside the fundamental hyperplanes as they contain the origin, observe that with our definition of root operators, we do not allow applying root operators to place foldings inside these hyperplanes. With this, we secure that all our galleries have the first alcove $\mathbf{c_f}$.

Remark 4.2.4. Observe with Notation 4.2.1, that the root operators e_α are specifically designed for application to minimal galleries that end in the fundamental Weyl chamber $\mathcal{C}_f$ with respect to the chosen root basis Φ^*: Given a minimal gallery that ends in $\mathcal{C}_f$ at distance far enough from the origin, it is possible to apply e_α for all positive roots, while minimal galleries ending in other Weyl chambers $\mathcal{C}_u$ with $u \neq e$ will not satisfy conditions (I) and (II) for at least one positive root $\alpha \in \Phi^+$. However, since $u(\Phi^*)$ forms a basis of roots for Φ as well, we can construct a new set of root operators ${}_ue_\alpha$, ${}_uf_\alpha$ with respect to this basis for minimal galleries ending in $\mathcal{C}_u$. As before, all minimal galleries that end in this Weyl chamber at a sufficient distance from the origin will allow the application of ${}_ue_\alpha$ for all positive roots $\alpha \in u(\Phi^*)$.

The following lemma collects some basic properties of generalized root operators. Along with several additional properties that we do not need here, they are proven for root operators in [GL05, Lemmas 5 - 7].

Lemma 4.2.5. *Use the notation as in Notation 4.2.1.*

(i) $e_\alpha(\gamma)$ *is defined if and only if* $M(\gamma, \alpha) \geq 2$. $e_\alpha(\gamma)$ *then ends in the vertex* $\nu - \alpha^\vee$.

(ii) $f_\alpha(\gamma)$ *is defined if and only if* $M(\gamma, \alpha) \geq \langle \nu, \alpha^\vee \rangle + 1$. $f_\alpha(\gamma)$ *then ends in the vertex* $\nu + \alpha^\vee$.

(iii) If $e_\alpha(\gamma)$ *is defined, then* $f_\alpha(e_\alpha(\gamma))$ *is defined and* $f_\alpha(e_\alpha(\gamma)) = \gamma$.

(iv) If $f_\alpha(\gamma)$ *is defined, then* $e_\alpha(f_\alpha(\gamma))$ *is defined and* $e_\alpha(f_\alpha(\gamma)) = \gamma$.

(v) If $e_\alpha(\gamma)$ or $f_\alpha(\gamma)$ is defined, then $e_\alpha(\gamma)$ and $f_\alpha(\gamma)$ is of the same type as γ.

PROOF. The items (i) to (v) follow immediately from Definition 4.2.2 and the fact that folding preserves the type of a gallery. □

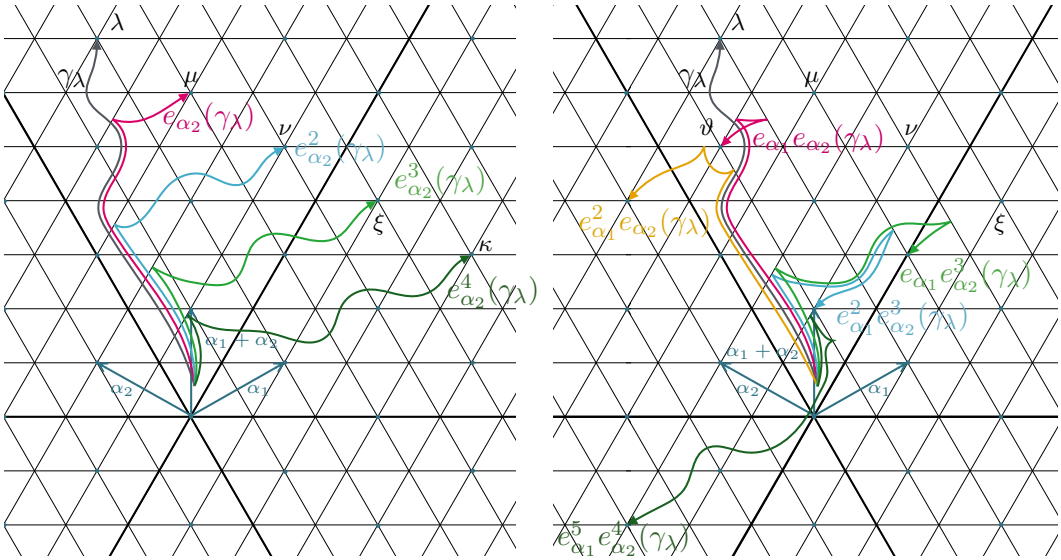

FIGURE 4.2. The two pictures show applications of root operators to the minimal vertex-to-vertex gallery γ_λ. The picture on the left shows multiple applications of the root operator e_{α_2} to γ_λ, such that the pink, blue, green, and dark green galleries are obtained. The picture on the right shows application of the two different root operators e_{α_2} and e_{α_1} to γ_λ, such that the 2-folded pink gallery is obtained. The orange, green, blue, and dark green gallery are constrcuted by applying the root operators iteratively to the pink gallery.

Example 4.2.6. Figure 4.2 illustrates the application of root operators to folded galleries. The pictures shows a minimal gallery γ_λ in grey. Observe that γ_λ is the canonically associated vertex-to-vertex gallery with the gate gallery γ_1 of λ discussed in Example 4.1.6. Application of the root operator e_{α_2} produces the folded gallery $e_{\alpha_2}(\gamma_\lambda)$ shown in pink in the left picture, which ends in μ. Since $\langle \mu, \alpha_2^\vee \rangle < M(e_{\alpha_2}(\gamma_\lambda), \alpha_2)$, we can apply the root operator e_{α_2} to the pink gallery again. This produces the gallery $e^2_{\alpha_2}(\gamma_\lambda)$ with a fold in the hyperplane $H_{\alpha_2,3}$. Observe that, again, we can apply the root operator iteratively two more times to obtain the galleries $e^3_{\alpha_2}(\gamma_\lambda)$ and $e^4_{\alpha_2}(\gamma_\lambda)$. For $e^3_{\alpha_2}(\gamma_\lambda)$ ending in $\xi \in T$, observe that $\langle \xi, \alpha_2^\vee \rangle + 1 = 0 \leq M(e^3_{\alpha_2}(\gamma_\lambda), \alpha_2) = 2$. Therefore, we can apply the root operator f_{α_2} to this gallery and obtain $f_{\alpha_2}(e^3_{\alpha_2}(\gamma_\lambda)) = e^2_{\alpha_2}(\gamma_\lambda)$. This illustrates Lemma 4.2.5 (iii). Note that with every application of e_{α_2}, resp. f_{α_2}, the fold along the hyperplane $H_{\alpha_2,j}$ it translated to a fold along the hyperplane $H_{\alpha_2,j-1}$, resp. $H_{\alpha_2,j+1}$.

The picture on the right of Figure 4.2 demonstrates the application of the two root operators e_{α_2} and e_{α_1} to the gallery γ_λ. This results in the 2-folded gallery with folding

pattern (α_2, α_1) which ends in $\vartheta \in T$ and is shown in pink. Checking the conditions stated in Definition 4.2.2, we see that it is allowed to apply both root operators again to the gallery. Examples of this iterative application of root operators are the galleries $e_{\alpha_1}^2 e_{\alpha_2}(\gamma_\lambda)$ shown in orange, $e_{\alpha_1} e_{\alpha_2}^3(\gamma_\lambda)$ shown in green, $e_{\alpha_1}^2 e_{\alpha_2}^3(\gamma_\lambda)$ shown in blue, and $e_{\alpha_1}^5 e_{\alpha_2}^4(\gamma_\lambda)$ shown in dark green. Observe that the application of e_{α_1} to the pink gallery $e_{\alpha_1} e_{\alpha_2}(\gamma_\lambda)$ produces a gallery with different folding pattern than the pink gallery, but that the folding pattern for all the other illustrated folded galleries is the same: The pink, the blue, the green, and the dark green galleries have the folding pattern (α_2, α_1). Invoking Theorems 3.3.3 and 3.3.9, we see that this is a positive folding pattern with respect to the Weyl chamber orientation induced by $w_0 \in W_0$, but not with respect to the Weyl chamber orientation induced by $s_1 s_2 \in W_0$. The orange gallery has the folding pattern $(\alpha_1, \alpha_1 + \alpha_2)$. Theorems 3.3.3 and 3.3.9 show that this is a positive folding pattern with respect to the Weyl chamber orientation defined by $s_1 s_2 \in W_0$ and $w_0 \in W_0$. This demonstrates that the application of root operators to folded galleries may also change the positivity and negativity of folds.

With the following lemma, we describe the observation on the parallelism classes of folds that we made in Example 4.2.6 in full generality. Compare also Example 4.3.1. The analogous result for root operators as introduced by Gaussent and Littelmann can be found in [GL05, Lemma 6].

Lemma 4.2.7 (Parallelism classes of folds and root operators)**.** *Use notation as in 4.2.1 and let the gallery γ be folded with folding pattern $(\alpha_{j,i})_{i\in[n]}$. Let $\alpha \in (\alpha_{j,i})_{i\in[n]}$. If e_α, resp. f_α, can be applied to γ and the gallery has no folds between $\mathbf{c}_j$ and $\mathbf{c}_{k-1}$, then $e_\alpha(\gamma)$, resp. $f_\alpha(\gamma)$, also has the folding pattern $(\alpha_{j,i})_{i\in[n]}$. In particular, if γ was positively folded with respect to a periodic orientation ϕ, then $e_\alpha(\gamma)$, resp. $f_\alpha(\gamma)$, is ϕ-positively folded too.*

Proof. Since the alcoves and panels p_i and $\mathbf{c}_i$ with $i \leq j-1$ and $j \geq k$ are fixed or translated when applying a root operator e_α or f_α, all folds contained in these parts of the gallery $e_\alpha(\gamma)$, resp. $f_\alpha(\gamma)$ are in hyperplanes of the same parallelism classes as the corresponding folds in γ. Since no folds are contained in between $\mathbf{c}_j$ and $\mathbf{c}_{k-1}$, the reflection of these alcoves due to the application of the root operator has no effect on the folds. If e_α can be applied, it holds that the fold in γ was at the panel p_k and that both alcoves $\mathbf{c}_{k-1}$ and $\mathbf{c}_k$ were on the same side of the panels supporting hyperplane $H_{\alpha,M}$. In $e_\alpha(\gamma)$ this fold will be translated into the panel p_j. And because of the reflection of the panel and alcoves in between, $\mathbf{c}_{j-1}$ and $\mathbf{c}_j$ will be on the same side of the panels supporting hyperplane and also on the same side of $H_{\alpha,M}$ as $\mathbf{c}_{k-1}$ and $\mathbf{c}_k$ in γ. The same argument holds for f_α, if applicable. Exchange M and $M-1$ and j and k. This proves the claim. □

Remark 4.2.8. Observe that the change of the folding pattern of a gallery γ due to the application of a root operator that we observed in Example 4.2.6 may also change the positivity or negativity of a fold in γ. Since we are usually interested in positively folded galleries, we will often restrict our application of root operators to galleries to the case of Lemma 4.2.7, where the folding pattern of the original gallery is preserved.

4.3. Folding pattern polytopes

We have discussed in Sections 3.2.1 and 3.3 that for a given Weyl chamber orientation ϕ_w of the Coxeter complex, all ϕ_w-positiely folded galleries have one of the folding patterns that are encoded in the Bruhat moment graph. To determine the Coxeter shadow of a group element x, it is therefore sufficient to compute all end alcoves of minimal galleries ending in $\mathbf{x}$ that were folded according to a folding pattern that applies to them and then construct the union of all these alcove sets for all possible folding patterns.

In Section 4.3.1 we introduce *folding pattern polytopes* for group elements x, with whom we will describe the set of all vertices of alcoves obtained by folding minimal galleries ending in $\mathbf{x}$ with a fixed folding pattern. Moreover, in Section 4.3.2 we will demonstrate with an example how to derive the whole Coxeter shadow by using folding pattern polytopes and Theorem 3.3.18.

4.3.1. Construction of a folding pattern polytope. Here we describe the set of coroot lattice points λ that are vertices $\mathrm{vtx}(\mathbf{y})$ of end alcoves of galleries $\gamma' : \mathbf{c_f} \rightsquigarrow \mathbf{y}$ that are obtained from minimal galleries $\gamma : \mathbf{c_f} \rightsquigarrow \mathbf{x}$ by folding γ with a fixed folding pattern $(\alpha_{j,i})_{i\in[n]}$. We will see that this set forms a lattice polytope in the coroot lattice T, and we will denote it as the *folding pattern polytope of* $(\alpha_{j,i})_{i\in[n]}$ *and* x. Together with Theorem 3.3.18 on the spherical direction of the end alcove of a folded gallery, these polytopes will construct the Coxeter shadow. Note that, in general, these polytopes are nonempty: for every folding pattern with respect to the Weyl chamber orientation ϕ_w we may find a minimal gallery ending in $\mathbf{x}$ inside the opposite Weyl chamber $\mathcal{C}_{ww_0}$, such that the folding pattern can be applied to a minimal gallery $\gamma : \mathbf{c_f} \rightsquigarrow \mathbf{x}$.

Our construction of the folding pattern polytopes will be as follows: We apply root operators $e_{\alpha_{j,i}}$ as often as possible to minimal, unfolded galleries in the ordering of the folding pattern. Given a minimal gallery $\gamma : \mathbf{c_f} \rightsquigarrow \mathbf{x} = t^\lambda \mathbf{w}$, note that in general it is not sufficient to apply all the root operator $e_{\alpha_{j,i}}$ $h_{\alpha_{j,i}}(\lambda)$-many times, since the ordering of the folds and the parallelism classes of hyperplanes after folding the gallery may change. The following example illustrates this problem:

Example 4.3.1. Consider the 2-folded gallery $e_{\alpha_1}e_{\alpha_2}(\gamma_\lambda)$ ending in $\vartheta \in T$ that is obtained from folding the minimal vertex-to-vertex gallery γ_λ with the folding pattern (α_2, α_1). Both galleries are shown in Figure 4.2.
Since $1 = \langle \vartheta, \alpha_1 \rangle < M(e_{\alpha_1}e_{\alpha_2}(\gamma_\lambda), \alpha_1) = 2$, we can apply the root operator e_{α_1} to the gallery $e_{\alpha_1}e_{\alpha_2}(\gamma_\lambda)$ again. By Definition 4.2.2, the part of the gallery located in between the panels $p_8 \subseteq H_{\alpha_1,1}$ and $p_{11} \subseteq H_{\alpha_1,2}$ is reflected along the wall $H_{\alpha_1,1}$ when applying e_{α_1}. This implies that also the first fold of the gallery at the panel $p_{10} \subseteq H_{\alpha_2,4}$ is reflected: It holds $s_{\alpha_1,1}(p_{10}) \subseteq H_{\alpha_1+\alpha_2,5}$. This has two significant consequences: First, the fold at the panel p_{10} is no longer inside a hyperplane of parallelism class α_2, but inside a hyperplane of class $\alpha_1 + \alpha_2$. Second, the ordering of the folds changes, because the application of e_{α_1} shifted the second fold of $e_{\alpha_1}e_{\alpha_2}(\gamma_\lambda)$ to a panel before the first fold of the gallery. Therefore, the constructed gallery $e_{\alpha_1}^2 e_{\alpha_2}(\gamma_\lambda)$ has the folding pattern $(\alpha_1, \alpha_1 + \alpha_2)$, which is different to the folding pattern of $e_{\alpha_1}e_{\alpha_2}(\gamma_\lambda)$.

Remark 4.3.2. Let γ be a minimal gallery that ends in $\mathcal{C}_u$. As discussed in Remark 4.2.4, the ability to apply root operators e_α to γ in order to obtain a ϕ-positively

folded gallery depends on the chosen root basis. In contrast, the application of the root operators ${}_ue_\alpha$ to γ is possible whenever the requirements of Definition 4.2.2 are met. To avoid unnecessary complications in our notation throughout the remaining chapter, we will always write e_α when referring to a root operator applied to a minimal gallery γ that ends in $\mathcal{C}_u$, instead of ${}_ue_\alpha$. This is beneficial for us, as we intend to apply root operators to minimal galleries, regardless of the Weyl chamber that contains their end vertex in our upcoming constructions.

We observed in Lemma 4.2.7 that we may avoid the changing of the folding pattern illustrated in Example 4.3.1 when applying root operators. For our definition of folding pattern polytopes, we will explicitly not allow the application of root operators that change the folding pattern.

Recall that folding a gallery is reflecting the part of the gallery behind the fold along the folding hyperplane. Therefore, multiple folds result in more than one reflection applied to the ending of the gallery. To simplify our notation below, we introduce an abbreviation for a product of reflections associated with a folding pattern:

Notation 4.3.3 (Reflections associated with folding patterns)**.** Let $(\alpha_{j,i})_{i\in[n]}$ be a folding pattern of length n. We denote by $u_k := s_{j,k-1}s_{j,k-2}\cdots s_{j,1}$ the product of the first $k-1$ (fundamental) reflections associated with the folding pattern, where $s_{j,i}$ is the reflection associated with the root $\alpha_{j,i}$.

It follows, that $u_k(\alpha_{j,k})$ describes the parallelism class of hyperplanes for the k-th fold. Before applying the first fold, the hyperplanes crossed by a minimal gallery are of the original parallelism classes. Observe that, correspondingly, $u_1 = e$. Be careful to note that applying u_k to panels or hyperplanes of a gallery does not give the exact affine hyperplane of the panels in the corresponding folded gallery. For this, we would require a product of affine reflections.

Example 4.3.4. Consider the minimal gallery $\gamma_\lambda : 0 \rightsquigarrow \lambda$ as shown in the pictures of Figure 4.2. The gallery $e_{\alpha_2}e_{\alpha_1}(\gamma_\lambda)$ shown in pink in the left picture is folded two times with the folding pattern (α_2, α_1). Consider the panel p_{11} in γ_λ. For the unfolded gallery γ_λ, the parallelism classes of the supporting hyperplanes of p_{11} is $\alpha_1+\alpha_2 = u_1(\alpha_1+\alpha_2) = e(\alpha_1+\alpha_2)$. That is: For the unfolded gallery and for panels inside galleries obtained from γ_λ before a first fold, the parallelism classes of the supporting hyperplanes are as in the unfolded gallery. By application of the root operator e_{α_2} to γ_λ, the last two alcoves,he panel p_{11} in between them, and the final vertex λ are reflected along the hyperplane $H_{\alpha_2,4}$. See also the pink gallery $e_{\alpha_2}(\gamma_\lambda)$ shown in the picture on the left of Figure 4.2. With the notion introduced above, we can derive the parallelism classes of the hyperplanes in the folded part of the gallery as $u_2(\alpha_j) = s_{\alpha_2}(\alpha_j)$. This implies for the supporting hyperplane of the panel p_{11} that it has parallelism class $u_2(\alpha_1 + \alpha_2) = s_{\alpha_2}(\alpha_1 + \alpha_2) = \alpha_1$ in the gallery $e_{\alpha_2}(\gamma_\lambda)$. Therefore, application of the root operator e_{α_1} to the gallery $e_{\alpha_2}(\gamma_\lambda)$ results in the gallery $e_{\alpha_2}e_{\alpha_1}(\gamma_\lambda)$, which has its second fold at the panel p_{11}. Although this gallery does not cross any further hyperplanes after the second fold, we could derive the parallelism classes of their supporting hyperplanes by applying $u_3 = s_{\alpha_1}u_2 = s_{\alpha_1}s_{\alpha_2}$ to the parallelism classes of the hyperplanes in the unfolded gallery γ_λ.

Using this, we are now ready to introduce folding pattern polytopes:

Definition 4.3.5 (Folding pattern polytope)**.** Let $\Sigma = \Sigma(W, S)$ be an affine Coxeter complex with periodic orientation ϕ. Let further $x = t^\lambda w \in W$ and let $(\alpha_{j,i})_{i\in[n]}$ be a folding pattern with respect to ϕ that is applicable to a given minimal gallery $\gamma : \mathbf{c_f} \rightsquigarrow \mathbf{x}$. Denote by $\max_i(\gamma) \in \mathbb{N}_0$ the upper bound on the number of applications of the root operator $e_{u_i(\alpha_{j,i})}$ to a gallery $e^{k_{i-1}}_{u_{i-1}(\alpha_{j,i-1})} \cdots e^{k_1}_{u_1(\alpha_{j,1})}(\gamma)$, such that the folded gallery has folding pattern $(\alpha_{j,i})_{i\in[n]}$. Define

$$\mathcal{A}_x := \bigcup_{\substack{\gamma:\mathbf{c_f}\rightsquigarrow\mathbf{x} \text{ minimal},\\ 1\le k_i\le \max_i}} \left\{ \operatorname{vtx}\left(e^{k_n}_{u_n(\alpha_{j,n})} \cdots e^{k_1}_{u_1(\alpha_{j,1})}(\gamma) \right) \right\}.$$

Then we call the set

$$\mathcal{P}(\mathbf{x}, (\alpha_{j,i})_{i\in[n]}) = \operatorname{conv}^*(\mathcal{A}_x)$$

the *folding pattern polytope of* $\mathbf{x}$ *for the pattern* $(\alpha_{j,i})_{i\in[n]}$.

Notation 4.3.6. Although we provide a definition of folding pattern polytopes for arbitrary $x = t^\lambda w \in W$, we will restrict our attention to group elements that are the gate for their vertex λ and λ being regular. In this case, we denote the vertex set $\mathcal{A}_x$ by $\mathcal{A}_\lambda$ and the folding pattern polytope by $\mathcal{P}(\mathbf{a}_\lambda, (\alpha_{j,i})_{i\in[n]})$.

Remark 4.3.7. Let $\Sigma = \Sigma(W, S)$ be an affine Coxeter complex with a periodic orientation ϕ. Consider $x, y \in W$ with $x = t^\lambda w$, $y = t^\lambda v$ and let $(\alpha_{j,i})_{i\in[n]}$ be a folding pattern with respect to ϕ. Even though the set $\mathcal{A}_x$, as defined in Definition 4.3.5, is a subset of the vertex shadow $\operatorname{Sh}^{\mathrm{vtx}}_\phi(x)$, and we have proven in Lemma 3.2.13 that $\operatorname{Sh}^{\mathrm{vtx}}_\phi(x) = \operatorname{Sh}^{\mathrm{vtx}}_\phi(y)$, it does not hold true in general that $\mathcal{A}_x = \mathcal{A}_y$.

Example 4.3.8. The vertex set $\mathcal{A}_\lambda$ for the folding pattern (α_2) of length 1 was computed above in Example 4.3.1. Compare also the left picture of Figure 4.2. All folded galleries obtained from the minimal gallery γ_λ drawn in grey are shown. Since the folding pattern has length 1 and the gallery γ_λ crosses all hyperplanes of class α_2 that separate $\mathbf{c_f}$ and λ, it follows that every folded gallery with folding pattern (α_2) obtained from an arbitrary minimal gallery starting in $\mathbf{c_f}$ and ending in λ ends in one of the end vertices of these four folded galleries. Observe that for folding patterns with length 1, the whole set $\mathcal{A}_\lambda$ can be constructed using an arbitrary minimal gate gallery $\gamma : \mathbf{c_f} \rightsquigarrow \mathbf{a}_\lambda$, because all minimal galleries cross the same set of hyperplanes that separate $\mathbf{c_f}$ and $\mathbf{a}_\lambda$. For a proof of this observation, refer to [Bro89, Section 4E]. From this we see, that $\operatorname{conv}^*(\mathcal{A}_\lambda) = \mathcal{P}(\mathbf{a}_\lambda, (\alpha_2)) = \operatorname{conv}^*(\mu, \kappa)$, and the folding pattern polytope contains precisely the four coroot lattice points $\{\mu, \nu, \xi, \kappa\}$.
The vertex set $\mathcal{A}_\lambda$ for the folding pattern (α_2, α_1) is shown as green dots in Figure 4.3. Notice that not every element of the vertex set can be obtained by application of root operators to the minimal gallery γ_λ shown in grey. Comparing Example 4.3.1 and the left picture of Figure 4.2, we observe that, for example, the coroot lattice point τ may be obtained by applying root operators to the gallery γ_λ. But the resulting gallery $e^2_{\alpha_1} e_{\alpha_2}(\gamma_\lambda)$ has the folding pattern $(\alpha_1, \alpha_1 + \alpha_2)$. Therefore, this construction of a folded gallery does not imply that $\tau \in \mathcal{A}_\lambda$. However, we find another minimal gallery $\tilde{\gamma}_\lambda$ as

shown in Figure 4.3 to which the root operators e_{α_2} and e_{α_1} may be applied to obtain a folded gallery with folding pattern (α_2, α_1). The resulting gallery $e_{\alpha_1}^2 e_{\alpha_2}(\tilde{\gamma}_\lambda)$ is shown in blue and ends in the coroot lattice point τ. These observations show that it is necessary to consider the set of all minimal galleries ending in λ when computing the set $\mathcal{A}_\lambda$.
Note that for both examples discussed here, the vertex set $\mathcal{A}_\lambda$ includes all coroot lattice points that are contained in the corresponding folding pattern polytope.

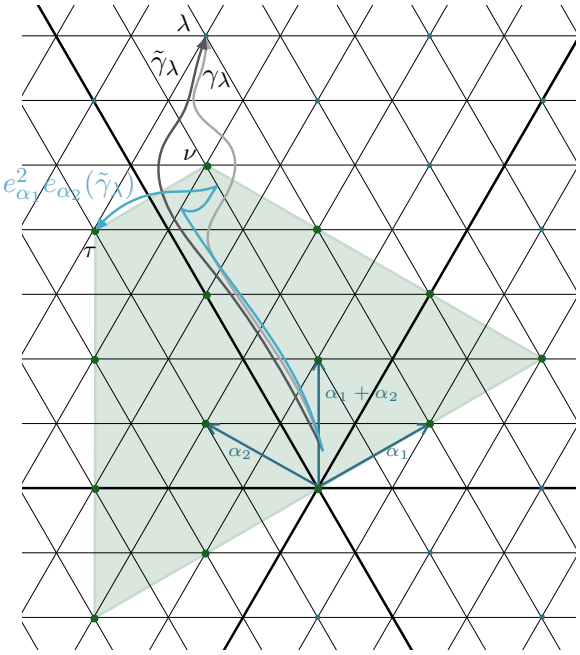

FIGURE 4.3. Folding pattern polytope $\mathcal{P}(\mathbf{a}_\lambda, (\alpha_2, \alpha_1))$. The blue gallery $e_{\alpha_1}^2 e_{\alpha_2}(\tilde{\gamma}_\lambda)$ illustrates an option to construct the vertex τ of the polytope.

Our observation from Example 4.3.8 motivates the following proposition:

Proposition 4.3.9. *Let $\Sigma = \Sigma(W, S)$ be an affine Coxeter complex with periodic orientation ϕ and let $\lambda \in T$ be regular with gate $\mathbf{a}_\lambda$. Let further $(\alpha_{j,i})_{i\in[n]}$ be a folding pattern for ϕ that can be applied to a minimal gallery $\gamma : \mathbf{c_f} \rightsquigarrow \mathbf{a}_\lambda$. Then*

$$\mathcal{P}(\mathbf{a}_\lambda, (\alpha_{j,i})_{i\in[n]}) \cap T = \mathcal{A}_\lambda.$$

PROOF. $\mathcal{A}_\lambda \subseteq \mathcal{P}(\mathbf{a}_\lambda, (\alpha_{j,i})_{i\in[n]}) \cap T$ is by construction of the folding pattern polytope. To demonstrate that $\mathcal{P}(\mathbf{a}_\lambda, (\alpha_{j,i})_{i\in[n]}) \cap T \subseteq \mathcal{A}_\lambda$, we assume that $\lambda \in \mathcal{C}_f$. For $\lambda \in \mathcal{C}_w \notin \mathcal{C}_f$, consider $w\Phi$ and apply the same arguments.
We first observe that $\mathcal{P}(\mathbf{a}_\lambda, (\alpha_{j,i})_{i\in[n]}) \subseteq \lambda + \mathcal{C}^-$ for the negative cone $\mathcal{C}^-$ (compare Definition 2.2.25). This follows from Lemma 4.2.5. Now let $\mu \in \mathcal{P}(\mathbf{a}_\lambda, (\alpha_{j,i})_{i\in[n]}) \cap T$. With $\mu \in T$, we can express μ as $\mu = \lambda - \sum_{\alpha\in\Phi} k_\alpha \alpha^\vee$ with $k_\alpha \in \mathbb{Z}$. But with Definition 4.3.5 for $\mathcal{A}_\lambda$ and $\mu \in \mathcal{P}(\mathbf{a}_\lambda, (\alpha_{j,i})_{i\in[n]})$, it follows that $\mu \in \mathrm{conv}(\mathcal{A}_\lambda)$, that is, $\mu = \lambda - \sum_{i\in[n]} k_i' \alpha_{j,i}^\vee$ with the bounds $1 \leq k_i' \leq \max_i$ and $k_i' \in \mathbb{R}$. This implies that we find an expression for μ as $\mu = \lambda - \sum_{\alpha\in\Phi} k_\alpha \alpha^\vee$ with $k_\alpha \in \mathbb{Z}$ and $k_\alpha = 0$ for all $\alpha \notin (\alpha_{j,i})_{i\in[n]}$. Together, this proves the claim. □

Open question 4.3.10. As proven in Proposition 4.3.9, the set $\mathcal{A}_\lambda$ is the set of all coroot lattice points that intersect with the folding pattern polytope $\mathcal{P}(\mathbf{a}_\lambda, (\alpha_{j,i})_{i\in[n]})$. Many of these points are contained in its interior. Recall that in Definition 4.3.5, the polytope is defined as the Euclidean convex hull of $\mathcal{A}_\lambda$. Given that $\mathcal{A}_\lambda$ may have a large cardinality, it is desirable to understand the structure and know the number of the extremal points of $\mathcal{P}(\mathbf{a}_\lambda, (\alpha_{j,i})_{i\in[n]})$.

Open question 4.3.11. There appears to be a potential connection between folding pattern polytopes and pseudo-Weyl polytopes: A λ-Weyl polytope is defined as $\mathcal{P}(\lambda) = \text{conv}^*(W \cdot \lambda)$, where $\text{conv}^*(\cdot)$ denotes the Euclidean convex hull. Weyl polytopes can also be characterized as the intersection of dual hyperplanes within the Coxeter complex. From this, pseudo-Weyl polytopes are constructed by translating the hyperplanes of a λ-Weyl polytope [Kam10].
The examples of folding pattern polytopes we have studied so far suggest that they might be pseudo-Weyl polytopes. It remains an open question to provide a proof for this observation and, if possible, to describe folding pattern polytopes in terms of pseudo-Weyl polytopes.
Additionally, it is worth noting that Ehrig explored connections between Mirković-Vilonen polytopes, which are pseudo-Weyl polytopes, and folded galleries as well [Ehr10].

4.3.2. Description of Coxeter Shadows of gates. Using the folding pattern polytopes, we can construct the entire Coxeter shadow of a gate $\mathbf{a}_\lambda = \mathbf{x}$ with $x = t^\lambda u$ and regular $\lambda \in T$ with respect to a given Weyl chamber orientation ϕ_w as follows: Use the Bruhat moment graph and Theorem 3.3.9 to derive all ϕ_w-positive folding patterns for minimal galleries ending in $\mathbf{a}_\lambda$. Afterwards, compute all corresponding folding pattern polytopes $\mathcal{P}(\mathbf{a}_\lambda, (\alpha_{j,i})_{i\in[n]})$. Besides that, use Theorem 3.3.18 for every applicable folding pattern to determine the spherical direction of the end alcoves of galleries obtained from minimal galleries ending in $\mathbf{a}_\lambda$ that are folded with the pattern. With this information, construct a set of alcoves for every folding pattern by combining all coroot lattice points contained within the computed folding pattern polytope with the spherical direction obtained in the previous step. The union of these alcove sets then gives the Coxeter shadow.
For the case of group elements $x = t^\lambda u$ that are the gate of their vertex λ, this answers the question which alcoves are contained within their Coxeter shadow:

Theorem 4.3.12 (Coxeter shadow of gates)**.** *Let (W, S) be an affine Coxeter system with (W_0, S_0) the associated spherical system. Let the Coxeter complex $\Sigma = \Sigma(W, S)$ be equipped with a Weyl chamber orientation ϕ_w. Let further $x = t^\lambda u$ be a group element such that $\lambda \in T$ is regular and $\mathbf{x}$ is the gate of λ. Then $y = t^\mu v \in \text{Sh}_{\phi_w}(x)$ if and only if there exists a ϕ_w-positive folding pattern $(\alpha_{j,i})_{i\in[n]}$ that is applicable to x such that $\mu \in \mathcal{P}(\mathbf{a}_\lambda, (\alpha_{j,i})_{i\in[n]})$ and v is the end node of the path labeled $(\alpha_{j,i})_{i\in[n]}$ starting in the node u in the undirected moment graph $\mathcal{G}^{un}_{W_0}$.*

Proof. Combine Proposition 4.3.9 and Theorem 3.3.18. □

Open question 4.3.13. It is a natural question to ask for a generalization of Theorem 4.3.12 for non-regular coroot lattice points λ. To apply similar methods as presented here, it is necessary to first answer Open question 4.1.4.

The remainder of this subsection is dedicated to the computation of an example illustrating Theorem 4.3.12.

Example 4.3.14. Consider a Coxeter group W of type $\tilde{\mathtt{A}}_2$ and the group element $x = t^\lambda w_0$ with $\mathbf{x} = \mathbf{a}_\lambda$ that is the last alcove of the galleries γ_λ and $\tilde{\gamma}_\lambda$ we discussed in Examples 4.2.6, 4.3.1 and 4.3.8. Compare also Figure 4.3. We want to compute the Coxeter shadow of x with respect to the Weyl chamber orientation ϕ_{w_0} induced by the unique longest element of the associated spherical Weyl group $w_0 \in W_0$.

For this, observe first that $\mathbf{x} \in \mathcal{C}_f$. It follows that, invoking Theorem 3.3.3, we may read off the possible folding patterns for x from the Bruhat moment graph $\mathcal{G}_{W_0}$ associated with W_0 as the label index sequences of directed paths starting in the node labeled e. For the Bruhat moment graph of $\mathtt{A}_2$, see Figure 1.1. We obtain the following folding patterns:

- 3 folding patterns of length 1: (α_1), (α_2), and $(\alpha_1 + \alpha_2)$;
- 4 folding patterns of length 2: (α_1, α_2), $(\alpha_1, \alpha_1+\alpha_2)$, (α_2, α_1), and $(\alpha_2, \alpha_1+\alpha_1)$;
- 4 folding patterns of length 3: $(\alpha_1, \alpha_2, \alpha_1)$, $(\alpha_1, \alpha_1 + \alpha_2, \alpha_2)$, $(\alpha_2, \alpha_1, \alpha_2)$, and $(\alpha_2, \alpha_1 + \alpha_2, \alpha_1)$.

Next, we compute the folding pattern polytopes for all these folding patterns. It holds $\langle \alpha_1, \lambda \rangle = 2$, $\langle \alpha_2, \lambda \rangle = 5$, and $\langle \alpha_1 + \alpha_2, \lambda \rangle = 7$. It follows with Lemma 4.1.7 that every minimal gallery $\gamma : \mathbf{c_f} \rightsquigarrow \mathbf{x}$ crosses 1 α_1-hyperplane, 4 α_2-hyperplanes, and 6 $\alpha_1 + \alpha_2$-hyperplanes. With our observations made in Example 4.3.8, we may use the minimal gallery γ_λ displayed in Figure 4.1 to compute the vertex sets $\mathcal{A}_\lambda$ for the three folding patterns (α_1), (α_2), and $(\alpha_1 + \alpha_2)$. We obtain

$$\begin{aligned}
\mathcal{A}_\lambda((\alpha_1)) &= \{\lambda - \alpha_1^\vee\};\\
\mathcal{A}_\lambda((\alpha_2)) &= \{\lambda - k\alpha_2^\vee \mid k \in [4]\};\\
\mathcal{A}_\lambda((\alpha_1 + \alpha_2)) &= \{\lambda - k(\alpha_1 + \alpha_2)^\vee \mid k \in [6]\}.
\end{aligned}$$

Recall that we computed $\mathcal{A}_\lambda((\alpha_2))$ in Example 4.2.6. For an illustration see the left picture of Figure 4.2.
We have $\mathrm{sph}(x) = w_0$. Invoking Theorem 3.3.18, we can derive the spherical directions of the end alcoves of galleries obtained from minimal galleries ending in $\mathbf{x}$ by applying the three folding patterns of length 1. Again, refer to Figure 1.1 for a picture of the moment graph. The spherical directions of the end alcoves are

- $s_2 s_1$ for the folding pattern (α_1),
- $s_1 s_2$ for the folding pattern (α_2),
- e for the folding pattern $(\alpha_1 + \alpha_2)$.

Together, we can construct the set of alcoves of $\mathrm{Sh}_{\phi_{w_0}}(x)$ that can be obtained as end alcoves of galleries by folding a minimal gallery of x once.

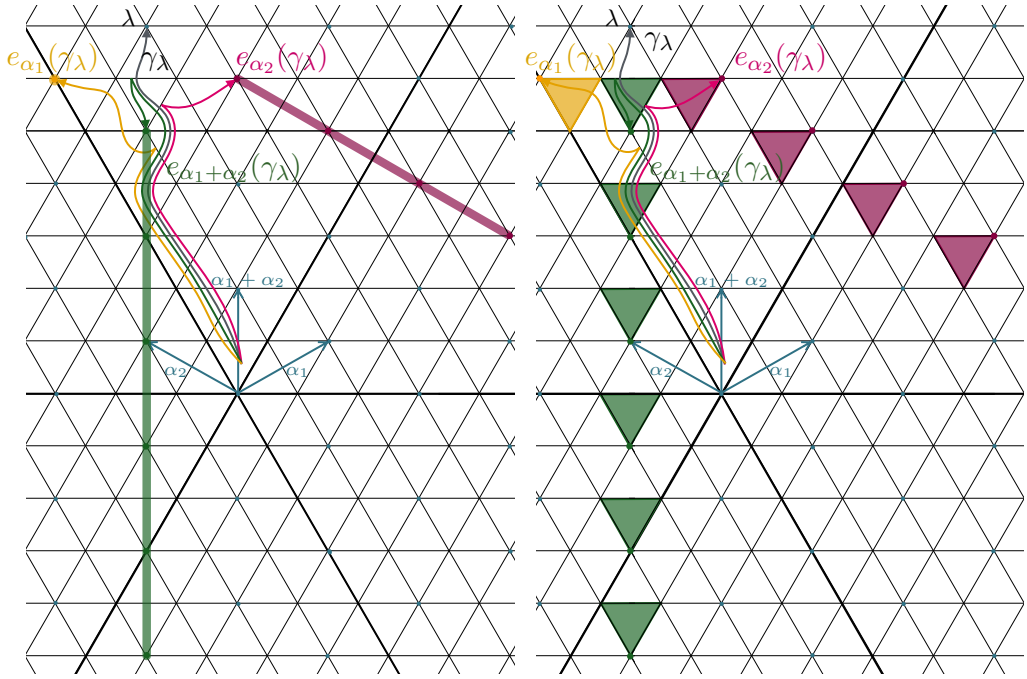

FIGURE 4.4. *On the left:* Illustration of the vertex sets $\mathcal{A}_\lambda$ and folding pattern polytopes for the gate alcove $\mathbf{a}_\lambda$ for the folding patterns (α_1) in orange, (α_2) in pink, and $(\alpha_1+\alpha_2)$ in green. *On the right:* The sets of corresponding end alcoves of galleries folded with these patterns.

The left picture in Figure 4.4 shows the vertex sets $\mathcal{A}_\lambda$ and folding pattern polytopes for the folding patterns of length 1. The picture on the right shows the set of alcoves.

Next we consider the 4 folding patterns of length 2:
Observe that we already computed the vertex set $\mathcal{A}_\lambda$ and the folding pattern polytope for (α_2, α_1) in Example 4.3.8. See also Figure 4.3. For the remaining three folding patterns of length 2, we obtain the following vertex sets:

$$\begin{aligned}
\mathcal{A}_\lambda((\alpha_1,\alpha_2)) &= \{\lambda - \alpha_1^\vee - k\alpha_2^\vee |\ k \in [5]\};\\
\mathcal{A}_\lambda((\alpha_1,\alpha_1+\alpha_2)) &= \{\lambda - \alpha_1^\vee - k(\alpha_1+\alpha_2)^\vee |\ k \in [4]\};\\
\mathcal{A}_\lambda((\alpha_2,\alpha_1+\alpha_2)) &= \{\lambda - k\alpha_2^\vee - (\alpha_1+\alpha_2)^\vee |\ k \in [4]\}.
\end{aligned}$$

We again apply Theorem 3.3.18 to derive the spherical directions of the end alcoves of galleries obtained from minimal galleries ending in $\mathbf{x}$ by applying the four folding patterns of length 2. The spherical directions of the end alcoves are

- s_1 for the folding pattern (α_1, α_2),
- s_2 for the folding pattern $(\alpha_1, \alpha_1+\alpha_2)$,
- s_2 for the folding pattern (α_2, α_1),
- s_1 for the folding pattern $(\alpha_2, \alpha_1+\alpha_2)$.

Together, we can construct the set of alcoves of $\mathrm{Sh}_{\phi_{w_0}}(x)$ that can be obtained as end alcoves of galleries by folding a minimal gallery of x twice positively with respect to ϕ_{w_0}. An illustration of the vertex sets $\mathcal{A}_\lambda$ and the constructed alcoves is provided in Figure 4.5.

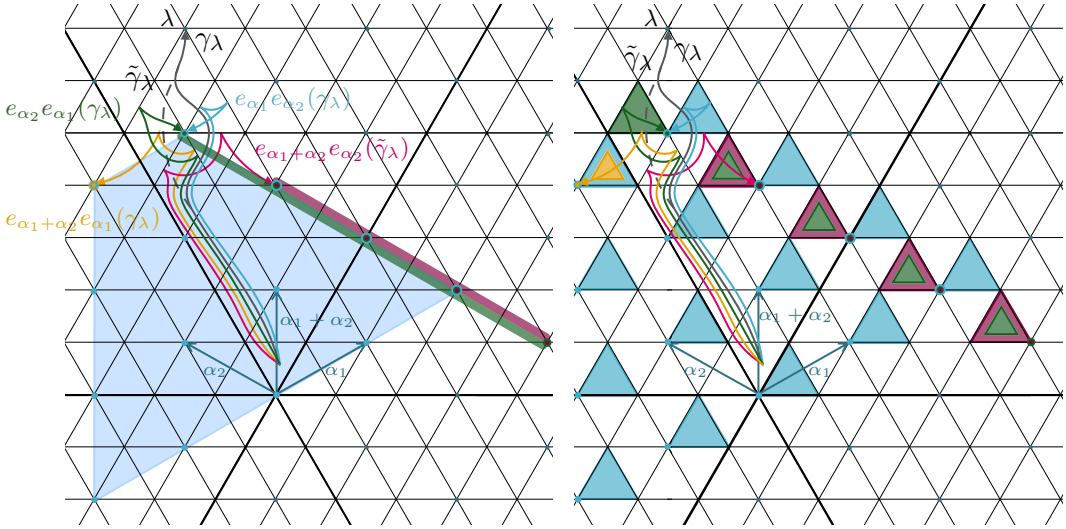

FIGURE 4.5. *On the left:* Illustration of the vertex sets $\mathcal{A}_\lambda$ and folding pattern polytopes for the gate alcove $\mathbf{a}_\lambda$ for the folding patterns $(\alpha_1, \alpha_1+\alpha_2)$ in orange, $(\alpha_2, \alpha_1+\alpha_2)$ in pink, (α_1, α_2) in green, and (α_2, α_1) in blue. *On the right:* The sets of corresponding end alcoves of galleries folded with these patterns. The dashed lines indicate where the galleries γ_λ and $\tilde{\gamma}_\lambda$ differ.

At last, we examine the 4 folding patterns of length 3 and obtain the following vertex sets:

$$\begin{aligned}
\mathcal{A}_\lambda((\alpha_1,\alpha_2,\alpha_1)) &= \{\lambda - k\alpha_1^\vee - l\alpha_2^\vee |\ 2 \le k \le 5,\ k \le l \le 5\};\\
\mathcal{A}_\lambda((\alpha_1,\alpha_1+\alpha_2,\alpha_2)) &= \emptyset;\\
\mathcal{A}_\lambda((\alpha_2,\alpha_1,\alpha_2)) &= \{\lambda - k\alpha_1^\vee - l\alpha_2^\vee |\ 2 \le k \le 5,\ k \le l \le 5\};\\
\mathcal{A}_\lambda((\alpha_2,\alpha_1+\alpha_2,\alpha_1)) &= \{\lambda - 4\alpha_2^\vee - (\alpha_1+\alpha_2)^\vee - k\alpha_1^\vee |\ k \in [3]\}.
\end{aligned}$$

By invoking Theorem 3.3.18 once more, we can derive the spherical directions of the end alcoves of galleries obtained from minimal galleries ending in $\mathbf{x}$ by applying the four folding patterns of length 3.

Together, we can construct the set of alcoves of $\mathrm{Sh}_{\phi_{w_0}}(x)$ that can be obtained as end alcoves of galleries by folding a minimal gallery of x thrice positively with respect to ϕ_{w_0}. These alcoves are illustrated in Figure 4.6. The union of the alcove sets constructed above gives the Coxeter shadow of x. An illustration is given in Figure 4.7.

Remark 4.3.15. Observe that the folding pattern polytopes have different dimensions: In the example discussed above, the polytopes of folding patterns with length 1 are 0- or

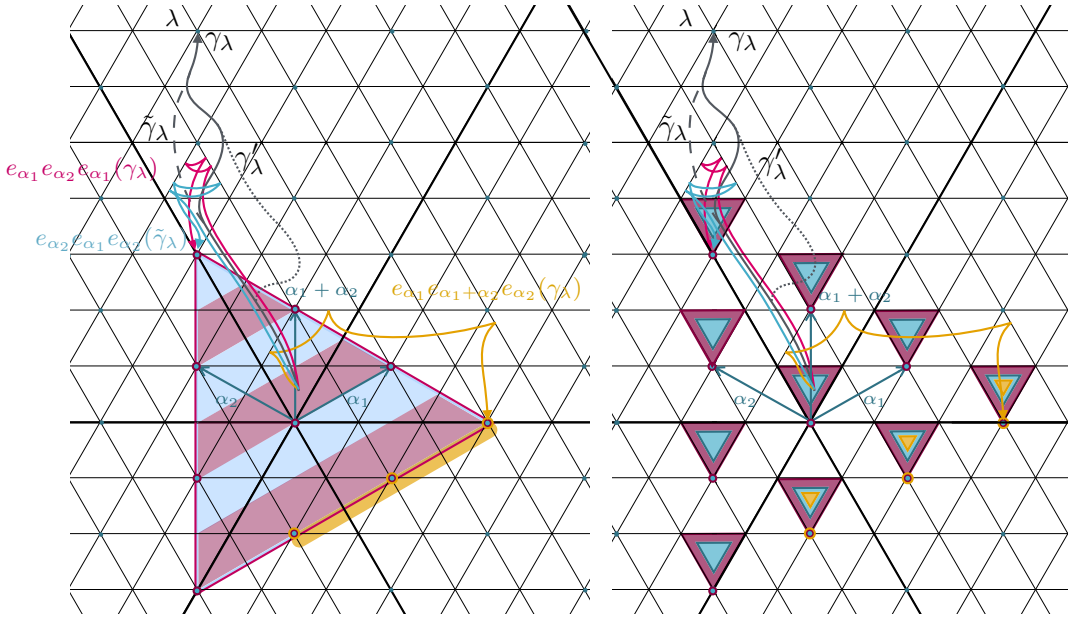

FIGURE 4.6. *On the left:* Illustration of the vertex sets $\mathcal{A}_\lambda$ and folding pattern polytopes for the gate alcove $\mathbf{a}_\lambda$ for the folding patterns $(\alpha_1, \alpha_2, \alpha_1)$ in pink, $(\alpha_2, \alpha_1, \alpha_2)$ in blue, and $(\alpha_2, \alpha_1 + \alpha_2, \alpha_1)$ in orange. *On the right:* The sets of corresponding end alcoves of galleries folded with these patterns. The dashed and dotted lines indicate where the galleries γ_λ, $\tilde{\gamma}_\lambda$, and γ'_λ differ.

1-dimensional, while the polytopes of folding patterns with length 2 and 3, if nonempty, have dimension 1 or 2.
Observe further that the alcove sets constructed from the folding pattern polytopes and application of Theorem 3.3.18 are not disjoint. For example, see Figure 4.7, where some of the alcoves of $\mathrm{Sh}_{\phi_{w_0}}(x)$ can be obtained by folding a suitable gallery once or three times. Alternatively, compare Figure 4.5, where $\mathcal{P}(\mathbf{a}_\lambda, (\alpha_1, \alpha_2)) \cap \mathcal{P}(\mathbf{a}_\lambda, (\alpha_2, \alpha_1 + \alpha_2)) = \mathcal{P}(\mathbf{a}_\lambda, (\alpha_2, \alpha_1 + \alpha_2))$ and the alcoves obtained from these folding pattern polytopes have the same spherical direction. This implies that some elements of the Coxeter shadow can be obtained as end alcoves of folded galleries by applying different folding patterns to suitable minimal galleries ending in $\mathbf{x}$. As a consequence, to compute the whole Coxeter shadow, it is not necessary to compute the folding pattern polytopes for all folding patterns, but a subset of them, to compute the whole Coxeter shadow in the example we discussed above.

This remarks motivates the following questions:

Open question 4.3.16. Given an affine Coxeter group of rank $n+1$ and a folding pattern $(\alpha_{j,i})_{i\in[k]}$ of length k, what is the dimension of the folding pattern polytope $\mathcal{P}(\mathbf{a}_\lambda, (\alpha_{j,i})_{i\in[k]})$?

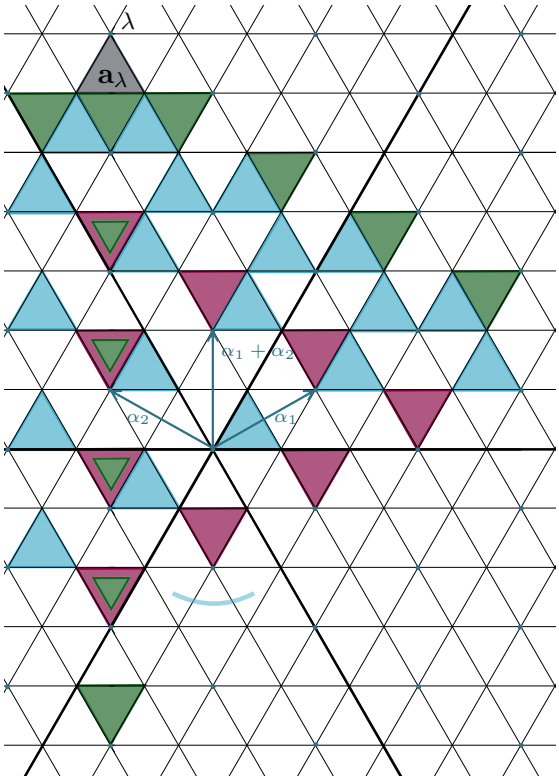

FIGURE 4.7. Shadow of a_λ with respect to ϕ_{w_0}. The orientation defining Weyl chamber is indicated by the light blue arc. The alcoves obtained by folding a minimal gallery for $\mathbf{a}_\lambda$ once are shown in green, by folding twice in blue, and folding three times in purple.

Open question 4.3.17. Let (W, S) be an affine Coxeter system, and let the associated Coxeter complex $\Sigma = \Sigma(W, S)$ be equipped with a Weyl chamber orientation ϕ_w. Consider $y \in \mathrm{Sh}_{\phi_w}(x)$ for $x = t^\lambda v$. It would be interesting to study the multiplicities of y in $\mathrm{Sh}_{\phi_w}(x)$, distinguishing between two different types: First, we can explore the *pattern multiplicity of y in* $\mathrm{Sh}_{\phi_w}(x)$, which is the number of folding patterns $(\alpha_{j,i})_{i\in[n]}$ such that there exists a minimal gallery $\gamma : \mathbf{c_f} \rightsquigarrow \mathbf{x}$ that can be ϕ_w-poyitively folded onto $\mathbf{y}$ following the folding pattern $(\alpha_{j,i})_{i\in[n]}$. Additionally, we could study the *gallery multiplicity of y in* $\mathrm{Sh}_{\phi_w}(x)$, which refers to the number of galleries $\gamma : \mathbf{c_f} \rightsquigarrow \mathbf{x}$ such that there exists a folding pattern $(\alpha_{j,i})_{i\in[n]}$ allowing the gallery to be ϕ_w-poyitively folded onto $\mathbf{y}$ following the folding pattern $(\alpha_{j,i})_{i\in[n]}$. This inquiry is closely related to the study of the *co-Shadow* $\mathrm{Sh}^{co}_\phi(x)$ *of x with respect to the orientation ϕ*, which denotes the set of group elements y for which there exists a minimal gallery $\gamma : \mathbf{c_f} \rightsquigarrow \mathbf{y}$ that can be ϕ-positively folded onto a gallery $\gamma' : \mathbf{c_f} \rightsquigarrow \mathbf{x}$.

4.4. Coxeter umbrae

We will now use our results from Section 4.3 to compute a subset of the Coxeter shadow with respect to Weyl chamber orientations for arbitrary group elements in affine Coxeter groups. For this, we introduce the notion of the *Coxeter umbra*.

However, we note the following connection between folding pattern polytopes and the vertex shadow beforehand.

Proposition 4.4.1 (Folding pattern polytopes and vertex shadow)**.** *Let $\Sigma = \Sigma(W, S)$ be an affine Coxeter complex with periodic orientation ϕ. Let further $x = t^\lambda w \in W$ with $\lambda \in T$ regular. Denote by $\mathscr{Fp}$ the set of folding patterns with respect to ϕ that are applicable to a minimal gallery $\gamma : \mathbf{c_f} \rightsquigarrow \mathbf{x}$. Then*

$$\mathrm{Sh}_\phi^{\mathrm{vtx}}(x) = \bigcup_{(\alpha_{j,i})_{i\in[n]} \in \mathscr{Fp}} \mathcal{P}(\mathbf{a}_\lambda, (\alpha_{j,i})_{i\in[n]}),$$

where $\mathbf{a}_\lambda$ denotes the gate of λ.

Proof. Combine Theorem 4.3.12 and Lemma 3.2.13. □

Given the folding pattern polytopes of the gate $\mathbf{a}_\lambda$ of a coroot lattice point λ, we can quickly derive a subset of the Coxeter shadow of an element $x = t^\lambda w$ by using the same method as in Section 4.3.2. We will use the following notation:

Notation 4.4.2. Let $\Sigma = \Sigma(W, S)$ be an affine Coxeter complex with periodic orientation ϕ. Let further $x = t^\lambda w \in W$ and $\mathbf{a}_\lambda$ be the gate of λ. Denote by $\mathscr{Fp}$ the set of folding patterns with respect to ϕ that are applicable to a minimal gallery $\gamma : \mathbf{c_f} \rightsquigarrow \mathbf{x}$. Recall that we denote by $\mathcal{A}_\lambda((\alpha_{j,i})_{i\in[n]})$ the coroot lattice points that intersect with the folding pattern polytope $\mathcal{P}(\mathbf{a}_\lambda, (\alpha_{j,i})_{i\in[n]})$. Then we denote for $(\alpha_{j,i})_{i\in[n]} \in \mathscr{Fp}$:

$$\mathcal{Y}_x((\alpha_{j,i})_{i\in[n]}) = \{\mathbf{y} = t^\lambda \mathbf{v} |\ \mu \in \mathcal{A}_\lambda((\alpha_{j,i})_{i\in[n]}),\ v \text{ is the end node of a path labeled } (\alpha_{j,i})_{i\in[n]} \text{ starting in } w \text{ in } \mathcal{G}^{un}_{W_0}\}.$$

Having this, we are ready to introduce Coxeter umbrae:

Definition 4.4.3 (Coxeter Umbra)**.** Let $\Sigma = \Sigma(W, S)$ be an affine Coxeter complex with periodic orientation ϕ. Let further $x = t^\lambda w \in W$ with $\lambda \in T$ regular. Denote by $\mathscr{Fp}$ the set of folding patterns with respect to ϕ that are applicable to a minimal gallery $\gamma : \mathbf{c_f} \rightsquigarrow \mathbf{x}$ and use the notation as in Notation 4.4.2. Then we define the *Coxeter Umbra* $\mathrm{Um}_\phi(x)$ *of x with respect to ϕ* as

$$\mathrm{Um}_\phi(x) = \bigcup_{(\alpha_{j,i})_{i\in[n]} \in \mathscr{Fp}} \mathcal{Y}_x((\alpha_{j,i})_{i\in[n]}),$$

where $\mathbf{a}_\lambda$ denotes the gate of λ.

Theorem 4.4.4 (Umbrae and shadows)**.** *Use the notation as in Definition 4.4.3. Then*

$$\mathrm{Um}_\phi(x) \subseteq \mathrm{Sh}_\phi(x).$$

Furthermore, if $\mathbf{x} = \mathbf{a}_\lambda$, then $\mathrm{Um}_\phi(x) = \mathrm{Sh}_\phi(x)$.

Proof. Combine Proposition 4.4.1 with Theorem 3.3.18. The equality follows from Definition 4.4.3 and Theorem 4.3.12. □

We close this section with the discussion of examples of Coxeter umbrae.

Example 4.4.5. Consider the three group elements $x = t^\lambda s_1$, $y = t^\lambda e$, $z = t^\lambda w_0 \in W_{\tilde{\mathtt{A}}_2}$ with $\lambda = 3\alpha_1 + 4\alpha_2$. Observe that $\mathbf{z} = \mathbf{a}_\lambda$ is the gate of λ. Fix the opposite Weyl chamber orientation $\phi = \phi_{w_0}$. We have discussed the folding pattern polytopes and the shadow of $\mathbf{a}_\lambda$ with respect to ϕ in Example 4.3.14. For this, we also computed the vertex sets $\mathcal{A}_\lambda$ for all applicable folding patterns and the umbra of x, y, and z there.
We will now compute the subset of $\mathrm{Sh}(x)$ that is given in Theorem 4.4.4. To derive the alcove sets $\mathcal{Y}_x((\alpha_{j,i})_{i\in[n]})$, use Theorem 3.3.18 to determine the spherical directions of the alcoves with vertices in $\mathcal{A}_\lambda((\alpha_{j,i})_{i\in[n]})$. Note that $\mathrm{sph}(x) = s_1$. We obtain

- e for the folding pattern (α_1);
- s_2s_1 for the folding patterns (α_2);
- s_1s_2 for the folding patterns $(\alpha_1 + \alpha_2)$;
- s_2 for the folding patterns (α_1, α_2) and $(\alpha_2, \alpha_1 + \alpha_2)$;
- w_0 for the folding patterns $(\alpha_1, \alpha_1 + \alpha_2)$ and (α_2, α_1);
- and s_1s_2 for the folding patterns $(\alpha_1, \alpha_2, \alpha_1)$, $(\alpha_2, \alpha_1, \alpha_2)$, $(\alpha_1, \alpha_1+\alpha_2, \alpha_2)$, and $(\alpha_2, \alpha_1 + \alpha_2, \alpha_1)$.

An illustration of the shadow, the vertex shadow, and the alcove sets $\mathcal{Y}_x$ is provided in Figure 4.8.

For $y = t^\lambda e$, we can compute the subset of $\mathrm{Sh}(x)$ that is described in Theorem 4.4.4 analogously. For the spherical directions of the alcoves in $\mathcal{Y}_y$ we obtain

- s_1 for the folding pattern (α_1);
- s_2 for the folding patterns (α_2);
- w_0 for the folding patterns $(\alpha_1 + \alpha_2)$;
- s_2s_1 for the folding patterns (α_1, α_2) and $(\alpha_2, \alpha_1 + \alpha_2)$;
- s_1s_2 for the folding patterns $(\alpha_1, \alpha_1 + \alpha_2)$ and (α_2, α_1);
- and w_0 for the folding patterns $(\alpha_1, \alpha_2, \alpha_1)$, $(\alpha_2, \alpha_1, \alpha_2)$, $(\alpha_1, \alpha_1 + \alpha_2, \alpha_2)$, and $(\alpha_2, \alpha_1 + \alpha_2, \alpha_1)$.

An illustration of the shadow, the vertex shadow, and the alcove sets $\mathcal{Y}_y$ is provided in Figure 4.9.

Remark 4.4.6. Observe that the alcoves of the Coxeter umbra cover all alcoves of the Coxeter shadow that are 'close' to the origin. In other words, the alcoves of the Coxeter shadow $\mathrm{Sh}_\phi(x)$ that cannot be constructed as alcoves of the sets $\mathcal{Y}_x$ are found at the outer boundary of the Coxeter shadow. Currently, this observation lacks a rigorous description.
On the other hand, there exist examples of group elements x with $\mathbf{x} \neq \mathbf{a}_\lambda$ where the Coxeter umbra covers up the entire Coxeter shadow. That is, in these cases we have set equality in Theorem 4.4.4. An example is illustrated in Figure 4.10.

These observations motivate the following two questions:

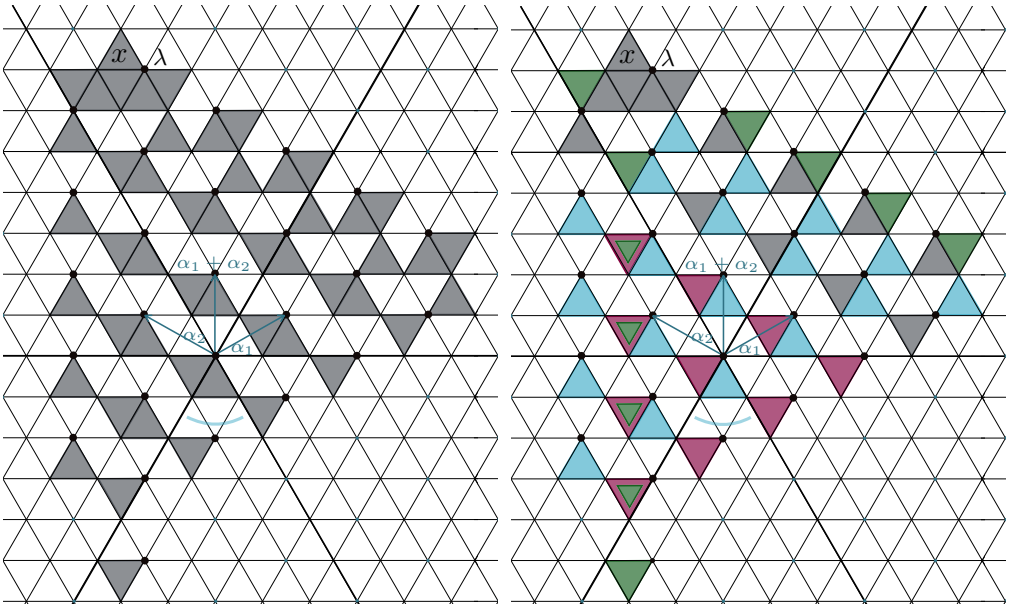

FIGURE 4.8. *On the left:* Coxeter shadow of $x = t^\lambda s_1$ with vertex shadow marked as black dots. The light blue arc indicates the orientation defining Weyl chamber. *On the right:* Coxeter shadow of x with highlighted alcove sets $\mathcal{Y}_x$ of the Coxeter umbra. The green alcoves are obtained from folding pattern polytopes with folding patterns of length 1, the blue alcoves from patterns of length 2, and the purple alcoves from pattern with length 3, respectively. The non-highlighted grey alcoves are not contained in the Coxeter umbra.

Open question 4.4.7. Let ϕ be a periodic orientation of the affine Coxeter complex $\Sigma = \Sigma(W, S)$, and let $x = t^\lambda w \in W$. Describe the set of alcoves $\mathcal{D} := \mathrm{Sh}_\phi(x) \setminus \mathrm{Um}_\phi(x)$ in terms of λ, w, and ϕ. This would then allow us to describe the Coxeter shadow as $\mathrm{Sh}_\phi(x) = \mathcal{D} \,\dot\cup\, \mathrm{Um}_\phi(x)$.

Open question 4.4.8. Let ϕ be a periodic orientation of the affine Coxeter complex $\Sigma = \Sigma(W, S)$, and let $x = t^\lambda w \in W$. We denote $\mathcal{D} := \mathrm{Sh}_\phi(x) \setminus \mathrm{Um}_\phi(x)$. Under what conditions on x and ϕ does it hold that $\mathcal{D} = \emptyset$? In other words, when is it true that $\mathrm{Sh}_\phi(x) = \mathrm{Um}_\phi(x)$?

Furthermore, the following question naturally arises:

Open question 4.4.9. It would be desirable to generalize the concept of folding pattern polytopes to other orientations. We conjecture that as long as the orientation is periodic, folding pattern polytopes should be convex polytopes of the coroot lattice. This is the next step in generalizing our findings to other orientations, specifically those induced by chimneys.

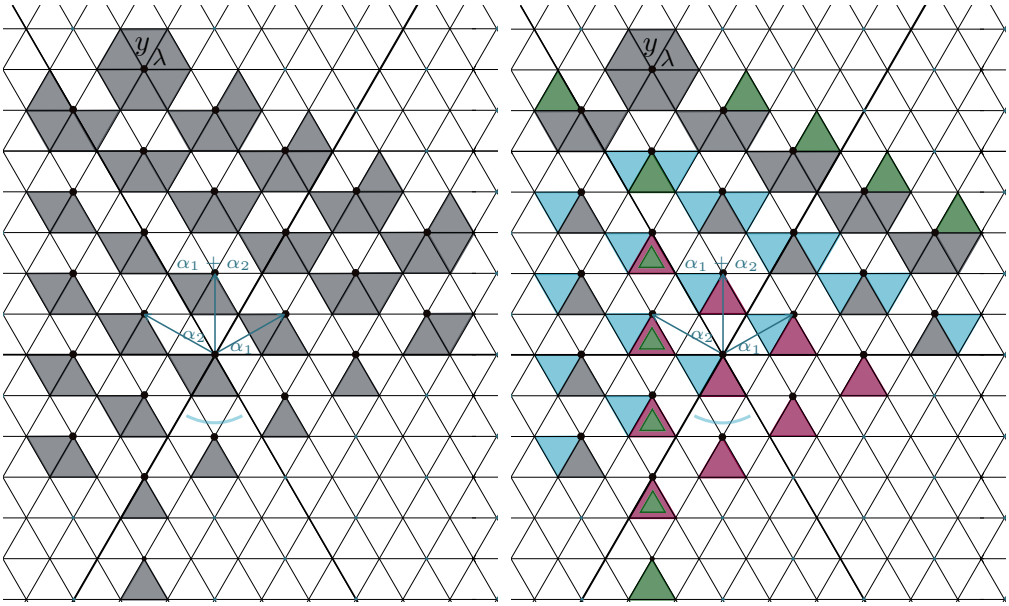

FIGURE 4.9. *On the left:* Coxeter shadow of $y = t^\lambda e$ with vertex shadow marked as black dots. The light blue arc indicates the orientation defining Weyl chamber. *On the right:* Coxeter shadow of y with highlighted alcove sets $\mathcal{Y}_y$ of the Coxeter umbra. The green alcoves are obtained from folding pattern polytopes with folding patterns of length 1, the blue alcoves from patterns of length 2, and the purple alcoves from pattern with length 3, respectively. The non-highlighted grey alcoves are not contained in the Coxeter umbra.

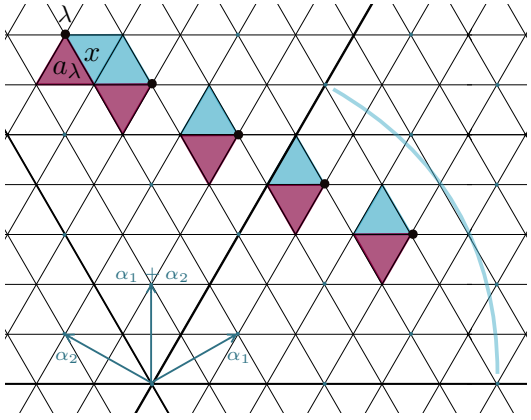

FIGURE 4.10. Coxeter shadow of $a_\lambda = t^\lambda w_0$ in purple and $x = t^\lambda s_2 s_1$ in blue with vertex shadow marked as black dots. The light blue arc indicates the orientation defining Weyl chamber.

Part III

Involutions in Coxeter groups

CHAPTER 5

Conjugacy classes of involutions in Coxeter groups

This chapter is based on the article [Rei+25]. Our goal is to combinatorially characterize the number cc_2 of conjugacy classes of involutions in any Coxeter group. For this, we will introduce the notion of higher rank odd graphs, which naturally generalizes the concept of odd graphs that was used previously to count the number of conjugacy classes of reflections (cf. [Bra+02]). Moreover, we will provide formulae for finite and affine types, besides computing cc_2 for all triangle groups and RACGs.

In Section 5.1 we set notation and establish the notion of Coxeter groups of *inc-type*. We will further collect some useful facts on them that allow us to transfer the problem of determining the number of conjugacy classes of involutions to the problem of counting the conjugacy classes of standard parabolic subgroups with irreducible components of inc-type. Section 5.2 introduces higher rank odd graphs and provides means to compute such graphs under specific conditions. Section 5.3.1 concerns technical results about conjugation of parabolic subgroups with nontrivial centers. In Section 5.3.2 we prove our main results. In Section 5.4 we explicitly compute and discuss cc_2, the number of conjugacy classes of involutions, for several subclasses of Coxeter groups, mostly applying Theorem 5.3.7 and the techniques from Section 5.2. More specifically, triangle groups are dealt with in Section 5.4.1, RACGs are discussed (with an alternative, geometric argument) in Section 5.4.2, and the final Section 5.4.3 concerns spherical and affine Coxeter groups. Given that the proofs of our results from Section 5.4.3 are extensive and repetitively utilize the same techniques as presented in Section 5.2, we will split them into Sections 5.5 and 5.6.

5.1. Coxeter groups of inc-type

We start by giving the definition of an involution:

Definition 5.1.1 (Involution)**.** An *involution* in W is a nontrivial element of order two. The *rank* of an involution is the rank of its parabolic closure.

Note that the rank of an involution thus depends on the chosen Coxeter system. Note further that all reflections are involutions, but not all involutions are reflections.

Example 5.1.2. Consider the Coxeter group $W_{\widetilde{\mathtt{C}}_2} = \langle s_0, s_1, s_2 \rangle$, where s_1, s_2 generate the finite Coxeter group of type $\mathtt{B}_2$. From the Coxeter diagram (see Figures A.1 and A.2), we read off that the relation $(s_1 s_2)^4 = 1$ holds. This implies that the element $w = s_1 s_2 s_1 s_2$ is an involution in both $W_{\mathtt{B}_2}$ and $W_{\widetilde{\mathtt{C}}_2}$.
Let $V = \mathbb{R}^2$ be equipped with the standard basis. We can describe s_1 as the reflection

along the vertical y-axis, represented by the matrix

$$s_1 = \begin{pmatrix} 1 & 0 \\ 0 & -1 \end{pmatrix}.$$

Similarly, s_2 represents the reflection along the line $x = y$ and is given by the matrix

$$s_2 = \begin{pmatrix} 0 & 1 \\ 1 & 0 \end{pmatrix}.$$

Now, we compute

$$s_1 s_2 = \begin{pmatrix} 0 & 1 \\ -1 & 0 \end{pmatrix},$$

which indicates that $s_1 s_2$ is a rotation by $\frac{\pi}{2}$. Next, we calculate w:

$$w = (s_1 s_2)^2 = \begin{pmatrix} -1 & 0 \\ 0 & -1 \end{pmatrix}.$$

This matrix represents a rotation by π, which only fixes the origin of V. Therefore, w is not a reflection.

Recall that the center of a group W is the set of group elements that commute with every element of W. For Coxeter groups, the classification of all groups with nontrivial center is well known. We recall this result in the following lemma.

Lemma 5.1.3 (Center of a Coxeter group)**.** *Let W be an irreducible Coxeter group. The center of W is nontrivial if and only if $W \cong W_\Gamma$ with Γ isomorphic to one of the diagrams in Figure 5.1. Moreover, in case Γ is one of the diagrams in Figure 5.1, the center of W_Γ is precisely the subgroup $\langle w_0 \rangle$, with w_0 the longest element.*

Proof. For W an infinite Coxeter group cf. [Dav08, Theorem D.2.10], [AB08, Proposition 2.73] or [Qi09]. For W spherical the 'if and only if' statement that Γ is isomorphic to one of the diagrams in Figure 5.1 follows from Coxeter's classification of finite irreducible Coxeter groups; see, for instance, [Ric82, Preliminaries, 1.9–1.12] or [Dav08, Remark 13.1.8]. The additional claim about the center being $\langle w_0 \rangle$ for the longest element w_0 has been long known for Weyl groups (see [Car72]), and can be readily checked for the remaining types `H` and `I`; for two elementary proofs, we refer the reader to [AB08, Corollary 1.91]. □

Notation 5.1.4. The Coxeter diagrams displayed in Figure 5.1 are referred to as the diagrams *of inc-type*. Moreover, we call W_Γ *of inc-type* if Γ is of *inc-type*. Here 'inc' abbreviates "irreducible with nontrivial center".

Remark 5.1.5. We remark that a subset $J \subseteq S$ generating an irreducible parabolic of inc-type is equivalent to the Coxeter system $(\langle J \rangle, J)$ satisfying the '(-1)-condition' (or 'being of (-1)-type) of Richardson; cf. [Ric82, Section 1.12]. We adopt new terminology since we deal directly with the group-theoretic condition about centers, whereas Richardson's (-1)-property is representation-theoretic, using root systems.

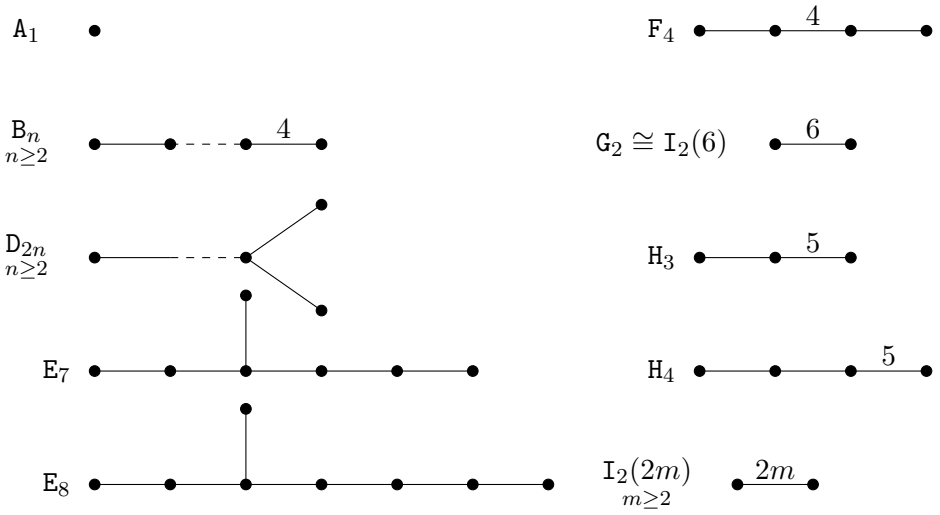

FIGURE 5.1. The Coxeter diagrams of inc-type yielding irreducible Coxeter groups with nontrivial centers.

Besides determining the center of (spherical) Coxeter groups, longest elements can also be used to represent conjugacy classes of involutions, as done below in Lemma 5.1.6. We note that Lemmas 5.1.6 and 5.1.7 correspond to part (a) of [Ric82, Theorem A]. We include a different proof which makes use of Springer's work [Spr82].

Lemma 5.1.6 (Involutions and longest elements)**.** *Let (W, S) be a Coxeter system of finite rank $|I|$ and let $c \in W$ be an involution. Then there exists a subset $J \subseteq I$ such that W_J is spherical, the longest element w_0 of W_J is central, and c is conjugate to w_0.*

PROOF. Consider the parabolic closure $\mathrm{Pc}(c)$. Since c has finite order, a result due to Tits (cf. [Dav08, Corollary D.2.9]) together with the minimality of parabolic closures implies that $\mathrm{Pc}(c)$ is in fact spherical. Moreover, $\mathrm{Pc}(c)$ is conjugate to some standard parabolic W_K with $|K|$ minimal; see, e.g., [Qi07, Theorem 3.4]. Thus, c is conjugate to some involution in W_K. In case W_K has irreducible components of classical types $\mathtt{A}_n$ to $\mathtt{G}_2$, apply [Spr82, Proposition 3] to conclude that such an involution is conjugate to the longest element of a (unique, standard) parabolic subgroup $W_J \subseteq W_K$ (with $J \subseteq K$) whose longest element is central. In case types $\mathtt{H}_n$ or $\mathtt{I}_2(n)$ are involved, one can directly check that the conclusion of Springer's proposition still holds true. Hence the lemma. □

Lemma 5.1.7 (Conjugated longest elements)**.** *Suppose W_J and W_K are standard parabolic subgroups whose irreducible components are of inc-type. Let c_J and c_K be the longest elements of W_J and W_K, respectively. Then $\mathrm{Pc}(c_J) = W_J$, $\mathrm{Pc}(c_K) = W_K$, and c_J is conjugate to c_K if and only if W_J and W_K are conjugate.*

PROOF. By Lemma 5.1.3, c_J is central. Since a reduced expression for c_J involves all letters of S_J and c_J commutes with all such generators, it follows that $\mathrm{Pc}(c_J) = W_J$. (Similarly for c_K.) Now assuming $c_J = wc_Kw^{-1}$, we obtain $W_J = \mathrm{Pc}(c_J) = \mathrm{Pc}(wc_Kw^{-1}) = w\mathrm{Pc}(c_K)w^{-1} = wW_Kw^{-1}$. The converse follows from Lemma 5.1.6. □

Lemmas 5.1.3, 5.1.6 and 5.1.7 imply that the number of conjugacy classes of involutions $\mathrm{cc}_2(W_\Gamma)$ is equal to the number of conjugacy classes of standard parabolic subgroups whose irreducible components are of inc-type.

5.2. Odd-adjacency and higher rank odd graphs

Recall that the odd graph Γ_{odd}, the graph obtained by deleting all edges labeled even or ∞ from a given Coxeter diagram, can be used to determine the number of conjugacy classes of reflections by counting the number of connected components of Γ_{odd}. See [Bra+02]. In this section, we generalize the concept of odd graphs and determine the number of conjugacy classes of involutions by counting connected components of these graphs. Notice that the odd graphs discussed here are not related to the family of odd graphs generalizing the Petersen graph as introduced by Biggs and Gardiner in the 1970s. See, e.g., [Big72].

5.2.1. Generalization of odd graphs. We start by introducing our notion of subgraph adjacency and odd-adjacency. Notice that our definition of subgraph adjacency is tailored to Coxeter diagrams and differs from the one commonly used in literature.

Definition 5.2.1 (Adjacent subgraphs)**.** Let Γ be a Coxeter diagram. Two full subgraphs Γ_J and Γ_K are *adjacent* if both Γ_J and Γ_K are isomorphic and the vertex sets $V(\Gamma_J) = S_J$ and $V(\Gamma_K) = S_K$ satisfy: $S_J \cap S_K = S_J \setminus \{s_j\} = S_K \setminus \{s_k\}$ with $s_j \neq s_k$.

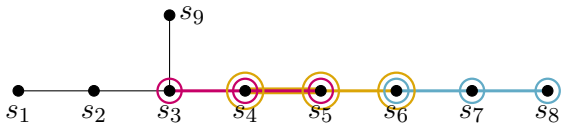

FIGURE 5.2. A Coxeter diagram of type $\widetilde{\mathtt{E}}_8$ with three subgraphs of type $\mathtt{A}_3$, highlighted in pink, orange, and blue.

Example 5.2.2. To illustrate adjacency of subgraphs, consider the affine Coxeter group $W_{\widetilde{\mathtt{E}}_8}$ of type $\widetilde{\mathtt{E}}_8$. Figure 5.2 shows its Coxeter diagram with three subdiagrams Γ_J,Γ_K, and Γ_L of type $\mathtt{A}_3$. They are spanned by the vertex sets $V(\Gamma_J) = \{s_3, s_4, s_5\}$, $V(\Gamma_K) = \{s_4, s_5, s_6\}$, as well as $V(\Gamma_L) = \{s_5, s_6, s_7\}$. It holds $\Gamma_J \cong \Gamma_K \cong \Gamma_L$. Since $V(\Gamma_J) \cap V(\Gamma_K) = V(\Gamma_J) \setminus \{s_3\} = V(\Gamma_K) \setminus \{s_6\}$, it follows that Γ_J and Γ_K are adjacent. But since $V(\Gamma_J) \cap V(\Gamma_L) = \emptyset$ and $V(\Gamma_K) \cap V(\Gamma_L) = \{s_6\}$, Γ_L is not adjacent to Γ_J nor to Γ_K.

We record a quick observation on the union of adjacent subgraphs of inc-type:

Lemma 5.2.3. *Let Γ be a Coxeter diagram and let Γ_J and Γ_K be two adjacent subgraphs. If Γ_J is of inc-type (see Figure 5.1) and of rank at least 2, then the standard parabolic subgroup generated by $V(\Gamma_J) \cup V(\Gamma_K) = S_{J\cup K}$ is infinite.*

PROOF. Let s_j be the unique vertex in $V(\Gamma_J)$ which is not in $V(\Gamma_K)$. Note that s_j is connected to some vertex in $V(\Gamma_J) \cap V(\Gamma_K)$. Thus the claim follows from the characterization of finite irreducible Coxeter groups. □

We now generalize the concept of odd-adjacency to higher rank parabolic subgroups.

Definition 5.2.4 (Odd-adjacent standard parabolics)**.** Let Γ be a Coxeter diagram. Two full subgraphs Γ_J and Γ_K are called *odd-adjacent* if the following hold:

(1) Γ_J and Γ_K are adjacent with $S_J \cap S_K = S_J \setminus \{s_j\} = S_K \setminus \{s_k\}$ and $s_j \neq s_k$;

(2) s_j is an isolated vertex of Γ_J and s_k is an isolated vertex of Γ_K;

(3) The vertices s_j and s_k are connected in Γ by an odd-labeled edge.

In this case, we also say that W_J and W_K are *odd-adjacent*. If $J = \{s\}$, $K = \{t\}$ are singletons and Γ_J and Γ_K are odd-adjacent, we also call the vertices $s, t \in V(\Gamma)$ odd-adjacent in Γ, in which case we call the edge $\{s, t\} \in E(\Gamma)$ an *odd edge*.

Example 5.2.5. To illustrate odd-adjacency, let us consider the affine Coxeter group $W_{\widetilde{\mathtt{E}}_8}$ again and compare Figure 5.3. Then the parabolic subgroup $W_{\{s_1,s_4,s_6,s_8,s_9\}}$ is odd-adjacent to the parabolic subgoup $W_{\{s_2,s_4,s_6,s_8,s_9\}}$, because the vertices corresponding to the generators s_1 and s_2 are odd-adjacent via the bold orange edge $\{s_1, s_2\}$.

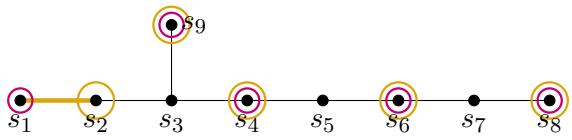

FIGURE 5.3. A Coxeter diagram of type $\widetilde{\mathtt{E}}_8$ with two odd-adjacent subgraphs of type $\mathtt{A}_1^5$, highlighted in pink and orange.

To simplify the upcoming definition of a higher rank odd graph, we introduce the graph-theoretic term of cocliques of *inc*-type.

Definition 5.2.6 (Inc-type cocliques)**.** Let Γ be a Coxeter diagram with vertex set $V(\Gamma) = S$. A vertex set $C \subseteq V(\Gamma)$ is called an *inc-type coclique* if the connected components of Γ_C are diagrams of inc-type. The *size* of an inc-type coclique is the cardinality of its vertex set.

Remark 5.2.7. Note that an inc-type coclique is not necessarily a coclique of Γ, but for subdiagrams of type $\sqcup_{i=1}^{k} \mathtt{A}_1$, the notions of coclique and inc-type coclique coincide. Notice further that inc-type cocliques are simply cocliques of graphs obtained from Γ by identifying (collapsing) all vertices contained in common full subgraphs of inc-types.

Example 5.2.8. The illustration in Figure 5.4 shows our concept of inc-type cocliques within a Coxeter diagram of type $\widetilde{\mathtt{E}}_8$. The vertices $C_1 = \{s_2, s_3, s_4, s_6, s_9\}$ span a subdiagram of type $\mathtt{D}_4 \sqcup \mathtt{A}_1$, which is highlighted in blue. Its connected components, spanned by the nodes labeled s_2, s_3, s_4, s_9 as well as the single node s_6, are subgroups of inc-type. Therefore, C_1 is an inc-type coclique. Note that C_1 is not a coclique in the usual graph-theoretic sense since the node labeled s_3 is adjacent to the nodes s_2, s_4, and s_9.
On the other hand, the vertex set $C_2 = \{s_1, s_7, s_8\}$ spans a subdiagram of type $\mathtt{A}_1 \sqcup \mathtt{A}_2$,

which is highlighted in pink. C_2 does not form an inc-type coclique because the subdiagram spanned by the nodes labeled s_7 and s_8 is of type $\mathtt{A}_2$ and, therefore, not of inc-type. Moreover, C_2 is not a coclique as well.

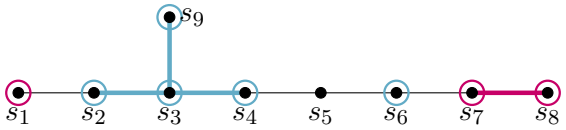

FIGURE 5.4. A Coxeter diagram of type $\widetilde{\mathtt{E}}_8$ with two subgraphs of type $\mathtt{D}_4 \sqcup \mathtt{A}_1$ and $\mathtt{A}_1 \sqcup \mathtt{A}_2$, highlighted in blue and pink.

Definition 5.2.9 (Higher rank odd graphs)**.** Let Γ be a Coxeter diagram with vertex set S indexed by I. For $k \geq 1$, the *k-odd graph* $\Gamma^k = (V(\Gamma^k), E(\Gamma^k))$ is defined as follows:

- The set of vertices $V(\Gamma^k)$ is the set of rank-k standard parabolic subgroups W_J for $J \subseteq I$ with S_J being an inc-type coclique of Γ;
- A pair of vertices W_J, W_K spans an edge in Γ^k if and only if W_J and W_K are odd-adjacent.

Note that $\Gamma^1 = \Gamma_{odd}$ with labels removed, and $\Gamma^k = \varnothing$ if $k > |V(\Gamma)|$. Moreover, it is known that $|\pi_0(\Gamma^1)|$ is independent of the chosen Coxeter system (W, S), see [MV24, Proposition 2.2].

Example 5.2.10. To illustrate the concept of higher rank odd graphs, we compute $\Gamma^5 = (V(\Gamma^5), E(\Gamma^5))$ for the Coxeter group $W_{\widetilde{\mathtt{E}}_8}$. A complete discussion of all k-odd graphs of this group can be found in Section 5.6.
We start by identifying all rank-5 standard parabolic subgroups of $W_{\widetilde{\mathtt{E}}_8}$, which have a generating set that is an inc-type coclique of $\Gamma_{\widetilde{\mathtt{E}}_8}$. Comparing Figure 5.1, we note that the diagram contains the inc-type cocliques

$$C_1 = \{s_2, s_3, s_4, s_6, s_9\},$$
$$C_2 = \{s_2, s_3, s_4, s_7, s_9\},$$
$$C_3 = \{s_2, s_3, s_4, s_8, s_9\},$$

which span the subgroups $W_{C_1} \cong W_{C_2} \cong W_{C_3}$ of type $\mathtt{D}_4 \sqcup \mathtt{A}_1$. The coclique C_1 is shown in Figure 5.4. Furthermore, the diagram $\Gamma_{\widetilde{\mathtt{E}}_8}$ contains the following inc-type cocliques:

$$C_4 = \{s_1, s_4, s_6, s_8, s_9\},$$
$$C_5 = \{s_2, s_4, s_6, s_8, s_9\}.$$

These sets of nodes span the subgroups $W_{C_4} \cong W_{C_5}$ of type $\mathtt{A}_1^5$. Therefore, the vertex set of Γ^5 is given as

$$V(\Gamma^5) = \{W_{C_1}, W_{C_2}, W_{C_3}, W_{C_4}, W_{C_5}\}.$$

Because the subdiagrams spanning W_{C_4} and W_{C_5} are odd-adjacent as shown in Example 5.2.5, the corresponding nodes in Γ^5 are connected by an edge. Observe further that the subdiagrams Γ_{C_1} and Γ_{C_2} are odd-adjacent since they only differ in one node and

the node labeled s_6 is adjacent via an odd-labeled edge to s_7. Similarly, Γ_{C_2} and Γ_{C_3} are odd-adjacent as well as they only differ by a single vertex, and the nodes s_7 and s_8 are adjacent along an odd-labeled edge. Therefore, we obtain the edge set $E(\Gamma^5)$ of Γ^5 as follows:

$$E(\Gamma^5) = \{\{W_{C_1}, W_{C_2}\}, \{W_{C_2}, W_{C_3}\}, \{W_{C_4}, W_{C_5}\}\}.$$

An illustration of Γ^5 is shown in Figure 5.5.

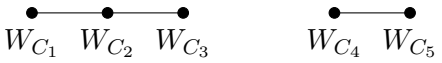

FIGURE 5.5. The 5-odd graph Γ^5 of the Coxeter diagram $\Gamma_{\widetilde{\mathrm{E}}_8}$.

Remark 5.2.11. Although we have introduced higher rank odd graphs Γ^k as graphs themselves, derived from a Coxeter diagram Γ, it turns out that $(V(\Gamma), V(\Gamma^k))$ can be interpreted as a *k-uniform hypergraph*. In this set-up, connected components in each Γ^k correspond to certain subgraphs of $(k-1)$-line graphs. We refer the reader to [Bre13] for more on hypergraph theory, and to [BHS77] for an introduction to s-line graphs.

5.2.2. Edges and connectivity of higher rank odd graphs. Next, we collect some conditions under which edges of Γ^k can be quickly derived. The first criterion is general, while the subsequent ones work for diagrams containing certain line subdiagrams. These criteria allow us to study connectivity in Γ^k for these particular cases.

For a given odd-edge $\{s_i, s_j\} \in E(\Gamma)$ the next lemma describes precisely which standard parabolic subgroups of inc-type are odd-adjacent via this edge. Recall that we denote by $N_\Gamma(K)$ the neighbourhood of a vertex set K in Γ.

Lemma 5.2.12 (Edges in Γ^m)**.** *Let $\Gamma = (S, E)$ be a Coxeter diagram and $\{s_i, s_j\} \in E$ be an odd edge, and let $\widetilde{\Gamma} = \Gamma \setminus N_\Gamma(s_i, s_j)$. If $m \geq 2$, then $\{\langle S_K, s_i\rangle, \langle S_K, s_j\rangle\} \in E(\Gamma^m)$ if and only if $S_K \subseteq V(\widetilde{\Gamma}) \setminus \{s_i, s_j\}$ is an inc-type coclique of size $m-1$. In particular, $\langle S_K, s_i\rangle$ and $\langle S_K, s_j\rangle$ are standard parabolic subgroups of W_Γ of rank m with irreducible components of inc-types.*

PROOF. Let first $\{\langle S_K, s_i\rangle, \langle S_K, s_j\rangle\} \in E(\Gamma^m)$. Then the vertices $\langle S_K, s_i\rangle$ and $\langle S_K, s_j\rangle$ of Γ^m are standard parabolic subgroups of rank m of inc-type. In particular, $|S_K \cup \{s_i\}| = m$ implies $|S_K| = m-1$. Since these two vertices form an edge in Γ^m by hypothesis, the parabolic subgroups $\langle S_K, s_i\rangle$ and $\langle S_K, s_j\rangle$ are odd-adjacent. Note that Definition 5.2.4 implies that $\langle S_K, s_i\rangle = W_L \times W_X$ and that $\langle S_K, s_j\rangle = W_M \times W_X$ for some index sets $L, X \subseteq K \cup \{i\}$, and $M, X \subseteq K \cup \{j\}$. In addition, $W_L \cong W_M \cong (\mathbb{Z}/2\mathbb{Z})^\ell$ for some $\ell \geq 1$. Moreover, $|L \setminus M| = |M \setminus L| = 1$ with $\{i\} = L \setminus M$, $\{j\} = M \setminus L$ and the edge $\{s_i, s_j\} \in E(\Gamma)$ is odd. Thus the standard parabolic subgroups $\langle s_i\rangle$, $\langle s_j\rangle$ commute with W_L, W_M and W_X. This implies that the intersection of $V(N_\Gamma(s_i, s_j))$ with $S_L \cup S_M \cup S_X$ is empty. Hence $S_K \subseteq V(\widetilde{\Gamma}) \setminus \{s_i, s_j\}$.
Conversely, let $S_K \subseteq V(\widetilde{\Gamma}) \setminus \{s_i, s_j\}$ be an inc-type coclique of $\widetilde{\Gamma}$ of size $m-1$. Then the standard parabolic subgroups $\langle S_K, s_i\rangle$ and $\langle S_K, s_j\rangle$ are of rank m. Further, the irreducible components of $\langle S_K, s_i\rangle$ and of $\langle S_K, s_j\rangle$ are of inc-type since s_i and s_j are not

adjacent to any vertex in S_K, hence $\langle S_K, s_i\rangle \cong W_K \times \langle s_i\rangle$ resp. $\langle S_K, s_j\rangle \cong W_K \times \langle s_j\rangle$. By assumption $\{s_i, s_j\} \in E(\Gamma)$ is an odd edge, thus $\{\langle S_K, s_i\rangle, \langle S_K, s_j\rangle\} \in E(\Gamma^m)$. □

Example 5.2.13. Figure 5.6 illustrates the construction of edges with Lemma 5.2.12 for the subgroups W_{C_4} and W_{C_5} discussed in Example 5.2.10 and pictured in Figure 5.3 above. The pair $\{s_1, s_2\}$ is an odd-edge in $\Gamma_{\widetilde{\mathtt{E}}_8}$. It holds $N_{\Gamma_{\widetilde{\mathtt{E}}_8}}(s_1, s_2) = \{s_3\}$. Since the vertex set $S_K := \{s_4, s_6, s_8, s_9\}$ is an inc-type coclique in $\Gamma_{\widetilde{\mathtt{E}}_8} \setminus \{s_3\}$, it follows that $\{\langle S_K, s_1\rangle, \langle S_K, s_2\rangle\} = \{\langle C_4\rangle, \langle C_5\rangle\} \in E(\Gamma^5)$.

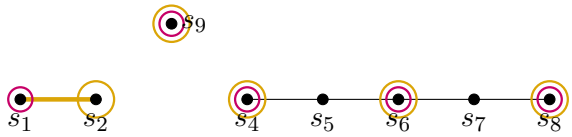

FIGURE 5.6. Illustration of $\Gamma_{\widetilde{\mathtt{E}}_8} \setminus N_{\Gamma_{\widetilde{\mathtt{E}}_8}}(s_1, s_2)$ with two subgraphs of type $\mathtt{A}_1^5$, marked with pink and orange circles.

The tools presented next concern path graphs (cf. Definition 2.1.4). These graphs are particularly useful as they show up as subdiagrams in most classical families of spherical and affine Coxeter diagrams. We start with the *Klapperschlangen*-Lemma.

Lemma 5.2.14 (Edge paths in Γ^k from odd sublines)**.** *Let Γ be a Coxeter diagram and let $W_J = W_L \times W_X, W_K = W_M \times W_X \in V(\Gamma^k)$ be distinct vertices in the k-odd graph Γ^k for some $k \geq 1$ with $W_L \cong W_M \cong (\mathbb{Z}/2\mathbb{Z})^\ell$, $\ell \in \mathbb{N}$. Suppose there exists a full subgraph $\mathcal{G} \subseteq \Gamma$ satisfying all of the following conditions:*

(1) The full subgraphs Γ_L and Γ_M corresponding to the union of the components of type $\mathtt{A}_1$ in W_J and W_K are both contained in $\mathcal{G}$;

(2) $\mathcal{G}$ is a path graph with odd edges only;

Then there exists an edge path connecting W_J to W_K in the k-odd graph Γ^k.

PROOF. The intuitive idea of the proof is to 'play' with the path graph $\mathcal{G}$ as a 'Klapperschlange' toy[1], folding it step-by-step to connect the given parabolics.

As $\mathcal{G}$ is a path graph, by Condition (2) we may linearly order its vertices as follows:

$$V(\mathcal{G}) = \{a_1, \ldots, a_m\},$$

where a_1 and a_m are the endpoints (leaves) of $\mathcal{G}$ and a_{i+1} is the obvious successor of a_i in this linear ordering. Note that any edges in Γ connecting any two $a_i, a_j \in V(\mathcal{G})$ must already be contained in $\mathcal{G}$ since $\mathcal{G}$ is assumed to be a full subgraph of Γ.

By definition, Γ_L and Γ_M are also full subgraphs of Γ, which in turn are, by Condition (1), contained in the full subgraph $\mathcal{G}$. By assumption $\Gamma_L \neq \Gamma_M$ and hence $|V(\mathcal{G})| = m > \ell =$

[1]The German word for 'rattlesnake'; 'Klapperschlangen' toys (or 'Zauberklapperschlangen') have wooden bits of same size that can be folded.

$|V(\Gamma_L)| = |V(\Gamma_M)|$. We may write

$$V(\Gamma_L) = \{a_{i_1}, \dots, a_{i_\ell} \mid i_1 < i_2 < \dots < i_\ell \text{ and } |i_f - i_h| \geq 2 \text{ for } f, h \in \{1, \dots, \ell\}\};$$
$$V(\Gamma_M) = \{a_{j_1}, \dots, a_{j_\ell} \mid j_1 < j_2 < \dots < j_\ell \text{ and } |j_f - j_h| \geq 2 \text{ for } f, h \in \{1, \dots, \ell\}\}.$$

Now suppose Γ_L and Γ_M only differ by one vertex, say $a_{i_\varphi} \in V(\Gamma_L) \setminus V(\Gamma_M)$ and $a_{j_\lambda} \in V(\Gamma_M) \setminus V(\Gamma_L)$ for some $\varphi, \lambda \in \{1, \dots, \ell\}$ with $\varphi \neq \lambda$. Without loss of generality, assume $i_\varphi < j_\lambda = i_\varphi + \eta$ with $\eta \geq 1$. In case $\eta = 1$, it is clear that W_L and W_M are odd-adjacent, hence also W_J and W_K are odd-adjacent and thus connected in Γ^k by an edge. So assume $\eta > 1$, in which case $|V(\mathcal{G})| = m > \ell + 1$. Looking at the intersection $V(\Gamma_L) \cap V(\Gamma_M)$ we see that, for every other vertex $a_{i_h} \in V(\Gamma_L) \setminus \{a_{i_\varphi}\}$ and $a_{j_f} \in V(\Gamma_M) \setminus \{a_{j_\lambda}\}$ with $i_h \neq j_f$, it holds

$$|i_h - j_\lambda| \geq 2 \leq |j_f - i_\varphi|.$$

In particular, we may search for the smallest possible indices $i_e < j_g \leq m$ with the following properties: the pair of distinct vertices $a_{i_e} \in V(\Gamma_L)$ and $a_{j_g} \in V(\Gamma_M) \setminus V(\Gamma_L)$ is such that none of the vertices a_{i_e+1}, a_{i_e+2}, …, a_{j_g-1} of the path graph $\mathcal{G}$ lying between a_{i_e} and a_{j_g} is contained in $V(\Gamma_L) \cup V(\Gamma_M)$. (Note that it might well be the case that $e = \varphi$ and $g = \lambda$. It could also happen that $a_{i_e} \in V(\Gamma_M)$.)

Given such indices i_e and j_g, we can 'fold the line' between those vertices a_{i_e} and a_{j_g} to create a path in Γ^k as follows: since all other elements of $(V(\Gamma_L) \cup V(\Gamma_M)) \setminus \{a_{i_e}, a_{j_g}\}$ lie before a_{i_e} or after a_{j_g}, it still holds true that

$$|i_h - (i_e + q)| \geq 2 \quad \text{for all} \quad a_{i_h} \in V(\Gamma_L) \setminus \{a_{i_e}\} \quad \text{and} \quad q \in \{1, \dots, j_g - i_e - 1\}.$$

Now define for each $p \in \{1, \dots, j_g - i_e\}$ the vertex set $V_p := \{a_{i_e+p}\} \cup V(\Gamma_L) \setminus \{a_{i_e}\} \subseteq \mathcal{G}$, and write $V(\Gamma_{L'})$ for the last term $V(\Gamma_{L'}) = V_{j_g - i_e}$. Take the parabolic subgroup W_p corresponding to the diagram spanned by $V_p \cup V(\Gamma_X)$. By construction, such a parabolic corresponds to a vertex of Γ^k that is odd-adjacent to W_{p+1}, and W_1 is odd-adjacent to W_J. Moreover, the generating set of the endpoint $W_{J'} := W_{V(\Gamma_{L'}) \cup V(\Gamma_X)}$ of this Γ^k-path simply replaces a_{i_e} by a_{j_g} while keeping the remaining vertices of Γ_J. Therefore $W_{J'}$ either coincides with W_K, or their Coxeter diagrams still differ by a single vertex. However, there is one less pair of indices $i_{e'} < j_{g'} \leq m$ such that $a_{i_{e'}} \in V(\Gamma_{L'})$ and $a_{j_{g'}} \in V(\Gamma_M) \setminus V(\Gamma_{L'})$ with the property that none of the vertices of $\mathcal{G}$ lying between $a_{i_{e'}}$ and $a_{j_{g'}}$ is contained in $V(\Gamma_{L'}) \cup V(\Gamma_M)$.

Thus, replacing W_J by $W_{J'}$ if necessary and iterating the above procedure for $W_{J'}$ and W_K instead, we inductively construct a path from W_J to W_K in Γ^k, as required.

In the remaining case, an inductive argument finishes off the proof. Indeed, if Γ_L and Γ_M differ by more than one vertex (hence $|V(\mathcal{G})| = m \geq \ell + 2$), we can iterate the procedure above to first construct an edge path in Γ^k from $W_J = W_L \times W_X$ to another vertex $W_{L''} \times W_X \in V(\Gamma^k)$ with $V(\Gamma_{L''}) \subseteq V(\mathcal{G})$ such that $\Gamma_{L''}$ and Γ_M differ by one vertex less than Γ_L and Γ_M. The lemma follows. □

Example 5.2.15. We demonstrate the central idea of Lemma 5.2.14 at the vertices $W_{\{s_1,s_3,s_8\}}$ and $W_{\{s_1,s_6,s_8\}}$ of the 3-odd graph corresponding to $W_{\widetilde{\mathbf{E}}_8}$. Using the notation introduced in the proof of Lemma 5.2.14, it holds $W_X = \emptyset$ and the graph $\mathcal{G}$ is spanned by

the nodes $V(\Gamma_{\widetilde{\mathtt{E}}_8})\backslash\{s_9\}$. We further have $V(\Gamma_L) = \{a_1, a_3, a_8\}$ and $V(\Gamma_M) = \{a_1, a_6, a_8\}$. It follows $a_{i_\varphi} = a_3$ and $a_{j_\lambda} = a_6$. With $p \in \{1, 2, 3\}$, we define the vertex sets

$$V_1 := \{a_4\} \cup \{a_1, a_8\},$$
$$V_2 := \{a_5\} \cup \{a_1, a_8\},$$
$$V_3 := \{a_6\} \cup \{a_1, a_8\} = V(\Gamma_M).$$

In Figure 5.7, the nodes of these sets are marked with blue, green, and pink circles, respectively. Now observe that the subgraphs spanned by these vertex sets are odd-adjacent in $\mathcal{G}$ since V_1 and V_2 as well as V_2 and V_3 differ by only a single node, and an odd-labeled edge connects these nodes. This odd-labeled path, which links a_3 and a_6, is highlighted with a bold line in $\mathcal{G}$ Figure 5.7. Together, this demonstrates that $W_{\{s_1,s_3,s_8\}}$ and $W_{\{s_1,s_6,s_8\}}$ are odd adjacent and the corresponding vertices are connected by an edge in Γ^3.

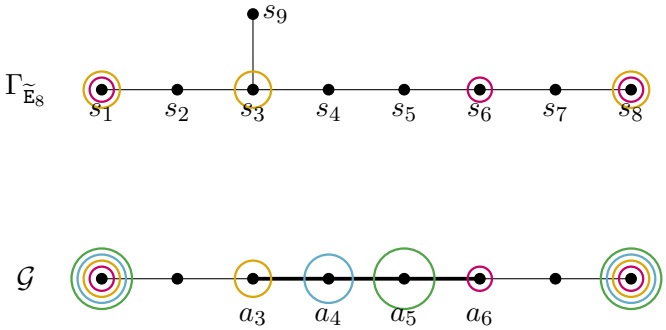

FIGURE 5.7. Illustration of the proof of Lemma 5.2.14 with two subgraphs of type $\mathtt{A}_1^3$ in a Coxeter diagram of type $\widetilde{\mathtt{E}}_8$ and the graph $\mathcal{G}$ below. A detailed explanation of the colours and shapes is given in Example 5.2.15.

The (sub)diagrams $\mathcal{G}$ appearing in Lemma 5.2.14 are depicted in Figure 5.8. A typical example of such a graph is the spherical Coxeter diagram of type $\mathtt{A}_n$.

Restricting to diagrams not containing subdiagrams of type $\mathtt{H}$, the arguments used in the proof of Lemma 5.2.14 also point out to the following observation.

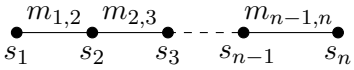

FIGURE 5.8. Odd-labeled path graph; if $m_{i,i+1} = 3$, the label is understood as omitted.

Proposition 5.2.16 (Vertices and connectivity in odd lines)**.** *Let Γ be a Coxeter path diagram as in Figure 5.8, with all edges odd, with $n = |V(\Gamma)| \geq 2$, and containing no subdiagram isomorphic to $\mathtt{H}_3$. Then $\Gamma^1 \cong \Gamma$ (as unlabeled, simplicial graphs) and the vertex set of Γ^k for $k \geq 2$ is given as follows:*

$$V(\Gamma^k) = \{\langle s_{j_1}, \ldots, s_{j_k}\rangle |\ j_1 < j_2 < \cdots < j_k,\ |j_f - j_h| \geq 2,\ f, h \in \{1, \ldots, k\}\},$$

in case $2 \leq k \leq \lceil \frac{n}{2} \rceil$*; otherwise* $V(\Gamma^k) = \varnothing$*. Moreover, for* $2 \leq k < n$*, the odd graph* Γ^k *consists of a single vertex if and only if* $n = 2\ell + 1$ *and* $k = \ell + 1$*; otherwise, if* Γ^k *has at least two vertices, then it is always connected.*

PROOF. By definition the only (relevant) subdiagrams of inc-type that are contained in such a graph Γ are of type $\mathtt{A}_1$. Compare Figure 5.1. This yields the description of the vertices of Γ^k. In particular, pigeonholing vertices of Γ to obtain potential vertices of Γ^k, one readily checks that Γ^k is empty for $k > \lceil \frac{n}{2} \rceil$. By the same principle, the only vertex of $\Gamma^{\ell+1}$ in case $n = 2\ell + 1$ corresponds precisely to the parabolic subgroup spanned by all vertices of Γ indexed by an odd number. The remaining claim about connectivity of Γ^k is a direct consequence of Lemma 5.2.14. □

After analysing odd lines, one quickly deduces similar properties for higher odd graphs of 'odd circles', depicted in Figure 5.9. A typical example of such a circle is the affine Coxeter diagram of type $\tilde{\mathtt{A}}_n$. In such a diagram we call s_{i+1} with $i + 1 \mod n + 1$ the *successor* of s_i, and similarly s_{i-1} with $i - 1 \mod n + 1$ is the *predecessor* of s_i.

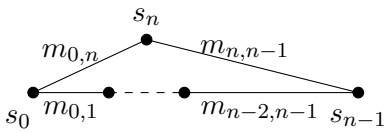

FIGURE 5.9. Odd-labeled circle; if an edge label equals three, the label is understood as omitted.

Lemma 5.2.17 (Vertices in odd circles)**.** *Fix* $n \geq 2$ *and let* Γ *be a Coxeter diagram as shown in Figure 5.9. That is,* Γ *is a circle on* $n + 1$ *vertices* $S = \{s_i \mid i \in \{0, \dots, n\}\}$ *whose edges are odd. Suppose further that* Γ *contains no subdiagram of type* $\mathtt{H}_3$*. Then* Γ^1 *is isomorphic to* Γ *(as unlabeled, simplicial graphs) and the vertices* $V(\Gamma^k)$ *of* Γ^k*, with* $2 \leq k \leq n$*, are of the form*

$$V(\Gamma^k) = \{\langle s_{j_1}, \dots, s_{j_k} \rangle \mid j_1 < j_2 < \cdots < j_k,\ |j_f - j_h| \geq 2 \bmod n + 1,\ f, h \in \{0, \dots, n\}\}\,.$$

In particular, Γ^k *is empty if and only if* $k > \lceil \frac{n}{2} \rceil$*. In the case* $k \leq \lceil \frac{n}{2} \rceil$*, a vertex* $\langle s_{j_1}, \dots, s_{j_k} \rangle \in V(\Gamma^k)$ *is isolated if and only if*

(1) $j_{m+1} = j_m + 2\ \forall m \in \{1, \dots, k\}$*, and*

(2) $j_k + 2 = j_1 \mod n + 1$*.*

PROOF. The description of $V(\Gamma^k)$ is obtained similarly to that in Proposition 5.2.16. Now, since every vertex s_i of Γ is odd-adjacent to s_{i-1} and to $s_{i+1} \mod n + 1$, we can always find in Γ^k a vertex odd-adjacent to $\langle s_{j_1}, \dots, s_{j_k} \rangle$ by exchanging one of the s_{j_m} by s_{j_m+1} or $s_{j_m-1} \mod n + 1$, except possibly when

(1) $j_{m+1} = j_m + 2$ for all $m \in \{1, \dots, k\}$ — in this case, every predecessor and successor of a generator s_{j_m} of the corresponding parabolic in $V(\Gamma^k)$ is odd-adjacent in Γ to another generator of the same parabolic. This contradicts the fact that the given parabolic has irreducible components of inc-type; and

(2) $j_k + 2 = j_1 \mod n+1$ — here, also the successor of s_{j_k} is adjacent in Γ^k to the predecessor of s_{j_1}.

Thus no rank-k parabolic that is odd-adjacent to the given vertex of Γ^k can be found. □

The previous results lay down some foundations to implement a practical algorithm to compute the higher rank odd graphs of Coxeter diagrams. In Section 5.4 we will use those to compute examples.

5.3. Conjugate parabolic subgroups

The main goal of this section is to prove Theorems 5.3.6 and 5.3.7, showing how to compute the number of conjugacy classes of involutions by counting connected components in Γ^k. Before doing so in Section 5.3.2, we establish a series of auxiliary results describing conjugation between parabolic subgroups in Section 5.3.1.

5.3.1. Conjugation of parabolics. We start the discussion with a combinatorial reformulation of a result by Krammer [Kra09, Section 3] and Deodhar [Deo82, Proposition 5.5].

Theorem 5.3.1 (Combinatorial Deodhar–Krammer Theorem)**.** *Let W_Γ be a Coxeter group with generating set $S = \{s_i |\ i \in I\}$ and W_J, W_K, $J, K \subseteq I$, $J \neq K$ be spherical standard parabolic subgroups. The subgroups W_J and W_K are conjugate if and only if*

(1) there exist a finite sequence of subdiagrams $\Gamma_1, \dots, \Gamma_m \subseteq \Gamma$ such that $V(\Gamma_1) = J$, $V(\Gamma_m) = K$ and Γ_i is adjacent to Γ_{i+1} for $i = 1, \dots, m-1$,

(2) for $i = 1, \dots, m-1$ the subgroup $W_{V(\Gamma_i) \cup V(\Gamma_{i+1})}$ is spherical and not of inc-type, and

(3) for $i = 1, \dots, m-1$ there exists $a_i \in W_{V(\Gamma_i) \cup V(\Gamma_{i+1})}$ such that $a_i W_{\Gamma_i} a_i^{-1} = W_{\Gamma_{i+1}}$.

As a consequence we obtain the following characterization of conjugacy for irreducible spherical standard parabolic subgroups with nontrivial center:

Lemma 5.3.2. *Let W_Γ be a Coxeter group with generating set S indexed by I. Suppose $J \neq K$ are subsets of I such that W_J and W_K are of inc-type. Then W_J is conjugate to W_K if and only if $J = \{j\}$, $K = \{k\}$ and there exists an odd-path from s_j to s_k in Γ.*

Proof. Applying Theorem 5.3.1 to conjugate parabolics of inc-type, we observe by item (2) and inspecting Figure 5.1, that such parabolics must have rank 1. As shown in [Bou02, p. 5, Proposition 3], two standard generators s_j and s_k are conjugate if and only if there exist $s_1, \dots, s_\ell \in V(\Gamma)$ such that $s_1 = s_j, s_\ell = s_k$ and with $\operatorname{ord}(s_i s_{i+1})$ odd for $i = 1, \dots, \ell - 1$. This is equivalent to the existence of an odd path in Γ from s_j to s_k, whence the result. □

For conjugated pairs of (not necessarily reduced) standard parabolics the following holds:

Lemma 5.3.3 (Conjugacy of irreducible components)**.** *Let W_Γ be a Coxeter group. Let W_J and W_K be standard parabolic subgroups of W_Γ. If W_J is conjugate to W_K, then the irreducible components of W_J are conjugate to the irreducible components of W_K.*

PROOF. By [Dav08, Proposition 4.5.10] the subgroup W_J is conjugate to W_K if and only if there exists $w \in W_\Gamma$ such that $wS_Jw^{-1} = S_K$. Further, the conjugation by w induces an isomorphism of graphs Γ_J and Γ_K. The lemma follows. □

Combining Lemmas 5.3.2 and 5.3.3 we obtain a splitting for the conjugated subgroups as follows:

Corollary 5.3.4. *Let W_J, W_K be distinct parabolic subgroups whose irreducible components are of inc-type in W_Γ. If W_J is conjugate to W_K, then there exist $\ell \in \mathbb{N}$ and a spherical standard parabolic W_X such that $W_J = (\mathbb{Z}/2\mathbb{Z})^\ell \times W_X$, $W_K = (\mathbb{Z}/2\mathbb{Z})^\ell \times W_X$, and $\mathbb{Z}/2\mathbb{Z}$ is not a direct factor of W_X.*

PROOF. Let $W_J = W_{X_1} \times \ldots \times W_{X_n}$ and $W_K = W_{Y_1} \times \ldots \times W_{Y_m}$ be the direct decompositions into irreducible components. Since the longest element in W_J resp. in W_K is central, the subgraphs of Γ induced by $X_1, \ldots, X_n$ resp. $Y_1, \ldots, Y_m$ are of inc-type.

If W_J is conjugated to W_K, then Lemma 5.3.3 shows that $n = m$ and there exists a permutation $\varphi\colon \{1, \ldots, n\} \to \{1, \ldots, n\}$ such that for $i = 1, \ldots, n$ the standard parabolic subgroup W_{X_i} is conjugated to $W_{Y_{\varphi(i)}}$. Let $i \in \{1, \ldots, n\}$. If the subgraph induced by X_i is not of type $\mathtt{A}_1$, then by Lemma 5.3.2 we obtain the equality $X_i = Y_{\varphi(i)}$.

By assumption $J \neq K$. Hence, after isolating the $\mathbb{Z}/2\mathbb{Z}$ factors of the direct product decompositions for W_J and W_K above, we obtain some $\ell \in \mathbb{N}$ and a (spherical) standard parabolic subgroup W_X such that $W_J = (\mathbb{Z}/2\mathbb{Z})^\ell \times W_X$ and $W_K = (\mathbb{Z}/2\mathbb{Z})^\ell \times W_X$ with $\mathbb{Z}/2\mathbb{Z}$ not a direct factor of W_X. □

A final ingredient for the proof of Theorem 5.3.6 is the following proposition describing conjugacy of parabolics by means of connecting odd-paths.

Proposition 5.3.5 (Conjugate, odd-connected parabolics)**.** *Let W_Γ be a Coxeter group. Let $W_J \cong (\mathbb{Z}/2\mathbb{Z})^\ell$ and $W_K \cong (\mathbb{Z}/2\mathbb{Z})^\ell$ be elementary abelian spherical standard parabolic subgroups of same rank. Then W_J is conjugate to W_K if and only if there exists a finite sequence of standard parabolic subgroups $W_1, \ldots, W_m$ such that $W_1 = W_J$, $W_m = W_K$ and W_i is odd-adjacent to W_{i+1} for $i = 1, \ldots, m-1$.*

PROOF. Let $W_J \cong W_K \cong (\mathbb{Z}/2\mathbb{Z})^\ell$ be conjugated. By Theorem 5.3.1 there exists a finite sequence of standard parabolic subgroups $W_{\Gamma_1}, \ldots, W_{\Gamma_m}$ with $V(\Gamma_1) = J$, $V(\Gamma_m) = K$ and Γ_i adjacent to Γ_{i+1} for all $i = 1, \ldots, m-1$. In particular, Γ_i and Γ_{i+1} differ by a single vertex. Moreover, Lemma 5.2.3 together with parts (2) and (3) of Theorem 5.3.1 implies that the vertices that differ between Γ_i and Γ_{i+1} must be connected via an odd-labeled edge in Γ since W_{Γ_i} and $W_{\Gamma_{i+1}}$ are conjugated via an element $a_i \in W_{V(\Gamma_i) \cup V(\Gamma_{i+1})}$. Hence W_{Γ_i} is odd-adjacent to $W_{\Gamma_{i+1}}$.

Conversely, let $W_J = W_1, W_2, \dots, W_m = W_K$ be a finite sequence of odd-adjacent standard parabolic subgroups. Let $\{s_1, \dots, s_e\}$ be a generating set for W_i and let $\{s_1, \dots, s_{e-1}, t_e\}$ be a set of generators for W_{i+1} with $i \in \{1, \dots, m-1\}$. Since W_i and W_{i+1} are odd-adjacent, then $\mathrm{ord}(s_e t_e) = q$ is odd. Define $w_i := s_e t_e s_e \cdots t_e$ where the length of w_i is $2q-1$. Then an easy calculation shows that $w_i W_i w_i^{-1} = W_{i+1}$. Iterating this process, it follows that the subgroups W_J and W_K are conjugated. □

5.3.2. (Proofs of the) main technical results. We are now ready to prove our main results of this chapter.

Theorem 5.3.6 (Conjugating parabolics with nontrivial centers)**.** *Let $\Gamma = (S, E)$ be a Coxeter diagram with $S = \{s_i |\ i \in I\}$ and $W = W_\Gamma$ the associated Coxeter group. For $J, K \subseteq I$, $J \neq K$ let W_J and W_K be the corresponding standard parabolic subgroups, and assume they are spherical with longest elements being central elements. Then the subgroup W_J is conjugate to W_K if and only if both following conditions hold:*

(1) There exist $\ell \in \mathbb{N}$ and $L, M, X \subseteq I$ such that $W_J = W_L \times W_X$ and $W_K = W_M \times W_X$ with $W_L \cong W_M \cong (\mathbb{Z}/2\mathbb{Z})^\ell$, and

(2) there exists a finite sequence of standard parabolic subgroups $W_1, \dots, W_m$ such that $W_1 = W_J$, $W_m = W_K$, and W_i is odd-adjacent to W_{i+1} for $i = 1, \dots, m-1$.

Proof. Item (1) is a consequence of Corollary 5.3.4. To check item (2), apply Proposition 5.3.5 to the abelian factors W_L and W_M.

Conversely, if W_J and W_K satisfy items (1) and (2), the claim follows immediately from Proposition 5.3.5 applied to the abelian factors. □

Theorem 5.3.7 (Counting conjugacy classes of involutions)**.** *Let Γ be a Coxeter diagram and, for each $k \geq 1$, let Γ^k be its corresponding k-odd graph. Then, the cardinality of the set of connected components of Γ^k is equal to the cardinality of the set of conjugacy classes of involutions of rank k in the corresponding Coxeter group W_Γ. The total number $\mathrm{cc}_2(W_\Gamma)$ of conjugacy classes is obtained as*

$$\mathrm{cc}_2(W_\Gamma) = \sum_{k=1}^{|V(\Gamma)|} |\pi_0(\Gamma^k)|.$$

Corollary 5.3.8 (Representing conjugacy classes of involutions)**.** *With notation as in Theorem 5.3.7, the connected components of Γ^k are in bijection with the conjugacy classes of involutions of rank k. To obtain a representative for such a conjugacy class, one may choose any vertex in the corresponding connected component in Γ^k and take as representative the longest element in the parabolic subgroup corresponding to it.*

Proof of Theorem 5.3.7 and Corollary 5.3.8. The conjugacy class of an arbitrary involution $c \in W_\Gamma$ is, by Lemma 5.1.6, represented by a central longest element in a suitably chosen spherical parabolic subgroup. (Note that this representative might be a standard generator.) The choice of a representative is unique up to conjugation, by Lemma 5.1.7. The set of conjugacy classes of involutions is thus completely described

once we know which parabolics of W_Γ whose irreducible components are of inc-type are conjugate to one another. But Theorem 5.3.6 shows that these conjugacy classes correspond bijectively to connected components of the k-odd graphs Γ^k. The theorem follows, as does Corollary 5.3.8. □

The following two open questions arise naturally from Theorem 5.3.7.

Open question 5.3.9. Investigate the complexity of the algorithm obtained from Theorem 5.3.7.

Open question 5.3.10. Is it possible to define a similar family of graphs which allows one to compute the number of conjugacy classes of torsion elements of order $m \neq 2$?

It remains to prove Corollary 5.3.11, presenting some results on Coxeter groups attaining certain bounds on the number of conjugacy classes of involutions.

Corollary 5.3.11 (The extreme cases)**.** *Let Γ be a Coxeter diagram of rank n.*

(1) Every involution in W_Γ is a reflection if and only if the diagram Γ is complete and every edge label in Γ is odd or ∞, in which case $\mathrm{cc}_2(W_\Gamma) = |\pi_0(\Gamma^1)| \leq n$.

(2) There is only one conjugacy class of involutions in W_Γ, i.e. $\mathrm{cc}_2(W_\Gamma) = 1$, if and only if the Coxeter diagram Γ is complete, the odd graph Γ^1 is connected, and every edge label in Γ is odd or ∞.

(3) If $n \geq 4$ and $\mathrm{cc}_2(W_\Gamma)$ is equal to the upper bound $2^n - 1$, then W_Γ is spherical and even, but not necessarily abelian.

(4) If W_Γ is not spherical, then $\mathrm{cc}_2(W_\Gamma) \leq 2^n - 2$. In case equality holds, then either $\Gamma = \overset{\infty}{\bullet\!-\!\bullet}$ (thus $W_\Gamma \cong D_\infty$) or Γ is a triangle with labels $2p$, $2q$, $2r \in \mathbb{N}$ (so that $W_\Gamma \cong \Delta(2p, 2q, 2r)$).

Proof. Let Γ be a Coxeter diagram of rank n. Since Γ^1 is always nonempty, by Theorem 5.3.7 there is only one conjugacy class of involutions in W_Γ if and only of $|\pi_0(\Gamma^1)| = 1$ and the vertex set of Γ^k is empty for $2 \leq k \leq n$. By definition of higher rank odd graphs, $V(\Gamma^k)$ is empty for $2 \leq k \leq n$ if and only if Γ is complete and every edge in Γ is odd or ∞. This proves item (1).

Further, by Theorem 5.3.7 every involution in W_Γ is a reflection if and only if $V(\Gamma^k)$ is empty for $2 \leq k \leq n$. The proof of part (1) shows that this is the case if and only if Γ is complete and every edge label in Γ is odd or ∞, hence item (2).

For items (3) and (4), first note that if the upper bounds are to be attained, then the k-odd graphs must have as many connected components as possible, which requires Γ to have only even or ∞ labels. Since W_Γ is trivially a parabolic subgroup of itself, then the highest odd graph Γ^n must be empty in case W_Γ is not spherical, so that the trivial upper bound decreases to $2^n - 2$.

To construct nonabelian (spherical) groups attaining the upper bound, define Γ as follows: if $n = 2k$ is even, Γ is the disjoint union of $k = n/2$ dihedral diagrams $\mathtt{I}_2(2m_1)$,

$\dots$, $\mathtt{I}_2(2m_k)$ with $m_i \geq 2$; in case $n = 2k+1$ is odd, Γ is the disjoint union of $\mathtt{I}_2(2m_1)$, $\dots$, $\mathtt{I}_2(2m_k)$ with one $\mathtt{A}_1$, again with $m_i \geq 2$. This concludes item (3). To finish off item (4), the previous paragraph shows that W_Γ must be even of rank ≤ 3. The two types of groups (infinite dihedral and even triangle) attaining the bound show up in Sections 5.4.1 and 5.4.2 below. □

Open question 5.3.12. The 'universal' upper bound for $\mathrm{cc}_2(W_\Gamma)$ can only be attained by infinite groups of rank at most three. That is, the bound $\mathrm{cc}_2(W_\Gamma) \leq 2^n - 2$ is not optimal if $|V(\Gamma)| \geq 4$ and W_Γ is infinite. In turn, lowering the bound down by one to $2^n - 3$, one can construct reducible examples in rank four with $\mathrm{cc}_2(W_\Gamma) = 13 = 2^4 - 3$; take, e.g., $\Gamma = \widetilde{\mathtt{C}}_2 \sqcup \mathtt{A}_1$.
Restricting ourselves to irreducible examples, the anonymous referee of [Rei+25] pointed out to a family of groups with (asymptotically) many conjugacy classes: Define Γ as a tree with one central vertex and k 'arms' of length two, such that all edge labels are (finite) even numbers ≥ 4. Thus Γ has $n = 2k+1$ vertices. After some deliberation and initial calculations, $\mathrm{cc}_2(W_\Gamma)$ seems to be roughly $2^{n-1} + k \cdot 2^{k-1}$ plus some constant C. These considerations leave open the following subtle problem: Is there a function $f : \mathbb{N}_{\geq 4} \to \mathbb{N}$ such that $\mathrm{cc}_2(W) \leq f(n)$ for all infinite irreducible Coxeter groups W of rank $n \geq 4$, with some (infinite, irreducible) Coxeter group W_0 of rank $n_0 \geq 4$ attaining equality $\mathrm{cc}_2(W_0) = f(n_0)$?

We finish this section by recording the additive properties for the number of conjugacy classes cc_m of elements of finite order m in free and direct products.

Lemma 5.3.13 (Free and direct products)**.** *Let G, H be groups and $m \geq 2$.*

(1) cc_m is additive on free products if finite. That is, suppose $\mathrm{cc}_m(G)$ and $\mathrm{cc}_m(H)$ are finite, then

$$\mathrm{cc}_m(G * H) = \mathrm{cc}_m(G) + \mathrm{cc}_m(H).$$

(2) Suppose that for every $(k,l) \in \mathbb{N} \times \mathbb{N}$ with $\mathrm{lcm}(k,l) = m$, the values $\mathrm{cc}_k(G)$ and $\mathrm{cc}_l(H)$ are finite, then the number of conjugacy classes of elements of order m of a direct product $G \times H$ is also finite and given by

$$\mathrm{cc}_m(G \times H) = \sum_{\substack{(k,l)\in\mathbb{N}\times\mathbb{N} \\ \mathrm{lcm}(k,l)=m}} \mathrm{cc}_k(G) \cdot \mathrm{cc}_l(H).$$

In particular, for a prime number p we have

$$\mathrm{cc}_p(G \times H) = \mathrm{cc}_p(G) + \mathrm{cc}_p(H) + \mathrm{cc}_p(G) \cdot \mathrm{cc}_p(H).$$

Proof. In case (1) let $w \in G * H$ be an element of order m. Using the action of $G * H$ on the associated Bass–Serre tree T_{G*T} one shows that w is contained in either a conjugate of G or of H, see [Ser80, I§6, Proposition 21]. Moreover, w cannot be simultaneously conjugated to an element of G and an element of H, since otherwise w would fix an edge in T_{G*H}. Additivity follows.

In case (2) let $w = (g, h) \in G \times H$ be of order m. In case either $g = 1$, respectively $h = 1$, an easy calculation shows that w is conjugated to an element of order m in H, resp. in G.

If $g \neq 1$ and $h \neq 1$, then $\mathrm{ord}(g) = a$, $\mathrm{ord}(h) = b$ with their least common multiple $\mathrm{lcm}(a, b) = m$. One easily checks that (g, h) can only be conjugated to an element in $G \setminus \{1\} \times H \setminus \{1\}$. Further, two elements $(g_1, h_1), (g_2, h_2)$ of order m in $G \setminus \{1\} \times H \setminus \{1\}$ are conjugated if and only if $\mathrm{lcm}(a, b) = m$, one has $\mathrm{ord}(g_1) = \mathrm{ord}(g_2) = a$, $\mathrm{ord}(h_1) = \mathrm{ord}(h_2) = b$ and g_1 is conjugated to g_2 and h_1 is conjugated to h_2. Hence, the statement. The conclusion for p prime follows readily. □

Open question 5.3.14. The number $\mathrm{cc}_2(W_\Gamma)$ is, by definition, a group-theoretic invariant of W_Γ. Also $|\pi_0(\Gamma_{odd})| = |\pi_0(\Gamma^1)|$ does not depend on Γ by [MV24, Proposition 2.2]. However, the connected components of higher rank odd graphs do a priori depend on the chosen Coxeter diagram Γ for W_Γ. It would be interesting to see how the higher rank odd graphs behave with respect to moves (such as twists [Müh00; Bra+02] or blow-ups [Müh06]) between the various Coxeter diagrams for a given group.

5.4. Applications to some subclasses of Coxeter groups

To provide extended examples we compute in Section 5.4.1 the number of conjugacy classes of involutions in any given triangle group and discuss in Section 5.4.2 the subclass of right-angled Coxeter groups. In Section 5.4.3 we determine cc_2 in all of the (irreducible) spherical and affine cases. Note that these results can be easily extended to reducible Coxeter groups by invoking Lemma 5.3.13.

5.4.1. Triangle Coxeter groups. The family of triangle groups, compare Definition 2.2.9, witnesses sharpness of the upper bounds for cc_2. Using Theorem 5.3.7, we now compute the number of conjugacy classes of involutions for all infinite triangle groups. We start by demonstrating this at an example:

Example 5.4.1. Consider the triangle group $\Delta(2, 4, 4)$. Its Coxeter diagram Γ is a path graph on three vertices connected by two edges, both labeled 4. Compare also Figure A.2. This structure implies that when constructing the odd graph Γ^1, both edges are omitted. As a result, Γ^1 consists of 3 isolated vertices and hence has 3 connected components. To compute Γ^2, we search for subdiagrams of inc-type in the diagram of $\Delta(2, 4, 4)$. We observe that it contains two subdiagrams of type $\mathtt{B}_2$, which are not odd-adjacent, and one subdiagram of type $\mathtt{A}_1^2$. This implies that Γ^2 also consists of 3 isolated vertices and has 3 connected components. Since the diagram Γ itself is not of inc-type, it follows that Γ^3 is empty. Together, this demonstrates that $\mathrm{cc}_2(\Delta(2, 4, 4)) = 6$.

The number of conjugacy classes of reflections is given by $|\pi_0(\Gamma^1)|$ (cf. [Bra+02, Lemma 3.6]) — our findings thus give quick means to check the discrepancy between the conjugacy classes of reflections and of involutions in $\Delta(p, q, r)$.

For $p, q, r \in \mathbb{N}$ we have

$$\mathrm{cc}_2(\Delta(p,q,r)) = \begin{cases} 6, & \text{if } p,q,r \text{ are even,} \\ 1, & \text{if } p,q,r \text{ are odd,} \\ 4, & \text{if exactly one edge label is odd,} \\ 2, & \text{if exactly one edge label is even;} \end{cases}$$

$$\mathrm{cc}_2(\Delta(\infty,q,r)) = \begin{cases} 5, & \text{if } q \text{ and } r \text{ are even,} \\ 1, & \text{if } q \text{ and } r \text{ are odd,} \\ 3, & \text{if } (q+r) \text{ is odd;} \end{cases}$$

$$\mathrm{cc}_2(\Delta(\infty,\infty,r)) = \begin{cases} 4, & \text{if } r \text{ is even,} \\ 2, & \text{if } r \text{ is odd.} \end{cases}$$

Finally, for the universal Coxeter group of rank three we have $\mathrm{cc}_2(\Delta(\infty,\infty,\infty)) = \mathrm{cc}_2(*_{i=1}^{3}\mathbb{Z}/2\mathbb{Z}) = 3$ by Corollary 5.3.11. This completes the list.

It is interesting to see that all possible values from 1 to $6 = 2^3 - 2$ are realized. We have no structural explanation for this phenomenon at the moment.

5.4.2. Right-angled Coxeter groups. Note that, for many RACGs, the number cc_2 of conjugacy classes of involutions can be computed by first looking at decompositions, applying Lemma 5.3.13 to reduce complexity, then invoking Theorem 5.3.7. Here we offer alternative means to determine cc_2 for such groups. The proof has a geometric flavour and for it we do not need the results from Sections 5.2 and 5.3.2, nor those of Richardson and Deodhar. Recall that we denote by Λ the presentation diagram of a right-angled Coxeter group $W(\Lambda)$, see Definition 2.2.10.

Proposition 5.4.2. *Let $W(\Lambda)$ be a right-angled Coxeter group. The number $\mathrm{cc}_2(W(\Lambda))$ of conjugacy classes of involutions in $W(\Lambda)$ is equal to the number of nontrivial cliques (i.e., complete subgraphs of rank at least one) in the defining graph Λ.*

Proof. Let $W(\Lambda)$ be a right-angled Coxeter group and let X be the associated Davis–Moussong complex (cf. [Dav08, Chapters 7 and 12]), on which $W(\Lambda)$ acts geometrically. We denote this action by $\Phi\colon W(\Lambda) \to \mathrm{Isom}(X)$.

Let $w \in W(\Lambda)$ be an involution. By the Bruhat–Tits fixed point theorem [AB08, Theorem 11.23] we know that $\mathrm{Fix}(\Phi(w))$ is nonempty. Since the action Φ is type-preserving, there exists a vertex in $F := \mathrm{Fix}(\Phi(w))$. Let then $y \in F$ be a vertex. By definition of X we have $y = gW(\Delta)$, where Δ is a nontrivial clique in Λ. Further, $w \in gW(\Delta)g^{-1}$.

We define $A_w := \bigcap_{g_iW(\Delta_i)\in F} g_iW(\Delta_i)g_i^{-1}$. Since we have $w \in g_iW(\Delta_i)g_i^{-1}$ for every $g_iW(\Delta_i) \in F$, the intersection A_w is nontrivial. Moreover, A_w is a parabolic subgroup since it is an intersection of parabolics; cf. [Qi07]. Thus $A_w = xW(\Delta')x^{-1}$ for some $x \in W$ and some nonempty clique Δ' in Λ. Hence $w \in A_w$ is conjugate to $v_1v_2\dots v_r$ where $V(\Delta') = \{v_1, \dots, v_r\}$.

Let now Δ_1 and Δ_2 be two nontrivial cliques. Let $w_1 = x_1 \dots x_n$ and $w_2 = y_1 \dots y_m$ be involutions where $V(\Delta_1) = \{x_1, \dots, x_n\}$ and $V(\Delta_2) = \{y_1, \dots, y_m\}$. If w_1 is conjugate to w_2, then the parabolic closure of w_1 is conjugate to the parabolic closure of w_2 by Lemma 5.1.7. As the parabolic closure of w_i is $W(\Delta_i)$, it follows from [AM15, Corollary 3.8] that $\Delta_1 = \Delta_2$. □

5.4.3. Spherical and affine Coxeter groups. The irreducible finite and affine Coxeter groups have been classified in a short list of infinite families $\mathtt{A}_n$, $\mathtt{B}_n = \mathtt{C}_n$, $\mathtt{D}_n$, $\mathtt{I}_2(m)$, $\tilde{\mathtt{A}}_n$, $\widetilde{\mathtt{B}}_n$, $\widetilde{\mathtt{C}}_n$, $\widetilde{\mathtt{D}}_n$ and some exceptional types. In this section we provide formulae for cc_2 for all such classical families. Combined with Lemma 5.3.13, this gives means to compute cc_2 for all finite Coxeter groups, as well as all direct and free products of all spherical and affine Coxeter groups. Since the proofs of these formulae require various case distinctions while making hard use of Lemma 5.2.14 in repeated arguments, we outsource them into Sections 5.5 and 5.6.

Theorem 5.4.3 (Families of spherical Coxeter groups)**.** *The number of conjugacy classes of involutions of Coxeter groups of types $\mathtt{A}_n$, $\mathtt{B}_n = \mathtt{C}_n$, $\mathtt{D}_n$, and $\mathtt{I}_2(n)$ is given by*

$$\mathrm{cc}_2(W_{\mathtt{A}_n}) = \begin{cases} k, & \text{if } n = 2k, \\ k+1, & \text{if } n = 2k+1; \end{cases}$$

$$\mathrm{cc}_2(W_{\mathtt{B}_n}) = \begin{cases} k^2 + 2k, & \text{if } n = 2k, \\ k^2 + 3k + 1, & \text{if } n = 2k+1; \end{cases}$$

$$\mathrm{cc}_2(W_{\mathtt{D}_n}) = \begin{cases} \frac{1}{2}(k^2 + 3k + 2), & \text{if } n = 2k, \\ \frac{1}{2}(k^2 + 3k), & \text{if } n = 2k+1. \end{cases}$$

$$\mathrm{cc}_2(W_{\mathtt{I}_2(n)}) = \begin{cases} 3, & \text{if } n = 2k, \\ 1, & \text{if } n = 2k+1. \end{cases}$$

The numbers of conjugacy classes of involutions of Coxeter groups of irreducible spherical exceptional types are as in the following table:

Type of Γ	$\mathtt{E}_6$	$\mathtt{E}_7$	$\mathtt{E}_8$	$\mathtt{F}_4$	$\mathtt{G}_2$	$\mathtt{H}_2$	$\mathtt{H}_3$	$\mathtt{H}_4$
$\mathrm{cc}_2(W_\Gamma)$	4	9	9	7	3	1	3	4

The next result summarizes our findings for the irreducible affine cases.

Theorem 5.4.4 (Affine Coxeter groups)**.** *The number of conjugacy classes of involutions of Coxeter groups of types $\tilde{\mathtt{A}}_n, \widetilde{\mathtt{B}}_n$, $\widetilde{\mathtt{C}}_n$, and $\widetilde{\mathtt{D}}_n$ for all n are given by the following formulae,*

respectively:

$$\mathrm{cc}_2(W_{\widetilde{\mathtt{A}}_n}) = \begin{cases} k, & \text{if } n = 2k, \\ k+2, & \text{if } n = 2k+1; \end{cases}$$

$$\mathrm{cc}_2(W_{\widetilde{\mathtt{B}}_n}) = \begin{cases} \frac{1}{3}k^3 + \frac{3}{2}k^2 + \frac{19}{6}k + 1, & \text{if } n = 2k, \\ \frac{1}{3}k^3 + 2k^2 + \frac{14}{3}k + 2, & \text{if } n = 2k+1; \end{cases}$$

$$\mathrm{cc}_2(W_{\widetilde{\mathtt{C}}_n}) = \begin{cases} 4k^2 + 2k, & \text{if } n = 2k, \\ 4k^2 + 6k + 2, & \text{if } n = 2k+1; \end{cases}$$

$$\mathrm{cc}_2(W_{\widetilde{\mathtt{D}}_n}) = \begin{cases} \frac{1}{6}(k+1)(k^2+5k+18), & \text{if } n = 2k, \\ \frac{1}{6}k(k^2+6k+11), & \text{if } n = 2k+1. \end{cases}$$

The number of conjugacy classes of involutions of Coxeter groups of irreducible affine exceptional types are as in the following table:

Type of Γ	$\widetilde{\mathtt{E}}_6$	$\widetilde{\mathtt{E}}_7$	$\widetilde{\mathtt{E}}_8$	$\widetilde{\mathtt{F}}_4$	$\widetilde{\mathtt{G}}_2$	$\widetilde{\mathtt{I}}_1$
$\mathrm{cc}_2(W_\Gamma)$	5	19	15	12	4	2

Remark 5.4.5. The number of classes of type $\widetilde{\mathtt{E}}_7$ has previously been computed by Richardson [Ric82, Example 3.4]. Note that Richardson found 20 conjugacy classes as he also considers the trivial element to be an involution.
The delicate behavior of conjugacy classes in type $\widetilde{\mathtt{D}}$ in particular also became clear in recent work of Milićević, Schwer, and Thomas [MST25].

Proposition 5.4.6 provides a formula for the number of conjugacy classes of involutions for all Coxeter groups whose Coxeter diagram is an odd-labeled circle, provided it contains no subdiagram of type $\mathtt{H}_3$. Note that this class includes groups of type $\tilde{\mathtt{A}}_n$. The relevant diagrams are shown in Figure 5.9 in Section 5.2.

Proposition 5.4.6 (Computing cc_2 in odd circles)**.** *Let $n \geq 2$ and Γ be a Coxeter diagram as shown in Figure 5.9, with only odd-edges and assuming Γ contains no subgraph isomorphic to $\mathtt{H}_3$. Then*

$$\mathrm{cc}_2(W_\Gamma) = \begin{cases} \ell, & \text{if } n = 2\ell, \\ \ell+2, & \text{if } n = 2\ell+1. \end{cases}$$

Proof. Lemma 5.2.17 implies that, for $k \leq \ell$, the graph Γ^k does not have isolated vertices. To determine the connected components of Γ^k in this case, the same argument as in the proof of Proposition 5.2.16 works, showing that Γ^k is always connected for $k \leq \ell$. (Note that here the distance between indices of generators of a given standard parabolic in Γ^k must also be at least 2, but now indices are taken $\mod n+1$.) Since Γ is a circle, taking $l > \ell$ gives $\Gamma^l = \varnothing$ for $n = 2\ell$; in turn, for $n = 2\ell+1$, the graph $\Gamma^{\ell+1}$ contains precisely two isolated vertices, namely $\langle s_0, s_2, s_4, \ldots, s_{2\ell}\rangle$ and $\langle s_1, s_3, s_5, \ldots, s_{2\ell+1}\rangle$. Finally, Γ^l for $l > \ell+1$ is also empty. This completes the proof. □

5.5. Proof of Theorem 5.4.3

This section is dedicated to the proofs of our findings on the number of conjugacy classes of involutions for the families of spherical Coxeter groups, as stated in Theorem 5.4.3.

PROOF OF THEOREM 5.4.3 FOR $\mathtt{A}_n$ AND $\mathtt{I}_2(n)$. The formula for type $\mathtt{A}$ is a straightforward corollary to Proposition 5.2.16. Type $\mathtt{I}_2$ is a triviality by the definition of higher rank odd graphs. □

It remains to prove the formulae for the families of type $\mathtt{B}$, $\mathtt{D}$, and the exceptional types. We start with type $\mathtt{B}$. For this, observe the following:

Lemma 5.5.1. *Consider a Coxeter group of type* $\mathtt{B}_n$ *with diagram* $\Gamma_{\mathtt{B}_n}$*. Then, all vertices of the* m*-odd-graph* Γ^m *are of the form*

$$\mathtt{B}_i \sqcup \mathtt{A}_1^{m-i},$$

with $i \in \{0, 1, \ldots, m\}$.

Remark 5.5.2. Notice that the notation $\mathtt{X}_0$ refers to an empty diagram of type $\mathtt{X}$.

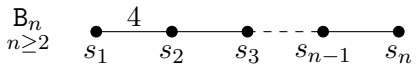

FIGURE 5.10. Coxeter diagram of $\mathtt{B}_n = \mathtt{C}_n$.

PROOF. For the sake of simplicity in our arguments below, we will refer to the nodes of $\Gamma_{\mathtt{B}_n}$ by their indexed generator, enumerating from left to right as shown in Figure 5.10. Recall that $\Gamma_{\mathtt{B}_n}$ has n nodes, with nodes s_1 and s_2 being adjacent via an edge labeled 4, while all other edges are labeled 3. Subgraphs spanned by the vertices $s_1, s_2, \ldots, s_\ell$ with $\ell \in \{2, \ldots, n\}$ are diagrams of type $\mathtt{B}_\ell$. Moreover, by choosing a set of pairwise non-adjacent vertices, one can obtain a collection of subgraphs of type $\mathtt{A}_1$ from $\Gamma_{\mathtt{B}_n}$. For this, notice that non-adjacency for these vertices means a distance of at least 2 between their index numbers. From these insights, it follows that one can identify subgraphs of the form $\mathtt{B}_i \sqcup \mathtt{A}_1^j$ with $i, j \in \mathbb{N}_0$ in a type $\mathtt{B}_n$ diagram. Furthermore, it is critical to observe that $\Gamma_{\mathtt{B}_n}$ does not encompass any other of the Coxeter diagrams presented in Figure 5.1, as it explicitly excludes $\mathtt{E}_7, \mathtt{E}_8, \mathtt{F}_4, \mathtt{G}_2, \mathtt{H}_3, \mathtt{H}_4$ alongside $\mathtt{I}_2(2\ell)$ and $\mathtt{D}_{2\ell}$ for $\ell \geq 2$. Consequently, the only subdiagrams within $\mathtt{B}_n$ that lead to irreducible Coxeter groups with nontrivial center manifest in the form $\mathtt{B}_i \sqcup \mathtt{A}_1^{m-i}$ with $i \in \{0, 1, \ldots, m\}$. Therefore, these specific subdiagrams represent the sole vertices of Γ^m. □

PROOF OF THEOREM 5.4.3 FOR $\mathtt{B}_n$. We see immediately from the structure of $\Gamma_{\mathtt{B}_n}$ that Γ^1 has 2 connected components for all $\mathtt{B}_n$, since all edge labels except for a single one of $\Gamma_{\mathtt{B}_n}$ are odd, so that Γ^1 is an unlabeled graph with two connected components. We now derive the closed formula by counting the connected components of Γ^m for the different types of subgraphs as given by Lemma 5.5.1. We discuss them separately below. Before this, we derive lower and upper bounds on the size of the subgraphs contained in $\Gamma_{\mathtt{B}_n}$: It follows from our arguments given in Lemma 5.5.1 above that the span of the

nodes labeled $s_1, s_2, \ldots, s_\ell$ with $\ell \in \{2, \ldots, n\}$ forms a subgraph of type $\mathtt{B}_\ell$. Hence, $\Gamma_{\mathtt{B}_n}$ contains a single subgraph of type $\mathtt{B}_2, \ldots, \mathtt{B}_n$ each.
Furthermore, we observed in Lemma 5.5.1 above that $\Gamma_{\mathtt{B}_n}$ contains up to $\lceil \frac{n}{2} \rceil$ many copies of type $\mathtt{A}_1$ subgraphs, located at every other node of the path between s_1 and s_n.

We now compute the number of connected components for the various types of subgraphs. Different types of subgraphs always yield different connected components in Γ^m because they are never adjacent since their diagrams are not isomorphic. However, subdiagrams of the same type can be adjacent. Compare Lemma 5.2.14.
For all the computations below, assume $n = 2k$ or $n = 2k + 1$.

Subdiagrams of type $\mathtt{B}_m$*:*
As discussed above, for $2 \leq m \leq n$, the graph $\Gamma_{\mathtt{B}_n}$ only contains one subdiagram of type $\mathtt{B}_m$, spanned by the vertices $s_1, s_2, \ldots, s_m$. Hence, this diagram produces an isolated vertex labeled $\langle s_0, s_1, \ldots, s_{m-1} \rangle$ in Γ^m, giving one connected component of the graph. It follows, that the number of conjucagy classes $\mathrm{cc}_2(W_{\mathtt{B}_n}, \mathtt{B}_m)$ of $\mathtt{B}_n$ obtained from subgroups of type $\mathtt{B}_m$ can be counted as:

$$\mathrm{cc}_2(W_{\mathtt{B}_n}, \mathtt{B}_m) = \sum_{m=2}^{n} 1 = n - 1.$$

Subdiagrams of type $\mathtt{A}_1^m$*:*
Subdiagrams of $\Gamma_{\mathtt{B}_n}$ of type $\mathtt{A}_1^m$ are characterized as m non-adjacent nodes. An application of Lemma 5.2.14 shows that many of these subdiagrams are connected as vertices in Γ^m since every edge of $\Gamma_{\mathtt{B}_n}$ except for (s_1, s_2) is odd-labeled. Subdiagrams containing the node labeled s_1 cannot be odd-adjacent to subdiagrams not containing s_1 since this node has degree 1 and its adjacent edge is labeled 4. Therefore, we distinguish two cases of subdiagrams to count the number of conjugacy classes of $\mathtt{B}_n$ obtained from subgroups of type $\mathtt{A}_1^m$:
Case 1: The node of $\Gamma_{\mathtt{B}_n}$ labeled s_1 is not contained in a vertex of Γ^m of the connected components under consideration.
To form vertices of Γ^m not containing s_1, one then has to choose m isolated nodes among the nodes labeled $s_2, \ldots, s_n$, which gives $2m - 1 \leq n - 1 \Leftrightarrow m \leq \frac{n}{2}$. Substituting $n = 2k$ yields $m \leq k$, and substituting $n = 2k + 1$ gives $m \leq k + \frac{1}{2}$. Using $m, k \in \mathbb{Z}$, this implies $m \leq k$. It thus follows from Lemma 5.2.14 that for fixed m and n, all vertices of Γ^m corresponding to subgraphs of $\Gamma_{\mathtt{B}_n}$ satisfying the conditions of this case are odd-adjacent. Hence, they are all contained in a common connected component of Γ^m.
Case 2: The node of $\Gamma_{\mathtt{B}_n}$ labeled s_1 is contained in all vertices of Γ^m of the connected components under consideration.
To form vertices of Γ^m that do contain s_1, one can pick $m - 1$ isolated nodes from nodes that are non-adjacent to s_1, that is, from $s_3, \ldots, s_n$. Therefore, we get $2(m - 1) - 1 \leq n - 2 \Leftrightarrow m \leq \frac{n+1}{2}$. For $n = 2k$, this is $m \leq k + \frac{1}{2}$. Since $m \in \mathbb{Z}$, we can also write $m \leq k$. For $n = 2k + 1$, we get $m \leq k + 1$. Again, invoking Lemma 5.2.14, we see that for fixed values of m and n, all subgraphs satisfying these constraints are odd-adjacent and therefore reside in a common connected component of Γ^m.
Considering both cases together, we can determine the number of conjugacy classes

$\mathrm{cc}_2(W_{\mathtt{B}_n}, \mathtt{A}_1^m)$ of $W_{\mathtt{B}_n}$ that arise from subgroups of type $\mathtt{A}_1^m$ as:

$$n = 2k: \qquad \mathrm{cc}_2(W_{\mathtt{B}_n}, \mathtt{A}_1^m) = \sum_{m=2}^{k} 1 + \sum_{m=2}^{k} 1 = 2(k-1);$$

$$n = 2k+1: \qquad \mathrm{cc}_2(W_{\mathtt{B}_n}, \mathtt{A}_1^m) = \sum_{m=2}^{k} 1 + \sum_{m=2}^{k+1} 1 = 2k-1.$$

Subdiagrams of type $\mathtt{A}_1^{m-i} \sqcup \mathtt{B}_i$*:*
Since we already counted the connected components of Γ^m with vertices associated with subgraphs of type $\mathtt{A}_1^m$ and $\mathtt{B}_m$ above, we will now focus on the case where $i \neq 0$ and $m > i$. This implies $m \geq 3$. According to Lemma 5.5.1, $\Gamma_{\mathtt{B}_n}$ contains subgraphs of type $\mathtt{B}_i$ for $i \in \{2, \ldots, n\}$. For the subdiagrams of type $\mathtt{A}_1^{m-i} \sqcup \mathtt{B}_i$ discussed here, we are interested in the subdiagrams spanned by the nodes labeled $s_1, \ldots, s_i$ for $i \leq n-2$. Next, we need to select $m-i$ isolated nodes from the set $\{s_{i+2}, \ldots, s_n\}$ in order to construct a subgraph of type $\mathtt{A}_1^{m-i} \sqcup \mathtt{B}_i$. The construction is as follows: Place $\mathtt{B}_i$ at the nodes labeled $s_1, \ldots, s_i$. To find $m-i$ isolated nodes spanning a subdiagram of type $\mathtt{A}_1^{m-i}$, it requires $2(m-i)$ nodes of $\Gamma_{\mathtt{B}_n}$. This leads us to the condition $i + 2(m-i) = 2m - i \leq n$. Combining this with the requirement that $m - i \geq 1$ provides $2 \leq i \leq n-2$, and $3 \leq m \leq \frac{n+i}{2}$. By substituting $n = 2k$, we find $2 \leq i \leq 2k-2$ and $3 \leq m \leq k + \frac{i}{2}$. For $n = 2k+1$, we obtain $2 \leq i \leq 2k-1$ and $3 \leq m \leq k + \frac{i+1}{2}$. The next step is to determine the number of connected components of Γ^m spanned by vertices corresponding to subgraphs of type $\mathtt{A}_1^{m-i} \sqcup \mathtt{B}_i$. As shown in Lemma 5.2.14, for fixed m and i, all subdiagrams of type $\mathtt{A}_1^{m-i} \sqcup \mathtt{B}_i$ that satisfy the stated conditions are odd-adjacent. Thus, they are all contained within a common connected component of Γ^m. We can count the number of conjugacy classes $\mathrm{cc}_2(W_{\mathtt{B}_n}, \mathtt{A}_1^{m-i} \sqcup \mathtt{B}_i)$ of $W_{\mathtt{B}_n}$ that correspond to subgroups of type $\mathtt{A}_1^{m-i} \sqcup \mathtt{B}_i$ as follows:

$$n = 2k: \qquad \mathrm{cc}_2(W_{\mathtt{B}_n}, \mathtt{A}_1^{m-i} \sqcup \mathtt{B}_i) = \sum_{i=2}^{2k-2} \sum_{m=i+1}^{k+\frac{i}{2}} 1 = (k-1)^2;$$

$$n = 2k+1: \qquad \mathrm{cc}_2(W_{\mathtt{B}_n}, \mathtt{A}_1^{m-i} \sqcup \mathtt{B}_i) = \sum_{i=2}^{2k-1} \sum_{m=i+1}^{k+\frac{i+1}{2}} 1 = k(k-1).$$

Sum of all conjucagy classes:
Eventually, the number of conjugacy classes of a Coxeter group of type $W_{\mathtt{B}_n}$ can be derived as follows:

$$\mathrm{cc}_2(W_{\mathtt{B}_n}) = 2 + \mathrm{cc}_2(W_{\mathtt{B}_n}, \mathtt{B}_m) + \mathrm{cc}_2(W_{\mathtt{B}_n}, \mathtt{A}_1^m) + \mathrm{cc}_2(W_{\mathtt{B}_n}, \mathtt{A}_1^{m-i} \sqcup \mathtt{B}_i);$$

$$n = 2k: \qquad \mathrm{cc}_2(W_{\mathtt{B}_n}) = 2 + 2k - 1 + 2(k-1) + (k-1)^2 = k^2 + 2k;$$

$$n = 2k+1: \qquad \mathrm{cc}_2(W_{\mathtt{B}_n}) = 2 + 2k + 2k - 1 + k(k-1) = k^2 + 3k + 1.$$

□

Notice that we gave an illustration of Γ^k for $\mathtt{B}_4$ in Figure 1.4. We continue with the proof of Theorem 5.4.3 for $W_{\mathtt{D}_n}$. As a preparation, we prove first:

Lemma 5.5.3. *Consider the affine Coxeter group* $\mathtt{D}_n$ *with diagram* $\Gamma_{\mathtt{D}_n}$*. Then, all vertices of the* m*-odd-graph* Γ^m *are of the form*

$$\mathtt{A}_1^{m-2j} \sqcup \mathtt{D}_{2j},$$

with $j \in \mathbb{N}_0$.

PROOF. To simplify speech in our arguments below, we will refer the nodes of $\Gamma_{\mathtt{D}_n}$ by their indexed generator, enumerated from left to right as shown in Figure 5.11. Recall that $\Gamma_{\mathtt{D}_n}$ has n nodes, with all edges labeled 3. Subgraphs spanned by the nodes labeled $s_n, s_{n-1}, \ldots, s_\ell$ with $\ell \in \{1, \ldots, n-3\}$ are diagrams of type $\mathtt{D}_{n-\ell+1}$. Furthermore, by selecting a set of pairwise non-adjacent nodes, one can obtain subgraphs of type $\mathtt{A}_1$ from $\mathtt{D}_n$. Notice that the condition of non-adjacency for subdiagrams of type $\mathtt{A}_1$ among the nodes labeled $s_1, s_2, \ldots, s_{n-2}$ necessitates distance of the index numbers of at least 2. Additionally, the nodes s_{n-1} and s_n are non-adjacent to each other and all nodes with indices less than or equal to $n-2$. From these observations, along with the fact that subdiagrams of type $\mathtt{D}_\ell$ are admissible as vertices of Γ^m only for even ℓ (compare Figure 5.1), we obtain that subgraphs of the form $\mathtt{A}_1^{m-2j} \sqcup \mathtt{D}_{2j}$ with $j \in \mathbb{N}_0$ are feasible for a diagram of type $\mathtt{D}_n$. Further, $\Gamma_{\mathtt{D}_n}$ does not contain any other Coxeter diagrams cataloged in Figure 5.1, as it does not contain $\mathtt{E}_7, \mathtt{E}_8, \mathtt{F}_4, \mathtt{G}_2, \mathtt{H}_3, \mathtt{H}_4$ as well as $\mathtt{I}_2(2\ell)$ and $\mathtt{B}_\ell$ for $\ell \geq 2$. Consequently, subdiagrams of the form $\mathtt{A}_1^{m-2j} \sqcup \mathtt{D}_{2j}$ with $j \in \mathbb{N}_0$ are the only subdiagrams of $\mathtt{D}_n$ that yield irreducible Coxeter groups with nontrivial center, thus defining the sole vertices of Γ^m. □

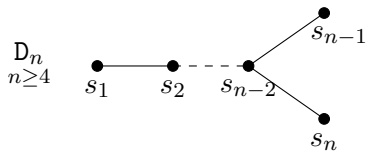

FIGURE 5.11. Coxeter diagram of $\mathtt{D}_n$.

PROOF OF THEOREM 5.4.3 FOR $\mathtt{D}_n$. From the structure of $\Gamma_{\mathtt{D}_n}$, it is evident that Γ^1 has a single connected component for all $\mathtt{D}_n$. This arises from the fact that all edge labels are odd, thereby yielding to Γ^1 being an unlabeled connected graph.
We derive the closed formula by counting the connected components of Γ^m for the different types of subgraphs as given by Lemma 5.5.3. We examine these different types in detail below. Beforehand, we derive lower and upper bounds on the size of the subgraphs contained in $\Gamma_{\mathtt{D}_n}$: As demonstrated in our preceding discussion in Lemma 5.5.3, the nodes labeled $s_n, s_{n-1}, \ldots, s_\ell$ with $\ell \in \{1, \ldots, n-3\}$ span a subgraph of type $\mathtt{D}_{n-\ell+1}$. Consequently, $\Gamma_{\mathtt{D}_n}$ contains precisely one subgraph of type $\mathtt{D}_{2j}$ for $j \in \{2, \ldots, \frac{n}{2}\}$.
Furthermore, we have observed in Lemma 5.5.3 above that $\Gamma_{\mathtt{D}_n}$ contains subdiagrams of type $\mathtt{A}_1$ and that these are isolated if the index numbers differ by more than 2. An exception arises for the nodes labeled s_{n-1} and s_n, which are solely adjacent to the node labeled s_{n-2}. This indicates, that $\Gamma_{\mathtt{D}_n}$ contains up to $k+1$ isolated copies of subdiagrams of type $\mathtt{A}_1$ for $n = 2k$ and $n = 2k+1$.

We will now compute the number of connected components associated with the various types of subgraphs. Different types of subgraphs invariably lead to different connected

components in Γ^m, as they cannot be odd-adjacent. This follows from the fact that their diagrams are not isomorphic. Nonetheless, subdiagrams of the same type can be adjacent, as shown, e.g., in Lemma 5.2.14.

Subdiagrams of type $\mathtt{D}_m = \mathtt{D}_{2j}$*:*
Given that only subdiagrams of the type $\mathtt{D}_m$ with m even are permissible, it follows that $m = 2j \geq 4$. Based on our analysis in Lemma 5.5.3, we already know that $\Gamma_{\mathtt{D}_n}$ contains a single subgraph of type $\mathtt{D}_m$ for $4 \leq m \leq n$. Thus, we have $j \leq \frac{n}{2} = k$ for $n = 2k$ and $j \leq \frac{n-1}{2} = k$ for $n = 2k+1$. This implies that for each even m, we obtain an isolated vertex of type $\mathtt{D}_m$ within the graph Γ^m. Therefore, we can quantify the number of conjucagy classes $\mathrm{cc}_2(W_{\mathtt{D}_n}, \mathtt{D}_m)$ of $\mathtt{D}_n$ that arise from subgroups of type $\mathtt{D}_m$ as follows:

$$\mathrm{cc}_2(W_{\mathtt{D}_n}, \mathtt{D}_m) = \sum_{j=2}^{k} 1 = k - 1.$$

Subdiagrams of type $\mathtt{A}_1^m$*:*
Subdiagrams of $\Gamma_{\mathtt{D}_n}$ of type $\mathtt{A}_1^m$ are characterized as m non-adjacent nodes. The application of Lemma 5.2.14 reveals that many of these subdiagrams are odd-adjacent, which indicates that the associated vertices in Γ^m are connected, given that every edge of $\Gamma_{\mathtt{D}_n}$ is odd-labeled. Note that subdiagrams that include both nodes labeled s_{n-1} and s_n cannot be odd-adjacent to those that do not contain both nodes. This restriction arises from the fact that these two nodes are only adjacent to the node labeled s_{n-2}. Consequently, the vertices of Γ^m associated with these subdiagrams are not contained within the same connected component. Thus, for counting the connected components of Γ^m, it is necessary to make a distinction between subdiagrams that encompass s_{n-1} and s_n, and those that do not include them.
We begin by examining subdiagrams that contain the nodes labeled s_{n-1} and s_n. It follows that $m \geq 2$. Next, it remains to choose $m-2$ isolated nodes of the nodes labeled $s_1, \ldots, s_{n-3}$. This gives $2(m-2) - 1 \leq n - 3 \Leftrightarrow m \leq \frac{n+2}{2}$. When we substitute $n = 2k$, we find $m \leq k + 1$. For $n = 2k + 1$, this results in $m \leq k + \frac{3}{2}$. Given that $m, k \in \mathbb{Z}$, this implies $m \leq k + 1$ in both cases. It then follows with Lemma 5.2.14 that for fixed m and n, all vertices of Γ^m that correspond to subgraphs of $\Gamma_{\mathtt{D}_n}$ and satisfy the conditions discussed are odd-adjacent. Consequently, they all belong to a common connected component of Γ^m.
Now, consider subdiagrams not containing both nodes s_{n-1} and s_n simultaneously. We must select m isolated nodes from the set of nodes labeled $s_1, \ldots, s_n$. If $2m - 1 \leq n - 2 \Leftrightarrow m \leq \frac{n-1}{2}$, we can find m isolated nodes, thereby yielding m subgraphs of type $\mathtt{A}_1$, exclusively from the nodes labeled $s_1, \ldots, s_{n-2}$. Invoking Lemma 5.2.14, we can ascertain that all subdiagrams of this type, including those that involve either s_{n-1} or s_n, are odd-adjacent. Consequently, the subdiagrams of type $\mathtt{A}_1^m$ for $2 \leq m \leq \frac{n-1}{2}$ that do not contain both s_{n-1} and s_n simultaneously are located within a shared connected component of Γ^m. By substituting $n = 2k$ and using $m \in \mathbb{Z}$, we find that $2 \leq m \leq k-1$. Considering $n = 2k + 1$ results in $2 \leq m \leq k$.
If $n - 2 < 2m - 1 \leq n - 1 \Leftrightarrow \frac{n-1}{2} < m \leq \frac{n}{2}$, we can identify up to two subdiagrams that meet our conditions: For $n = 2k$, we observe $k - \frac{1}{2} < m \leq k \Leftrightarrow m = k$. This leads to an identification of the two subdiagrams spanned by $s_1, s_3, s_5, \ldots, s_{n-1}$ and $s_1, s_3, s_5, \ldots, s_{n-3}, s_n$. Since these are not odd-adjacent in $\Gamma_{\mathtt{D}_n}$, they each establish a

connected component in Γ^m. For $n = 2k+1$, we obtain $k < m \leq k+\frac{1}{2}$, which has no solution for $m \in \mathbb{Z}$. As a result, no subdiagram of type $\mathtt{A}_1^m$ exists within these constraints. In conclusion, we can enumerate the conjugacy classes $\mathrm{cc}_2(W_{\mathtt{D}_n}, \mathtt{A}_1^m)$ of $W_{\mathtt{D}_n}$ derived from subgroups of type $\mathtt{A}_1^m$ as follows:

$$n = 2k: \qquad \mathrm{cc}_2(W_{\mathtt{D}_n}, \mathtt{A}_1^m) = \sum_{m=2}^{k+1} 1 + \sum_{m=2}^{k-1} 1 + 2 = k + k - 2 + 2 = 2k;$$

$$n = 2k+1: \qquad \mathrm{cc}_2(W_{\mathtt{D}_n}, \mathtt{A}_1^m) = \sum_{m=2}^{k+1} 1 + \sum_{m=2}^{k} 1 = k + k - 1 = 2k - 1.$$

Subdiagrams of type $\mathtt{D}_{2j} \sqcup A_1^{m-2j}$*:*
Since we have already counted the connected components of Γ^m of type A_1^m and $\mathtt{D}_m$ above, we will focus exclusively on the case where $j \neq 0$ and $m - 2j > 0$ here. Therefore, we require $m \geq 5$. From our prior observations in Lemma 5.5.3, we know that $\Gamma_{\mathtt{D}_n}$ contains subgraphs of type $\mathtt{D}_m$ for $m \leq n$. Thus, we conclude $j \leq \frac{n}{2} = k$ for $n = 2k$, and $j \leq \frac{n-1}{2} = k$ when $n = 2k+1$. Observe that two subgraphs of type $\mathtt{A}_1^{m-2j} \sqcup \mathtt{D}_{2j}$ and $\mathtt{A}_1^{m'-2j'} \sqcup \mathtt{D}_{2j'}$ can only be odd-adjacent if $m = m'$ and $j = j'$, as they are not isomorphic as diagrams otherwise. This implies that for different values of j, we can count the connected components of m separately. Since $j \neq 0$, we will first consider the subgraph of type $\mathtt{D}_{2j}$. Given the structure of $\Gamma_{\mathtt{D}_n}$, this subgraph can only be spanned by the nodes labeled $s_{n-2j+1}, \ldots, s_{n-1}, s_n$. For a vertex of Γ^m with the desired type, we must choose $m - 2j$ feasible isolated nodes from the remaining nodes labeled $s_1, \ldots, s_{n-2j}$. Note that we cannot select the node labeled s_{n-2j} because it is odd-adjacent to s_{n-2j+1}. Therefore, we can place the isolated nodes at $s_1, \ldots, s_{n-2j-1}$. To ensure all $m - 2j$ nodes remain isolated from each other, it requires a total of $2(m-2j)-1$ nodes from $s_1, \ldots, s_{n-2j-1}$. Consequently, we derive that $2(m-2j) - 1 \leq n - 2j - 1 \Leftrightarrow 2m - 2j \leq n \Leftrightarrow m \leq \frac{n+2j}{2}$. For $n = 2k$, we can reformulate to $m \leq k + j$. For $n = 2k+1$, we obtain $m \leq k + j + \frac{1}{2}$. However, since $k, j \in \mathbb{Z}$, this yields the same upper bound. Observe that we explicitly do not allow $m = 2j$. Thus we do not consider subgraphs of type $\mathtt{D}_{2j}$ as a subclass of $\mathtt{D}_{2j} \sqcup \mathtt{A}_1^{m-2j}$ in this context. Finally, it only remains to quantify the number of connected components of Γ^m defined by the vertices corresponding to these subgraphs of $\Gamma_{\mathtt{D}_n}$. Lemma 5.2.14 shows that all the vertices defined by the subgraphs of the same type and size described above are odd-adjacent. Therefore, Γ^m contains one connected component of type $\mathtt{D}_{2j} \sqcup A_1^{m-2j}$ for every $2 \leq j \leq k$, $2j + 1 \leq m \leq k + j$.
In summary, we can count the number of conjugacy classes $\mathrm{cc}_2(W_{\mathtt{D}_n}, \mathtt{D}_{2j} \sqcup \mathtt{A}_1^{m-2j})$ of $W_{\mathtt{D}_n}$ for $n = 2k$ and $n = 2k+1$ obtained from subgroups of type $\mathtt{D}_{2j} \sqcup A_1^{m-2j}$ as:

$$\mathrm{cc}_2(W_{\mathtt{D}_n}, \mathtt{D}_{2j} \sqcup \mathtt{A}_1^{m-2j}) = \sum_{j=2}^{k} \sum_{m=2j+1}^{k+j} 1 = \frac{1}{2}(k-1)(k-2).$$

Sum of all conjucagy classes:
In conclusion, we can derive the number of conjugacy classes of a Coxeter group of type $W_{\mathtt{D}_n}$ to:

$$\mathrm{cc}_2(W_{\mathtt{D}_n}) = 1 + \mathrm{cc}_2(W_{\mathtt{D}_n}, \mathtt{D}_m) + \mathrm{cc}_2(W_{\mathtt{D}_n}, \mathtt{A}_1^m) + \mathrm{cc}_2(W_{\mathtt{D}_n}, \mathtt{A}_1^{m-2j} \sqcup \mathtt{D}_{2j});$$

$$n = 2k: \qquad \mathrm{cc}_2(W_{\mathtt{D}_n}) = 1 + k - 1 + 2k + \frac{1}{2}(k-1)(k-2) = \frac{1}{2}(k^2 + 3k + 2);$$
$$n = 2k+1: \qquad \mathrm{cc}_2(W_{\mathtt{D}_n}) = 1 + k - 1 + 2k - 1 + \frac{1}{2}(k-1)(k-2) = \frac{1}{2}(k^2 + 3k).$$

□

It remains to present the proofs for the numbers of conjugacy classes of the exceptional types of spherical Coxeter groups:

Proof of Theorem 5.4.3 for the exceptional types. To determine the number of conjugacy classes of the exceptional types of spherical Coxeter groups, we use arguments similar to those in Lemma 5.2.14 and count the number of subdiagrams of the types presented in Figure 5.1.
$\mathrm{cc}_2(\mathtt{E}_6)$*:*

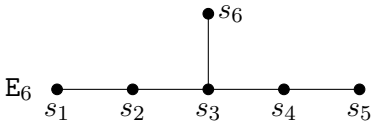

Figure 5.12. Coxeter diagram of $\mathtt{E}_6$.

Since all edges of $\Gamma_{\mathtt{E}_6}$ are odd-labeled, Γ^1 is a connected graph. Comparing Figure 5.1, we observe that for $m = 2$ and $m = 3$, the diagram $\Gamma_{\mathtt{E}_6}$ contains only subgraphs of type $\mathtt{A}_1^m$. The structure of $\Gamma_{\mathtt{E}_6}$ resembles that of a path graph with an additional edge attached to the node labeled s_3. Invoking Lemma 5.2.14, we conclude that all these subgraphs are odd-adjacent and form a connected component in Γ^m. This implies that Γ^2 and Γ^3 are connected graphs. Moreover, it is impossible to find 4 isolated nodes in $\Gamma_{\mathtt{E}_6}$, indicating that Γ^4 does not include vertices representing subgroups of type $\mathtt{A}_1^4$. However, $\Gamma_{\mathtt{E}_6}$ does feature a subdiagram of type $\mathtt{D}_4$, which is spanned by the nodes labeled s_2, s_3, s_4, s_6 (see also Figure 5.12). For $m \geq 5$, $\Gamma_{\mathtt{E}_6}$ lacks the required subdiagrams listed in Figure 5.1. Consequently, we find that $\Gamma^5 = \emptyset$ and $\Gamma^6 = \emptyset$. In summary, the number of conjugacy classes of a Coxeter group of type $\mathtt{E}_6$ is as follows:

$$\mathrm{cc}_2(W_{\mathtt{E}_6}) = 1 + 1 + 1 + 1 + 0 + 0 = 4.$$

$\mathrm{cc}_2(\mathtt{E}_7)$*:*

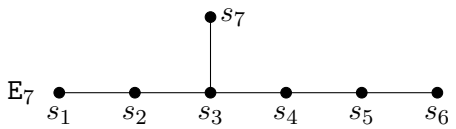

Figure 5.13. Coxeter diagram of $\mathtt{E}_7$.

Since all edges of $\Gamma_{\mathtt{E}_7}$ are odd-labeled, Γ^1 is a connected graph. Comparing Figure 5.1 as for $\mathtt{E}_6$ above, we observe that for $m = 2$ and $m = 3$ the diagram $\Gamma_{\mathtt{E}_7}$ contains only subgraphs of type $\mathtt{A}_1^m$. Note that $\Gamma_{\mathtt{E}_7}$ has the structure of a path graph with an additional edge connected to the node labeled s_3. Using the arguments from Lemma 5.2.14, we see that for $m = 2$, all subgraphs of type $\mathtt{A}_1^2$ are odd-adjacent and thus form a connected component within Γ^2. For Γ^3, we find 2 connected components of the graph with vertices representing subgroups of type $\mathtt{A}_1^3$. The nodes labeled s_4 and s_7 are only adjacent to the node s_3 and have a distance of 2 to their neighboring nodes in their spanned path subgraph. Therefore, the subdiagram spanned by s_4, s_6, s_7 is not odd-adjacent to other subdiagrams of type $\mathtt{A}_1^3$, such as those spanned by s_2, s_4, s_7 or s_1, s_3, s_5. For $m = 4$, the diagram $\Gamma_{\mathtt{E}_7}$ contains subdiagrams of type $\mathtt{A}_1^4$ and $\mathtt{D}_4$ from the list presented in Figure 5.1. Again, applying Lemma 5.2.14, we find that all subdiagrams of type $\mathtt{A}_1^4$ are odd-adjacent and therefore belong to a common connected component of Γ^4. Additionally, $\Gamma_{\mathtt{E}_6}$ contains a single subdiagram of type $\mathtt{D}_4$ spanned by the nodes labeled s_2, s_3, s_4, s_7. Because of its type, this subdiagram is not odd-adjacent to the other subdiagrams of type $\mathtt{A}_1^4$ discussed earlier, resulting in its corresponding vertex in Γ^4 forming a separate connected component. Thus, Γ^4 has two connected components. For $m = 5$, note that $\Gamma_{\mathtt{E}_7}$ does not contain a subdiagram of type $\mathtt{A}_1^5$; it only includes a subdiagram of type $\mathtt{D}_4 \sqcup \mathtt{A}_1$ spanned by the nodes labeled s_2, s_3, s_4, s_6, s_7 according to the list of graphs shown in Figure 5.1. Hence, Γ^5 contains a single vertex and, therefore, has one connected component. For $m = 6$, $\Gamma_{\mathtt{E}_7}$ contains only the subdiagram of type $\mathtt{D}_6$, spanned by the nodes labeled $s_2, s_3, s_4, s_5, s_6, s_7$. Similar to Γ^5, we conclude that Γ^6 has a single connected component. For $m = 7$, we observe that $\Gamma_{\mathtt{E}_7}$ itself is of inc-type, indicating that Γ^7 has one connected component as well.
Eventually, we can summarize the number of conjugacy classes of a Coxeter group of type $\mathtt{E}_7$ to:

$$\mathrm{cc}_2(W_{\mathtt{E}_7}) = 1 + 1 + 2 + 2 + 1 + 1 + 1 = 9.$$

$\mathrm{cc}_2(\mathtt{E}_8)$*:*

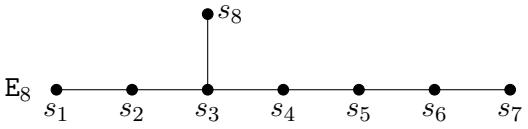

FIGURE 5.14. Coxeter diagram of $\mathtt{E}_8$.

Using the same arguments as presented in the proof for $W_{\mathtt{E}_6}$ above, we observe that Γ^1, Γ^2, and Γ^3 each have one connected component consisting of vertices of the type $\mathtt{A}_1^m$. For $m = 4$, note that $\Gamma_{\mathtt{E}_8}$ contains a subgraph of type $\mathtt{D}_4$, which is spanned by the nodes s_2, s_3, s_4, s_8. It further contains several subgraphs of type $\mathtt{A}_1^4$. Again, Lemma 5.2.14 shows that all subgraphs of this type are odd-adjacent, thereby forming a connected component in Γ^4. Since the corresponding subgroups are not isomorphic to $\mathtt{D}_4$, the vertex of Γ^4 representing this subgroup is not odd-adjacent to the other nodes. Thus, Γ^4 has two connected components.

For $m = 5$, similar to $W_{\mathtt{E}_7}$, we find that the diagram only contains a subgraph of type $\mathtt{D}_4 \sqcup \mathtt{A}_1$ from the list displayed in Figure 5.1. Consequently, Γ^5 consists of a single node and therefore has one connected component.
For $m = 6$, we identify a subgraph of type $\mathtt{D}_6$ that is spanned by the nodes labeled $s_2, s_3, s_4, s_5, s_6, s_8$. Note that we cannot find a subgraph of type $\mathtt{D}_4 \sqcup \mathtt{A}_1^2$ because we cannot identify two isolated nodes in $\Gamma_{\mathtt{E}_8}$ with a subgraph of type $\mathtt{D}_4$ spanned by the nodes labeled s_2, s_3, s_4, s_8. Hence, Γ^6 consists of one vertex and has one connected component.
For $m = 7$, we only find the subgraph spanned by the nodes labeled $s_1, s_2, s_3, s_4, s_5, s_6, s_8$ of type $\mathtt{E}_7$. This implies, again, that Γ^7 has one connected component.
Finally, for $m = 8$, since $\Gamma_{\mathtt{E}_8}$ is of inc-type, we find the entire graph as a subgraph and obtain that Γ^8 has one connected component.
Given these observations, we can summarize the number of conjugacy classes of a Coxeter group of type $\mathtt{E}_8$:

$$\mathrm{cc}_2(W_{\mathtt{E}_8}) = 1 + 1 + 1 + 2 + 1 + 1 + 1 + 1 = 9.$$

$\mathrm{cc}_2(\mathtt{F}_4)$*:*

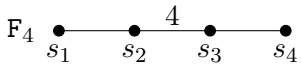

FIGURE 5.15. Coxeter diagram of $\mathtt{F}_4$.

Since $\Gamma_{\mathtt{F}_4}$ is a path graph and the edge connecting the nodes labeled s_2 and s_3 is the only edge with an even label, Γ^1 has two connected components, which are spanned by the nodes labeled s_1, s_2 and s_3, s_4.
For $m = 2$, observe that Γ^m contains vertices representing subgraphs of type $\mathtt{A}_1^2$ and subgraphs of type $\mathtt{B}_2$. The only subgraph of $\Gamma_{\mathtt{F}_4}$ of type $\mathtt{B}_2$ is spanned by the nodes labeled s_2, s_3. Since groups of type $\mathtt{B}_2$ are not isomorphic to groups of type $\mathtt{A}_1^2$, this vertex is not connected to vertices representing other subgroups in Γ^2, thus forming a separate connected component. Subgroups of type $\mathtt{A}_1^2$ are represented by the nodes labeled s_1, s_3, and s_1, s_4, and s_2, s_4. The nodes labeled s_3 and s_4 are adjacent along an odd-labeled edge, making the first two subdiagrams odd-adjacent. Additionally, the nodes labeled s_1 and s_2 are also adjacent along an odd edge, ensuring that the last two subdiagrams are odd-adjacent as well. This guarantees that all corresponding vertices of Γ^2 are connected and form a connected component. Together, this shows that Γ^2 has two connected components.
For $m = 3$, note that $\Gamma_{\mathtt{F}_4}$ only contains two subdiagrams of type $\mathtt{B}_3$ from the list displayed in Figure 5.1, which are spanned by the nodes labeled s_1, s_2, s_3, and s_2, s_3, s_4. Since the nodes labeled s_1 and s_4 are not adjacent in $\Gamma_{\mathtt{F}_4}$, the corresponding vertices in Γ^3 are not connected, resulting in 2 connected components in Γ^3.
Finally, for Γ^4, we observe that $\Gamma_{\mathtt{F}_4}$ itself is of inc-type, which indicates that Γ^4 has one connected component.
In summary, we can derive the number of conjugacy classes of a Coxeter group of type

$\mathtt{F}_4$ as follows:

$$\mathrm{cc}_2(W_{\mathtt{F}_4}) = 2 + 2 + 2 + 1 = 7.$$

$\mathrm{cc}_2(\mathtt{G}_2)$*:*

$\mathtt{G}_2 \cong \mathtt{I}_2(6)$ 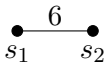

FIGURE 5.16. Coxeter diagram of $\mathtt{G}_2$.

Since $\Gamma_{\mathtt{G}_2}$ contains two nodes and the single edge of $\Gamma_{\mathtt{G}_2}$ connecting them is even labeled, Γ^1 comprises two isolated vertices and therefore has two connected components. Additionally, as $\Gamma_{\mathtt{G}_2}$ itself is of inc-type, Γ^2 consists of a single isolated node, resulting in one connected component. Thus, we can count the number of conjugacy classes of a Coxeter group of type $\mathtt{G}_2$ as:

$$\mathrm{cc}_2(W_{\mathtt{G}_2}) = 2 + 1 = 3.$$

$\mathrm{cc}_2(\mathtt{H}_2)$*:*

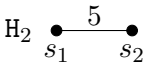

FIGURE 5.17. Coxeter diagram of $\mathtt{H}_2$.

Since $\Gamma_{\mathtt{H}_2}$ has two nodes and the sole edge of $\Gamma_{\mathtt{G}_2}$ is odd-labeled, it follows that Γ^1 is an unlabeled connected graph and therefore has one connected component. Furthermore, since $\Gamma_{\mathtt{H}_2}$ is not of inc-type, Γ^2 is empty.
Therefore, we can determine the number of conjugacy classes of a Coxeter group of type $\mathtt{H}_2$ as follows:

$$\mathrm{cc}_2(W_{\mathtt{H}_2}) = 1 + 0 = 1.$$

$\mathrm{cc}_2(\mathtt{H}_3)$*:*

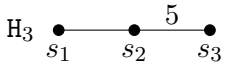

FIGURE 5.18. Coxeter diagram of type $\mathtt{H}_3$.

Since all edges of $\Gamma_{\mathtt{H}_3}$ are odd-labeled, and the graph contains no isolated nodes, we conclude that Γ^1 is a connected graph with one connected component.
For Γ^2, observe that $\Gamma_{\mathtt{H}_3}$ contains the two isolated nodes labeled s_1 and s_3, which together

form a subdiagram of type $\mathtt{A}_1^2$. As this is the only contained subdiagram with two nodes from the list in Figure 5.1, Γ^2 consists of an isolated vertex, resulting in one connected component.
Regarding Γ^3, we recall that $\Gamma_{\mathtt{H}_3}$ itself is of inc-type. Thus, Γ^3 also consists of one isolated vertex and has one connected component.
In summary, the total number of conjugacy classes of a Coxeter group of type $\mathtt{H}_3$ can be expressed as:

$$\mathrm{cc}_2(W_{\mathtt{H}_3}) = 1 + 1 + 1 = 3.$$

$\mathrm{cc}_2(\mathtt{H}_4)$*:*

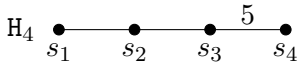

FIGURE 5.19. Coxeter diagram of $\mathtt{H}_4$.

Since all edges of $\Gamma_{\mathtt{H}_4}$ are odd-labeled and the graph is connected, Γ^1 is a connected graph with a single connected component.
For Γ^2, note that $\Gamma_{\mathtt{H}_4}$ contains subdiagrams of type $\mathtt{A}_1^2$, which are spanned by the nodes labeled s_1, s_3, and s_1, s_4, and s_2, s_4. According to Lemma 5.2.14, these are all odd-adjacent and thus form a connected component in Γ^2. Since $\Gamma_{\mathtt{H}_4}$ does not include any other subdiagrams from the list mentioned in Figure 5.1 with two nodes, Γ^2 also has one connected component.
In Γ^3, there exists a vertex corresponding to a subdiagram of type $\mathtt{H}_3$ spanned by the nodes labeled s_2, s_3, and s_4. As $\Gamma_{\mathtt{H}_4}$ contains no other subdiagrams from Figure 5.1, Γ^3 consists of one isolated vertex and has one connected component.
For Γ^4, since $\Gamma_{\mathtt{H}_4}$ itself is of inc-type, we find that Γ^4 also consists of one isolated vertex and has one connected component.
In summary, we can conclude that the number of conjugacy classes of a Coxeter group of type $\mathtt{H}_4$ is:

$$\mathrm{cc}_2(W_{\mathtt{H}_4}) = 1 + 1 + 1 + 1 = 4.$$

□

5.6. Proof of Theorem 5.4.4

This section provides proofs of our findings regarding the numbers of conjugacy classes of involutions for the families and exceptional types of affine Coxeter groups, as presented in Theorem 5.4.4.

PROOF OF THEOREM 5.4.4 FOR $\tilde{\mathtt{A}}_n$, $\widetilde{\mathtt{G}}_2$, AND $\widetilde{\mathtt{I}}_1$. The formula for type $\tilde{\mathtt{A}}_n$ follows immediately from the more general Proposition 5.4.6. Types $\widetilde{\mathtt{G}}_2$ and $\widetilde{\mathtt{I}}_1$ were already covered above: $W_{\widetilde{\mathtt{I}}_1} \cong \mathbb{Z}/2\mathbb{Z} * \mathbb{Z}/2\mathbb{Z}$ and $W_{\widetilde{\mathtt{G}}_2} \cong \Delta(2,3,6)$, hence $\mathrm{cc}_2(W_{\widetilde{\mathtt{I}}_1}) = 2$ and $\mathrm{cc}_2(W_{\widetilde{\mathtt{G}}_2}) = 4$. □

To verify the remainder of Theorem 5.4.4, we will distinguish between the three infinite families and the exceptional types, starting with $\widetilde{\mathtt{B}}_n$. First, observe the following:

Lemma 5.6.1. *Consider the affine Coxeter group $\widetilde{\mathtt{B}}_n$ with diagram $\Gamma_{\widetilde{\mathtt{B}}_n}$. Then, all vertices of the m-odd-graph Γ^m are of the form*

$$\mathtt{B}_i \sqcup \mathtt{A}_1^l \sqcup \mathtt{D}_{2j},$$

with $i, j, l \in \mathbb{N}_0$.

Remark 5.6.2. Recall that the notation $\mathtt{X}_0$ refers to an empty diagram of type $\mathtt{X}$.

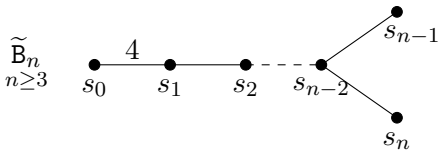

FIGURE 5.20. Coxeter diagram of $\widetilde{\mathtt{B}}_n$.

PROOF. To simplify our notation below, we will refer the nodes of $\Gamma_{\widetilde{\mathtt{B}}_n}$ by their indexed generator, enumerating from left to right as shown in Figure 5.20. Recall that $\Gamma_{\widetilde{\mathtt{B}}_n}$ has $n+1$ nodes, with node s_0 and s_1 being adjacent via an edge labeled 4, while all other edges are labeled 3. Subgraphs spanned by the vertices $s_0, s_1, \ldots, s_\ell$ where $\ell \in \{2, \ldots, n-1\}$ or $s_0, s_1, \ldots, s_{n-2}, s_n$ are diagrams of type $\mathtt{B}_{\ell+1}$ and $\mathtt{B}_n$, respectively. Further, subgraphs spanned by the vertices $s_n, s_{n-1}, \ldots, s_\ell$ for $\ell \in \{1, \ldots, n-3\}$ are diagrams of type $\mathtt{D}_{n-\ell+1}$. By selecting a set of m pairwise non-adjacent nodes, one can also create subgraphs of type $\mathtt{A}_1^m$ from $\widetilde{\mathtt{B}}_n$. Note that non-adjacency among the nodes $s_0, s_1, \ldots, s_{n-2}$ implies that the indices must differ by at least two. Additionally, s_{n-1} and s_n are non-adjacent to each other and all vertices with index numbers less than or equal to $n-2$. From these observations, along with the fact that subdiagrams of type $\mathtt{D}_\ell$ are only permitted as vertices of Γ^m when ℓ is even, we conclude that subgraphs of the form $\mathtt{B}_i \sqcup \mathtt{A}_1^l \sqcup \mathtt{D}_{2j}$ with $i, j, l \in \mathbb{N}_0$ are valid for a $\widetilde{\mathtt{B}}_n$ diagram. Furthermore, we observe that $\Gamma_{\widetilde{\mathtt{B}}_n}$ does not contain $\mathtt{E}_7, \mathtt{E}_8, \mathtt{F}_4, \mathtt{G}_2, \mathtt{H}_3, \mathtt{H}_4$ as well as $\mathtt{I}_2(2\ell)$ for $\ell \geq 2$. Thus, subdiagrams of the form $\mathtt{B}_i \sqcup \mathtt{A}_1^l \sqcup \mathtt{D}_{2j}$ with $i, j, l \in \mathbb{N}_0$ are indeed the only subdiagrams of $\widetilde{\mathtt{B}}_n$ yielding irreducible Coxeter groups with nontrivial centers. Therefore, these are the only vertices of Γ^m. □

PROOF OF THEOREM 5.4.4 FOR $\widetilde{\mathtt{B}}_n$. We can observe immediately from the structure of Γ that Γ^1 has 2 connected components for all $\widetilde{\mathtt{B}}_n$, since all edge labels except for one of $\Gamma_{\widetilde{\mathtt{B}}_n}$ are odd. This results in Γ^1 being an unlabeled graph with two connected components.
Next, we will derive the closed formula by counting the connected components of Γ^m for the various types of subgraphs described in Lemma 5.6.1. We will discuss them separately below. Before we proceed with that, let us first establish lower and upper bounds on the size of the subgraphs contained in $\Gamma_{\widetilde{\mathtt{B}}_n}$:
Based on our arguments given in Lemma 5.6.1, we find that the span of the nodes labeled $s_0, s_1, \ldots, s_\ell$ with $\ell \in \{2, \ldots, n-1\}$ forms a subgraph of type $\mathtt{B}_{\ell+1}$. Additionally, the

nodes labeled $s_0, s_1, \ldots, s_{n-2}, s_n$ yield a subgraph of type $\mathtt{B}_n$. Therefore, $\Gamma_{\widetilde{\mathtt{B}}_n}$ contains one subgraph of type $\mathtt{B}_2, \ldots, \mathtt{B}_{n-2}$ each, and two subgraphs of type $\mathtt{B}_n$.
Furthermore, as noted in Lemma 5.6.1, $\Gamma_{\widetilde{\mathtt{B}}_n}$ also contains subgraphs of type $\mathtt{D}_{n-\ell+1}$ that are spanned by the nodes labeled $s_\ell, s_{\ell+1}, , \ldots, s_n$. Depending on the parity of n, this implies that $\Gamma_{\widetilde{\mathtt{B}}_n}$ contains subgraphs of type $\mathtt{D}_{2j}$ for $j \in \{2, \ldots, \frac{n}{2}\}$ when n is even, and for $j \in \{2, \ldots, \frac{n-1}{2}\}$ when n is odd. Additionally, $\Gamma_{\widetilde{\mathtt{B}}_n}$ contains up to $3 + \lfloor \frac{n-3}{2} \rfloor$ subgraphs of type $\mathtt{A}_1$. The type $\mathtt{A}_1^{3+\lfloor \frac{n-3}{2} \rfloor}$ subgraph contains the nodes labeled s_0, s_{n-1}, s_n, and every second node along the path in between s_0 and s_{n-3}.

We will now compute the number of connected components for the different types of subgraphs. Note that different types of subgraphs always yield different connected components in Γ^m since they are never adjacent as their diagrams are not isomorphic. However, subdiagrams of the same type can be odd-adjacent, as discussed in Lemma 5.2.14. For all the computations that follow, assume $n = 2k$ or $n = 2k + 1$.

Subdiagrams of type $\mathtt{B}_m$*:*
We distinguish between two cases:
Case 1: $2 \leq m \leq n - 1$. In this scenario, the graph $\Gamma_{\widetilde{\mathtt{B}}_n}$ contains only one subdiagram of type $\mathtt{B}_m$, which is spanned by the nodes labeled $s_0, s_1, \ldots, s_{m-1}$. As a result, this diagram produces an isolated vertex in Γ^m, labeled $\langle s_0, s_1, \ldots, s_{m-1} \rangle$, defining one connected component of the graph.
Case 2: $m = n$. As noted in Lemma 5.6.1, when $m = n$, $\Gamma_{\widetilde{\mathtt{B}}_n}$ contains two subdiagrams of type $\mathtt{B}_m$. These subdiagrams are spanned by the nodes labeled $s_0, s_1, \ldots, s_{n-2}$ and either s_{n-1} or s_n. Although these only differ by a single vertex and are isomorphic, there is no edge connecting s_{n-1} and s_n in $\Gamma_{\widetilde{\mathtt{B}}_n}$. Consequently, these subdiagrams are not odd-adjacent, resulting in two isolated vertices in Γ^m labeled $\langle s_0, s_1, \ldots, s_{n-1} \rangle$ and $\langle s_0, s_1, \ldots, s_{n-2}, s_n \rangle$. This gives rise to two connected components of the graph Γ^m. Thus, the number of conjucagy classes $\mathrm{cc}_2(W_{\widetilde{\mathtt{B}}_n}, \mathtt{B}_m)$ of $\widetilde{\mathtt{B}}_n$ obtained from subgroups of type $\mathtt{B}_m$ can be determined as:

$$\mathrm{cc}_2(W_{\widetilde{\mathtt{B}}_n}, \mathtt{B}_m) = 2 + \sum_{m=2}^{n-1} 1 = 2 + n - 2 = n.$$

Subdiagrams of type $\mathtt{A}_1^m$*:*
Subdiagrams of $\Gamma_{\widetilde{\mathtt{B}}_n}$ of type $\mathtt{A}_1^m$ are characterized as m pairwise non-adjacent nodes. Invoking Lemma 5.2.14, we observe that numerous of these subdiagrams are connected as vertices in Γ^m, given that every edge of $\Gamma_{\widetilde{\mathtt{B}}_n}$, aside from (s_0, s_1), is odd-labeled. Subdiagrams that comprise the node labeled s_0 cannot be odd-adjacent to those that do not contain s_0 since this node has degree 1 and its adjacent edge is labeled 4. Consequently, we need to distinguish between two cases of subdiagrams in order to count the number of conjugacy classes of $\widetilde{\mathtt{B}}_n$:
Case 1: The node labeled s_0 is not contained in any vertex of Γ^m of the connected components under consideration.
First, observe the following: The nodes of $\Gamma_{\widetilde{\mathtt{B}}_n}$ labeled s_{n-1} and s_n both have degree 1 and are adjacent to the common node labeled s_{n-2}. Hence, subdiagrams of type $\mathtt{A}_1^m$ that contain both nodes labeled s_{n-1} and s_n simultaneously are not odd-adjacent to subdiagrams that do not include both of these nodes. Therefore, the corresponding vertices of

Γ^m are not contained in a common connected component. It follows that, for counting the connected components of Γ^m, we need to distinguish between vertices that include the nodes labeled s_{n-1} and s_n, and those that do not contain them.
We start by considering subdiagrams that contain s_{n-1} and s_n. This implies $m \geq 2$. It then remains to choose $m-2$ isolated nodes from those labeled $s_1, \dots, s_{n-3}$, which gives $2(m-2)-1 \leq n-3 \Leftrightarrow m \leq \frac{n+2}{2}$. Substituting $n = 2k$ yields $m \leq k+1$, and substituting $n = 2k+1$ gives $m \leq k + \frac{3}{2}$. Since $m, k \in \mathbb{Z}$, this implies $m \leq k+1$. By invoking Lemma 5.2.14, we observe that for fixed m and n, all vertices of Γ^m corresponding to subgraphs of $\Gamma_{\widetilde{\mathtt{B}}_n}$ satisfying the conditions of this case are odd-adjacent. Thus, they are all contained in a common connected component of Γ^m.
Now, consider subdiagrams that do not contain both nodes labeled s_{n-1} and s_n. One has to choose m isolated nodes from those labeled $s_1, \dots, s_n$. If $2m-1 \leq n-2 \Leftrightarrow m \leq \frac{n-1}{2}$, a subgraph of type $\mathtt{A}_1^m$ can also be realized by only using the nodes labeled $s_1, \dots, s_{n-2}$. Therefore, all of these subgraphs, including those containing s_{n-1} or s_n, are odd-adjacent because the node labeled s_{n-2} is adjacent via an odd-labeled edge to the nodes labeled s_{n-1} and s_n. Consequently, the subdiagrams of type $\mathtt{A}_1^m$ for $2 \leq m \leq \frac{n-1}{2}$ that do not comprise s_0, and simultaneously do not comprise s_{n-1} and s_n, are all contained in a common connected component of Γ^m. If $n-2 < 2m-1 \leq n-1 \Leftrightarrow \frac{n-1}{2} < m \leq \frac{n}{2}$, we can find up to two subdiagrams that satisfy our conditions. For $n = 2k$, we have $k - \frac{1}{2} < m \leq k \Leftrightarrow m = k$, resulting in two subdiagrams spanned by $s_1, s_3, s_5, \dots, s_{n-1}$ and $s_1, s_3, s_5, \dots, s_{n-3}, s_n$. Since these are not odd-adjacent in $\Gamma_{\widetilde{\mathtt{B}}_n}$, each forms a separate connected component in Γ^m. For $n = 2k+1$, we find $k < m \leq k + \frac{1}{2}$, which has no solution for $m \in \mathbb{Z}$. Hence, no subdiagram of type $\mathtt{A}_1^m$ exists with these constraints.
Case 2: The node labeled s_0 is contained in all vertices of Γ^m of the connected components under consideration.
As in Case 1, we differentiate between subgraphs that contain both nodes labeled s_{n-1} and s_n and those that do not. First, we examine subgraphs that include the nodes labeled s_{n-1} and s_n simultaneously. To select from nodes which are non-adjacent to s_0, s_{n-1}, and s_n, we need to choose $m-3$ isolated nodes from $s_2, \dots, s_{n-3}$. This requirement leads to $m \geq 3$. Furthermore, we derive $2(m-3)-1 \leq n-4 \Leftrightarrow m \leq \frac{n+3}{2}$. For $n = 2k$, this translates to $3 \leq m \leq k + \frac{3}{2}$. Since $m \in \mathbb{Z}$, we can also express this as $3 \leq m \leq k+1$. When $n = 2k+1$, we find $3 \leq m \leq k+2$. Again, according to Lemma 5.2.14, for fixed values of m and n, all subgraphs that meet these criteria are odd-adjacent and thus belong to a common connected component of Γ^m.
Next, we consider subgraphs that do not contain both nodes s_{n-1} and s_n. When selecting the node labeled s_0, we must choose $m-1$ other isolated nodes from the set of nodes labeled $s_2, \dots, s_n$. If $2(m-1)-1 \leq n-3 \Leftrightarrow m \leq \frac{n}{2}$, then all isolated nodes of the subgraph can be selected from $s_0, \dots, s_{n-2}$. Therefore, all selected subgraphs, including those containing either s_{n-1} or s_n, are odd-adjacent, and the corresponding vertices in Γ^m are contained in a common connected component. If $n-5 < 2(m-2)-1 \leq n-4 \Leftrightarrow \frac{n}{2} < m \leq \frac{n+1}{2}$, we can find up to two subdiagrams of type $\mathtt{A}_1^m$ that satisfy our conditions. For $n = 2k$, we get $k < m \leq k + \frac{1}{2}$. Since $m \in \mathbb{Z}$, this implies that no subdiagram of type $\mathtt{A}_1^m$ meets our conditions. In the case where $n = 2k+1$, we get $k + \frac{1}{2} < m \leq k+1 \Leftrightarrow m = k+1$. Here, we identify two subdiagrams that fulfill the requirements: One spanned by $s_0, s_2, s_4, \dots, s_{n-1}$ and the other by $s_0, s_2, s_4, \dots, s_{n-3}, s_n$. These two are not odd-adjacent in $\Gamma_{\widetilde{\mathtt{B}}_n}$, meaning they

each constitute a separate connected component in Γ^m.
By considering both cases, we can count the number of conjugacy classes $\mathrm{cc}_2(W_{\widetilde{\mathtt{B}}_n}, \mathtt{A}_1^m)$ of $W_{\widetilde{\mathtt{B}}_n}$ arising from subgroups of type $\mathtt{A}_1^m$ as:

$$\begin{aligned} n = 2k: \qquad \mathrm{cc}_2(W_{\widetilde{\mathtt{B}}_n}, \mathtt{A}_1^m) &= \sum_{m=2}^{k+1} 1 + \sum_{m=2}^{k-1} 1 + \sum_{m=3}^{k+1} 1 + 2 + \sum_{m=2}^{k} 1 \\ &= k + k - 2 + k - 1 + 2 + k - 1 = 4k - 2; \\ n = 2k+1: \qquad \mathrm{cc}_2(W_{\widetilde{\mathtt{B}}_n}, \mathtt{A}_1^m) &= \sum_{m=2}^{k+1} 1 + \sum_{m=2}^{k} 1 + \sum_{m=3}^{k+2} 1 + 2 + \sum_{m=2}^{k} 1 \\ &= k + k - 1 + k + 2 + k - 1 = 4k. \end{aligned}$$

Subdiagrams of type $\mathtt{A}_1^{m-i} \sqcup \mathtt{B}_i$*:*
We have already counted the connected components of Γ^m related to subgraphs of type $\mathtt{A}_1^m$ and $\mathtt{B}_m$ above. Therefore, we now focus on the case $i \neq 0$ and $m > i$, which implies $m \geq 3$. According to Lemma 5.6.1, $\Gamma_{\widetilde{\mathtt{B}}_n}$ contains subgraphs of type $\mathtt{B}_i$ for $i \in \{2, \ldots, n\}$. For the subdiagrams of type $\mathtt{A}_1^{m-i} \sqcup \mathtt{B}_i$ that we are examining now, we are interested in those of them that are spanned by the nodes labeled $s_0, \ldots, s_{i-1}$ for $i \leq n-2$. Next, we must choose $m-i$ isolated nodes from $s_{i+1}, \ldots, s_n$ to form a subgraph of type $\mathtt{A}_1^{m-i} \sqcup \mathtt{B}_i$. To simplify the counting of connected components in Γ^m, we differentiate between three cases:
Case 1: The subgraph of type $\mathtt{A}_1^{m-i} \sqcup \mathtt{B}_i$ is formed using only the nodes labeled $s_0, \ldots, s_{n-2}$. Note that in this scenario, we will not use both nodes labeled s_{n-1} and s_n together in the subgraph of type $\mathtt{A}_1^{m-i}$. We place $\mathtt{B}_i$ at the nodes labeled $s_0, \ldots, s_{i-1}$. To identify $m-i$ isolated nodes that span a subdiagram of type $\mathtt{A}_1^{m-i}$, we will require a path subgraph with $2(m-i)$ nodes from $\Gamma_{\widetilde{\mathtt{B}}_n}$. This implies $i + 2(m-i) = 2m - i \leq n-1$. Combining this with $m - i \geq 1$, we derive $2 \leq i \leq n-3$ and $3 \leq m \leq \frac{n-1+i}{2}$. If we substitute $n = 2k$, we obtain $2 \leq i \leq 2k-3$ and $3 \leq m \leq k + \frac{i-1}{2}$. For $n = 2k+1$, this gives $2 \leq i \leq 2k-2$ and $3 \leq m \leq k + \frac{i}{2}$. Finally, we need to determine the number of connected components of Γ^m that are spanned by vertices corresponding to subgraphs of type $\mathtt{A}_1^{m-i} \sqcup \mathtt{B}_i$. Lemma 5.2.14 shows that for fixed values of m and i, all subdiagrams of type $\mathtt{A}_1^{m-i} \sqcup \mathtt{B}_i$ satisfying the conditions mentioned in this case are odd-adjacent. Therefore, they all belong to a common connected component of Γ^m.
Case 2: The subgraph of type $\mathtt{A}_1^{m-i} \sqcup \mathtt{B}_i$ cannot be spanned by only using the nodes labeled $s_0, \ldots, s_{n-2}$ and does not contain both nodes labeled s_{n-1} and s_n.
In other words, the subdiagram cannot be spanned by the nodes $s_0, \ldots, s_{n-2}$ and requires one of the nodes s_{n-1} or s_n. As in case 1, we require the i nodes labeled $s_0, \ldots, s_{i-1}$ to span a subgraph of type $\mathtt{B}_i$, along with additional $2(m-i)$ nodes in a path subgraph for $m-i$ isolated nodes for $\mathtt{A}_1^{m-i}$. Consequently, case 2 only occurs when $i + 2(m-i) = n \Leftrightarrow 2m - i = n$. Given $m - i \geq 1$, it follows $2 \leq i \leq n-2$. Furthermore, the solutions of $2m - i = n$ depend on the parity of n: If $n = 2k$, then i must be even. If $n = 2k+1$, then i must be odd. To determine the number of connected components of Γ^m that are spanned by vertices discussed in this case, we note the following: For $3 \leq i \leq n-2$ and i even when $n = 2k$, resp. i odd for $n = 2k+1$, we can identify two subdiagrams of $\Gamma_{\widetilde{\mathtt{B}}_n}$ that satisfy the conditions of this case. Specifically, they are spanned by the nodes labeled $s_0, \ldots, s_{i-1}, s_{i+1}, \ldots, s_{n-3}, s_{n-1}$ and $s_0, \ldots, s_{i-1}, s_{i+1}, \ldots, s_{n-3}, s_n$.

Note that $s_{i+1+2(m-i)-4} = s_{2m-i-3} = s_{n-3}$. These two subdiagrams are not odd-adjacent in $\Gamma_{\widetilde{\mathtt{B}}_n}$ since both nodes labeled s_{n-1} and s_n have degree 1 and are adjacent to the node labeled s_{n-2}. Therefore, the vertices of Γ^m obtained from these subdiagrams each form a separated connected component.

Case 3: The subgraph of type $\mathtt{A}_1^{m-i} \sqcup \mathtt{B}_i$ contains the nodes labeled s_{n-1} and s_n.

Since $i \neq 0$, this implies that $m \geq 4$, $m - i \geq 2$, and $i \leq n-2$. As above, we place the subgraph of type $\mathtt{B}_i$ at the nodes labeled $s_0, \ldots, s_{i-1}$. Additionally, we want to select $m-i-2$ isolated nodes from the set labeled $s_i, \ldots, s_{n-3}$, and we will also include s_{n-1} and s_n as isolated nodes to form a subdiagram of type $\mathtt{A}_1^{m-i}$. This leads us to $i+2(m-i-2) \leq n-2 \Leftrightarrow 2m-i \leq n+2$. From this, we obtain the bounds $2 \leq i \leq n-2$ and $i+2 \leq m \leq \frac{n+2+i}{2}$. By substituting $n = 2k$, we obtain $i+2 \leq m \leq k+1+\frac{i}{2}$ for the second constraint. Similarly, for $n = 2k+1$, we get $i+2 \leq m \leq k+1+\frac{i+1}{2}$. Again, as Lemma 5.2.14 shows, for fixed values of n, m, all the subgraphs discussed in this case are odd-adjacent in $\Gamma_{\widetilde{\mathtt{B}}_n}$ and therefore contained in a common connected component of Γ^m.

In summary, we can count the conjugacy classes $\mathrm{cc}_2(W_{\widetilde{\mathtt{B}}_n}, \mathtt{A}_1^{m-i} \sqcup \mathtt{B}_i)$ of $W_{\widetilde{\mathtt{B}}_n}$ that correspond to subgroups of type $\mathtt{A}_1^{m-i} \sqcup \mathtt{B}_i$ as:

$$\begin{aligned} n = 2k: \qquad \mathrm{cc}_2(W_{\widetilde{\mathtt{B}}_n}, \mathtt{A}_1^{m-i} \sqcup \mathtt{B}_i) &= \sum_{i=2}^{2k-3} \sum_{m=i+1}^{k+\frac{i-1}{2}} 1 + \sum_{i=1}^{k-1} 2 + \sum_{i=2}^{2k-2} \sum_{m=i+2}^{k+1+\frac{i}{2}} 1 \\ &= (k-2)(k-1) + 2(k-1) + (k-1)^2; \\ n = 2k+1: \qquad \mathrm{cc}_2(W_{\widetilde{\mathtt{B}}_n}, \mathtt{A}_1^{m-i} \sqcup \mathtt{B}_i) &= \sum_{i=2}^{2k-2} \sum_{m=i+1}^{k+\frac{i}{2}} 1 + \sum_{i=1}^{k-1} 2 + \sum_{i=2}^{2k-1} \sum_{m=i+2}^{k+1+\frac{i+1}{2}} 1 \\ &= (k-1)^2 + 2(k-1) + k(k-1). \end{aligned}$$

Subdiagrams of type $\mathtt{D}_{2j} \sqcup A_1^{m-2j}$*:*

Since we already counted the connected components of Γ^m of type A_1^m above, we will focus only on the case where $j \neq 0$ here, which requires $m \geq 4$. From our previous observations in Lemma 5.6.1, we know that $\Gamma_{\widetilde{\mathtt{B}}_n}$ contains subgraphs of type $\mathtt{D}_m$ for $m \leq n$. Therefore, we have $j \leq \frac{n}{2} = k$ for $n = 2k$ and $j \leq \frac{n-1}{2} = k$ for $n = 2k+1$. Note that two subgraphs of the types $\mathtt{A}_1^{m-2j} \sqcup \mathtt{D}_{2j}$ and $\mathtt{A}_1^{m'-2j'} \sqcup \mathtt{D}_{2j'}$ can only be odd-adjacent if $m = m'$ and $j = j'$. This is because they are not isomorphic as diagrams otherwise. This observation allows us to count the connected components of Γ^m for different values of j separately. In doing so, we will distinguish between two cases:

Case 1: The node labeled s_0 in $\Gamma_{\widetilde{\mathtt{B}}_n}$ is not included in a vertex of Γ^m of the connected component under consideration.

This case distinction is possible because subgraphs of $\Gamma_{\widetilde{\mathtt{B}}_n}$ that include the node labeled s_0 cannot be odd-adjacent to subgraphs that do not contain it. This is because the node has degree 1 and is only adjacent to the node labeled s_1 by an edge labeled 4. Therefore, in this case, we are only searching for subgraphs of type $\mathtt{D}_{2j} \sqcup \mathtt{A}_1^{m-2j}$ within the graph spanned by $s_1, \ldots, s_n$, which equals the diagram $\Gamma_{\mathtt{D}_n}$. Given that $j \neq 0$, we first consider the subgraph of type $\mathtt{D}_{2j}$. Due to the structure of $\Gamma_{\widetilde{\mathtt{B}}_n}$, this subgraph can only be spanned by the nodes labeled $s_{n-2j+1}, \ldots, s_{n-1}, s_n$. Compare Figure 5.20. For a vertex of Γ^m, we need to select $m-2j$ feasible isolated nodes from the remaining

nodes labeled $s_1, \ldots, s_{n-2j}$. Note that we cannot choose the node labeled s_{n-2j} since it is odd-adjacent to s_{n-2j+1}. Consequently, we can select the isolated nodes from the set labeled $s_1, \ldots, s_{n-2j-1}$. To ensure that all the $m-2j$ nodes are isolated from each other, we require a total of $2(m-2j)-1$ nodes from $s_1, \ldots, s_{n-2j-1}$. From this, we derive that $2(m-2j)-1 \leq n-2j-1 \Leftrightarrow 2m-2j \leq n \Leftrightarrow m \leq \frac{n+2j}{2}$. For $n=2k$, we can rewrite this as $m \leq k+j$. For $n=2k+1$, we obtain $m \leq k+j+\frac{1}{2}$. However, since $k, j \in \mathbb{Z}$, both cases yield the same upper bound. Note that we explicitly allow $m=2j$, meaning we also consider subgraphs of type $\mathtt{D}_{2j}$ as a subclass of $\mathtt{D}_{2j} \sqcup \mathtt{A}_1^{m-2j}$. Finally, it remains to quantify the number of connected components of Γ^m defined by the vertices corresponding to these subgraphs of $\Gamma_{\mathtt{B}_n}$. According to Lemma 5.2.14, all vertices defined by the subgraphs of the same type and size that we discussed above are odd-adjacent. Therefore, Γ^m has one connected component of type $\mathtt{D}_{2j} \sqcup A_1^{m-2j}$ for every $2 \leq j \leq k$, $m \leq k+j$ in this case.

Case 2: The node of $\Gamma_{\widetilde{\mathtt{B}}_n}$ labeled s_0 is contained in all vertices of Γ^m within the connected component under consideration.

Observe that case 1 and case 2 together encompass all possible connected components of Γ^m. As in case 1, we have $j \neq 0$, and a subgraph of type $\mathtt{D}_{2j}$ can only be spanned by the nodes labeled $s_{n-2j+1}, \ldots, s_{n-1}, s_n$. Consequently, we need to choose $m-2j$ feasible isolated nodes from the remaining nodes labeled $s_0, \ldots, s_{n-2j}$. However, we cannot select the node labeled s_{n-2j} since it is odd-adjacent to s_{n-2j+1}. Additionally, since we must include the node s_0, we cannot choose the node labeled s_1. Together, they would form a subgraph of type $\mathtt{B}_2$ and subgraphs of the form $\mathtt{D}_{2j} \sqcup \mathtt{A}_1^{m-2j-i} \sqcup \mathtt{B}_i$ will be discussed below. Not including the node s_1 leads to two implications: First, it implies that $2j \leq n-1$, ensuring that the subgraph of type $\mathtt{D}_{2j}$ does not contain the node labeled s_1. Second, after selecting the isolated node s_0, one must choose $m-2j-1$ feasible isolated nodes from $s_2, \ldots, s_{n-2j-1}$. From this, we derive $2(m-2j-1)-1 \leq n-2j-2 \Leftrightarrow 2m-2j-1 \leq n \Leftrightarrow m \leq \frac{n+2j+1}{2}$. Substituting $n=2k$ and using $k, j \in \mathbb{Z}$, we obtain $m \leq k+j$. Moreover, for the case $n=2k+1$, we find that $m \leq k+j+1$. As above, applying Lemma 5.2.14 shows that all vertices defined by the subgraphs of the same type and size described above are odd-adjacent. Consequently, Γ^m in this case has one connected component of type $\mathtt{D}_{2j} \sqcup A_1^{m-2j}$ for each $2 \leq j \leq \frac{n-1}{2}$, with $m \leq k+j$ for $n=2k$, or $m \leq k+j+1$ for $n=2k+1$.

Summarizing our results for both cases, we can count the conjugacy classes $\mathrm{cc}_2(W_{\widetilde{\mathtt{B}}_n}, \mathtt{D}_{2j} \sqcup \mathtt{A}_1^{m-2j})$ of $W_{\widetilde{\mathtt{B}}_n}$ obtained from subgroups of type $\mathtt{D}_{2j} \sqcup A_1^{m-2j}$ as:

$$n=2k: \qquad \mathrm{cc}_2(W_{\widetilde{\mathtt{B}}_n}, \mathtt{D}_{2j} \sqcup \mathtt{A}_1^{m-2j}) = \sum_{j=2}^{k} \sum_{m=2j}^{k+j} 1 + \sum_{j=2}^{k-1} \sum_{m=2j+1}^{k+j} 1 = (k-1)^2;$$

$$n=2k+1: \qquad \mathrm{cc}_2(W_{\widetilde{\mathtt{B}}_n}, \mathtt{D}_{2j} \sqcup \mathtt{A}_1^{m-2j}) = \sum_{j=2}^{k} \sum_{m=2j}^{k+j} 1 + \sum_{j=2}^{k} \sum_{m=2j+1}^{k+j+1} 1 = k(k-1).$$

Subdiagrams of type $\mathtt{D}_{2j} \sqcup \mathtt{A}_1^{m-2j-i} \sqcup \mathtt{B}_i$*:*

Since we already counted the numbers of conjugacy classes corresponding to subgraphs of type $\mathtt{D}_{2j} \sqcup \mathtt{A}_1^{m-2j}$, $\mathtt{A}_1^{m-i} \sqcup \mathtt{B}_i$, $\mathtt{B}_m$, and $\mathtt{A}_1^m$ above, we will assume $i \geq 2$, $j \geq 2$, and therefore $m \geq 6$. Based on our observations regarding subgraphs of type $\mathtt{D}_{2j}$ above,

this implies $2 \leq j \leq \frac{n-2}{2}$. Let us consider subgraphs of type $\mathtt{D}_{2j}$ first. From the structure of $\Gamma_{\widetilde{\mathtt{B}}_n}$, we determine that a subgraph of type $\mathtt{D}_{2j}$ is spanned by the nodes labeled $s_{n-2j+1}, \ldots, s_{n-1}, s_n$. Out of the remining free nodes $s_0, \ldots, s_{n-2j}$, we can select nodes from $s_0, \ldots, s_{n-2j-1}$ to span subgraphs of type $\mathtt{B}_i$ and $\mathtt{A}_1^{m-2j-i}$ without selecting odd-adjacent nodes to the subgraph of type $\mathtt{D}_{2j}$. Thus, for $2 \leq i \leq n-2j$, we can find a subgraph of type $\mathtt{B}_i$ spanned by the nodes labeled $s_0, \ldots, s_{i-1}$. The nodes $s_{i+1}, \ldots, s_{n-2j-1}$ are then available for selection for the subgraphs of type $\mathtt{A}_1^{m-2j-i}$. To ensure we choose non-adjacent nodes for the subgraphs of type $\mathtt{A}_1^{m-2j-i}$, we derive the following boundary condition on m: $2(m-2j-i)-1 \leq n-2j-i-1 \Leftrightarrow m \leq \frac{n+i}{2}+j$. For $n=2k$, this can be expressed as $m \leq k+j+\frac{i}{2}$, whereas for $n=2k+1$, it becomes $m \leq k+j+\frac{i+1}{2}$. Again, it follows from Lemma 5.2.14 that all vertices of Γ^m defined by subgraphs of type $\mathtt{D}_{2j} \sqcup \mathtt{A}_1^{m-2j-i} \sqcup \mathtt{B}_i$ with fixed $i, j \in \mathbb{Z}$ are odd-adjacent. Consequently, for every $2 \leq j \leq \frac{n-2}{2}$ and for all $2 \leq i \leq n-2j$, Γ^m contains one connected coponent of vertices of type $\mathtt{D}_{2j} \sqcup \mathtt{A}_1^{m-2j-i} \sqcup \mathtt{B}_i$. Therefore, we can derive the number of conjugacy classes $\mathrm{cc}_2(W_{\widetilde{\mathtt{B}}_n}, \mathtt{D}_{2j} \sqcup \mathtt{A}_1^{m-2j-i} \sqcup \mathtt{B}_i)$ of $W_{\widetilde{\mathtt{B}}_n}$ obtained from subgroups of type $\mathtt{D}_{2j} \sqcup \mathtt{A}_1^{m-2j-i} \sqcup \mathtt{B}_i$, as:

$$\begin{aligned}
n=2k: \quad \mathrm{cc}_2(W_{\widetilde{\mathtt{B}}_n}, \mathtt{D}_{2j} \sqcup \mathtt{A}_1^{m-2j-i} \sqcup \mathtt{B}_i) &= \sum_{j=2}^{k-1} \left(\sum_{i=1}^{k-j} \sum_{m=2i+2j}^{k+i+j} 1 + \sum_{i=1}^{k-j-1} \sum_{m=2i+2j+1}^{k+j+i} 1 \right) \\
&= (k-2)(k-1)\frac{2k-3}{6}; \\
n=2k+1: \quad \mathrm{cc}_2(W_{\widetilde{\mathtt{B}}_n}, \mathtt{D}_{2j} \sqcup \mathtt{A}_1^{m-2j-i} \sqcup \mathtt{B}_i) &= \sum_{j=2}^{k-1} \left(\sum_{i=1}^{k-j} \sum_{m=2i+2j}^{k+i+j} 1 + \sum_{i=1}^{k-j} \sum_{m=2i+2j+1}^{k+j+i+1} 1 \right) \\
&= k(k-2)\frac{k-1}{3}.
\end{aligned}$$

Sum of all conjucagy classes:
Finally, we can derive the number of conjugacy classes of a Coxeter group of type $W_{\widetilde{\mathtt{B}}_n}$ as:

$$\begin{aligned}
\mathrm{cc}_2(W_{\widetilde{\mathtt{B}}_n}) = 2 &+ \mathrm{cc}_2(W_{\widetilde{\mathtt{B}}_n}, \mathtt{B}_m) + \mathrm{cc}_2(W_{\widetilde{\mathtt{B}}_n}, \mathtt{A}_1^m) + \mathrm{cc}_2(W_{\widetilde{\mathtt{B}}_n}, \mathtt{A}_1^{m-i} \sqcup \mathtt{B}_i) \\
&+ \mathrm{cc}_2(W_{\widetilde{\mathtt{B}}_n}, \mathtt{D}_{2j} \sqcup \mathtt{A}_1^{m-2j}) + \mathrm{cc}_2(W_{\widetilde{\mathtt{B}}_n}, \mathtt{D}_{2j} \sqcup \mathtt{A}_1^{m-2j-i} \sqcup \mathtt{B}_i);
\end{aligned}$$

$$\begin{aligned}
n=2k: \quad \mathrm{cc}_2(W_{\widetilde{\mathtt{B}}_n}) &= 2 + 2k + 4k - 2 + (k-2)(k-1) + 2(k-1) + (k-1)^2 \\
&\quad + (k-1)^2 + (k-2)(k-1)\frac{2k-3}{6} \\
&= \frac{1}{3}k^3 + \frac{3}{2}k^2 + \frac{19}{6}k + 1; \\
n=2k+1: \quad \mathrm{cc}_2(W_{\widetilde{\mathtt{B}}_n}) &= 2 + 2k + 1 + 4k + (k-1)^2 + 2(k-1) + k(k-1) \\
&\quad + k(k-1) + k(k-2)\frac{k-1}{3} \\
&= \frac{1}{3}k^3 + 2k^2 + \frac{14}{3}k + 2.
\end{aligned}$$

□

We continue our proof of Theorem 5.4.4 for $W_{\widetilde{\mathtt{C}}_n}$. As a preparation, we first prove:

Lemma 5.6.3. *Consider the affine Coxeter group $\widetilde{\mathtt{C}}_n$ with diagram $\Gamma_{\widetilde{\mathtt{C}}_n}$. Then, all vertices of the m-odd-graph Γ^m are of the form*

$$\mathtt{B}_i \sqcup \mathtt{A}_1^j,$$

with $i, j \in \mathbb{N}_0$.

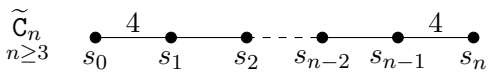

FIGURE 5.21. Coxeter diagram of $\widetilde{\mathtt{C}}_n$.

PROOF. Similar to Lemma 5.6.1 above, we will refer to the nodes of $\Gamma_{\widetilde{\mathtt{C}}_n}$ by their indexed generator, enumerating from left to right as illustrated in Figure 5.21. Notice that $\Gamma_{\widetilde{\mathtt{C}}_n}$ has $n+1$ nodes of degree 2. Among these, the nodes s_0 and s_1, as well as s_{n-1} and s_n, are adjacent through an edge labeled 4, while all other edges are labeled 3. Subgraphs spanned by the nodes labeled $s_0, s_1, \ldots, s_\ell$ with $\ell \in \{2, \ldots, n-1\}$ are diagrams of type $\mathtt{B}_{\ell+1}$. Due to the symmetry of $\Gamma_{\widetilde{\mathtt{C}}_n}$, the subdiagrams spanned by the nodes $s_{n-\ell}, s_{n-\ell+1}, \ldots, s_{n-1}, s_n$ are also diagrams of type $\mathtt{B}_{\ell+1}$. Furthermore, nodes that are pairwise non-adjacent form collections of subdiagrams of type $\mathtt{A}_1$. Regarding this, notice that nodes of $\Gamma_{\widetilde{\mathtt{C}}_n}$ are non-adjacent if and only if the distance of their index numbers is greater than 1. From these observations, it follows that one can find subdiagrams of the form $\mathtt{B}_i \sqcup \mathtt{A}_1^j$ where $j \in \mathbb{N}_0$, $i \in \mathbb{N}_0 \setminus \{1\}$ within $\Gamma_{\widetilde{\mathtt{C}}_n}$. Additionally, $\Gamma_{\widetilde{\mathtt{C}}_n}$ does not contain any other Coxeter diagrams of inc-type. Therefore, the subdiagrams described above are the only ones within this graph that yield irreducible Coxeter groups with nontrivial center and, consequently, the only vertices of Γ^m. □

PROOF OF THEOREM 5.4.4 FOR $\widetilde{\mathtt{C}}_n$. We can immediately observe from the structure of $\Gamma_{\widetilde{\mathtt{C}}_n}$ that Γ^1 has 3 connected components for all groups of type $\widetilde{\mathtt{C}}_n$. Compare also Figure 5.21.
Following the method we used for groups of type $\widetilde{\mathtt{B}}_n$ above, we now compute the number of connected components of Γ^m with $m \geq 4$ for the different types of subgraphs of Γ, as determined in Lemma 5.6.3 above.

Subdiagrams of type $\mathtt{B}_m$:
We find that the diagram $\Gamma_{\widetilde{\mathtt{C}}_n}$ contains two subdiagrams of type $\mathtt{B}_m$. These are spanned by the nodes labeled $s_0, s_1, \ldots, s_{m-1}$ and $s_{n-m+1}, s_{m-n+2}, \ldots, s_{n-1}, s_n$ for $2 \leq m \leq n$. Since they differ in more than one vertex, these subdiagrams are not odd-adjacent and yield two isolated vertices in Γ^m. Consequently, we obtain:

$$n = 2k: \qquad \mathrm{cc}_2(W_{\widetilde{\mathtt{C}}_n}, \mathtt{B}_m) = \sum_{i=2}^{2k} 2 = 2(2k-1) = 4k-2;$$

$$n = 2k+1: \qquad \mathrm{cc}_2(W_{\widetilde{\mathtt{C}}_n}, \mathtt{B}_m) = \sum_{i=2}^{2k+1} 2 = 2(2k) = 4k.$$

Subdiagrams of type $\mathtt{A}_1^m$*:*
First, observe that the nodes labeled s_0, s_n in the diagram Γ are not odd-adjacent to any other node of $\Gamma_{\widetilde{\mathtt{C}}_n}$. This means that all subdiagrams of type $\mathtt{A}_1^m$ containing either s_0, s_1, both simultaneously, or neither, are only odd-adjacent to other subdiagrams of the same type that also include s_0, s_1, both simultaneously, or neither. Using Lemma 5.2.14, we conclude that all vertices of Γ^m corresponding to subdiagrams of type $\mathtt{A}_1^m$ that contain the node labeled s_0, or s_1, both simultaneously, or neither, are contained in a common connected component of the graph.
Now, recall that $\Gamma_{\widetilde{\mathtt{C}}_n}$ contains $n+1$ nodes. To identify a subgraph of type $\mathtt{A}_1^m$, we need at least $2m-1$ nodes of $\Gamma_{\widetilde{\mathtt{C}}_n}$. If $2m-1 \leq n-1$, it is possible to find subgraphs of type $\mathtt{A}_1^m$ that do not include the nodes labeled s_0 and s_n. Thus, for $m \leq \frac{n}{2}$, the graph Γ^m has four connected components for subgraphs of this type. When $2m-1 = n \Leftrightarrow m = \frac{n+1}{2}$, subgraphs of type $\mathtt{A}_1^m$ must contain at least one of the nodes labeled s_0 and s_n. As a result, Γ^m will then have three connected components for subgraphs of this type. If $2m-1 = n+1 \Leftrightarrow m = \frac{n+2}{2}$, subgraphs of type $\mathtt{A}_1^m$ will include both nodes labeled s_0 and s_n. In this case, Γ^m will have only one connected component containing vertices corresponding to subgraphs of this type. In conclusion, we can count the number of conjugacy classes $\mathrm{cc}_2(W_{\widetilde{\mathtt{C}}_n}, \mathtt{A}_1^m)$ of $W_{\widetilde{\mathtt{C}}_n}$ obtained from subgroups of type $\mathtt{A}_1^m$ as follows:

$$n = 2k: \qquad \mathrm{cc}_2(W_{\widetilde{\mathtt{C}}_n}, \mathtt{A}_1^m) = \sum_{i=2}^{k} 4 + 1 = 4k - 3;$$

$$n = 2k+1: \qquad \mathrm{cc}_2(W_{\widetilde{\mathtt{C}}_n}, \mathtt{A}_1^m) = \sum_{i=2}^{k} 4 + 3 = 4k - 1.$$

Subdiagrams of type $\mathtt{A}_1^{m-i} \sqcup \mathtt{B}_i$*:*
First, note that subdiagrams of type $\mathtt{A}_1^{m-i} \sqcup \mathtt{B}_i$, where $i \neq 0$, require $m \geq 3$. Additionally, a subgraph of type $\mathtt{A}_1^{m-i} \sqcup \mathtt{B}_i$ requires $2m-i$ nodes from the diagram $\Gamma_{\widetilde{\mathtt{C}}_n}$. Since $\Gamma_{\widetilde{\mathtt{C}}_n}$ has $n+1$ nodes, it follows that $2m-i \leq n+1$. Now, suppose $m \geq n+1$. From this, we get $2n+2-i \leq n+1 \Leftrightarrow n+1 \leq i$. This leads to a contradiction with our earlier observations about subgraphs of type $\mathtt{B}_m$. Consequently, we conclude that $m \leq n$. From this, it also follows that $i \leq n-1$, since $i < m \leq n$. Recall that we can identify two not odd-adjacent subdiagrams of type $\mathtt{B}_i$ for $i \in \{2, \ldots, n-1\}$. These subdiagrams are spanned by the nodes $s_0, s_1, \ldots, s_{i-1}$ and $s_{n-i+1}, s_{n-i+2}, \ldots, s_n$. If $i = n-1$, we can construct two non odd-adjacent subdiagrams of type $\mathtt{A}_1 \sqcup \mathtt{B}_{n-1}$, spanned by the nodes labeled $s_0, s_1, \ldots, s_{n-2}, s_n$ and $s_0, s_2, s_3, \ldots, s_n$. This results in two connected components of Γ^m. For $i \in \{2, \ldots, n-2\}$, it follows $m \leq n-1$, since $2m-i \leq n+1$. If we then further have $2m-i \leq n \Leftrightarrow m \leq \frac{n+i}{2}$, we can find subgraphs of type $\mathtt{A}_1^{m-i} \sqcup \mathtt{B}_i$ such that the set of spanning nodes may either include both nodes of degree 1 of $\Gamma_{\widetilde{\mathtt{C}}_n}$ or exclude them: We can locate a subdiagram of type $\mathtt{B}_i$ at $s_0, s_1, \ldots, s_{i-1}$ or at $s_{n-i+1}, s_{n-i+2}, \ldots, s_n$. In addition, we find $m-i$ isolated nodes that span a subdiagram of type $\mathtt{A}_1^{m-i}$. These nodes are taken from the sets $A := \{s_{i+1}, \ldots, s_n\}$, resp. $B := \{s_0, \ldots, s_{n-i-1}\}$. Since $|A| = |B| = n-i$ and given that $n-i \geq 2m-2i > 2(m-i)-1$, we can also find $m-i$ isolated nodes as a subset of $A \setminus \{s_n\}$, resp. $B \setminus \{s_0,\}$. Consequently, no node of degree 1 is spanning the subgraph. Now, observe that subdiagrams of type $\mathtt{A}_1^{m-i} \sqcup \mathtt{B}_i$, which do not contain a degree-1-node in their $\mathtt{A}_1^{m-i}$-part, are only odd-adjacent to subdiagrams that

are not containing it as well. Furthermore, subdiagrams of type $\mathtt{A}_1^{m-i} \sqcup \mathtt{B}_i$ that include a degree-1-node in the $\mathtt{A}_1^{m-i}$-part are only odd-adjacent to subdiagrams that also contain a degree-1-node. With Lemma 5.2.14, we observe that all subdiagrams of type $\mathtt{A}_1^{m-i} \sqcup \mathtt{B}_i$ that contain the same subdiagram of type $\mathtt{B}_i$, and that either do not contain (resp. do contain) a degree-1-node in their $\mathtt{A}_1^{m-i}$-part, are contained in a common connected component of Γ^m.
Otherwise, if $\frac{n+i}{2} < m \leq n-1$, we again find two not odd-adjacent subdiagrams of type $\mathtt{B}_i$ as mentioned before. In this case, the $\mathtt{A}_1^{m-i}$-part of a subdiagram of type $\mathtt{A}_1^{m-i} \sqcup \mathtt{B}_i$ is always spanned by a set of nodes containing the second node of Γ with degree 1. Invoking Lemma 5.2.14 once more, we conclude that two connected components of Γ^m are spanned by vertices derived from these subdiagrams. In total, this proves that there are 4 connected components of Γ^m with vertices representing subdiagrams of type $\mathtt{A}_1^{m-i} \sqcup \mathtt{B}_i$. Thus, we can count the number of conjugacy classes $\mathrm{cc}_2(W_{\widetilde{\mathtt{C}}_n}, \mathtt{A}_1^{m-i} \sqcup \mathtt{B}_i)$ of $W_{\widetilde{\mathtt{C}}_n}$ that arise from subgroups of type $\mathtt{A}_1^{m-i} \sqcup \mathtt{B}_i$ as follows:

$$
\begin{aligned}
n = 2k: \qquad \mathrm{cc}_2(W_{\widetilde{\mathtt{C}}_n}, \mathtt{A}_1^{m-i} \sqcup \mathtt{B}_i) &= 2 + \sum_{i=2}^{2k-2} \left(\sum_{m=i+1}^{k+\frac{i}{2}} 4 \right) + \sum_{i=2}^{2k-2} \left(\sum_{m=k+\frac{i}{2}+1}^{k+\frac{i+1}{2}} 2 \right) \\
&= 2 + \sum_{i=1}^{k-1} \left(\sum_{m=2i+1}^{k+i} 4 \right) + \sum_{i=1}^{k-2} \left(\sum_{m=2i+2}^{k+i} 4 \right) + \sum_{i=1}^{k-2} 2 \\
&= 4k^2 - 6k + 2; \\
n = 2k+1: \qquad \mathrm{cc}_2(W_{\widetilde{\mathtt{C}}_n}, \mathtt{A}_1^{m-i} \sqcup \mathtt{B}_i) &= 2 + + \sum_{i=2}^{2k-1} \left(\sum_{m=i+1}^{k+\frac{i+1}{2}} 4 \right) + \sum_{i=2}^{2k-1} \left(\sum_{m=k+\frac{i+1}{2}+1}^{k+1+\frac{i}{2}} 2 \right) \\
&= 2 + \sum_{i=1}^{k-1} \left(\sum_{m=2i+1}^{k+i} 4 \right) + \sum_{i=1}^{k-1} \left(\sum_{m=2i+2}^{k+i+1} 4 \right) + \sum_{i=1}^{k-1} 2 \\
&= 4k^2 - 2k.
\end{aligned}
$$

Sum of all conjucagy classes:
Eventually, we can calculate the number of conjugacy classes of a Coxeter group of type $W_{\widetilde{\mathtt{C}}_n}$ for $n \geq 4$ as follows:

$$
\begin{aligned}
& \mathrm{cc}_2(W_{\widetilde{\mathtt{C}}_n}) = 3 + \mathrm{cc}_2(W_{\widetilde{\mathtt{C}}_n}, \mathtt{B}_m) + \mathrm{cc}_2(W_{\widetilde{\mathtt{C}}_n}, \mathtt{A}_1^m) + \mathrm{cc}_2(W_{\widetilde{\mathtt{C}}_n}, \mathtt{A}_1^{m-i} \sqcup \mathtt{B}_i); \\
n = 2k: \qquad & \mathrm{cc}_2(W_{\widetilde{\mathtt{C}}_n}) = 3 + 2(2k-1) + 4k - 3 + 4k^2 - 6k + 2 = 4k^2 + 2k; \\
n = 2k+1: \qquad & \mathrm{cc}_2(W_{\widetilde{\mathtt{C}}_n}) = 3 + 2(2k) + 4k - 1 + 4k^2 - 2k = 4k^2 + 6k + 2.
\end{aligned}
$$

□

We proceed with the proof of Theorem 5.4.4 by deriving the formula for groups of type $\widetilde{\mathtt{D}}_n$. As a preparation, we show first:

Lemma 5.6.4. *Consider the affine Coxeter group $\widetilde{\mathtt{D}}_n$ with diagram $\Gamma_{\widetilde{\mathtt{D}}_n}$. Then, all vertices of the m-odd-graph Γ^m are of the form*

$$\mathtt{D}_{2i} \sqcup \mathtt{A}_1^{m-2i-2j} \sqcup \mathtt{D}_{2j},$$

with $i, j \in \mathbb{N}_0$.

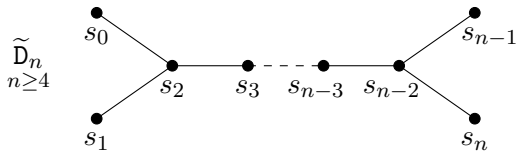

FIGURE 5.22. Coxeter diagram of $\widetilde{\mathtt{D}}_n$.

PROOF. As in Lemma 5.6.1, we refer to the nodes of $\Gamma_{\widetilde{\mathtt{D}}_n}$ by their indexed generator, enumerating them from left to right as shown in Figure 5.22. Observe that $\Gamma_{\widetilde{\mathtt{D}}_n}$ has $n+1$ nodes. The nodes s_0, s_1, s_{n-1}, s_n each have degree 1, while the nodes s_2 and s_{n-2} have degree 3. All remaining nodes having degree 2. Additionally, all edges are labeled 3. The subdiagrams spanned by the nodes $s_0, s_1, \ldots, s_\ell$ with $\ell \in \{3, \ldots, n-2\}$, are diagrams of type $\mathtt{D}_{\ell+1}$. Due to the symmetry of Γ, subdiagrams spanned by the nodes $s_{n-\ell}, s_{n-\ell+1}, \ldots, s_n$ are also of type $\mathtt{D}_{\ell+1}$. Moreover, by selecting a set of pairwise non-adjacent nodes, one can find a collection of subdiagrams of type $\mathtt{A}_1$, which form subdiagrams of type $\mathtt{A}_1^m$. Observe that two nodes $s_i, s_j \in \{s_2, \ldots, s_{n-2}\}$ are non-adjacent if the distance of their index numbers is at least two. Additionally, the nodes labeled s_0 and s_1 are not adjacent, nor are s_{n-1} and s_n. From this observation, and considering that subdiagrams of type $\mathtt{D}_{\ell+1}$ can only be vertices of Γ^m when ℓ is odd, we conclude that subdiagrams of the form $\mathtt{D}_{2i} \sqcup \mathtt{A}_1^{m-2i-2j} \sqcup \mathtt{D}_{2j}$ with $i, j \in \mathbb{N}_0$ are possible in $\Gamma_{\widetilde{\mathtt{D}}_n}$. Furthermore, note that $\Gamma_{\widetilde{\mathtt{D}}_n}$ does not contain any other Coxeter diagrams of inc-type. Therefore, subdiagrams of the form $\mathtt{D}_{2i} \sqcup \mathtt{A}_1^{m-2i-2j} \sqcup \mathtt{D}_{2j}$ with $i, j \in \mathbb{N}_0$ are indeed the only subdiagrams of $\Gamma_{\widetilde{\mathtt{D}}_n}$ that yield irreducible Coxeter groups with nontrivial center, making them the only vertices of Γ^m. □

PROOF OF THEOREM 5.4.4 FOR $\widetilde{\mathtt{D}}_n$. We can see right away from the structure of $\Gamma_{\widetilde{\mathtt{D}}_n}$ that Γ^1 is always connected, as all edge labels of $\Gamma_{\widetilde{\mathtt{D}}_n}$ are odd.
Next, we will derive the formula by counting the connected components of Γ^m for the various types of subdiagrams as given in Lemma 5.6.4. We will discuss each type of subdiagram separately below.

Subdiagrams of type $\mathtt{D}_{2i} = \mathtt{D}_m$:
As observed in Lemma 5.6.4 above, we identify subdiagrams of type $\mathtt{D}_{2i} = \mathtt{D}_m$ for m even, $4 \leq m \leq n$. When $m < n$, these subdiagrams are spanned by the nodes labeled $s_0, s_1, \ldots, s_{2i-1}$ and $s_{n-2i+1}, s_{n-2i+2}, \ldots, s_n$. Since the nodes labeled s_0, s_1, s_{n-1}, and s_n are pairwise non odd-adjacent, these two subdiagrams of type $\mathtt{D}_{2i}$ are also not odd-adjacent. In the case where $m = n$ and n is even, we find 4 not odd-adjacent subdiagrams of type $\mathtt{D}_m$. These are spanned by the nodes labeled as follows: $s_0, s_1, \ldots, s_{n-1}$, and $s_0, s_1, \ldots, s_{n-2}, s_n$, and $s_0, s_2, s_3, \ldots, s_n$, and $s_1, s_2, \ldots, s_n$. Moreover, since the nodes

of $\Gamma_{\widetilde{\mathtt{D}}_n}$ with degree 1 are pairwise not odd-adjacent, all four of these subdiagrams are also not odd-adjacent and form isolated vertices of Γ^m. Note that for n odd, we do not have inc-type subdiagrams of type $\mathtt{D}_n$. Therefore, we can count the number of connected components $\mathrm{cc}_2(W_{\widetilde{\mathtt{D}}_n}, \mathtt{D}_{2i})$ of $W_{\widetilde{\mathtt{D}}_n}$ obtained from subgroups of type $\mathtt{D}_{2i}$ as follows:

$$n = 2k: \qquad \mathrm{cc}_2(W_{\widetilde{\mathtt{D}}_n}, \mathtt{D}_{2i}) = 2 + \sum_{i=2}^{k} 2 = 2 + 2(k-1) = 2k;$$

$$n = 2k+1: \qquad \mathrm{cc}_2(W_{\widetilde{\mathtt{D}}_n}, \mathtt{D}_{2i}) = \sum_{i=2}^{k} 2 = 2(k-1) = 2k-2.$$

Subdiagrams of type $\mathtt{A}_1^m$*:*
We observed in Lemma 5.6.4 that we can identify pairwise not odd-adjacent nodes in $\Gamma_{\widetilde{\mathtt{D}}_n}$ representing subgroups of type $\mathtt{A}_1$ by selecting nodes from the set $\{s_2, \ldots, s_{n-2}\}$ that have a distance of at least 2 in their index numbers. Additionally, note that the nodes labeled s_0, s_1, and s_{n-1}, s_n, are both odd-adjacent to the same node labeled s_2, resp. s_{n-2}. Moreover, the nodes labeled s_0, s_1, resp. s_{n-1}, s_n, are not adjacent. See also Figure 5.22. It follows that the vertices of Γ^m that include the nodes s_0, s_1 or s_{n-1}, s_n are not odd-adjacent to vertices that do not contain these nodes. Consequently, to count the number of connected components of Γ^m, we can distinguish five cases:
Case 1: The subdiagram of type $\mathtt{A}_1^m$ includes the nodes labeled $\{s_0, s_1, s_{n-1}, s_n\}$. It follows immediately that $m \geq 4$ and $n \geq 4$. By selecting the four isolated nodes s_0, s_1, s_{n-1}, s_n, we can form a subdiagram of type $\mathtt{A}_1^4$. Additionally, we can choose more isolated nodes from the subset $\{s_3, \ldots, s_{n-3}\}$. While maintaining a minimum distance of index numbers of at least 2 between any two chosen nodes, we can select up to $\lceil \frac{(n-3)-2}{2} \rceil$ isolated nodes. Depending on the parity of n, this results in up to $\frac{2k-4}{2} = k-2$ isolated nodes for $n = 2k$, and similarly, up to $\frac{2k+1-5}{2} = k-2$ isolated nodes for $n = 2k+1$. Thus, it holds for $n = 2k$: $4 \leq m \leq 4 + k - 2 = k + 2$. And for $n = 2k+1$ it holds: $4 \leq m \leq 4 + k - 2$. By applying Lemma 5.2.14, we can conclude that for a fixed value of m, all vertices of Γ^m obtained from a subgraph of type $\mathtt{A}_1^m$ in case 1 are contained within a common connected component of the graph. Therefore, for both $n = 2k$ and $n = 2k+1$, the number of connected components of Γ^m in case 1 can be expressed as:

$$\mathrm{cc}_2(W_{\widetilde{\mathtt{D}}_n}, \mathtt{A}_1^m, \text{ case 1}) = \sum_{m=4}^{k+2} 1 = k - 1.$$

Case 2: The subdiagram of type $\mathtt{A}_1^m$ includes the nodes labeled $\{s_0, s_1\}$ and does not include the nodes s_{n-1} and s_n simultaneously. We select the two nodes labeled s_0 and s_1 as subdiagrams of type $\mathtt{A}_1$. Note that both nodes are adjacent to the node labeled s_2, which means we cannot find another isolated subdiagram of type $\mathtt{A}_1$ at this node. When seeking $m-2$ additional subdiagrams of type $\mathtt{A}_1$, we distinguish between two cases: For $m-2 \leq \frac{n-3}{2}$, we can choose the $m-2$ isolated nodes from the nodes labeled $s_2, \ldots, s_{n-2}$. Invoking Lemma 5.2.14, we see that the vertices of Γ^m obtained from these subdiagrams are odd-adjacent to subdiagrams of type $\mathtt{A}_1^m$ that also include s_{n-1} or s_n, along with s_0 and s_1. Therefore, for $m-2 \leq k-2$, when $n = 2k$, and $m-2 \leq k-1$, when $n = 2k+1$, we obtain one connected component of Γ^m in this case.
For the case when $n = 2k$ even and $m = k+1$, we find two subdiagrams of type $\mathtt{A}_1^m$ that satisfy the conditions of this case. These subdiagrams are spanned by the nodes

labeled $s_0, s_1, s_3, s_5, \ldots, s_{n-3}, s_{n-1}$ and $s_0, s_1, s_3, s_5, \ldots, s_{n-3}, s_n$. Since the nodes labeled s_{n-1} and s_n are not adjacent in $\Gamma_{\widetilde{\mathtt{D}}_n}$, these subdiagrams are not odd-adjacent, and the corresponding vertices of Γ^m each form a separate connected component of the graph. Finally, note that we cannot find more than $k+1$ isolated nodes in $\Gamma_{W_{\widetilde{\mathtt{D}}_n}}$ in this case because we have restricted our selections to avoid choosing s_{n-1} and s_n simultaneously with s_0 and s_1. Thus, we count the number of connected components of Γ^m in this case as:

$$n = 2k: \qquad \mathrm{cc}_2(W_{\widetilde{\mathtt{D}}_n}, \mathtt{A}_1^m, \text{ case 2}) = 2 + \sum_{m=2}^{k} 1 = 2 + k - 1 = k + 1;$$

$$n = 2k+1: \qquad \mathrm{cc}_2(W_{\widetilde{\mathtt{D}}_n}, \mathtt{A}_1^m, \text{ case 2}) = \sum_{m=2}^{k+1} 1 = k.$$

Case 3: The subdiagram of type $\mathtt{A}_1^m$ includes the nodes labeled s_{n-1}, s_n, but it does not contain both nodes s_0 and s_1 simultaneously. Due to the symmetry of $\Gamma_{\widetilde{\mathtt{D}}_n}$, we can determine the number of connected components using the same reasoning as in case 2 above:

$$n = 2k: \qquad \mathrm{cc}_2(W_{\widetilde{\mathtt{D}}_n}, \mathtt{A}_1^m, \text{ case 3}) = k + 1;$$

$$n = 2k+1: \qquad \mathrm{cc}_2(W_{\widetilde{\mathtt{D}}_n}, \mathtt{A}_1^m, \text{ case 3}) = k.$$

Case 4: The subdiagram of type $\mathtt{A}_1^m$ includes either the node labeled s_0 or s_1, as well as either s_{n-1} or s_n, and it is not odd-adjacent to subdiagrams that do not contain these two nodes. This situation arises when the subdiagram contains two of the nodes with degree 1 on each outer side of the diagram, along with every second node in between them. Given that $\Gamma_{\widetilde{\mathtt{D}}_n}$ has $n+1$ nodes, this implies that n has to be even. Futhermore, we have $m = \frac{n-2}{2} + 1 = \frac{2k-2}{2} + 1 = k$. Now, observe that in this case, we find four vertices of Γ^m derived from subgraphs of type $\mathtt{A}_1^m$. The following combinations of nodes span these subgraphs:

(1) $s_0, s_3, s_5, \ldots, s_{n-3}, s_{n-1}$;

(2) $s_1, s_3, s_5, \ldots, s_{n-3}, s_{n-1}$;

(3) $s_0, s_3, s_5, \ldots, s_{n-3}, s_n$;

(4) and $s_1, s_3, s_5, \ldots, s_{n-3}, s_n$.

Note that all four vertices are isolated in Γ^m because they differ in non-adjacent nodes. Consequently, if $n = 2k$ even, we obtain four connected components of Γ^m. If $n = 2k+1$ is odd, no vertices of Γ^m satisfy the conditions of this case. Thus:

$$n = 2k: \qquad \mathrm{cc}_2(W_{\widetilde{\mathtt{D}}_n}, \mathtt{A}_1^m, \text{ case 4}) = 4;$$

$$n = 2k+1: \qquad \mathrm{cc}_2(W_{\widetilde{\mathtt{D}}_n}, \mathtt{A}_1^m, \text{ case 4}) = 0.$$

Case 5: The subdiagram of type $\mathtt{A}_1^m$ includes at most one node from $\{s_0, s_1, s_{n-1}, s_n\}$. Since two nodes from the set $\{s_1, \ldots, s_{n-1}\}$ are isolated if and only if their index numbers have a distance of at least 2, it follows from the symmetry of $\Gamma_{\widetilde{\mathtt{D}}_n}$ that $m \leq 1 + \frac{n-3}{2}$. This observation leads to the following conclusions: For $n = 2k$, we have $m \leq k-1$, and for $n = 2k+1$, we have $m \leq k$. With Lemma 5.2.14 and the fact that the node labeled s_1 (resp. s_{n-2}) is odd-adjacent to the nodes labeled s_0 and s_2 (resp. s_{n-1} and s_n), it

follows that for fixed m, all vertices of Γ^m that arise from subdiagrams satisfying the conditions of case 5 are odd-adjacent, which means they are all contained in a common connected component of the graph. As a result, we count one connected component for every such m. This gives:

$$n = 2k: \qquad \mathrm{cc}_2(W_{\widetilde{\mathtt{D}}_n}, \mathtt{A}_1^m, \text{ case 5}) = \sum_{m=2}^{k-1} 1 = k-2;$$

$$n = 2k+1: \qquad \mathrm{cc}_2(W_{\widetilde{\mathtt{D}}_n}, \mathtt{A}_1^m, \text{ case 5}) = \sum_{m=2}^{k} 1 = k-1.$$

In summary, after considering all five cases, we can calculate the number of connected components $\mathrm{cc}_2(W_{\widetilde{\mathtt{D}}_n}, \mathtt{A}_1^m)$ of $W_{\widetilde{\mathtt{D}}_n}$ obtained from subgroups of type $\mathtt{A}_1^m$ to:

$$n = 2k: \qquad \mathrm{cc}_2(W_{\widetilde{\mathtt{D}}_n}, \mathtt{A}_1^m) = k-1+k+1+k+1+4+k-2 = 4k+3;$$
$$n = 2k+1: \qquad \mathrm{cc}_2(W_{\widetilde{\mathtt{D}}_n}, \mathtt{A}_1^m) = k-1+k+k+0+k-1 = 4k-2.$$

Subdiagrams of type $\mathtt{D}_{2i} \sqcup \mathtt{A}_1^{m-2i}$*:*
Since $i \geq 2$ and $m > 2i$, it follows that $m \geq 5$. Recall that $\Gamma_{\widetilde{\mathtt{D}}_n}$ contains two subdiagrams of type $\mathtt{D}_{2i}$ for each $i \in \{2, \ldots, \lfloor \frac{n}{2} \rfloor\}$. These subdiagrams are spanned by the nodes labeled $s_0, s_1, \ldots, s_{2i-1}$ and $s_{n-2i+1}, s_{n-2i+2} \ldots, s_n$. In the following discussion, we consider subdiagrams of type $\mathtt{D}_{2i} \sqcup \mathtt{A}_1^{m-2i}$ which contain a subdiagram of type $\mathtt{D}_{2i}$ spanned by $s_0, s_1, \ldots, s_{2i-1}$ first.
Notice that, with the subdiagram of type $\mathtt{D}_{2i}$ being spanned by the nodes labeled $s_0, s_1, \ldots, s_{2i-1}$, we need to select $m-2i$ isolated nodes from the nodes that are labeled $s_{2i}, s_{2i+1}, \ldots, s_n$ to construct a subdiagram of type $\mathtt{A}_1^{m-2i}$. Since $m > 2i$ and the nodes labeled s_{n-1} and s_n are both adjacent to the node labeled s_{n-2}, the subdiagram $\mathtt{D}_{2i}$ must not include the node s_{n-2}. This leads to $2i-1 < n-2 \Leftrightarrow i < \frac{n-1}{2}$. Therefore, we obtain $2 \leq i \leq k-1$ for both cases $n = 2k$ and $n = 2k+1$. To count the number of connected components of Γ^m obtained from subdiagrams of type $\mathtt{D}_{2i} \sqcup \mathtt{A}_1^{2i-m}$, we differentiate into three cases:
Case 1: The set of nodes that spans the subdiagram of type $\mathtt{D}_{2i} \sqcup \mathtt{A}_1^{m-2i}$ includes the nodes labeled s_{n-1}, s_n. Since both of these nodes are adjacent to the node labeled s_{n-2} and have degree 1, subdiagrams of type $\mathtt{D}_{2i} \sqcup \mathtt{A}_1^{m-2i}$ with fixed values of m and i are never odd-adjacent to subdiagrams of this type that do not include these two nodes. Recall that $2 \leq i \leq k-1$. We place two copies of $\mathtt{A}_1$ at the nodes labeled s_{n-1} and s_n. Additionally, we can place $m-2i-2$ more copies of $\mathtt{A}_1$ at the nodes labeled $s_{2i+1}, s_{2i+2}, \ldots, s_{n-3}$. This results in $2(m-2i-2) \leq n-2-(2i+1)+1 \Leftrightarrow m-2i-2 \leq \frac{n-2-2i}{2}$. For $n = 2k$ and $n = 2k+1$, we derive $2 \leq m-2i \leq k-i+1$. Applying Lemma 5.2.14 shows that for fixed values of m and i, all vertices of Γ^m obtained from subdiagrams we discussed in this case are contained within the same connected component of the graph. Therefore, we count the number of connected components from this case as:

$$\mathrm{cc}_2(W_{\widetilde{\mathtt{D}}_n}, \mathtt{D}_{2i} \sqcup \mathtt{A}_1^{m-2i}, \text{ case 1}) = \sum_{i=2}^{k-1} \left(\sum_{m=2i+2}^{k+i+1} 1 \right) = (k-2)\frac{k-1}{2}.$$

Case 2: Consider subdiagrams of type $\mathtt{D}_{2i} \sqcup \mathtt{A}_1^{m-2i}$ with $m = k+i$, and ensure that the set of nodes spanning the subdiagram does not include both nodes labeled s_{n-1} and s_n simultaneously. The condition $m = k+i$ implies that the subdiagram cannot be spanned

without using the nodes labeled s_{n-1} and s_n: As noted earlier, since $\mathtt{D}_{2i}$ is spanned by the $2i$ nodes $s_0, \ldots, s_{2i-1}$, there are $n-2i+1$ remaining nodes in $\Gamma_{\widetilde{\mathtt{D}}_n}$. To place $m-2i$ copies of $\mathtt{A}_1$ there while using exactly one of the nodes s_{n-1} and s_n, we require the conditions $2(m-2i) \leq n-2i \Leftrightarrow m \leq \frac{n}{2}+i$, and simultaneously $n-2i-1 < 2(m-2i) \Leftrightarrow \frac{n}{2}+i-\frac{1}{2} < m$. Combining these results, we find that $k+i-\frac{1}{2} < m \leq k+i \Leftrightarrow m = k+i$ for $n = 2k$, and $k+i < m \leq k+\frac{1}{2}+i$ for $n = 2k+1$. Therefore, this case applies only when $n = 2k$. Next, for fixed $2 \leq i \leq k-1$ with $m = k+i$, we can identify two subdiagrams of type $\mathtt{D}_{2i} \sqcup \mathtt{A}_1^{m-2i}$. These are spanned by the nodes labeled $s_0, s_1, \ldots, s_{2i-1}, s_{2i+1}, s_{2i+3}, \ldots, s_{n-1}$ and $s_0, s_1, \ldots, s_{2i-1}, s_{2i+1}, s_{2i+3}, \ldots, s_n$ (resp. $s_0, s_1, \ldots, s_{2i-1}, s_n$). Since the nodes labeled s_{n-1} and s_n are not adjacent, these subdiagrams are not odd-adjacent and are therefore contained in two different connected components of Γ^m. Consequently, the number of connected components in this case totals:

$$n = 2k: \qquad \mathrm{cc}_2(W_{\widetilde{\mathtt{D}}_n}, \mathtt{D}_{2i} \sqcup \mathtt{A}_1^{m-2i}, \text{ case 2}) = \sum_{i=2}^{k-1} 2 = 2k-4.$$

Case 3: Consider subdiagrams of type $\mathtt{D}_{2i} \sqcup \mathtt{A}_1^{m-2i}$ that can be spanned without using the nodes labeled s_{n-1} and s_n. Given $m > 2i$, the contained subdiagram of type $\mathtt{D}_{2i}$ must not be spanned by a set of nodes containing $s_{n-3}, s_{n-2}, s_{n-1}$ and s_n. This leads to the condition $2i \leq n-3 \Leftrightarrow i \leq \frac{n-3}{2}$. Thus, for $n = 2k$, we have $2 \leq i \leq k-2$, and $2 \leq i \leq k-1$ for $n = 2k+1$. For each fixed i, the graph $\Gamma_{\widetilde{\mathtt{D}}_n}$ will then have $n+1-2i$ additional nodes. Without placing a copy of $\mathtt{A}_1$ at either of the nodes labeled s_{n-1} and s_n, it follows from $2(m-2i) \leq n-1-2i \Leftrightarrow m \leq \frac{n-1}{2}+i$ that $m \leq k+i-1$ for $n = 2k$, and $m \leq k+i$ for $n = 2k+1$. Or, $1 \leq m-2i \leq k-i$, for $n = 2k+1$, and $1 \leq m-2i \leq k-i-1$, for $n = 2k$. Since both nodes labeled s_{n-1} and s_n are adjacent to the node labeled s_{n-2}, all subdiagrams of type $\mathtt{A}_1^{m-2i}$ spanned by a subset of $s_{2i+1}, s_{2i+2}, \ldots, s_n$ are odd-adjacent. Consequently, we can apply Lemma 5.2.14, which indicates that all the subdiagrams of type $\mathtt{D}_{2i} \sqcup \mathtt{A}_1^{m-2i}$ that correspond to vertices in Γ^m are contained within a common connected component of the graph. Thus, we count the connected components for this case as:

$$n = 2k: \qquad \mathrm{cc}_2(W_{\widetilde{\mathtt{D}}_n}, \mathtt{D}_{2i} \sqcup \mathtt{A}_1^{m-2i}, \text{ case 3}) = \sum_{i=2}^{k-2} \left(\sum_{m=2i+1}^{k+i-1} 1 \right) = (k-3)\frac{k-2}{2};$$

$$n = 2k+1: \qquad \mathrm{cc}_2(W_{\widetilde{\mathtt{D}}_n}, \mathtt{D}_{2i} \sqcup \mathtt{A}_1^{m-2i}, \text{ case 3}) = \sum_{i=2}^{k-1} \left(\sum_{m=2i+1}^{k+i} 1 \right) = (k-2)\frac{k-1}{2}.$$

Observe that due to the symmetry of $\Gamma_{\widetilde{\mathtt{D}}_n}$, when considering subdiagrams of type $\mathtt{D}_{2i} \sqcup \mathtt{A}_1^{m-2i}$, with the subdiagram of type $\mathtt{D}_{2i}$ containing the nodes labeled s_{n-1} and s_n, we obtain the same results as discussed in cases 1,2, and 3 above, simply by adjusting the index numbers of the nodes $s_0, \ldots, s_n$ accordingly. Compare Figure 5.22 again for clarity. Therefore, when we combine all three cases and multiply the results by 2, we arrive at the total count of connected components $\mathrm{cc}_2(W_{\widetilde{\mathtt{D}}_n}, \mathtt{D}_{2i} \sqcup \mathtt{A}_1^{m-2i})$ of $W_{\widetilde{\mathtt{D}}_n}$ obtained

from subgroups of type $\mathtt{D}_{2i} \sqcup \mathtt{A}_1^{m-2i}$:

$$\begin{aligned} n = 2k: \qquad \mathrm{cc}_2(W_{\widetilde{\mathtt{D}}_n}, \mathtt{D}_{2i} \sqcup \mathtt{A}_1^{m-2i}) &= 2\left((k-2)\frac{k-1}{2} + 2k - 4 + (k-3)\frac{k-2}{2}\right) \\ &= 2k(k-2). \\ n = 2k+1: \qquad \mathrm{cc}_2(W_{\widetilde{\mathtt{D}}_n}, \mathtt{D}_{2i} \sqcup \mathtt{A}_1^{m-2i}) &= 2\left((k-2)\frac{k-1}{2} + (k-2)\frac{k-1}{2}\right) \\ &= 2(k-2)(k-1). \end{aligned}$$

Subdiagrams of type $\mathtt{D}_{2i} \sqcup \mathtt{A}_1^{m-2i-2j} \sqcup \mathtt{D}_{2j}$*:*
Since we have already considered subdiagrams of type $\mathtt{A}_1^m$ and $\mathtt{D}_{2i} \sqcup \mathtt{A}_1^{m-2i}$ above, we assume that $i, j \geq 2$, which implies that $m \geq 8$. Recall that subdiagrams of type $\mathtt{D}_{2i}$, resp. $\mathtt{D}_{2j}$, are spanned by the nodes labeled $s_0, s_1, \ldots, s_{2i-1}$, resp. $s_{n-2j+1}, \ldots s_n$. Therefore, we have $2i \leq n-4 \Leftrightarrow i \leq k-2$. For fixed i, the diagram $\Gamma_{\widetilde{\mathtt{D}}_n}$ contains $n-2i+1$ additional nodes that do not span the subdiagram $\mathtt{D}_{2i}$. For the second isolated subdiagram of type $\mathtt{D}_{2j}$, we then find $2j \leq n - 2i \Leftrightarrow j \leq k - i$. With these two subdiagrams of type $\mathtt{D}_{2i}$ and $\mathtt{D}_{2j}$ being spanned by $2i + 2j$ of the $n + 1$ nodes of $\Gamma_{\widetilde{\mathtt{D}}_n}$, we can select $m - 2i - 2j$ isolated nodes from the remaining $n+1-2i-2j$ nodes of the graph to find subdiagrams of type $\mathtt{A}_1^{m-2i-2j}$. Note that two nodes of the set $\{s_2, \ldots s_{n-2}\}$ are isolated in $\Gamma_{\widetilde{\mathtt{D}}_n}$ if and only if the distance of their index numbers is at least two. Consequently, we have that $m - 2i - 2j \leq \frac{1}{2}(n + 1 - 2i - 2j - 1) = k - i - j$. Applying Lemma 5.2.14, we find that for every feasible choice of m, i, j, all vertices of Γ^m obtained from subgraphs of type $\mathtt{D}_{2i} \sqcup \mathtt{A}_1^{m-2i-2j} \sqcup \mathtt{D}_{2j}$ are contained within a common connected component of the graph. Thus, we can calculate the number of connected components $\mathrm{cc}_2(W_{\widetilde{\mathtt{D}}_n}, \mathtt{D}_{2i} \sqcup \mathtt{A}_1^{m-2i-2j} \sqcup \mathtt{D}_{2j})$ of $W_{\widetilde{\mathtt{D}}_n}$ obtained from subgroups of type $\mathtt{D}_{2i} \sqcup \mathtt{A}_1^{m-2i-2j} \sqcup \mathtt{D}_{2j}$ as:

$$\begin{aligned} n = 2k,\ n = 2k+1: \qquad \mathrm{cc}_2(W_{\widetilde{\mathtt{D}}_n}, \mathtt{D}_{2i} \sqcup \mathtt{A}_1^{m-2i-2j} \sqcup \mathtt{D}_{2j}) &= \sum_{i=2}^{k-2}\left(\sum_{j=2}^{k-i}\left(\sum_{m=0}^{k-i-j} 1\right)\right) \\ &= (k-3)(k-2)\frac{k-1}{6}. \end{aligned}$$

Sum of all conjucagy classes:
Eventually, we can derive the number of conjugacy classes of a Coxeter group of type $W_{\widetilde{\mathtt{D}}_n}$ as:

$$\begin{aligned} \mathrm{cc}_2(W_{\widetilde{\mathtt{D}}_n}) &= 1 + \mathrm{cc}_2(W_{\widetilde{\mathtt{D}}_n}, \mathtt{D}_m) + \mathrm{cc}_2(W_{\widetilde{\mathtt{D}}_n}, \mathtt{A}_1^m) + \mathrm{cc}_2(W_{\widetilde{\mathtt{D}}_n}, \mathtt{D}_{2i} \sqcup \mathtt{A}_1^{m-2i}) \\ &\quad + \mathrm{cc}_2(W_{\widetilde{\mathtt{D}}_n}, \mathtt{D}_{2i} \sqcup \mathtt{A}_1^{m-2i-2j} \sqcup \mathtt{D}_{2j}); \\ n = 2k: \qquad \mathrm{cc}_2(W_{\widetilde{\mathtt{D}}_n}) &= 1 + 2k + 4k + 3 + 2k(k-2) + (k-3)(k-2)\frac{k-1}{6} \\ &= \frac{1}{6}(k+1)(k^2+5k+18); \\ n = 2k+1: \ \mathrm{cc}_2(W_{\widetilde{\mathtt{D}}_n}) &= 1 + 2k - 2 + 4k - 2 + 2(k-2)(k-1) + (k-3)(k-2)\frac{k-1}{6} \\ &= \frac{1}{6}k(k^2+6k+11). \end{aligned}$$

□

We conclude the proof of Theorem 5.4.4 by proving the formulae for the exceptional types of affine Coxeter groups:

PROOF OF THEOREM 5.4.4 FOR THE EXCEPTIONAL TYPES: To determine the number of conjugacy classes for the exceptional types of affine Coxeter groups, we employ similar arguments as those used in Lemma 5.2.14 and count the number of subdiagrams of inc-types shown in Figure 5.1.
$\mathrm{cc}_2(\widetilde{\mathtt{E}}_6)$*:*

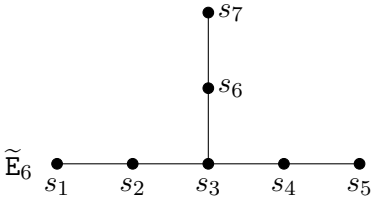

FIGURE 5.23. Coxeter diagram of $\widetilde{\mathtt{E}}_6$.

First, observe that $\Gamma_{\widetilde{\mathtt{E}}_6}$ is an odd-labeled connected graph, which implies that Γ^1 has one connected component. Furthermore, according to the list presented in Figure 5.1, $\Gamma_{\widetilde{\mathtt{E}}_6}$ contains only (copies of) $\mathtt{A}_1$ and $\mathtt{D}_4$ as subdiagrams of inc-type. Thus, for $m = 2$ and $m = 3$, it only includes subdiagrams of type $\mathtt{A}_1^2$ and$\mathtt{A}_1^3$, respectively. Since $\Gamma_{\widetilde{\mathtt{E}}_6}$ has the structure of two path graphs that are glued together at the node labeled s_3, we can apply the arguments of Lemma 5.2.14 to conclude that all these subdiagrams are odd-adjacent. This indicates that the corresponding vertices in Γ^2 and Γ^3 are connected. Therefore, both Γ^2 and Γ^3 have one connected component each.
For $m = 4$, we find that $\Gamma_{\widetilde{\mathtt{E}}_6}$ contains a subdiagram of type $\mathtt{D}_4$, which is spanned by the nodes labeled s_2, s_3, s_4, s_6. As there are no other subdiagrams of this type, the corresponding vertex in Γ^4 is isolated. Additionally, there are four non-adjacent nodes labeled s_1, s_3, s_5, s_7 in the graph, representing a subgroup of type $\mathtt{A}_1^4$, which also forms an isolated vertex in Γ^4. Since this is the only subgroup of this type, we can conclude that Γ^4 has two connected components.
For Γ^5, Γ^6, and Γ^7, we find no subgraphs of $\Gamma_{\widetilde{\mathtt{E}}_6}$ as listed in Figure 5.1, hence these graphs are empty.
In summary, we can count the connected components of $W_{\widetilde{\mathtt{E}}_6}$ as:

$$\mathrm{cc}_2(W_{\widetilde{\mathtt{E}}_6}) = 1 + 1 + 1 + 2 + 0 + 0 + 0 = 5.$$

$\mathrm{cc}_2(\widetilde{\mathtt{E}}_7)$*:*

Since $\Gamma_{\widetilde{\mathtt{E}}_7}$ is an odd-labeled connected graph, Γ^1 is an unlabeled connected graph that consists of a single connected component. It follows from the structure of the graph that $\Gamma_{\widetilde{\mathtt{E}}_7}$ contains only subdiagrams of type $\mathtt{A}_1, \mathtt{D}_4, \mathtt{D}_6$, and $\mathtt{E}_7$ from the list of subdiagrams of inc-type as presented in Figure 5.1. See also Figure 5.24. For Γ^2 and Γ^3, we conclude that $\Gamma_{\widetilde{\mathtt{E}}_7}$ includes only subdiagrams of type $\mathtt{A}_1^2$, resp. $\mathtt{A}_1^3$, given by two and three non-adjacent nodes in the graph, respectively. Note that $\Gamma_{\widetilde{\mathtt{E}}_7}$ is a path graph, with an additional edge

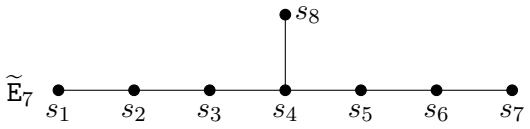

FIGURE 5.24. Coxeter diagram of $\widetilde{\mathtt{E}}_7$.

glued to the node labeled s_4. Based on this and the arguments used in Lemma 5.2.14, we observe that for $m = 2$, all of these subgraphs are odd-adjacdent. Hence, they are contained within a common connected component of Γ^2. This demonstrates that Γ^2 is indeed a connected graph.

For $m = 3$, we observe that not all subdiagrams of type $\mathtt{A}_1^3$ are odd-adjacent. Specifically, the two subdiagrams spanned by the nodes labeled s_1, s_3, s_8 and s_5, s_7, s_8 are not adjacent to any other subdiagram of this type. This is because their nodes are only adjacent to other nodes that have a distance of 2 or less from two of the contained nodes. Consequently, the corresponding vertices in Γ^3 are isolated. In contrast, for every other subdiagram of type $\mathtt{A}_1^3$, for instance, the one spanned by the nodes labeled s_1, s_3, s_5 or s_2, s_5, s_8, the arguments of Lemma 5.2.14 confirm that these are indeed odd-adjacent. This implies that the corresponding vertices in Γ^4 are part of a common connected component. Overall, this shows that Γ^3 consists of 3 connected components.

For Γ^4, we note that the diagram contains a single subgraph of type $\mathtt{D}_4$, which is spanned by the nodes labeled s_3, s_4, s_5, and s_8. Since all other subdiagrams represent groups that are not isomorphic to $\mathtt{D}_4$, the corresponding vertex in Γ^4 is isolated. Additionally, $\Gamma_{\widetilde{\mathtt{E}}_7}$ contains three sets of subgraphs of type $\mathtt{A}_1^4$, with none of the representatives from one set being odd-adjacent to any graph in another set. The first set consists of one subgraph spanned by the nodes labeled s_1, s_3, s_5, and s_7. This graph is not odd-adjacent to any other subgraph of this type in $\Gamma_{\widetilde{\mathtt{E}}_7}$ since all spanning nodes have a distance of exactly 2 to their adjacent neighbors. Therefore, the corresponding vertex in Γ^4 is isolated. The second set comprises subdiagrams containing the nodes labeled s_1, s_3, s_8, and one of the nodes labeled s_5, s_6, or s_7. By applying Lemma 5.2.14, we see that these are odd-adjacent subdiagrams of the same type, and thus they are contained within a common connected component in Γ^4. The third includes subdiagrams that contain the nodes labeled s_5, s_7, s_8, along with one of the nodes labeled s_1, s_2, or s_3. Again, using Lemma 5.2.14, we find that these subdiagrams are odd-adjacent and of the same type, meaning they are part of a common connected component in Γ^4. In conclusion, this shows that Γ^4 has 4 connected components.

For Γ^5, we note that $\Gamma_{\widetilde{\mathtt{E}}_7}$ contains a single subgraph of type $\mathtt{A}_1^5$, which is spanned by the nodes labeled s_1, s_3, s_5, s_7, s_8. The corresponding vertex in Γ^5 is isolated, thus forming a connected component. Additionally, we identify two subdiagrams of type $\mathtt{D}_4 \sqcup \mathtt{A}_1$, which are spanned by the nodes labeled s_1, s_3, s_4, s_5, s_8 and s_3, s_4, s_5, s_7, s_8. Since the nodes labeled s_1 and s_7 are not adjacent, these two subdiagrams are also not odd-adjacent, indicating that the corresponding vertices in Γ^5 are isolated. Together, this shows that Γ^5 has 3 connected components.

For Γ^6, note that $\Gamma_{\widetilde{\mathtt{E}}_7}$ contains two subdiagrams of type $\mathtt{D}_6$. The first is spanned by the nodes labeled $s_1, s_2, s_3, s_4, s_5, s_8$, and the second by the nodes labeled $s_3, s_4, s_5, s_6, s_7, s_8$.

Since these two subdiagrams differ in more than one node, they are not odd-adjacent and thus form two isolated vertices in Γ^6. Additionally, we find a single subgraph of type $\mathtt{D}_4 \sqcup \mathtt{A}_1^2$, spanned by the nodes labeled $s_1, s_3, s_4, s_5, s_7, s_8$. This subgraph also corresponds to an isolated vertex in Γ^6. In total, this shows that Γ^6 consists of 3 connected components.
For Γ^7, we identify two subdiagrams of type $\mathtt{E}_7$, which are spanned by the nodes labeled $s_1, s_2, s_3, s_4, s_5, s_6, s_8$, and $s_2, s_3, s_4, s_5, s_6, s_7, s_8$. Since the nodes labeled s_1 and s_7 are not adjacent, these subdiagrams are not odd-adjacent, resulting in the corresponding vertices in Γ^7 being isolated. Additionally, we find two subdiagrams of type $\mathtt{D}_6 \sqcup \mathtt{A}_1$ that are spanned by the nodes labeled $s_1, s_3, s_4, s_5, s_6, s_7, s_8$, and $s_1, s_2, s_3, s_4, s_5, s_7, s_8$. Again, since the nodes labeled s_2 and s_6 are not adjacent, the corresponding vertices in Γ^7 are isolated. Since these are the only contained subgraphs of inc-type spanned by 7 nodes, we conclude that Γ^7 has 4 connected components.
Furthermore, because $\Gamma_{\widetilde{\mathtt{E}}_7}$ itself is not of inc-type, it follows that $\Gamma^8 = \emptyset$. Thus, we can determine the number of conjugacy classes of $W_{\widetilde{\mathtt{E}}_7}$ to:

$$\mathrm{cc}_2(W_{\widetilde{\mathtt{E}}_7}) = 1 + 1 + 3 + 4 + 3 + 3 + 4 + 0 = 19.$$

$\mathrm{cc}_2(\widetilde{\mathtt{E}}_8)$*:*

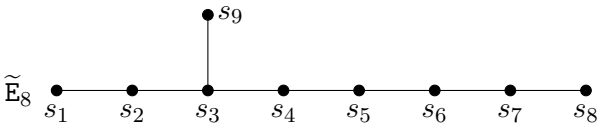

FIGURE 5.25. Coxeter diagram of $\widetilde{\mathtt{E}}_8$.

Since all edges of $\Gamma_{\widetilde{\mathtt{E}}_8}$ are odd-labeled and the diagram is connected, it follows that Γ^1 is also connected and, consequently, has one connected component.
Comparing Figure 5.25 with Figure 5.1, we observe that $\Gamma_{\widetilde{\mathtt{E}}_6}$ can only contain (copies) of subdiagrams of inc-types $\mathtt{A}_1, \mathtt{D}_4, \mathtt{D}_6, \mathtt{D}_8, \mathtt{E}_7$, and $\mathtt{E}_8$. Note that $\Gamma_{\widetilde{\mathtt{E}}_8}$ has the structure of a path graph with an additional edge attached to the node labeled s_3. For Γ^2 and Γ^3, this implies that $\Gamma_{\widetilde{\mathtt{E}}_8}$ contains only subdiagrams of types $\mathtt{A}_1^2$ and $\mathtt{A}_1^3$, respectively. Using the arguments from Lemma 5.2.14, we can see that these subgraphs are all odd-adjacent. Hence, the corresponding vertices in Γ^2 and Γ^3 are connected. Therefore, both Γ^2 and Γ^3 each have only one connected component.
For Γ^4, we identify a single subdiagram of type $\mathtt{D}_4$ and several subdiagrams of type $\mathtt{A}_1^4$. The subdiagram of type $\mathtt{D}_4$ is spanned by the nodes labeled s_2, s_3, s_4, s_9. This corresponds to an isolated vertex in Γ^4 because the group is not isomorphic to a group of type $\mathtt{A}_1^4$. Most of the subdiagrams of type $\mathtt{A}_1^4$ are odd-adjacent, as can be seen with the arguments of Lemma 5.2.14; we omit the listing of them here. Consequently, all of these odd-adjacent subdiagrams of type $\mathtt{A}_1^4$ are contained within a common connected component of Γ^4. Notably, there is a single subdiagram of type $\mathtt{A}_1^4$ spanned by the nodes labeled s_4, s_6, s_8, s_9, which is not odd-adjacent to any other subdiagram of this type. This arises from the fact that all spanning nodes are at a distance 2 from another node spanning the subgraph, and they are not adjacent to nodes with a distance greater than

2 from other spanning nodes. Consequently, this diagram is not odd-adjacent to another subdiagram of type $\mathtt{A}_1^4$ and is represented by an isolated vertex in Γ^4. In conclusion, this shows that Γ^4 has 3 connected components.
Further observe that the diagram $\Gamma_{\widetilde{\mathtt{E}}_8}$ contains three subdiagrams of type $\mathtt{D}_4 \sqcup \mathtt{A}_1$. These are all odd-adjacent due to Lemma 5.2.14. They are spanned by the nodes labeled s_2, s_3, s_4, s_9, and one of the isolated nodes s_6, s_7, or s_8. The corresponding vertices in Γ^5 form a connected component. Additionally, $\Gamma_{\widetilde{\mathtt{E}}_8}$ contains two subdiagrams of type $\mathtt{A}_1^5$. These are spanned by the nodes labeled s_4, s_6, s_8, s_9, along with one of the two nodes labeled s_1, or s_2. Again, using Lemma 5.2.14, we find that these two subdiagrams are odd-adjacent. Hence, the corresponding vertices in Γ^5 are part of a common connected component. Based on our observations regarding subdiagrams of inc-type that are included in $\Gamma_{\widetilde{\mathtt{E}}_8}$, we conclude that these two classes of subgraphs are the only ones present in Γ^5. Therefore, Γ^5 consists of two connected components. Compare also Example 5.2.10
For Γ^6, we observe that $\Gamma_{\widetilde{\mathtt{E}}_8}$ contains a single subgraph of type $\mathtt{D}_6$, which is spanned by the nodes labeled $s_2, s_3, s_4, s_5, s_6, s_9$. Additionally, there is a single subgraph of type $\mathtt{D}_4 \sqcup \mathtt{A}_1^2$, spanned by the nodes labeled $s_2, s_3, s_4, s_6, s_8, s_9$. Since the groups represented by these subgraphs are not isomorphic, they correspond to two isolated vertices in Γ^6. Furthermore, as noted earlier, $\Gamma_{\widetilde{\mathtt{E}}_8}$ contains no other subgraphs of inc-type. Therefore, it follows that Γ^6 has 2 connected components.
For Γ^7, we observe that $\Gamma_{\widetilde{\mathtt{E}}_8}$ contains a single subgraph of type $\mathtt{E}_7$. This subgraph is spanned by the nodes labeled $s_1, s_2, s_3, s_4, s_5, s_6$, and s_9. Additionally, there is a single subgraph of type $\mathtt{D}_6 \sqcup \mathtt{A}_1$, which is spanned by the nodes labeled $s_2, s_3, s_4, s_5, s_6, s_9$, and s_8. Therefore, Γ^7 consists of 2 connected components.
For Γ^8, we identify three subgraphs corresponding to vertices in the graph: The first subdiagram of type $\mathtt{D}_8$ is spanned by the nodes labeled $s_2, s_3, s_4, s_5, s_6, s_7, s_8, s_9$. The second subdiagram of type $\mathtt{E}_7 \sqcup \mathtt{A}_1$ is spanned by the nodes labeled $s_1, s_2, s_3, s_4, s_5, s_6, s_8, s_9$. And the third subdiagram of type $\mathtt{E}_8$ is spanned by the nodes labeled $s_1, s_2, s_3, s_4, s_5, s_6, s_7, s_9$. Since the corresponding groups are pairwise non-isomorphic, these diagrams correspond to isolated vertices in Γ^8. Thus, Γ^8 has 3 connected components.
Since $\Gamma_{\widetilde{\mathtt{E}}_8}$ is not of inc-type, Γ^8 is empty.
Together, we can count the conjugacy classes of $W_{\widetilde{\mathtt{E}}_8}$ as follows:

$$\mathrm{cc}_2(W_{\widetilde{\mathtt{E}}_8}) = 1 + 1 + 1 + 3 + 2 + 2 + 2 + 3 + 0 = 15.$$

$\mathrm{cc}_2(\widetilde{\mathtt{F}}_4)$*:*

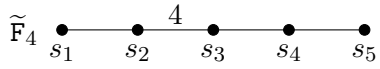

FIGURE 5.26. Coxeter diagram of $\widetilde{\mathtt{F}}_4$.

Since $\Gamma_{\widetilde{\mathtt{F}}_4}$ is a path graph with one edge labeled 4 and all other edges odd-labeled, it follows that Γ^1 consists of two connected components. For Γ^2, we note that $\Gamma_{\widetilde{\mathtt{F}}_4}$ contains subdiagrams of inc-type with two vertices of types $\mathtt{B}_2$ and $\mathtt{A}_1^2$. Precisely, we identify a single subdiagram of type $\mathtt{B}_2$, which is spanned by the nodes labeled s_2 and s_3. This diagram corresponds to an isolated vertex in Γ^2. Further, we find two classes of subdiagrams

of type $\mathtt{A}_1^2$. The first class includes subdiagrams spanned by the nodes labeled s_1 and s_3, s_4, or s_5, as well as s_2 and s_4 or s_5. Invoking Lemma 5.2.14, these are odd-adjacent subdiagrams, which means their corresponding vertices in Γ^2 belong to a common connected component. The second class consists of the subdiagram spanned by the nodes labeled s_3 and s_5. This subdiagram is not odd-adjacent to the subdiagrams discussed beforehand, meaning the corresponding vertex in Γ^2 is isolated. In summary, this shows that Γ^2 has 3 connected components.
For Γ^3, we identify subdiagrams of the types $\mathtt{A}_1^3$, $\mathtt{B}_2 \sqcup \mathtt{A}_1$, and $\mathtt{B}_3$ from the list presented in Figure 5.1 in $\Gamma_{\widetilde{\mathtt{F}}_4}$. The nodes labeled s_1, s_3, and s_5 span the only subdiagram of type $\mathtt{A}_1^3$. It corresponds to an isolated vertex in Γ^3. We also find two subdiagrams of type $\mathtt{B}_3$, which are spanned by the nodes labeled s_1, s_2, s_3, and s_2, s_3, s_4. Since the nodes labeled s_1 and s_4 are not adjacent, these two subgraphs are not odd-adjacent, meaning the corresponding vertices in Γ^3 are disconnected and form two separated connected components. Additionally, we find a subdiagram of type $\mathtt{B}_2 \sqcup \mathtt{A}_1$, spanned by the nodes labeled s_2, s_3, s_5, which also corresponds to an isolated vertex in the graph Γ^3. Altogether, this demonstrates that Γ^3 has 4 connected components.
For Γ^4, we identify a single subdiagram of type $\mathtt{F}_4$ spanned by the nodes labeled $s_1 s_2, s_3$, and s_4, which corresponds to an isolated vertex in Γ^4. We also find a single subdiagram of type $\mathtt{B}_4$, spanned by the nodes labeled s_2, s_3, s_4, s_5, which likewise corresponds to an isolated vertex in Γ^4. Furthermore, we find a single subdiagram of type $\mathtt{B}_3 \sqcup \mathtt{A}_1$, spanned by the nodes labeled s_1, s_2, s_3, and s_5. Together, this shows that Γ^4 has 3 connected components.
Since $\Gamma_{\widetilde{\mathtt{F}}_4}$ itself is not of inc-type, we conclude that Γ^5 is empty.
In summary, we can count the conjugacy classes of $W_{\widetilde{\mathtt{F}}_4}$ as follows:

$$\mathrm{cc}_2(W_{\widetilde{\mathtt{F}}_4}) = 2 + 3 + 4 + 3 + 0 = 12.$$

$\mathrm{cc}_2(\widetilde{\mathtt{G}}_2)$*:*

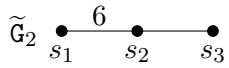

FIGURE 5.27. Coxeter diagram of $\widetilde{\mathtt{G}}_2$.

Since $W_{\widetilde{\mathtt{G}}_2} \cong \Delta(2, 3, 6)$, it follows with our findings in Section 5.4.1 that $\mathrm{cc}_2(\widetilde{\mathtt{G}}_2) = 4$.

$\mathrm{cc}_2(\widetilde{\mathtt{I}}_1)$*:*

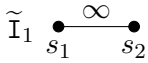

FIGURE 5.28. Coxeter diagram of $\widetilde{\mathtt{I}}_1$.

Since $W_{\widetilde{\mathtt{I}}_1} \cong \mathbb{Z} \setminus 2\mathbb{Z} * \mathbb{Z} \setminus 2\mathbb{Z}$, it follows with Lemma 5.3.13 that $\mathrm{cc}_2(\widetilde{\mathtt{I}}_1) = 2$. This closes the proof. □

Part IV

Sequel

CHAPTER 6

Further questions and research impetus

The results presented in this thesis open up several avenues for further research. Throughout this work, we have identified some research problems and explicitly marked them as *open questions*. The purpose of this section is to consolidate these questions into a coherent overview and, where appropriate, to provide additional explanatory remarks. For the reader's convenience, we provide a reference for every question to the relevant passage in the thesis where it was initinally discussed.

Further questions from Chapter 3

- Open question 3.2.10: Proposition 3.2.9 describes a connection between Coxeter shadows and intervals of the form $[1, x]$ in Bruhat order. Notice that one can also use shadows to describe other intervals $[x, y]$ in Bruhat order (cf. [GS20, Remark 6.10]). For this, consider $\mathrm{Sh}_{\phi_+}(y)$ and derive all elements represented by alcoves $\mathbf{z} \in \mathrm{Sh}_{\phi_+}(y)$, such that a minimal gallery $\gamma : \mathbf{c_f} \rightsquigarrow \mathbf{z}$ can be folded onto $\mathbf{x}$. Motivated by these results, it is an open question to describe connections between Coxeter shadows and other order relations.

- Open question 3.2.16: Definition 3.2.8 enables the construction of Coxeter shadows in arbitrary Coxeter groups; however, to date, they have not been studied in hyperbolic Coxeter groups. For this, it is necessary to further develop the theory of orientations in hyperbolic Coxeter complexes to implement the concept of braid-invariance, which, to our knowledge, remains open. This issue was previously mentioned in [Sch22].

- Open question 3.2.29: Recall that Weyl chamber orientations of affine Coxeter complexes are a special case of chimney-induced orientations. In Example 3.2.27, we observed that chimney shadows, which do not meet the assumptions of Proposition 3.2.28, are subsets of the Weyl chamber shadows with missing alcoves contained in a cone that is *cut off* from the shadow. It remains open question to describe these cones in relation to the chimney. As a first step for this, it would be interesting to precisely describe how the orientations of the hyperplanes change as a sector moves from being far away from the gallery to being closer to it.
  Recall further, that every (J, y)-chimney ξ that is represented by a sector containing more than one alcove (and thus, containing infinitely many, cf. [Mil+24, Lemma 3.10]) is represented by sectors bounded by two adjacent hyperplanes of the same parallelism class. Since this parallelism class corresponds to a panel in the boundary complex $\partial\Sigma$, which lies within certain Weyl chambers, it might

be wothwhile to study the chimney orientation $\phi_{J,y}$ in relation to these Weyl chamber orientations of Σ.

- Open question 3.3.16: Recall that we introduced the set $\mathcal{X}(\mathcal{C}_v, \phi_w)$ of alcoves $\mathbf{x}$ to which every ϕ_w-positive folding pattern can be applied for at least one minimal gallery $\gamma : \mathbf{c_f} \rightsquigarrow \mathbf{x}$. As observed in Example 3.3.15, the naive construction presented in Proposition 3.3.14 only provides a proper subset of $\mathcal{X}(\mathcal{C}_v, \phi_w)$. It remains to give a sharp (geometric) description. Furthermore, it could be interesting to study $\mathcal{X}(\mathcal{C}_v, \phi)$ with respect to other types of orientations ϕ. We assume that the study of $\mathcal{X}(\mathcal{C}_v, \phi_w)$ might provide insights to the co-shadow, see also Open question 4.3.17.

- Open question 3.3.19: It is an open question to investigate potential connections between the folding patterns of galleries in relation to other orientations of the Coxeter complex and different order relations of the group. The concept of folding patterns, as introduced in Definition 3.2.5, only provides information about the parallelism class of the hyperplanes involved in the folds. While this is useful for periodic orientations, it requires modification for non-periodic orientations. In such cases, it is necessary to develop a notion of folding patterns that incorporates information about the height of the hyperplanes where the folds occur. Jacinta Torres and the author are currently exploring this question. This may also help to generalize the results of Chapter 4.

Further questions from Chapter 4

- Open question 4.1.4: We describe gates of irregular coroot lattice points in affine Coxeter complexes of dimension 2 in Lemma 4.1.3. It is open to generalize this result to Coxeter complexes of higher dimension to obtain a general description of irregular gates. This would be the next step in generalizing Theorem 4.3.12, compare also Open question 4.3.13.

- Open question 4.3.10: As proven in Proposition 4.3.9, the set $\mathcal{A}_\lambda$ is the set of all coroot lattice points that intersect with the folding pattern polytope $\mathcal{P}(\mathbf{a}_\lambda, (\alpha_{j,i})_{i\in[n]})$. Many of these points are contained in its interior. Recall that in Definition 4.3.5, the polytope is defined as the Euclidean convex hull of $\mathcal{A}_\lambda$. Given that $\mathcal{A}_\lambda$ may have a large cardinality, it is desirable to understand the structure and know the number of the extremal points of $\mathcal{P}(\mathbf{a}_\lambda, (\alpha_{j,i})_{i\in[n]})$. This would give a more compact description of the folding pattern polytope.

- Open question 4.3.11: There appears to be a potential connection between folding pattern polytopes and pseudo-Weyl polytopes: A λ-Weyl polytope is defined as $\mathcal{P}(\lambda) = \mathrm{conv}^*(W \cdot \lambda)$, where $\mathrm{conv}^*(\cdot)$ denotes the Euclidean convex hull. Weyl polytopes can also be characterized as the intersection of dual hyperplanes within the Coxeter complex. From this, pseudo-Weyl polytopes are constructed by translating the hyperplanes of a λ-Weyl polytope [Kam10].
  The examples of folding pattern polytopes we have studied so far suggest that they might be pseudo-Weyl polytopes. It remains an open question to provide a proof for this observation and, if possible, to describe folding pattern polytopes in terms of pseudo-Weyl polytopes.
  Additionally, it is worth noting that Ehrig explored the connections between

Mirković-Vilonen polytopes, which are pseudo-Weyl polytopes, and folded galleries as well [Ehr10].

- Open question 4.3.13: It is a natural question to ask for a generalization of Theorem 4.3.12 for non-regular coroot lattice points λ. To apply similar methods as presented in this thesis, it is necessary to first answer Open question 4.1.4.

- Open question 4.3.16: Given an affine Coxeter group of rank $n+1$ and a folding pattern $(\alpha_{j,i})_{i\in[k]}$ of length k, what is the dimension of the folding pattern polytope $\mathcal{P}(\mathbf{a}_\lambda, (\alpha_{j,i})_{i\in[k]})$?

- Open question 4.3.17: Let (W, S) be an affine Coxeter system, and let the associated Coxeter complex $\Sigma = \Sigma(W, S)$ be equipped with a Weyl chamber orientation ϕ_w. Consider $y \in \mathrm{Sh}_{\phi_w}(x)$ for $x = t^\lambda v$. It would be interesting to study the multiplicities of y in $\mathrm{Sh}_{\phi_w}(x)$, distinguishing between two different types: First, we can explore the *pattern multiplicity of y in* $\mathrm{Sh}_{\phi_w}(x)$, which is the number of folding patterns $(\alpha_{j,i})_{i\in[n]}$ such that there exists a minimal gallery $\gamma : \mathbf{c_f} \rightsquigarrow \mathbf{x}$ that can be ϕ_w-poyitively folded onto $\mathbf{y}$ following the folding pattern $(\alpha_{j,i})_{i\in[n]}$. Additionally, we could study the *gallery multiplicity of y in* $\mathrm{Sh}_{\phi_w}(x)$, which refers to the number of galleries $\gamma : \mathbf{c_f} \rightsquigarrow \mathbf{x}$ such that there exists a folding pattern $(\alpha_{j,i})_{i\in[n]}$ allowing the gallery to be ϕ_w-poyitively folded onto $\mathbf{y}$ following the folding pattern $(\alpha_{j,i})_{i\in[n]}$. Multiplicities are connected to the study of structure constants in Hecke algebras, cf. [Sch06a; Ram06]. This inquiry is closely related to the study of the *co-Shadow* $\mathrm{Sh}^{co}_\phi(x)$ *of x with respect to the orientation ϕ*, which denotes the set of group elements y for which there exists a minimal gallery $\gamma : \mathbf{c_f} \rightsquigarrow \mathbf{y}$ that can be ϕ-positively folded onto a gallery $\gamma' : \mathbf{c_f} \rightsquigarrow \mathbf{x}$.

- Open question 4.4.7: Let ϕ be a periodic orientation of the affine Coxeter complex $\Sigma = \Sigma(W, S)$, and let $x = t^\lambda w \in W$. Describe the set of alcoves $\mathcal{D} := \mathrm{Sh}_\phi(x) \setminus \mathrm{Um}_\phi(x)$ in terms of λ, w, and ϕ. This would then allow us to describe the Coxeter shadow as $\mathrm{Sh}_\phi(x) = \mathcal{D} \dot\cup \mathrm{Um}_\phi(x)$.

- Open question 4.4.8: Let ϕ be a periodic orientation of the affine Coxeter complex $\Sigma = \Sigma(W, S)$, and let $x = t^\lambda w \in W$. We denote $\mathcal{D} := \mathrm{Sh}_\phi(x) \setminus \mathrm{Um}_\phi(x)$. Under what conditions on x and ϕ does it hold that $\mathcal{D} = \emptyset$? In other words, when is it true that $\mathrm{Sh}_\phi(x) = \mathrm{Um}_\phi(x)$?

- Open question 4.4.9: It would be desirable to generalize the concept of folding pattern polytopes to other orientations. We conjecture that as long as the orientation is periodic, folding pattern polytopes should be convex polytopes of the coroot lattice. This is the next step in generalizing our findings of Chapter 4 to other orientations, specifically those induced by chimneys.

Further questions from Chapter 5

- Open question 5.3.9: Recall that we used higher rank odd graphs to determine the number of conjugacy classes of involutions in Theorem 5.3.7. It is open to investigate the complexity of the algorithm obtained from this.

- Open question 5.3.10: As we introduced the family of higher rank odd graphs Γ^k to compute the number of conjugacy classes of involutions in Coxeter groups, is it possible to define a similar family of graphs that allows one to compute the number of conjugacy classes of torsion elements of order $m \neq 2$?

- Open question 5.3.12: The 'universal' upper bound for $\mathrm{cc}_2(W_\Gamma)$ can only be attained by infinite groups of rank at most three. That is, the bound $\mathrm{cc}_2(W_\Gamma) \leq 2^n - 2$ is not optimal if $|V(\Gamma)| \geq 4$ and W_Γ is infinite. In turn, lowering the bound down by one to $2^n - 3$, one can construct reducible examples in rank four with $\mathrm{cc}_2(W_\Gamma) = 13 = 2^4 - 3$; take, e.g., $\Gamma = \widetilde{\mathtt{C}}_2 \sqcup \mathtt{A}_1$.
  Restricting ourselves to irreducible examples, the anonymous referee of [Rei+25] pointed out to a family of groups with (asymptotically) many conjugacy classes: Define Γ as a tree with one central vertex and k 'arms' of length two, such that all edge labels are (finite) even numbers ≥ 4. Thus Γ has $n = 2k + 1$ vertices. After some deliberation and initial calculations, $\mathrm{cc}_2(W_\Gamma)$ seems to be roughly $2^{n-1} + k \cdot 2^{k-1}$ plus some constant C.
  These considerations leave open the following subtle problem: Is there a function $f : \mathbb{N}_{\geq 4} \to \mathbb{N}$ such that $\mathrm{cc}_2(W) \leq f(n)$ for all infinite irreducible Coxeter groups W of rank $n \geq 4$, with some (infinite, irreducible) Coxeter group W_0 of rank $n_0 \geq 4$ attaining equality $\mathrm{cc}_2(W_0) = f(n_0)$?

- Open question 5.3.14: The number $\mathrm{cc}_2(W_\Gamma)$ is, by definition, a group-theoretic invariant of W_Γ. Also $|\pi_0(\Gamma_{odd})| = |\pi_0(\Gamma^1)|$ does not depend on Γ by [MV24, Proposition 2.2]. However, the connected components of higher rank odd graphs do a priori depend on the chosen Coxeter diagram Γ for W_Γ. It would be interesting to see how the higher rank odd graphs behave with respect to moves (such as twists [Müh00; Bra+02] or blow-ups [Müh06]) between the various Coxeter diagrams for a given group.

Bibliography

[AB08] Peter Abramenko and Kenneth S. Brown. *Buildings. Theory and applications*. Vol. 248. Graduate Texts in Mathematics. New York: Springer, 2008, pp. xxii+747. DOI: 10.1007/978-0-387-78835-7.

[AM15] Yago Antolín and Ashot Minasyan. "Tits alternatives for graph products". In: *J. reine angew. Math.* 704 (2015), pp. 55–83. DOI: 10.1515/crelle-2013-0062.

[BB06] Anders Bjorner and Francesco Brenti. *Combinatorics of Coxeter Groups*. Graduate Texts in Mathematics. Springer Berlin Heidelberg, 2006.

[Ber01] Claude Berge. *Theory of Graphs*. [Transl. by A. Doig] Originally published: The theory of graphs and its applications. London : Methuen, 1962. Mineola, NY: Dover Publ., 2001.

[BH99] Martin R. Bridson and André Haeflier. *Metric spaces of non-positive curvature*. Vol. 319. Grundlehren der mathematischen Wissenschaften. Berlin–Heidelberg: Springer, 1999. DOI: 10.1007/978-3-662-12494-9.

[BHS77] Jean-Claude Bermond, Marie-Claude Heydemann, and Dominique Sotteau. "Line graphs of hypergraphs I". In: *Discrete Math.* 18.3 (1977), pp. 235–241. DOI: 10.1016/0012-365X(77)90127-3.

[Big72] Norman Biggs. "An Edge-Colouring Problem". In: *The American Mathematical Monthly* 79.9 (1972), pp. 1018–1020. DOI: 10.1080/00029890.1972.11993176.

[Bou02] Nicolas Bourbaki. *Lie Groups and Lie Algebras. Chapters 4 – 6*. Berlin – Heidelberg: Springer Science & Business Media, 2002.

[Bra+02] Noel Brady et al. "Rigidity of Coxeter groups and Artin groups". In: *Geom. Dedicata* 94 (2002), pp. 91–109. DOI: 10.1023/A:1020948811381.

[Bre13] Alain Bretto. *Hypergraph theory. An introduction*. Mathematical Engineering. Cham: Springer, 2013, pp. xiii+119. DOI: 10.1007/978-3-319-00080-0.

[Bro89] Kenneth S. Brown. *Buildings*. 1st ed. Éléments de mathématique. Springer Science & Business Media New York 1989, 1989. DOI: doi:10.1007/978-1-4612-1019-1.

[Car72] Roger W. Carter. "Conjugacy classes in the Weyl group". In: *Compos. Math.* 25 (1972), pp. 1–59.

[CL11] Pierre-Emmanuel Caprace and Jean Lécureux. "Combinatorial and group-theoretic compactifications of buildings". eng. In: *Annales de l'institut Fourier* 61.2 (2011), pp. 619–672.

[Coh94] Arjeh M. Cohen. "Recent results on Coxeter groups". In: *Polytopes: abstract, convex and computational*. Proceedings of the NATO Advanced Study Institute, Scarborough, Ontario, Canada, Aug 20–Sep 3, 1993. Dordrecht: Kluwer Academic Publishers, 1994, pp. 1–19.

[Cox35] Harold S. M. Coxeter. "The Complete Enumeration of Finite Groups of the Form $r_i^2 = (r_i r_j)^{k_{ij}} = 1$". In: *Journal of the London Mathematical Society* s1-10.1 (1935), pp. 21–25. DOI: 10.1112/jlms/s1-10.37.21.

[Dav08] Michael W. Davis. *The geometry and topology of Coxeter groups*. Vol. 32. London Mathematical Society Monographs. Princeton University Press, 2008. DOI: 10.1515/9781400845941.

[Deo82] Vinay V. Deodhar. "On the root system of a Coxeter group". In: *Comm. Algebra* 10.6 (1982), pp. 611–630. DOI: 10.1080/00927878208822738.

[Die05] Reinhard Diestel. *Graph Theory (Graduate Texts in Mathematics)*. Springer, Aug. 2005.

[Ehr10] Michael Ehrig. "MV-polytopes via affine buildings". In: *Duke Mathematical Journal* 155.3 (2010), pp. 433–482. DOI: 10.1215/00127094-2010-062.

[Ehr34] Charles Ehresmann. "Sur la Topologie de Certains Espaces Homogénes". In: *Annals of Mathematics* 35.2 (1934), pp. 396–443. DOI: 10.2307/1968440.

[Fie07] Peter Fiebig. "Sheaves on affine Schubert varieties, modular representations and Lusztig's conjecture". In: *Journal of the American Mathematical Society* 24 (Nov. 2007). DOI: 10.2307/25801449.

[Fie10] Peter Fiebig. "Lusztig's conjecture as a moment graph problem". In: *Bulletin of the London Mathematical Society* 42.6 (Aug. 2010), pp. 957–972. DOI: 10.1112/blms/bdq058.

[Fie16] Peter Fiebig. "Moment graphs in representation theory and geometry". In: *Advanced Studies in Pure Mathematics 71, Schubert Calculus — Osaka 2012* (2016), pp. 75–96.

[Fro00] Ferdinand G. Frobenius. "Über die Charaktere der symmetrischen Gruppe". In: *Sitz. Ber. Preuss. Akad.* (1900), pp. 516–534.

[GKM97] Mark Goresky, Robert Kottwitz, and Robert MacPherson. "Equivariant cohomology, Koszul duality, and the localization theorem". In: *Inventiones mathematicae* 131.1 (Dec. 1, 1997), pp. 25–83. DOI: 10.1007/s002220050197.

[GKP00] Meinolf Geck, Sungsoon Kim, and Götz Pfeiffer. "Minimal length elements in twisted conjugacy classes of finite Coxeter groups". In: *J. Algebra* 229.2 (2000), pp. 570–600.

[GL05] Stéphane Gaussent and Peter Littelmann. "LS Galleries, the Path Model, and MV Cycles". In: *Duke Mathematical Journal* 127 (Mar. 2005). DOI: 10.1215/S0012-7094-04-12712-5.

[Gör+06] Ulrich Görtz et al. "Dimensions of some affine Deligne-Lusztig varieties". en. In: *Annales scientifiques de l'École Normale Supérieure* Ser. 4, 39.3 (2006), pp. 467–511. DOI: 10.1016/j.ansens.2005.12.004.

[GP00] Meinolf Geck and Götz Pfeiffer. *Characters of finite Coxeter groups and Iwahori-Hecke algebras*. Vol. 21. London Mathematical Society Monographs. New Series. The Clarendon Press, Oxford University Press, New York, 2000, pp. xvi+446.

[GP19] Jérémie Guilhot and James Parkinson. "A proof of Lusztig's conjectures for affine type G2 with arbitrary parameters". In: *Proceedings of the London*

Mathematical Society 118.5 (2019), pp. 1188–1244. DOI: 10.1112/plms.12211.

[GP93] Meinolf Geck and Götz Pfeiffer. "On the irreducible characters of Hecke algebras". In: *Adv. Math.* 102.1 (1993), pp. 79–94. DOI: 10.1006/aima.1993.1056.

[GR01] Chris Godsil and Gordon Royle. *Algebraic Graph Theory*. Vol. 207. Graduate Texts in Mathematics. New York: Springer, 2001. DOI: 10.1007/978-1-4613-0163-9.

[GS20] Marius Graeber and Petra Schwer. "Shadows in Coxeter Groups". In: *Annals of Combinatorics* 24.1 (Feb. 2020), pp. 119–147. DOI: 10.1007/s00026-019-00485-0.

[Hit10] Petra Hitzelberger. "Kostant convexity for affine buildings". In: *Forum Mathematicum* 22.5 (2010), pp. 959–971. DOI: 10.1515/forum.2010.051.

[HN12] Xuhua He and Sian Nie. "Minimal length elements of finite Coxeter groups". In: *Duke Math. J.* 161.15 (2012), pp. 2945–2967. DOI: 10.1215/00127094-1902382.

[How80] Robert B. Howlett. "Normalizers of parabolic subgroups of reflection groups". In: *J. London Math. Soc. (2)* 21.1 (1980), pp. 62–80. DOI: 10.1112/jlms/s2-21.1.62.

[Hum90] James E. Humphreys. *Reflection Groups and Coxeter Groups*. Cambridge Studies in Advanced Mathematics. Cambridge University Press, 1990. DOI: 10.1017/CBO9780511623646.

[Kam10] Joel Kamnitzer. "Mirković-Vilonen cycles and polytopes". In: *Annals of Mathematics* 171.1 (2010), pp. 245–294.

[KM04] Michael Kapovich and John Millson. "A path model for geodesics in Euclidean buildings and its applications to representation theory". In: *Groups, Geometry, and Dynamics* 2 (2004), pp. 405–480. DOI: 10.4171/GGD/46.

[Kra09] Daan Krammer. "The conjugacy problem for Coxeter groups". In: *Groups Geom. Dyn.* 3.1 (2009), pp. 71–171. DOI: 10.4171/ggd/52.

[Lit94] Peter Littelmann. "A Littlewood-Richardson rule for symmetrizable Kac-Moody algebras". In: *Inventiones mathematicae* 116.1 (1994), pp. 329–346. DOI: 10.1007/BF01231564.

[Lit95] Peter Littelmann. "Paths and Root Operators in Representation Theory". In: *Annals of Mathematics* 142.3 (1995), pp. 499–525.

[Lus03] George Lusztig. *Hecke algebras with unequal parameters*. CRM Monograph Series. American Mathematical Society Providence, 2003.

[Mar21] Timothée Marquis. "Cyclically reduced elements in Coxeter groups". In: *Ann. Sci. Éc. Norm. Supér. (4)* 54.2 (2021), pp. 483–502. DOI: 10.24033/asens.2463.

[Mat64] Hideya Matsumoto. "Générateurs et relations des groupes de Weyl généralisés". In: *C. r. de l'Académie des Sciences Paris* 258 (1964), pp. 3419–3422.

[Mil+24] Elizabeth Milićević et al. "A Gallery Model for Affine Flag Varieties via Chimney Retractions". In: *Transformation Groups* 29.2 (June 1, 2024), pp. 773–821. DOI: 10.1007/s00031-022-09726-8.

[Mou88] Gabor Moussong. *Hyperbolic Coxeter groups*. PhD Thesis, Budapest, Hungary. 1988.

[MST15] Elizabeth Milićević, Petra Schwer, and Anne Thomas. "Dimensions of Affine Deligne–Lusztig Varieties: A New Approach via Labeled Folded Alcove Walks

and Root Operators". In: *Memoirs of the American Mathematical Society* 261 (Apr. 2015). DOI: 10.1090/memo/1260.

[MST22] Elizabeth Milićević, Petra Schwer, and Anne Thomas. *Affine Deligne-Lusztig varieties and folded galleries governed by chimneys*. 2022. arXiv: 2006.16288 [math.AG].

[MST23] Elizabeth Milićević, Petra Schwer, and Anne Thomas. "Chimney retractions in affine buildings encode orbits in affine flag varieties". In: *Innovations in Incidence Geometry: Algebraic, Topological and Combinatorial* 20.2–3 (Sept. 2023), pp. 395–430. DOI: 10.2140/iig.2023.20.395.

[MST24] Elizabeth Milićević, Petra Schwer, and Anne Thomas. *The geometry of conjugation in Euclidean isometry groups*. Preprint. 2024. arXiv: 2407.08078.

[MST25] Elizabeth Milićević, Petra Schwer, and Anne Thomas. "The geometry of conjugation in affine Coxeter groups". In: *Int. J. Alg. Comp.* (2025). DOI: 10.1142/S0218196725500109.

[Müh00] Bernhard Mühlherr. "On isomorphisms between Coxeter groups". In: vol. 21. 1-3. Special issue dedicated to Dr. Jaap Seidel on the occasion of his 80th birthday (Oisterwijk, 1999). 2000, p. 189. DOI: 10.1023/A:1008347930052.

[Müh06] Bernhard Mühlherr. "The isomorphism problem for Coxeter groups". In: *The Coxeter legacy*. Amer. Math. Soc., Providence, RI, 2006, pp. 1–15.

[MV24] Philip Möller and Olga Varghese. "On quotients of Coxeter groups". In: *J. Algebra* 639 (2024), pp. 516–531. DOI: 10.1016/j.jalgebra.2023.09.048.

[Qi07] Dongwen Qi. "A note on parabolic subgroups of a Coxeter group". In: *Expo. Math.* 25.1 (2007), pp. 77–81. DOI: 10.1016/j.exmath.2006.05.001.

[Qi09] Dongwen Qi. "A note on irreducible, infinite Coxeter groups". In: *Expo. Math.* 27.1 (2009), pp. 87–91. DOI: 10.1016/j.exmath.2008.07.001.

[Ram06] Arun Ram. *Alcove walks, Hecke algebras, spherical functions, crystals and column strict tableaux*. 2006. DOI: 10.4310/PAMQ.2006.v2.n4.a4.

[Rei+25] Anna Reimann et al. "Involutions in Coxeter groups". In: *Algebras and Representation Theory* 28.2 (2025), pp. 647–667. DOI: 10.1007/s10468-025-10332-x.

[Rei24] Anna Reimann. *Folded galleries and moment graphs*. 2024. arXiv: 2410.12578 [math.CO].

[Ric82] Roger W. Richardson. "Conjugacy classes of involutions in Coxeter groups". In: *Bulletin of the Australian Mathematical Society* 26.1 (1982), pp. 1–15. DOI: 10.1017/S0004972700005554.

[Rou01] Guy Rousseau. "Exercices métriques immobiliers". In: *Indag. Mathem. (N.S.)* 12(3) (Sept. 2001), pp. 383–405.

[Rou77] Guy Rousseau. "Immeubles des groupes réducitifs sur les corps locaux". In: *Publications Mathématiques d'Orsay* (1977). Thése de doctorat.

[Sch06a] Christoph Schwer. "Galleries and q-analogs in combinatorial representation theory". PhD thesis. Universität zu Köln, 2006.

[Sch06b] Christoph Schwer. "Galleries, Hall-Littlewood polynomials, and structure constants of the spherical Hecke algebra". In: *International Mathematics Research Notices* (2006). DOI: 10.1155/imrn/2006/75395.

[Sch08] Issai Schur. "Über die Darstellung der symmetrischen Gruppe durch lineare homogene Substitutionen". In: *Sitz. Ber. Preuss. Akad.* (1908), pp. 664–678.

[Sch22] Petra Schwer. "Shadows in the Wild - Folded Galleries and Their Applications". In: *Jahresbericht der Deutschen Mathematiker-Vereinigung* 124.1 (Mar. 1, 2022), pp. 3–41. DOI: 10.1365/s13291-021-00244-2.

[Ser80] Jean-Pierre Serre. *Trees*. [Transl. by J. Stillwell]. Berlin–New York: Springer-Verlag, 1980, pp. ix+142. DOI: 10.1007/978-3-642-61856-7.

[Spe37] Wilhelm Specht. "Darstellungstheorie der Hyperoktaedergruppe". In: *Math. Z.* 42 (1937), pp. 629–640. DOI: 10.1007/BF01160099.

[Spr82] Tonny A. Springer. "Some remarks on involutions in Coxeter groups". In: *Comm. Algebra* 10.6 (1982), pp. 631–636. DOI: 10.1080/00927878208822739.

[Tit69] Jacques Tits. "Le probléme des mots dans les groupes de Coxeter". In: *Symposia Mathematica (INDAM, Rome, 1967/68)* 1 (1969), pp. 175–185.

[Ver68] Daya-Nand Verma. "Structure of certain induced representations of complex semisimple Lie algebras". In: *Bulletin of the American Mathematical Society* 74.1 (1968), pp. 160–166.

[You30a] Alfred Young. "On quantitative substitutional analysis. IV". In: *Proc. Lond. Math. Soc. (2)* 31.1 (1930), pp. 253–272. DOI: 10.1112/plms/s2-31.1.253.

[You30b] Alfred Young. "On quantitative substitutional analysis. V". In: *Proc. Lond. Math. Soc. (2)* 31.1 (1930), pp. 273–288. DOI: 10.1112/plms/s2-31.1.273.

APPENDIX A

Coxeter diagrams of finite and affine Coxeter groups

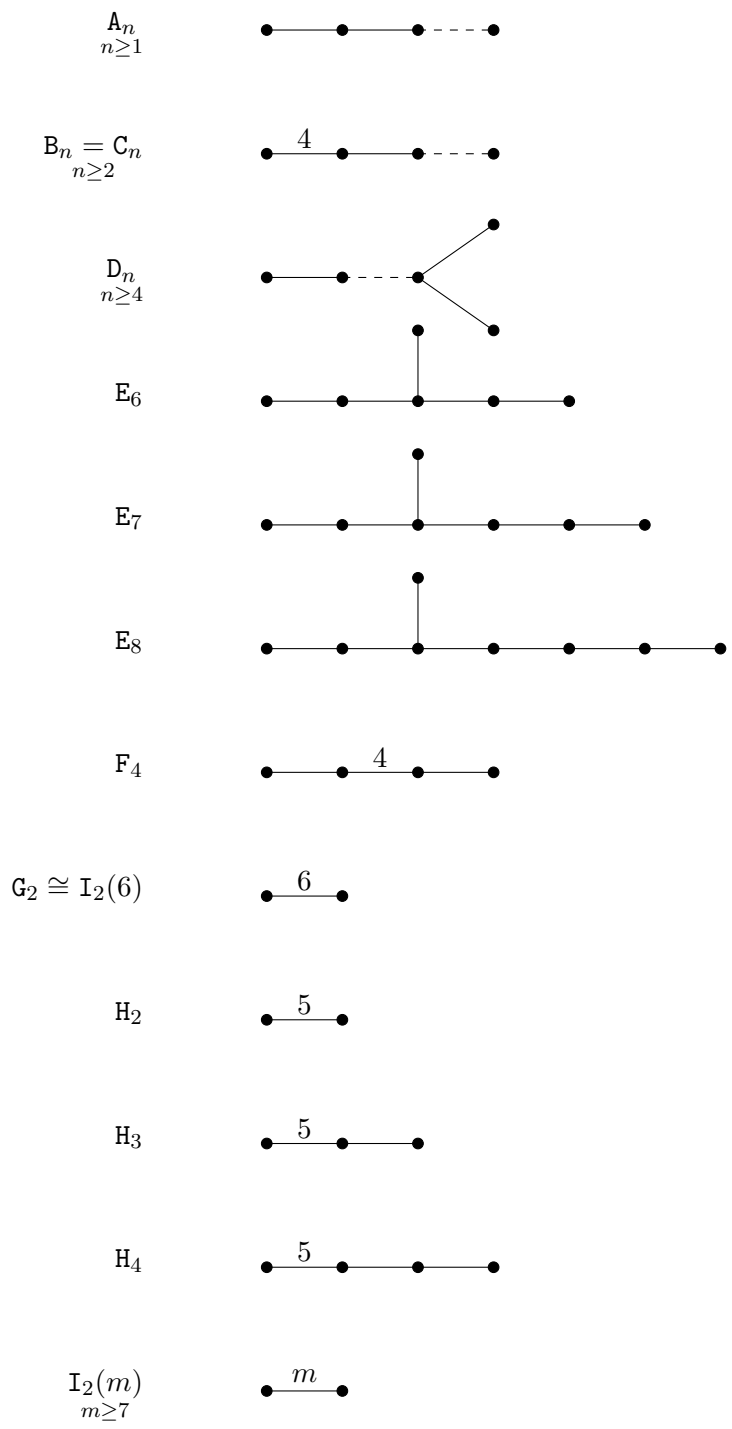

FIGURE A.1. Coxeter diagrams of the finite irreducible Coxeter groups.

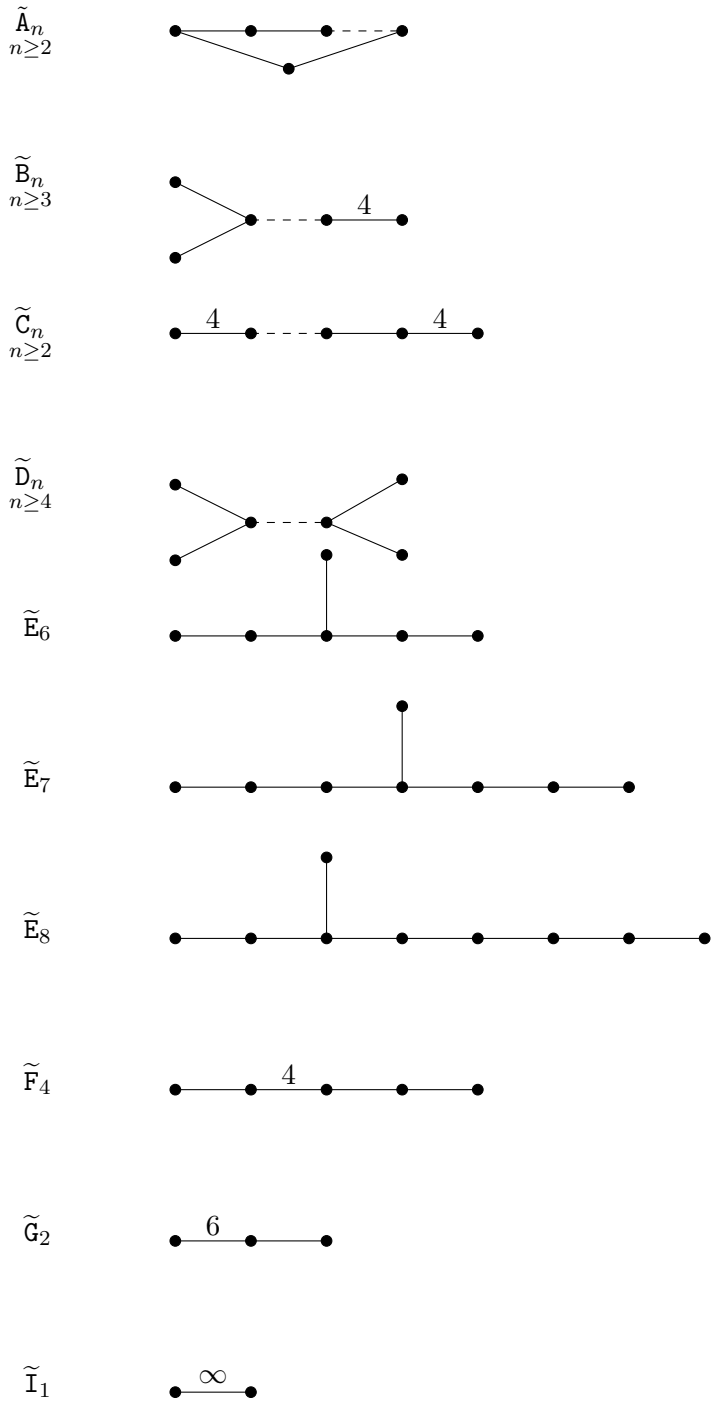

FIGURE A.2. Coxeter diagrams of the infinite irreducible Coxeter groups.

Author contributions

Anna Reimann: Combinatorial aspects of Coxeter groups

This thesis is a collection of research results that were partly published earlier as contributions to the collaborative article [Rei+25], partly contained in the single-author paper [Rei24], and partly unpublished. The following review presents sources and author contributions for all contents of this work that contain research results:

Chapter 2: Section 2.1 contains no new results, but collects notions and notation from well-founded literature resources. Definitions 2.1.3, 2.1.5, 2.1.7 and 2.1.8 are taken from the author's collaborative work [Rei+25], where compiling and articulating the necessary graph theoretic foundations was part of the first author's responsibility. The examples in this section were computed specifically for this thesis.
Section 2.2 is compiled from various sources, including established literature, the author's paper [Rei24], the collaborative research article [Rei+25], and unpublished material. Section 2.2.1 is based on the preliminaries sections of [Rei24] and [Rei+25], but includes unpublished examples and further details. Section 2.2.3 did not appear in any of the author's previous works. Sections 2.2.2 and 2.2.4 are based on [Rei24], but also contain unpublished examples and further elaborations. The first part of Section 2.2.5, along with the parts concerning Weyl chamber orientations, is based on [Rei24] as well, while the parts addressing chimney orientation are included in this thesis exclusively.

Chapter 3: Large piles of this chapter, especially Sections 3.1, 3.2.1 and 3.3, are based on the author's article [Rei24]. The content of Proposition 3.1.7 and Lemma 3.1.11, and Examples 3.1.10 and 3.1.12, has not yet been published. Section 3.2.2 was not included in [Rei24]; in particular, Lemmas 3.2.13 and 3.2.21 and Propositions 3.2.18 and 3.2.23, along with the examples and open questions presented there, are unpublished research results of the author.

Chapter 4: This chapter is entirely based on the author's work and, to our knowledge, does not contain any research results that have been previously published.

Chapter 5: Sections 5.1 to 5.4 of this chapter are based on the collaborative article [Rei+25], while Examples 5.1.2, 5.2.2, 5.2.5, 5.2.8, 5.2.10, 5.2.13, 5.2.15 and 5.4.1 presented in these sections were developed specifically for this thesis and did not appear in the article. The research question that motivated the study of conjugacy classes of involutions in Coxeter groups and the approach using generalized higher-rank odd graphs was proposed by the author's colleagues Santos Rego, Schwer, and Varghese. It was the author's contribution to present Lemma 5.2.12, which enables the computation of the number of conjugacy classes for various examples and establishes the foundations for Lemma 5.2.14 and Proposition 5.2.16, which were developed collaboratively by all co-authors. Furthermore, the author derived and proved the closed formulae for the number of conjugacy classes, as presented in Theorems 5.4.3 and 5.4.4. The author also contributed to reviewing the existing literature, the collection of relevant material, and the writing of the manuscript.
The contents of Sections 5.5 and 5.6 were developed solely by the author and have not yet been published.